

ETUDE SUR LA DETECTION DES PHENOMENES AEROSPATIAUX RARES

Volume n° 4

SOMMAIRE DU VOLUME N° 4

oooooooooooooooooooooooooooo

Ce volume se compose de 3 parties :

III.5.1. Prosuection systématique

Correspondances avec 17 pays, par ordre alphabétique :

- Afrique du Sud
- , Belgique
- , Brésil
- , **Canada**
- , Colombie
- Danemark
- , **Equateur**
- , Espagne
- , Etats-Unis
- Grande-Bretagne
- , Hongrie
- , Indonésie
- Nouvelle-Zélande
- , Pays-Bas
- , République Fédérale d'Allemagne
- , Tunisie
- Uruguay

III.5.2. Echanges avec les Etats-Unis.

Comptes-rendus de visites :

- , au S.E.A.N.
- chez Monsieur Mac Crosky (Prairie)

III.5.3. Echanges avec la Tchécoslovaquie.

correspondances avec Monsieur Ceplecha, et compte-rendu de visite à son observatoire (Réseau européen de détection des météores),

III.5. ANNEXE : correspondances et visites à l'étranger.

III.5.1. Prospection systématique.

Cette partie de l'annexe au chapitre III présente toutes les correspondances échangées dans le cadre des prises de contact systématiques décrites au para. III.1.1 ■

Le signe ⊕ ajouté en marge d'une adresse signifie qu'une lettre du second type y a été envoyée.

LISTE des 75 AMBASSADES DESTINATAIRES

Afrique du Sud	Israël
Albanie	Italie
Algérie	Japon
Arabie Saoudite	Koweït
Argentine	Liban
Australie	Maroc
Autriche	Mexique
Belgique	Nicaragua
Bolivie	Norvège
Bésil	Nouvelle Zélande
Bulgarie	Ouganda
Canada	Pakistan
Chili	Pays-Bas
Chine	Panama
Colombie	Pérou
Congo	Philippines
Corée	Pologne
Costa Rica	Portugal
Côte d'Ivoire	Qatar
Cuba	R.D.A.
Danemark	R.F.A.
Egypte	République Malgache
Emirats Arabes Réunis	Roumanie
Equateur	Sri Lanka
Espagne	Suède
Etats - Unis	Suisse
Ethiopie	Tchécoslovaquie
Finlande	Thaïlande
Grande-Bretagne	Tunisie
Grèce	Turquie
Guatemala	U.R.S.S.
Guinée	Uruguay
Haïti	Vénézuéla
Hongrie	Viet-Nam
Inde	Yougoslavie
Indonésie	Zaïre
Irlande	Zambie
Islande	

Lettre adressée aux ambassades parisiennes

François LOUANGE
Ingénieur - Conseil

9, rue Sainte-Anastase,
75003 PARIS
Tél. : (1) 277.49.56

NO SIRET : 319532503 00012

à l'attention de
Monsieur l'Attaché Scientifique

Paris, le 19/04/82

Monsieur,

chargé par un service du Centre National d'Etudes Spatiales d'effectuer une étude sur l'état actuel des recherches dans un **domaine** scientifique **particulier**, je me permets de m'adresser à vous, ainsi qu'à vos homologues **d'autres ambassades parisiennes**.

Le problème étudié, dont vous pourrez trouver **ci-joint** un exposé succinct, concerne la **détection** des phénomènes aérospatiaux rares, pour laquelle une collaboration et des échanges de données **pourraient** s'avérer fructueux pour les chercheurs des différentes disciplines concernées.

Pourriez-vous me faire savoir si dans votre pays des laboratoires de recherche ou **d'autres organismes s'intéressent** à la détection des phénomènes aérospatiaux rares (chutes de météorites, foudre, ...) et **s'ils utilisent** des moyens de détection **systématique** (radars, caméras, **images** de satellites, ...) ? Dans **l'affirmative**, vous serait-il possible de me mettre en contact avec ces laboratoires ou organismes, ou à défaut de me **fournir** des **renseignements** sur leurs activités et les moyens techniques dont ils disposent dans ce **domaine** ?

En vous **remerciant** à l'avance pour votre collaboration, je vous prie d'agréer, Monsieur, l'expression de ma parfaite consiaération,

F. Louange

ETUDE DE LA DETECTION DES PHENOMENES AEROSPATIAUX RARES

.....

Depuis plusieurs années, l'étude de phénomènes aérospatiaux rares a été entreprise au sein du CNES. Cette tâche, confiée au **GEPAN** (Groupe **d'Etude** des Phénomènes Aérospatiaux Non-identifiés) a conduit à mettre au point des méthodes efficaces de collecte et d'analyse d'informations originales concernant des phénomènes aérospatiaux fugitifs, non prévisibles et généralement non reproductibles. Certains de ces phénomènes sont connus et déjà étudiés (météorites, décharges d'électricité atmosphérique ...) ; d'autres restent probablement à expliquer.

Tous ces phénomènes ont en commun que de nombreuses **informations** les concernant se présentent sous forme de témoignages humains. C'est donc sur l'étude de tels témoignages (recueillis et transmis par la Gendarmerie Nationale) que le **GEPAN** a, d'abord fait porter son effort principal ; il a ainsi pu établir que, sous réserve de certaines précautions méthodologiques, il **est** parfaitement possible d'extraire de telles informations des données exploitables pour une recherche scientifique. Celles-ci, bien que largement ignorées de nos **jours** par les chercheurs, revêtent un caractère unique, des informations équivalentes ne pouvant être totalement fournies par d'éventuels systèmes instrumentaux ; il faut voir là deux voies d'acquisition de données, indépendantes et complémentaires, concernant les phénomènes aérospatiaux rares.

Lors de sa dernière réunion (janvier 82), le Conseil Scientifique du **GEPAN** a recommandé que soit entreprise une étude sur **les** possibilités techniques et les besoins de détection systématique des phénomènes aérospatiaux rares. Ce travail comporte un recensement et une analyse préalable portant sur les points suivants :

- ♦ **les** besoins actuels des laboratoires de recherche scientifique et autres organismes intéressés **par** certains de ces phénomènes (protection de l'environnement, par exemple) ;
- ♦ les moyens de détection actuels (radars, caméras grand **champ...**), **implantés** en France ou à l'étranger ;
- ♦ les extensions opportunes, sous forme d'adaptation de systèmes **existants** ou développement de systèmes originaux.

Les résultats de ce premier travail d'enquête devront conduire prochainement tous les partenaires intéressés à débattre sur le choix d'une proposition concrète de mise en place de systèmes de détection et de diffusion de données.

Lettre adressée aux laboratoires et organismes

François LOUANGE

Ingenieur - Conseil

9 rue Sainte-Anastase,

75003 PARIS

Tel. : (1) 277.49.56

tic SIRET : 319532503 00012

Paris, / /82

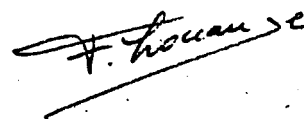
Monsieur,

je suis chargé par un service du C.N.E.S. (Centre National d'Etudes Spatiales) d'effectuer une étude de l'état actuel des moyens et des besoins dans le domaine de la détection des phénomènes aérospatiaux rares. Ce sujet, qui est brièvement présenté dans le papier ci-joint, recouvre tous les phénomènes sporadiques et imprévisibles qui peuvent se produire dans la Basse atmosphère, comme la foudre, les étoiles filantes,...

La première étape de ce travail consiste naturellement à passer en revue, dans la mesure du possible, les systèmes existants susceptibles de présenter un intérêt pour cette détection (radars, caméras à grand champ, détecteurs électromagnétiques,...). Dans cette optique, j'ai pris contact, en France, avec l'aviation civile, l'armée, la météorologie nationale, les spécialistes des météores et météorites, de la protection de l'environnement, etc... J'ai également écrit à plusieurs ambassades à Paris, et le représentant de votre pays m'a aimablement communiqué votre adresse.

Si vous disposez d'information sur des systèmes de détection utilisés dans votre pays, je vous serais très reconnaissant de bien vouloir m'envoyer quelques données techniques.

Dans l'attente de votre réponse, je vous prie d'agréer, Monsieur, l'expression de ma parfaite considération,.



François LOUANGE
Ingénieur - Conseil

9, rue Sainte-Anastase,
75008 PARIS
Tél. : (1) 277.49.56

No SIPET : 319032503 00012

Paris, / /82

Sir,

I have been appointed by a department of the french national space research centre C.N.E.S. to undertake a survey of existing **means** and needs in the field of detection of rare aerospace phenornena. This topic, **which** is briefly described in the attached **paper**, includes **all sporadic** and non-predictible **luminous** phenonena that may occur in low atmosphere, **such as** lightnings, fireballs, etc.. .

The first step in this work is **obviously** to review, as far as possible, **all** existing systems that are likely to be useful for **such** a detection (radars, wide field caneras, electrornagnetic detectors,...). **With** this in view, I got into touch, in Frânce, with **civilian** aviation, armies, **meteorologists**, **specia-**
lists of fireballs and meteorites, protection of environment, etc... I **also** sent a letter to various **embassies** in Paris, and your country's representati-
ve kindly sent me your address.

If you have information on detection **systems** that are used in your country, I would be nost grateful for **receiving** from you some technical data.

Looking forward to hear of you, I remain

Yours sincerely,

F. Louange

STUDY ON DETECTION OF RARE AEROSPACE PHENOMENA

A study of rare aerospace phenomena has been conducted for several years by a department of CNES : entrusted with this task, the GEPAN (Groupe d'Etude des Phénomènes Aérospatiaux ?Ton-identifiés) developed efficient methods to collect and analyze original information concerning transient, unpredictable and generally non-reproducible aerospace phenomena. Some of these phenomena are known and already under study (e.g. meteorites, discharge of atmospheric electricity ...); others are probably still to be explained.

All these phenomena have in common that most information is available through human testimonies. For this reason, GEPAN has devoted most of its efforts to the study of such testimonies (collected and transmitted by the french "Gendarmerie Nationale^H), and has established that it is perfectly feasible to extract from this information valuable data for scientific research, provided some methodological precautions are taken. Such data, although generally ignored nowadays by researchers, take on a unique character, as no equivalent information could be totally provided by technical equipments; one should see there two independant and complementary means of data acquisition about rare aerospace phenomena.

During its last meeting (in January 1982), GEPAN's Scientific Board recommended to undertake a study on technical possibilities and actual needs for detection of rare aerospace phenomena. This work includes a survey and a preliminary analysis of the following points :

- present needs of scientific research laboratories and other institutions interested in some of these phenomena (e.g. for protection of the environment);
- existing detection means (radars, wide field cameras ...), implemented in France or abroad;
- convenient extensions, either as adaptation of existing means or as development of original systems.

The results of this initial work will soon enable all interested parties to discuss the choice of a concrete proposal aiming at the set-up of detection and data dissemination systems.

François LOUANGE
Ingenieur - Conseil

8, rue **Sainle-Anastase.**
75003 PARIS
Tél : (1) 277.49.56

no SIRET : 319532503 00012

Paris, / /82

Muy Señor mio,

he sido encargado por un departamento del centro frances de **investigacion** espacial C.N.E.S. de un estudio de los **medios** y de las necesidades existente en el campo de la deteccion de los fenomenos aerospaciales **raros**. Este tema, brevemente **presentado** en el **papel adjunto**, **atañe a todos** los fenomenos luminosos eçporadicos Y im-
previsibles que **pueden** ocurrir en la atmosfera **baja**, tal como el **rayo**, **meteoritos**, etc...

La primera etapa de este trabajo consiste **naturalmente** en un estudio de los **sistemas** actuales que **podrian** ser utiles para una tal deteccion (radares, **camaras de gran campo**, detectores **electromagneticos**,...). Con esta idea, ne he puesto en **contacto**, en Francia, con la **aviacion** civil, el ejercito, meteorologos, especialistas en **me-
teoros** y meteoritos, **proteccion** del medio ambiente, etc. He escrito **tambien cartas** para varias **embajadas** en Pa-
ris, y el representante de Su pais me **facilito amabla-
mente** Su **direccion**.

Si Ud tiene informacion sobre sistenas de deteccion **u-
tilizados** en Su pais, Le agradeceria mucho si me **man-
dara** algunos datos tecnicos.

En la espera de Su contestacion, Le **saludo muy atenta-
mente**,

F. Louange

ESTUDIO DE LA DETECCION DE LOS FENOMENOS AEROSPACIALES RAROS

Hace ya varios años que el CNES estudia fenómenos aerospaciales raros, gracias a uno de sus departamentos : el GEPAN (Groupe d'Etude des Phénomènes Aérospatiaux Non-identifiés). El trabajo de investigación consecuente ha permitido desarrollar varios métodos eficaces para la colecta y el análisis de informaciones originales sobre los fenómenos aerospaciales fugaces, que no pueden ser previstos ni generalmente reproducidos. Algunos de esos fenómenos son ya conocidos y estudiados (meteoritos, descargas de electricidad atmosférica ...); otros quedan por explicar.

El punto común de todos esos fenómenos es que la mayor parte de sus informaciones se presenta en forma de testimonios. En consecuencia, el GEPAN empezó sobre todo por el estudio de los testimonios (recogidos y transmitidos por la "Gendarmerie Nationale"); de esa manera el GEPAN ha podido establecer que, si se respetan ciertas precauciones metodológicas, es perfectamente posible extraer de tales informaciones datos explotables en una investigación científica.

Esas informaciones, aunque bastante ignoradas por los investigadores actuales, son de un carácter único, puesto que no pueden ser obtenidas totalmente gracias a sistemas instrumentales eventuales. Luego es preciso reconocer que hay dos métodos de adquisición, independientes y complementarios, de los datos que concierne los fenómenos aerospaciales raros.

En la última reunión del Consejo Científico del GEPAN (en Enero 1982), se ha aconsejado emprender un estudio sobre las posibilidades técnicas y las necesidades de detección sistemática de los fenómenos aerospaciales raros. Ese trabajo comporta un recensamiento y un análisis previo sobre los siguientes puntos :

- las necesidades actuales de los laboratorios de investigación científica y de los otros organismos interesados por algunos de esos fenómenos (por ejemplo : la protección del medio ambiente);
- los sistemas actuales de detección (radares, cámaras de gran campo ...) que existen en Francia o en el extranjero;
- las extensiones oportunas, bajo la forma de adaptación de sistemas que existen ya, o del desarrollo de nuevos sistemas.

Los resultados de este trabajo primero de encuesta permitieron proximate que todos los interesados puedan discutir de proposiciones concretas sobre la instalación de sistemas de detección y de difusión de datos.

A F R I Q U E du S U D

TÉLÉPHONE : 555-92-37
TÉLÉG. : NAVORS PARIS
TELEX : NAVORS 203964



AMBASSADE D'AFRIQUE DU SUD
BUREAU DU CONSEILLER SCIENTIFIQUE

59, QUAI D'ORSAY
78007 PARIS

Votre réf. :

Notre réf. :

le 23 avril 1982

M. François Louange
Ingenieur-Conseil
9, rue Sainte-Anastase
75003 PARIS

Monsieur,

Je fais référence à votre lettre du 19 avril 1982.

Il existe trois Instituts en Afrique du Sud auxquels vous pourriez écrire concernant la détection des phénomènes aérospatiaux rares:

- 1) The National Institute for Telecommunications Research
CSIR
PO Box 3718
2000 Johannesburg

Ils ont autrefois étudié la foudre et il est possible qu'ils continuent leurs recherches sur ce phénomène. Un dossier sur des rapports d'OVNIS est également mis à jour.

- 2) The National Electrical Engineering Research Institute
CSIR
PO Box 395
0001 PRETORIA

A présent, cet Institut s'occupe de la détection de décharges d'électricité atmosphérique sur l'Afrique du Sud, par moyen d'enregistrement électronique.

- 3) The South African Astronomical Observatory
PO Box 9
Observatory
CAPE TOWN 7935

Je ne suis pas au courant des recherches effectuées par cet Institut mais vous pourriez demander directement si l'on fait des recherches sur les chutes de météorites.

Dans tous les cas, vous devriez vous adresser au Directeur de l'Institut, de préférence, en anglais.

Veuillez agréer, Monsieur, l'expression de mes sentiments les plus distingués.


J.A. BRINK
Conseiller Scientifique

JAB/ph

CSIR



Council for Scientific and Industrial Research

National Institute for Telecommunications Research

P.O. Box 3718 Johannesburg 2000 South Africa • Telegrams Navorstel Yeoville 2198 Tel (011) 648-1150/6

Our ref. 5/8/2(4)2

Your ref.

28 July 1982

Mr. F. Louange
9, Rue Sainte-Anastase
75003, PARIS.

Dear Mr. Louange,

OBSERVATIONS OF RARE AEROSPACE PHENOMENA

The only phenomenon of the class mentioned in your enquiry that is specifically studied here on a continuing basis is that of lightning. I should mention that in large parts of South Africa lightning is a frequent occurrence, though predictable only in a statistical sense.

The National Institute for Electrical Engineering Research operates a country-wide network of lightning counters and also carries out a programme of research into the parameters of lightning with the aid of a lightning mast and associated measuring equipment.

This Institute, the National Institute for Telecommunications Research, carries out research into the physics of lightning using a system of spaced vhf receivers to obtain three-dimensional images of lightning with very high spatial and temporal resolution.

Apart from the above examples there is no conscious attempt to keep a watch for rare phenomena. Of course if any such phenomena were reported the reports would be judged against routine meteorological observations, records of the existing civil and military radar networks, and so on.

Yours sincerely,

R.W. VICE

DIRECTOR

RWV/msm

CSIR

Council for Scientific and Industrial Research

National Electrical Engineering Research Institute

P O Box 395, Pretoria, 0001 South Africa • Telex 3-630 SA Telegrams Navorselek Tel. (012) 86-9211

Our ref. NEERI/Ek/1

Your ref.

BY AIRMAIL

Mr Francois Louange
9 rue Sainte-Anastase
75003 PARIS
France

Dear Mr Louange

Lightning detection

Your **letter** of 21 May 1982 refers. We have for a number of years been engaged in lightning research, mainly with the **purpose** of **determining** the effects that lightning ground flashes have on electrical installations.

The method of detection is by the characteristic components of the frequency spectrum of a lightning flash which reaches the ground. The position of the flash **is then** determined in two ways:

- (a) By **cameras taking** a 360 ° picture of the horizon or by TV **cameras** covering a smaller area of interest.
- (b) By comparing the two **signals** induced in a crossed loop antenna.

A lightning ground flash counter, based on the **typical** frequency characteristic of lightning flashes striking the ground, has also been developed by us and **is presently** used to determine the geographical distribution of lightning ground flashes in South Africa. In **conjunction** with this we are operating a microcomputer based system developed **by** Lightning Location and Protection of Tucson, USA, which uses a crossed loop antenna for **lightning** detection and location.

We are also operating **another** system in **conjunction** with a German **organization**, which monitors global lightning distribution using low frequency crossed loop antennae. The system **has** a range of **several** thousand **kilo-**metres and stations are **currently situated** in Berlin, Tel Aviv and Pretoria.

I/2

--- I hope that the **above** information will be of use to you. I also enclose a review paper which **summarises** current lightning research **activities** in South Africa. Should you require more details, please do not hesitate to contact us **again**.

Yours sincerely



H Kröniger
Lightning Research Division
Electric Power Department

Presidential Address

Lightning research in Southern Africa

by R B Anderson



President of the Institute 1979



Dr R B Anderson

Dr Ralph Blyth Anderson was born in 1916 in Bulawayo and educated at the Milton High School there. In 1937, he was awarded the degree of **BSc** (Engineering) at Cape Town.

He worked with the Southern Rhodesia **Electricity** Supply Commission and, together with Mr **R D** Jenner, was awarded the **Gold** Medal of the Institute for a paper on Lightning published in the Transactions in 1954. In 1965 he **joined** the **CSIR** and is now Head of the Power Electrical Engineering Division of the National Electrical Engineering Research Institute.

He was appointed Convenor of **the Working** Group 33.01 (Lightning) of Study Committee No. **33** of CIGRÉ (**International** Conference on Large Electric **Systems** at High Tension) as from January 1970 **after** service with the Working **Group** since 1963. He was awarded the degree of Doctor of **Philosophy** by the University of Cape Town in December, **1972** for a **thesis** entitled 'The Lightning **Discharge**.'

Dr Anderson is the **author** of a number of papers, many jointly with **colleagues**.

Lightning research in Southern Africa*

R B Anderson

SINOPSISIS

The paper reviews the development of the lightning discharge from the initial stage of charge separation, through to the mechanisms of the discharge within a thundercloud and finally in its path to earth. At the same time, attention is drawn to the considerable contributions made by scientists and engineers in Southern Africa. The classical works of Schonland and Malan, together with their contemporary colleagues, figure high on the list but they are followed by other no less enthusiastic investigators, each of whom added yet another contribution to the knowledge of lightning, or applied it to the protection of systems be they electric power, communications, buildings or simply to the safety of human beings. The various lightning parameters are discussed together with the means whereby they have been or are being measured; these include the multiple stroke flash, the lightning current magnitude and its shape and the lightning flash density in the Republic. Finally, the optimisation of the protection of power and communication systems is discussed, and the application of lightning data to the philosophy of the protection of buildings and of people. In conclusion, the review illustrates that while a great deal of knowledge of lightning has been acquired over the years there are still many areas where further research is urgently needed in order that protective measures may be improved with benefit to the safety and prosperity of all peoples of the country.

OPSOMMING

Die referaat bied 'n oorsig van die ontwikkeling van die weerligontlading, vanaf die beginstadium van ladingskeiding tot die meganismes van ontlading binne die donderwolk en uiteindelik in sy pad na die aarde. Die aandag word terselfdertyd gevestig op die aansienlike bydraes deur Suid-Afrikaanse wetenskaplikes en ingenieurs. Die klassieke werk van Schonland en Malan en hulle tydgenote staan hoog aangeskrewe, maar hulle is gevolg deur ander wat nie minder entoesiasies was nie, en elkeen 'n bydrae gemaak het tot die kennis oor weerlig of tot die beveiliging van elektriese kragstelsels, kommunikasiestelsels, geboue of die veiligheid van mense. Die verskillende weerligparameters word bespreek, asook die metodes waarvolgens dit gemeet is of word: dit sluit in die multi-straal ontlading, grootte van die weerligstroom en die golfvorm daarvan, en die weerligdigtheid in die Republiek. Die optimisering van die beveiliging van krag- en kommunikasiestelsels word ten slotte bespreek, asook die toepassing van weerligdata ten opsigte van die beskerming van geboue en mense. Laastens toon die oorsig dat, alhoewel 'n groot hoeveelheid kennis deur die jare oor weerlig ingewin is, daar nog baie gebiede is waar verdere navorsing dringend benodig word sodat beveiligingsmaatreels verbeter kan word tot voordeel van die veiligheid en voorspoed van almal in die land.

1 Introduction

In this review it is intended to describe, rather circumspectly perhaps, the development of the lightning discharge, and to draw, at the same time, special attention to the contributions made by South Africans (and Rhodesians) to the advancement of the science and the engineering implications of the phenomena.

First of all, compared to the global situation (Fig 1), the isokeraunic level, reaching over 100 thunderstorm days per annum in some parts of South Africa, is one of the highest for an area having a comparatively advanced industrial development with its network of electric power and communication systems. Thus it was no great wonder that the problems which faced the country were tackled by its scientists and engineers early in the century, soon after the development of electric transmission and distribution systems had begun.

In fact, these difficulties were referred to in the early annals of this Institute, and the first paper directly describing the relation of atmospheric phenomena to the production of overvoltages in overhead electric transmission lines was presented by G V Adendorff⁽¹⁾ in 1911 and published in Vol 2 of the Transactions of the Institute.

Considering the fact that little knowledge was available compared to the present day, this paper recorded some very close estimates of lightning parameters and also some unusual theories. For example, the estimated breakdown potential for air at 33 kV cm⁻¹ resulted in a lightning potential of the order of 5 × 10⁹ V. The discharge was assumed to be highly oscillatory having a frequency of 50 to 500 kHz; it lasted two or three microseconds and delivered a current of 10 kA.

The author strongly advocated overhead grounded

wires to guard against direct strokes of lightning to power lines, for 'if the discharge is very heavy, as usually is the case, the probabilities are that a portion of the section struck will completely disappear...'

The paper concludes with the following paragraph:

'The whole question of atmospheric phenomena in this country is of such vast importance to the electrical engineer that a complete study of the whole subject should receive his careful consideration. Any time spent would be amply repaid with the thought that the progress of our electrical knowledge on the subject was being made more rapid and secure'.

However, serious research into lightning in South Africa was only to begin in the 1930s, mainly at the instigation of a Mr T P Pask of the Victoria Falls and Transvaal Power Company (VFP) who again extolled the necessity for lightning research in a paper⁽²⁾ to the Institute in early 1930, which resulted in the setting up of the 'Lightning Investigation Committee' under his Chairmanship in December of that year⁽³⁾.

In January 1932, Bernard Price, then President of the VFP, announced that Dr B F J Schonland was carrying out work in connection with lightning, as a result of which he, Schonland, was invited to take charge of the 'Lightning Research Sub-Committee'.

In the following month E C Halliday⁽⁴⁾ obtained the first photographs of lightning (Fig 2) with a camera having rotating lenses and modelled on the former camera designed by C V Boys and constructed by the University of the Witwatersrand.

As a result of a successful appeal for funds subsequently made by the SAIEE, several cameras were made and a mobile van equipped by the summer of 1932, and, with the help of H Collens^{(5) (6)} of the VFP, 11 good photographs of lightning were obtained (Fig 3).

D J Malan joined the team in 1934 and together they produced the many learned publications which pave the world the most advanced and unique information about

*Presidential Address delivered to The South African Institute of Electrical Engineers on 28th February, 1979.



Fig 1 Global Isokeraunic Map (Thunderstorm days).



Fig 2 First high speed picture of lightning in South Africa taken by E C Halliday(*) with a rotating lens camera.



Fig 3 High speed pictures of lightning by Schonland et al/(**) using a modified rotating lens camera.

lightning this century. These have been listed by T E Allibone⁽⁷⁾, an eminent British scientist, in his biographical memoirs of Schonland written for the Royal Society in 1973 for which the writer is also indebted for some of the historical information included herein. Allibone was closely associated with Schonland with whom he came out some joint work on the spark discharge to be mentioned later.

Schonland was appointed the first director of the Bernard Price Institute of Geophysical Research when it was established in 1937, and where work on lightning continued mainly under Malan until the latter's death in 1970. It is also fitting to recall that F J Hewitt joined the Institute just after World War 2 with an interest in radar and he was later to be the first to use this new tool for further research on lightning^{(8) (9)}.

After the war, Schonland was appointed the first

President of the Council for Scientific and Industrial Research (CSIR) when it was officially established in December 1945, but returned to the Bernard Price Institute five years later and continued with Malan to finish off their previous work.

Other South Africans reporting in the literature associated with the work of these pioneering scientists on lightning were D B Hodges, P G Gane and N D Clarence, and no doubt there were many more who were in some way connected with this unprecedented effort.

On the engineering side there were also a number of dedicated investigators, for example E F Rendell and H D Gaff⁽¹⁰⁾ of the VFP who presented a paper to the Institute in 1933 dealing with the problems of lightning protection of power systems for which the authors were

awarded the first Gold Medal of the Institute. Then C F Boyce, I C Ramsay and D P J Retief produced, in 1955, the now classic monograph⁽¹¹⁾ on the protection of open-wire communication systems against damage caused by lightning.

Finally, R B Anderson with R D Jenner summarised eight years of lightning investigation on a 88 kV transmission line in Rhodesia in two papers^{(12) (13)} to the SAIEE in 1948 and 1954 respectively, the latter also enjoying the distinction of the second Gold Medal award to the authors.

Two eminent contributors from the United Kingdom, who undoubtedly left their mark on the lightning scene in this country, were B L Goodlet⁽¹⁴⁾ who inspired many students during his professorship at the University of Cape Town, commencing during the writer's final year in 1937, and indirectly, but no less effectively, R H Golde through his classic paper on lightning with C E R Bruce⁽¹⁵⁾. Nearly 30 years later he was also invited to review the subject of lightning protection⁽¹⁶⁾ on the occasion of the SAIEE Golden Jubilee in 1969.

The more recent outcome of this great heritage of research into lightning is now vested in the CSIR in collaboration with the Electricity Supply Commission (ESCOM), the South African Bureau of Standards (SABS) and other statutory organisations interested in the application of the research to engineering systems, as will be further referred to in this review.

2 The origin of lightning

It is possibly surprising that even today the true mechanism of the generation of electricity in a thundercloud is not known for certain, and this is primarily due to the great difficulty, not to speak of the danger, of making direct measurements within clouds.

First attempts in this direction started with the measurement of the electrostatic fields within and under thunderclouds and the field changes during lightning discharges, together with the charge on precipitation and using electrometers and weather balloons; the results of this work, unfortunately, led to two opposing viewpoints. Firstly, C T R Wilson⁽¹⁷⁾, in 1929, maintained that positive ions were carried up to the top of the cloud, leaving the base negative, and thus assisting to maintain the earth's positive fair weather electric field; on the other hand, Simpson⁽¹⁸⁾ and his workers maintained that the base of the cloud was the seat of origin of positive electricity; the classic falling and breaking drop theories were also evolved at that time to explain how the charge could be separated within a cloud. Schonland and his father-in-law, J Craib, measured the electric field polarity of thunderclouds in South Africa and in 1927 published their results⁽¹⁹⁾ supporting the Wilson theory of a generally bipolar thundercloud with negative charge at the base. This was confirmed in later measurements by Halliday⁽²⁰⁾ in 1932. They also indicated that 90 per cent of all discharges originated from negative cloud charge and that from three to five discharges were within clouds for each one discharge to ground. However, there was also sufficient evidence to suggest that small positive charge centres could exist at the cloud base or in the air below the cloud, thus accounting for some discharges they

called 'air' discharges, which did not terminate on the earth and for the positive charge which was occasionally measured on rain drops. Simpson also thought that a branching discharge could only occur from a positively charged electrode thus supporting his theory. However, Allibone demonstrated to Schonland that branching could occur from either a positive or a negative polarity electrode and they published⁽²¹⁾ this information in 1931 thus supporting the deduction that a branched lightning flash to ground, emanating from the base of a thundercloud, could originate from a negative charge accumulation.

Reverting now to the present day, according to Moore and Vonnegut⁽²²⁾ there are two main theories of charge separation which are, however, still the centre of much controversy; they name the precipitation powered process and the convective electrification mechanism respectively.

In the first, the principal mechanism for the separation of charge is the vertical separation of larger hydro-meteors (water drops or hail pellets) from smaller ones as a result of their different terminal velocities and the various theories differ only in the way in which the hydro-meteors of different sizes come to carry different electric charges. For example, water drops which are polarised within an existing electric field will separate charge if the drop splits into large and small drops after the collision. Similarly, super-cooled water drops freezing suddenly will splinter off minute pieces of ice which will be positively charged, leaving a solid hail pellet negatively charged, and these will separate in a strong updraught.

In the second and more recently devised mechanism, the cloud particles are the principle charge carriers separated by the differential convective motions in opposition to forces imposed by the electric field, as shown in Fig 4 (after Vonnegut⁽²³⁾).

These charges are assumed to be derived in the first instance from a pre-existing electric field which creates ions during the normal ionic current flow and which are then captured by the cloud particles; a positive feedback occurs, thereby strengthening the field and speeding up the mechanism accordingly until breakdown occurs.

Moore concludes by saying that 'a single mechanism may be the primary agency responsible for the electrification of all thunderstorms; however, many scientists active in the field now incline to the view expressed by

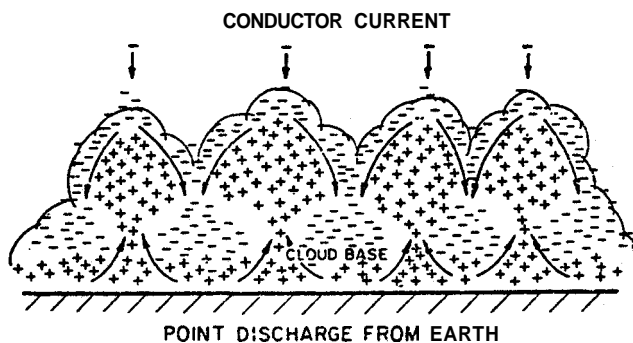


Fig 4 The convection electrification mechanism for charge separation in thunderclouds after Vonnegut⁽²³⁾.

Schonland, Chalmers and others, that several processes are capable of giving rise to lightning'. The best that can be done is to set out some conditions and observations which must be explained by any theory purporting to describe the detailed mechanism of cloud electrification.

Unfortunately, some of the proposed mechanisms of charge separation result in charge distributions within a thundercloud which could be significantly different from the simple bipolar model originally suggested by Schonland and Malan and depicted in Fig 5. Nevertheless, until such time as further information is available it can serve to represent a basic single cell within the cloud, to be replaced approximately every 20 minutes or so with another adjacent cell as described by Held and Carte⁽²⁴⁾ of the National Physical Research Laboratory of the CSIR. They used a 10 cm radar and all-sky camera at the radar site at Houtkopen near Pretoria and together with the analysis of reports from some 4 000 voluntary observers in an area of about 1 000 km² were able to conclude that lightning was observed more frequently near the leading edge of precipitation than elsewhere, thereby suggesting a possible connection between the charge separation mechanism and precipitation. On the other hand, hail was most often accompanied by lightning, but not always, thus suggesting that the hail process alone could not be responsible for the production of lightning.

Also in recent years, Proctor of the National Institute for Telecommunications Research (NITR) of the CSIR has developed a hyperbolic system of obtaining three-dimensional radio pictures of lightning⁽²⁵⁾⁽²⁶⁾ by using a number of VHF receivers, spread some 30 to 40 km apart and a recording system capable of accurately locating the position of sources of radiation (or noise) by measuring the time of arrival of the signals at the various receivers.

This ingenious method of recording was used to obtain the first unique pictures of lightning within clouds (Fig 6) and when combined with records from a 3 cm radar he was able to obtain some information from 12 flashes which led him to the conclusion that 'lightning had a

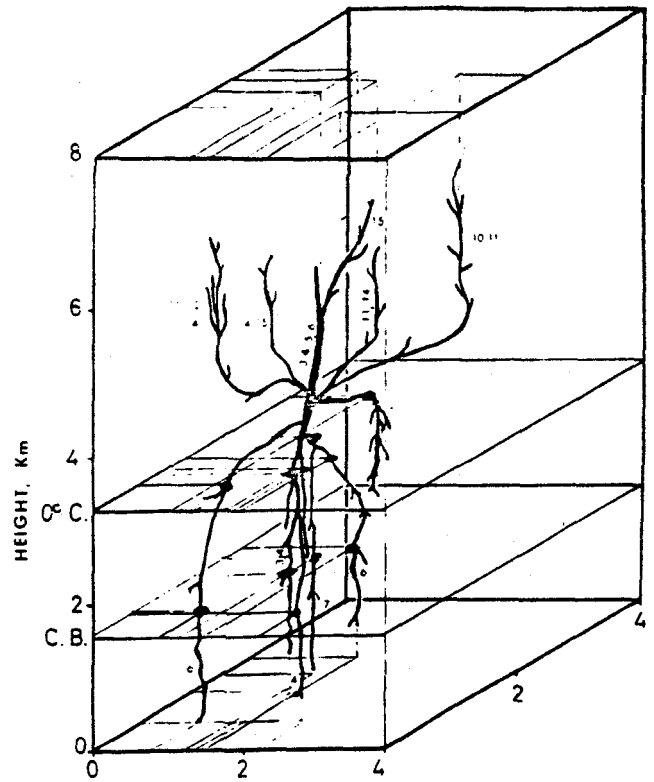


Fig 6 A unique radio picture of lightning after Proctor⁽²⁵⁾ CB = Cloud Base 0°C = Zero temperature level. (The sequence in which branches radiate is indicated by the small numerals).

marked tendency to begin at or near precipitation boundaries and to track edges of the precipitation patterns. Eleven flashes giving rise to high noise pulse rates began inside the precipitation and the only flash with a low pulse rate began just outside the precipitation boundary'.

These various observations therefore tend to support the theory linking the charge separation process with hydrometeors, be they hail pellets or liquid water drops, and that it is likely to be related to the precipitation mechanism itself. However, Proctor produced three-

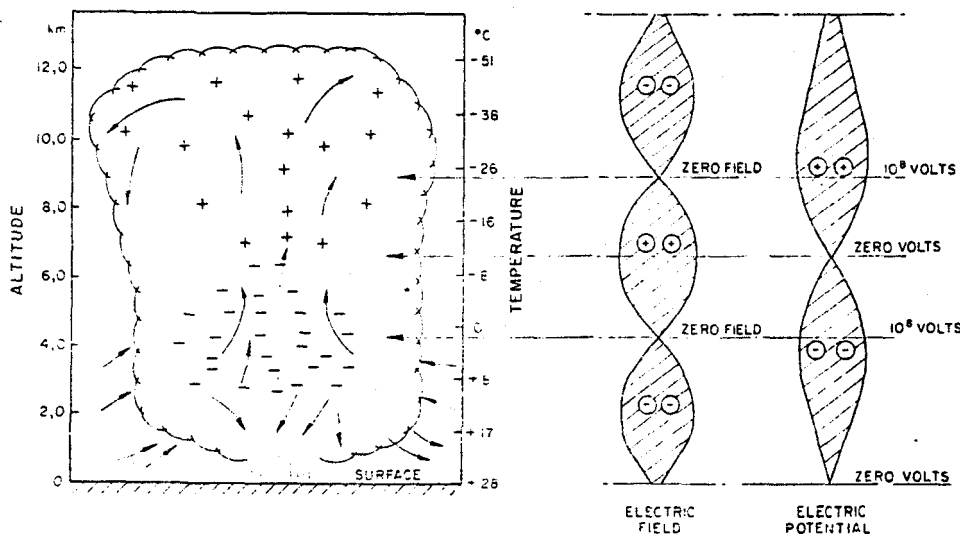


Fig 5 The conventional bi-polar thundercloud after Schonland and Malan with electric field and potential Conditions added.

dimensional pictures of five intra-cloud flashes and eleven cloud to ground flashes, and judging from the disposition of his streamers, most were not vertically orientated as in the classic bipolar thundercloud and in fact many were horizontal and spread out, sometimes several kilometers in extent. This considerable horizontal spread of streamers and thus of the distribution of charges has also been observed by Few⁽²⁷⁾ using acoustic methods and it may therefore be concluded that even though initial charge separation may take place in a vertical or near vertical direction, the charge of one sign can spread out horizontally and furthermore may physically move presumably as a consequence of upward and downward directed air draughts.

The possibility of the existence of both positive and negative charge centres separated horizontally is further borne out by electric field measurements at ground level carried out at the CSIR by Eriksson⁽²⁸⁾ and shown in Fig 7, indicating that field intensities of about equal magnitude were possible with both polarities and furthermore that while the strong negative fields occurred during the height of overhead thunderstorms, positive fields occurred in the later stages when the storm had passed over and during which time positive lightning flashes to ground also occurred more frequently (see Anderson⁽²⁹⁾); this would suggest that either the negative charge had been dissipated, leaving a large positive charge aloft at the end of the storm, or that the positive charges moved downwards by convection in the wake of a storm.

Thus, not only is the manner in which charge separates in the cloud still uncertain, but also how these charges are distributed, and it will take much additional

investigation of conditions within the cloud itself to obtain a statistically significant answer.

3 The mechanism of the discharge

The mechanism of the initial electrical breakdown of the media within a thundercloud itself is not precisely known for the same reasons as for the lack of knowledge regarding charge generating processes, and a solution of one of these processes would assist the understanding of the other. Basic measurements have been made, however, both in the laboratory and within clouds themselves which have enabled some theoretical considerations to be made.

Firstly, the breakdown strength of media somewhat resembling that in clouds has been determined in the laboratory — namely between falling water drops or ice particles etc, and this varies between 0.4×10^6 and $1 \times 10^6 \text{ Vm}^{-1}$ compared with $3 \times 10^6 \text{ Vm}^{-1}$ for air at NTP. Furthermore, a recent laboratory measurement by Griffiths and Latham⁽³⁰⁾ showed that no corona discharge could be produced from ice at temperatures below $-18 \text{ }^\circ\text{C}$. The highest electric field measurement measured to date in clouds is $0.4 \times 10^6 \text{ Vm}^{-1}$ using rockets, but it can be seen from physical models that the chance of making the measurement at the exact time and place of maximum field intensity in a cloud is very small.

On the other hand, the breakdown strength of air itself, reduces with altitude from about $3 \times 10^6 \text{ Vm}^{-1}$ at sea level, to 2×10^6 at about 3 km altitude and is less than $1 \times 10^6 \text{ Vm}^{-1}$ at about 9 km altitude and higher, so that the cloud boundaries at lower levels would at least comprise an insulation barrier to a discharge within a cloud which would tend to explain why long horizontal discharges seek out a rain shaft as a means to descend to the earth.

Reference to Fig 5 on the other hand, shows that for a bipolar cell, maximum field intensities are achieved at the upper and lower charge boundaries, and also in the charge separation area, and these therefore are regions within a cloud where initial breakdown can be expected to start.

Anderson⁽³¹⁾ has shown that if the two opposing cloud charges are enclosed in a cylinder in which the length exceeds twice the diameter, the maximum field intensity occurs at the extremities of the cylinder whereas for a shorter and larger diameter cylinder, the maximum stress occurs in the centre between the two charges. If one ignores the possibility of discharges from the upper charge where temperatures are much less than $-20 \text{ }^\circ\text{C}$, following Griffiths and Latham — then the first case favours the initiation of a discharge towards the earth from the lower end of the cylinder (or the boundary of the lower charge) while in the second case an intra-cloud discharge would be initiated in the area corresponding to where charge separation was occurring.

There is some evidence that charge separation takes place in the area around the $-8 \text{ }^\circ\text{C}$ isotherm and above, namely about 6 km above sea level (Anderson⁽³²⁾), and intra-cloud flashes would therefore be expected to be initiated in this region and five cases examined by

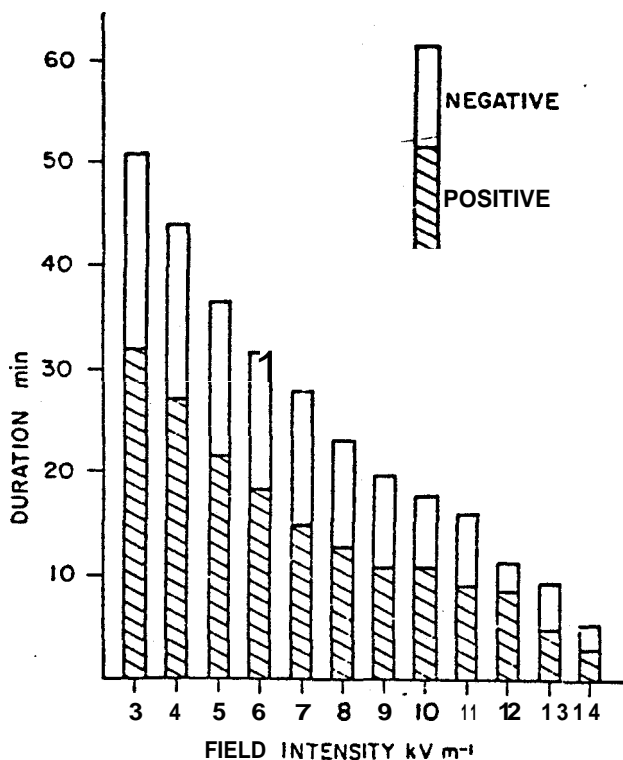


Fig 7 Distribution of durations of electric field intensities after Eriksson⁽²⁸⁾.

Proctor⁽²⁶⁾ did in fact do this. Flashes to the earth therefore would be expected to be initiated below 6 km and possibly even below the zero isotherm. about 5 km, where mostly water drops would be encountered. **Again**, Proctor observed the **majority** of his ground flashes to occur within zones of active precipitation and that initial sources of radiation **originated** around the zero isotherm **region**.

The only other known direct measurements of the altitudes of charges involved in ground flashes **come** from the work of Krehbiel et al⁽³³⁾ who, using a **multi-station** high speed field change measurement technique, calculated the origin of two strokes to be around 7 km and 5 km altitude respectively.

Clearly, more measurements of the direct type used by Proctor, for **example**, will **provide** further data from which the charge distribution within clouds and the origin of flashes **can** be more accurately determined.

Following on questions as to the origin of lightning flashes, the next stage, namely the development of the discharge to ground, was first of **all** postulated by **Schonland**⁽³⁴⁾ (see Fig 8). He envisaged breakdown from a pocket of negative charge which was **then** lowered by **means** of a stepped leader, most frequently branched,

centre, the negative charge first **neutralised** the positive charge and **then** recharges the channel **negatively prior** to breakdown for a second stroke and so on, repeating the process so long as there were negative pockets of charge available as shown in the latter **portion** of Fig 8.

Ten **years later**, namely 1951, Malan with **Schonland**⁽³⁵⁾ deduced from slow **field** change measurements **during** the **intervals** between strokes that the successive strokes appeared to originate from higher and higher altitudes and **thus** evolved a mechanism to account for successive breakdown which assumed also that the channel became positive after the first return stroke and the positive streamers developed further into the charge volume till neutral. The channel could **then** be recharged negatively for a subsequent stroke (see Fig 9). The necessity to assume **separate** pockets of charge **thus fell** away.

However, **Hewitt**⁽⁶⁾ who was the first to use radar to detect the progress of streamers within a cloud was able to **state**⁽⁹⁾ that positive streamer advancement **occurred** from the ionised channel to **several** new charge centres and discharges did not necessarily **occur** in a set sequence or to **charge** centres ascending in **height**.

Finally, to add to **these**, **Anderson**⁽³¹⁾ found that in **order** to allow for a rather low potential gradient **along**

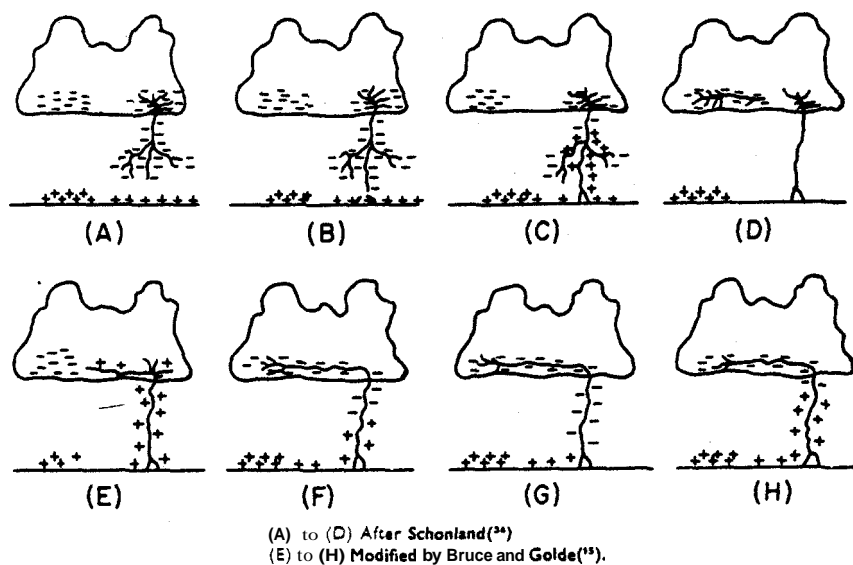


Fig 8 Diagram illustrating lightning leader and return stroke mechanism.

towards the earth. Upon **making** contact positive charge rose up the channel to neutralise the negative charge, and this **then** completed the first stroke. Other pockets of negative charge could thereafter break down by **means** of streamers directed towards the ionised channel and upon **making** contact be **discharged**. This gave **rise** to a high speed dart leader in place of the initial stepped leader but otherwise following the **same** pattern for any further number of **isolated** pockets, **thus making** up the **so-called** multiple stroke flash.

This **mechanism was** only questioned in 1941 by Bruce & Golde⁽¹⁵⁾ who suggested that after the **completion** of the first stroke the channel remained positively charged and streamers developed to new negative charge centres from the top of the channel. Upon reaching a

a leader of about $1 \times 10^5 \text{ Vm}^{-1}$ a substantial positive charge **was** required in the upper extremities of the channel and **thus** he evolved yet another mechanism (see Fig 10). This assumed that the conducting channel existing between two **opposing electric** charges **will always** be bipolar by induction thereby assisting **its** extension at both extremities **so** long as the main charges exist. Also **since** positive charge **carried** on **relatively** heavy ions could not **advance** up the lightning channel fast enough when the leader **contacted** the earth, he surmised that the return stroke **consisted** of an **over-discharge** of electrons to the earth, **leaving** the positive ions in the channel concentrated mainly at the cloud end. The field strength at the lower end could **then fall** to a sufficiently low **level** to **ensure** a rapid **de-**

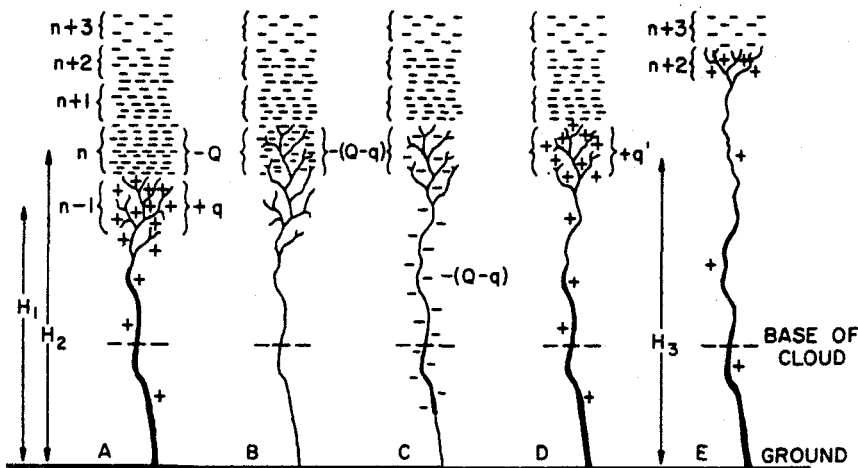


Fig 9 Sequence of events for ground strokes after Maian and Schonland⁽²⁴⁾.

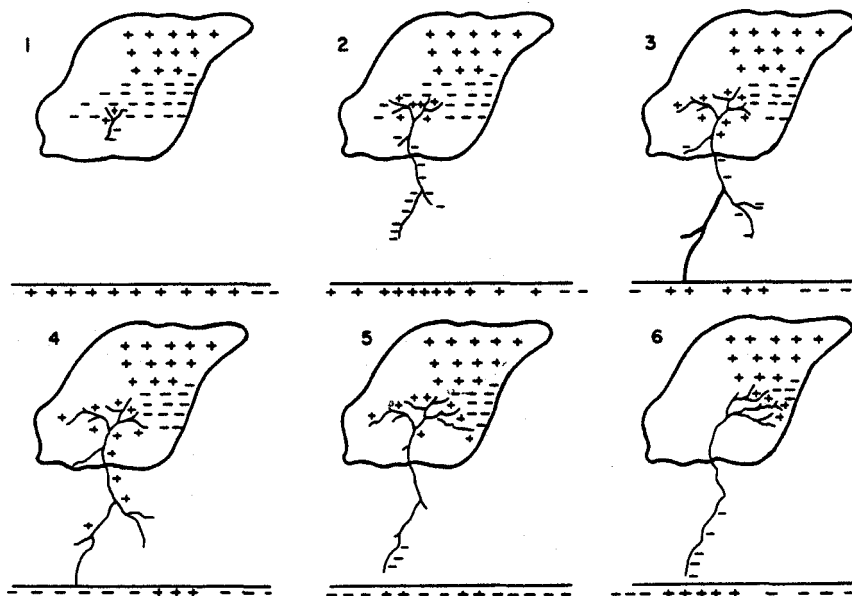


Fig 10 Revised mechanism of a lightning flash to ground after Anderson⁽²¹⁾.

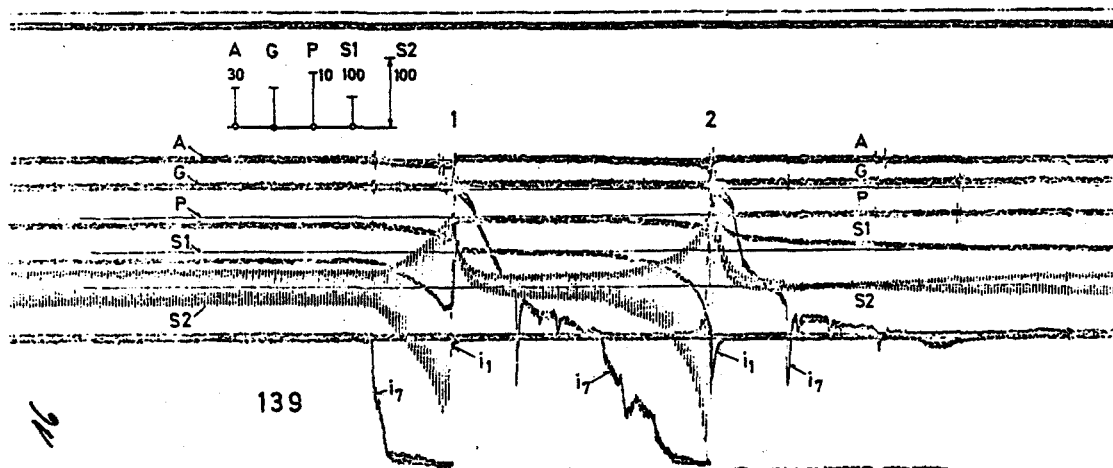
ionisation of the channel and contact with earth could thereby be broken. Some milliseconds would then elapse during which the positive streamers at the top of the channel advanced into a new region of negative cloud charge, first of all neutralising the excess positive ion charge in the channel and then recharging the channel again by lowering more negative charge to the lower extremity till breakdown again occurred at the lower end — this time only over a relatively short de-ionised path. This relatively slow recharging process is graphically supported by field strength records of Berger's⁽²⁶⁾ showing, for example, (see Fig 11) that the field change which occurs prior to successive strokes is of the same duration as for the leader — namely, 20-30 ms and is independent of the extremely fast dart leader which precedes breakdown in subsequent strokes.

Again, according to the above hypothesis, the over-discharge of electrons during the return stroke produced a larger field change relative to that of the leader and was thus able to explain how the charge distribution along

a leader channel need not be uniform as had previously been deduced, and could therefore be linear or even exponential.

The valuable experimental work of Proctor⁽²⁶⁾ has added further information with which to assess the above hypotheses. Of interest to the present discussion, for example, is that all lightning flashes to ground were accompanied by at least one and very often more than one stepped leader which would begin in adjacent regions, thus indicating a multi-origin type of discharge rather than a single discharge, as illustrated in Fig 6.

Secondly, branches in the upper regions of ground flashes fanned out over considerable horizontal distances amounting sometimes to several kilometers and these were not necessarily involved in a discharge to ground in any particular order. This therefore differs from earlier notions of adjacent charge centres being involved in successive strokes or that discharges should necessarily be from centres which were progressively located higher or more distant than the preceding one.



S2 = electric field intensity from fieldmill mounted on San Salvatore Tower
 Calibration of S2 - 100 kV/m shown
 Frequency of S2 - 1 150 Hz approx
Fig II An oscillographic record of a two stroke lightning flash after Berger⁽²⁶⁾.

First streamers, presumably **during** leader development progressed at between $1,0$ and $2,0 \times 10^5 \text{ms}^{-1}$ which was the **same order** as measured by Schonland et al⁽³⁴⁾. He also found that sources of radiation active **during** the last stages or return strokes originated from streamers that progressed at very high speeds of the **order** of $1,4 \times 10^8 \text{ms}^{-1}$ and were faster **than** the streamers active **during** dart leaders which averaged $6,5 \times 10^7 \text{ms}^{-1}$.

This supports the suggestion that a **relatively** large positive charge is induced at the top of the lightning discharge channel towards the end of the return stroke **thus** greatly intensifying the field **strength** and **giving rise** to the faster development of streamers.

The development of dart leaders either **during** the stepped leader process or **during** successive following strokes **appears** not to be associated with the leader **charging process** described but rather with the burst of luminosity in the step dart or in the last breakdown step of a following stroke.

It is pertinent here to mention the **mechanism** which occurs when lightning leaders approach near the earth. First of **all**, there have been many cases photographed where it is apparent that even from flat terrain, **such** as a beach, there is a short upward streamer which **ris**es to **meet** the descending lightning leader. One photograph (Fig 12) reported by Krider⁽³⁷⁾ shows lightning striking uneven ground where **several** short streamers **arise**, of which only one contacted the main leader channel. It is also a common feature of a laboratory long spark between a **negative** rod and positive plane but it **does** not occur with the reverse, ie, when the plane is negative. It **is thus** a fact that a positive tipped streamer **can** easily develop from a plane — more especially, however, if it **contains** rough points or protrusions.

In the case of structures, upward streamers were more likely to **start** sooner from **those having** a high so-called slenderness ratio, ie, the **length** exceeds the **diameter** (see Ref 38 and Fig 13). **Thus**, upward streamers could develop from **trees** or **thin** structures **during** the approach of a leader before a streamer from the nearby earth and it would **then depend** on the relative velocity of the streamer and that of the leader and **its** geometric



Fig 12 Lightning striking ground showing upward streamers after Krider⁽³⁷⁾.

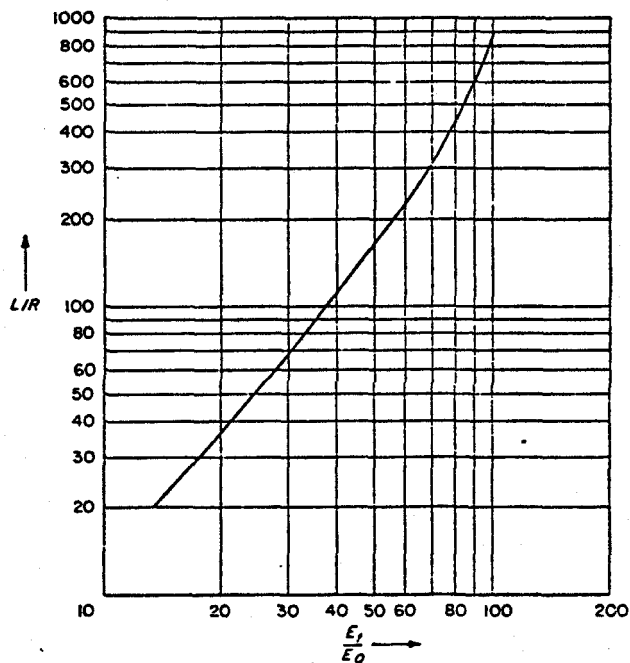


Fig 13 Ratio of the field intensity E_t at the top of a structure to the ambient inducing electric field intensity E_o for given ratios of structure dimension L/R (L = length; R = radius) after Anderson⁽³⁸⁾.

distance and direction whether the upward streamer reached the lightning channel before the latter reached the earth, thereby determining whether the structure was the termination point for the lightning or not.

However, the inimportance of these upward leaders and their effect on strikes to structures has been particularly emphasised by the South African contribution to the science, leading to the proposal that currently accepted electro-geometric models for lightning strikes to transmission towers should be modified.

4 Lightning flash parameters

4.1 Multiple strokes

As the following Table 1 shows, multiple stroke lightning is a common occurrence, especially in Southern Africa, ranging as it does from single stroke flashes to those exceeding 20 strokes.

TABLE 1 Percentage of lightning flashes having the number of strokes indicated

Observer	Number of flashes	% number of flashes having the indicated number of strokes					
		1	2	3	4	5	6 and above
Malan ⁽⁴⁰⁾	530	13	19	18	20	12	18
Anderson ⁽⁴¹⁾	1430	36	16	12	8	7	21
Pierce ⁽⁴²⁾	373	38	27	17	9	4	5
Berger ⁽⁴³⁾	153	65	13	10	3	4	5
Carte ⁽⁴⁴⁾	877	65	14	8	5	2	6
Eriksson ⁽⁴⁵⁾	428	52	20	6	9	5	8
2	9 263	50	30	7	5	3	5

Field change measurements were used to obtain the data by Malan and Anderson in Southern Africa and by Pierce in the UK. Berger, on the other hand, observed lightning stroke currents directly for strokes to the masts on Mt Salvatore in Lugano, Switzerland and indicated a much larger proportion of single stroke flashes — equalled only in Carte's data taken over several seasons in South Africa using slowly rotating cameras to separate out the component strokes.

Eriksson, however, employed two separate techniques at the CSIR. Firstly, he used direct visual observation with a closed circuit television and a video tape recorder which, however, a resolution of better than 20ms between frames could not be obtained. Secondly, a new instrument termed a Multiple Stroke Discriminator was developed with a resolution better than 10 ms, which could accumulate data on multiple strokes over a period, hence the large number of observations.

Reasons why there should be such differences in the observations shown in Table 1 are not readily forthcoming since a physical explanation is needed to explain such a variable number of strokes per flash whilst at the same time allowing the peak current per stroke to vary over a large range, as shown later.

According to the writer's hypothesis⁽³¹⁾, the two factors chiefly influencing the flash are the rate of charge generation, and the rate at which such charges separate physically. The former controls the amount of charge made available in a given time which can give rise to high or low currents per stroke whilst the latter controls the

potential of the cloud and its consequent field gradients. Rapid charge separation therefore results in large areas where breakdown fields can be attained, hence the possibility of a multiplicity of strokes irrespective of the amount of charge available. However, many simultaneous measurements would be required to substantiate such a hypothesis. In addition, there is the question of continuing current observed to follow some components strokes of a flash, most frequently the last. The physical mechanism suggests that the rapid extension of streamers tapping more negative charge toward the end of a return stroke could supply negative charge to the channel in excess of the positive charge generated on the leader, thus preventing it from deionising after contact with the earth — whereupon current will continue to flow till it can no longer be supported by the particular charge centre.

While the numbers of multiple strokes in a flash show some variability as between observers, there is remarkably good agreement with regard to the time intervals between and the total duration of flashes reported by various investigators. Table 3 indicates the distribution of time intervals (found to be closely log-normal) and Table 3 the durations of multiple flashes which appear to have an irregular distribution by comparison.

TABLE 2 Time intervals between strokes of a multiple stroke flash

Observer	Number	Percent having intervals exceeding tabled values		
		95%	50%	5%
Schonland et al ⁽⁴⁶⁾	109	5 ms	35 ms	250 ms
Anderson ⁽⁴¹⁾	3 585	7 ms	35 ms	200 ms
Berger ⁽⁴⁷⁾	133	7 ms	33 ms	150 ms

TABLE 3 Total duration of multiple stroke flashes

Observer	Number	Percent having durations exceeding tabled values		
		95%	50%	5%
Malan ⁽⁴⁰⁾	530	30 ms	200 ms	600 ms
Anderson ⁽⁴¹⁾	1 430	< 10 ms	180 ms	600 ms
Berger ⁽⁴⁷⁾	39	31 ms	180 ms	900 ms

It may thus be concluded that while there may be some factor influencing the proportion of multiple stroke flashes — for example, very severe storms may tend to produce greater numbers — nevertheless, the close agreement, at least on median values of time interval and duration of multiple stroke flashes, suggests that these are governed by some common physical restraint.

However, these parameters are of direct importance to the protection and operation of systems since equipment should be able to withstand the resulting repeated surges and for the periods concerned. Furthermore, high speed switching reclosure of systems can only be undertaken outside the limits of the total duration of flashes and it is also of concern that while a circuit breaker may be opened on the occurrence of the first

stroke of a flash, it is thereafter subjected to open circuit doubling of incoming surges until such time as it can be reclosed.

4.2 Lightning currents

Following on pre-war measurements of the peak magnitude of lightning currents by means of magnetic links by Lewis and Foust⁽⁴⁶⁾ in the USA, Anderson and Jenner⁽⁴³⁾ conducted a similar investigation on a 160 km, 88 kV transmission line in Rhodesia; this took eight years to complete and netted 140 measurements which, however, lacked data below 20 kA owing to the relative insensitivity of the magnetic links used.

Later Berger⁽⁴⁷⁾ accumulated over 160 oscillographic results of currents measured in downward flashes to the 70 m television towers on Mt San Salvatore, Lugano, Switzerland. The lower limit of current magnitude was

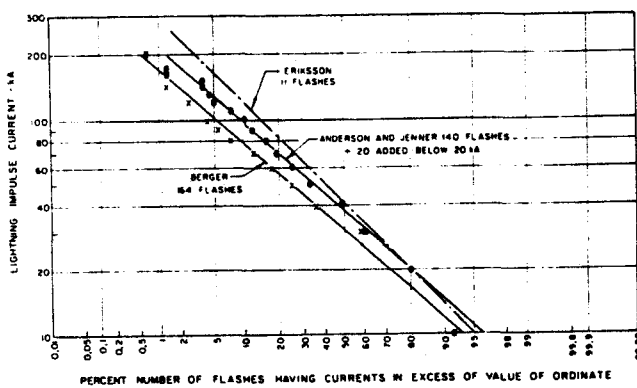


Fig 14 Cumulative frequency distribution of peak values of lightning flash current. Data from Anderson and Jenner⁽⁴³⁾ Berger⁽⁴⁷⁾ and Eriksson⁽⁴⁹⁾.

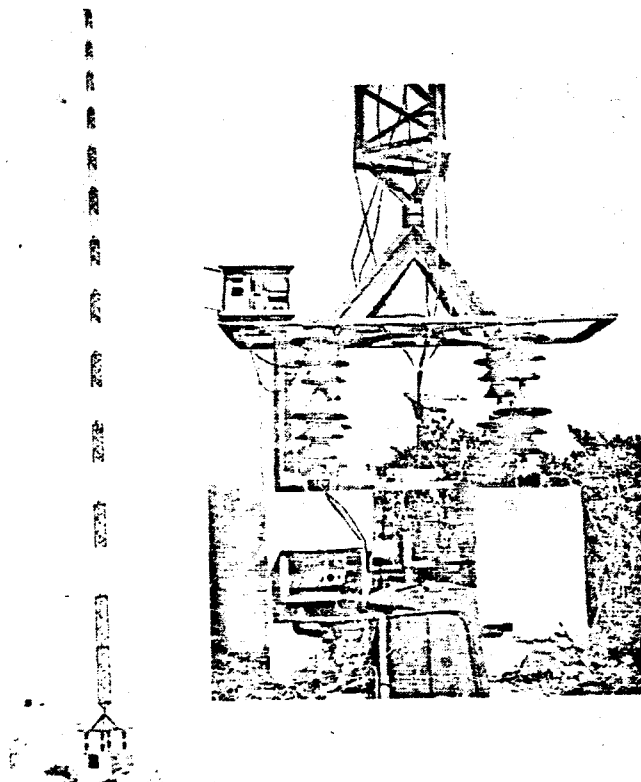


Fig 15 The 60 m insulated research mast at Scientia, Pretoria Eriksson⁽⁴⁹⁾.

1 kA and about 10 per cent were below 20 kA. If this proportion is added to the Rhodesian results they can be compared as shown in Fig 14. This indicated that the median value of peak current from the Rhodesian results was about 40 kA compared with about 30 kA from Berger's data, and this, among other differences referred to above, led to the decision to start making measurements directly in the Republic.

Accordingly, a mast of 60 m height was sited on a relatively low-lying hill at the CSIR, Pretoria, with the intention that this situation should closely simulate natural lightning conditions compared with those, say, on high mountains, which might just influence the type of discharge (see Fig 15).

This mast is unique in that it is completely insulated from the earth and all measuring equipment is situated conveniently at the base and the signals are led in by a short, low impedance connection to totally metal-enclosed instrumentation. It is furthermore equipped with a power supply which is insulated from the mains supply system by using a motor generator set having an insulating shaft. A stand-by generator is automatically switched on should the mains supply system fail.

Oscillograms of the type shown in Fig 16 were obtained by Eriksson⁽⁴⁹⁾ and eleven results were achieved over a period of five years. The distribution, which also has a median value of about 40 kA, is shown for comparison on Fig 14 indicating a trend to higher maximum values than previously recorded by Berger.

In this challenging paper⁽⁴⁸⁾, Eriksson has examined all previous data regarding current measurements to structures of different heights and as a result he questions the validity of a previously accepted hypothesis that an increasing number of higher current values are sustained with increasing height of the towers upon which they are measured. Conversely, according to his analysis of the

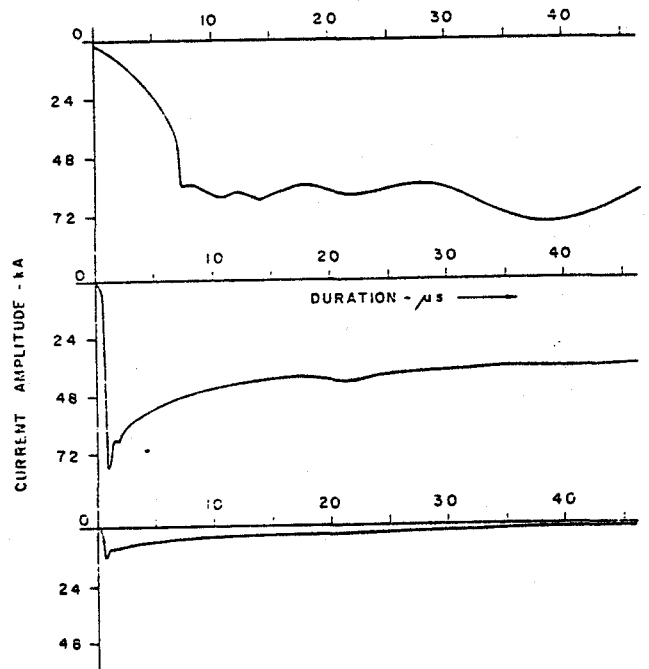


Fig 16 Oscillogram of the current of a multiple stroke lightning flash after Eriksson⁽⁴⁹⁾.

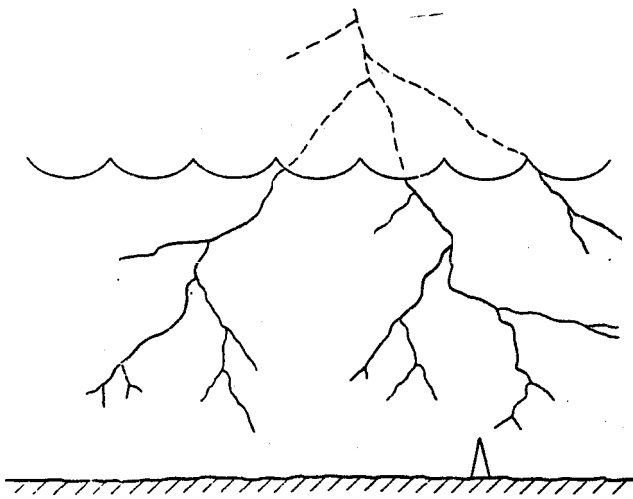
data. he shows that the **median** value of **peak** currents to open **ground** should not be less **than those** measured on **tall** structures; in **fact**, a **median** current of about 40 kA peak should hold, whatever the height of the structure. This value is **higher than** previously accepted values for protective design **purposes** in the literature, where distributions having a **median** value of 30 kA and even below 20 kA have been used, and therefore it has important consequences for transmission line design.

Eriksson's **findings** could be further substantiated if an explanation **could** be found to counter the theoretical basis for the previous hypothesis, and he suggests that this could be derived from the concept of the rather spatial and diffuse distribution of charge in a **macro-system** for the leader with its branches whereas the contact between this system and, **say**, a mast to be struck, **will** be dependent **mainly** on the **effect** of the proximity of the micro-system of a branch leader with its local charge (see Fig 17).

This mechanism could **certainly** give rise to the possibility of a lack of correlation between the striking distance and lightning current to a structure, thereby compromising the accepted concept of an **electro-geometric model** — **since** even **small** striking distances could be associated with large current magnitude if, for **example**, one of the branches of an otherwise heavily branched and charged leader happened to contact a short upward leader from a slender structure. **Subsequently**, Eriksson⁽⁵⁰⁾ secured a video tape recording which illustrates the mechanism very neatly (see Fig 18).

However, if **such** heavily charged branched leader was also proportionately larger in **lateral** dimensions it would make contact with a **tall** structure from a greater distance **than** a lightly charged leader, **thus maintaining** the hypothesis it was hoped could be refuted.

HYPOTHESIZE SPATIALLY DIFFUSE NATURE OF LEADER CHARGE



EVIDENCE

- "COMPLEX" GROUND FLASHES
- INCOMPLETE UPWARD LEADERS
- "ROOT" - BRANCHING

Fig 17 A hypothetical spatially diffused lightning leader after Eriksson^(*).

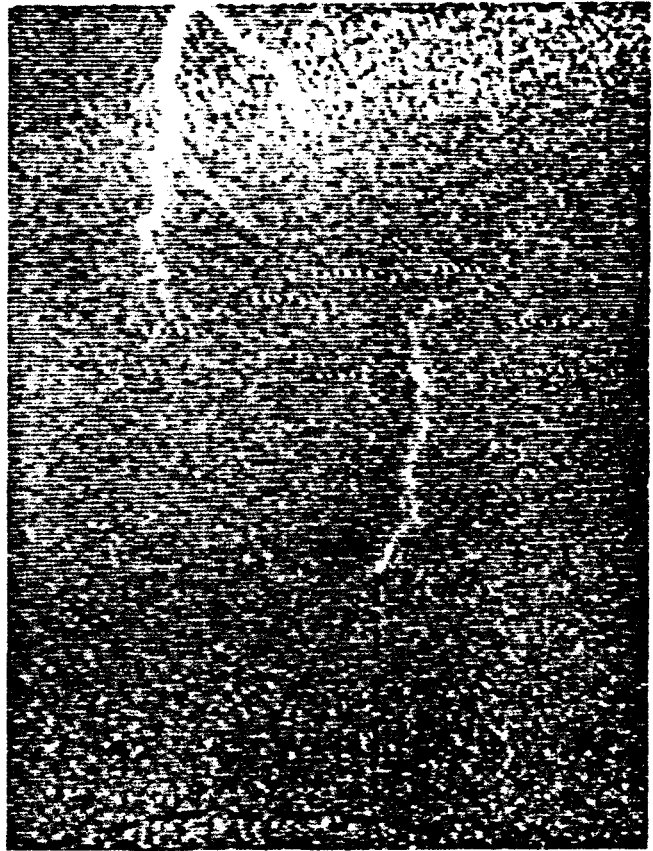


Fig 18 A video tape record of a near lightning discharge to the 60 m research mast after Eriksson⁽⁵⁰⁾.

On the other hand, the writer has **proposed**⁽⁵¹⁾ that if the more heavily charged leaders have also a higher downward velocity relative to the **velocity** of the upward streamer from the structure, **then it** could reach the earth in a proportionately **lesser** time, thereby equalising the probability of either high or low current leaders **making** contact with the structure (see Fig 19).

In an altogether unique experiment the striking distance of **lightning is** being measured by Eriksson⁽⁴⁹⁾ using two video **cameras** sighted on the 60 m mast at Pretoria from two directions approximately at right angles and from the resulting geometric photograph he **can** determine the striking distance and its relationship to current magnitude. To date, three direct measurements were obtained of distance of 90, 150 and 220 m but the corresponding currents were about 20, 85 and 40 kA **respectively, indicating** negligible correlation. Many more results are **obviously** needed, however, to substantiate his proposition.

The height **does**, however, affect the number of flashes to the tower as Eriksson⁽⁴⁹⁾ shows, and the higher the tower the more it tends to **produce** upwards leader to the **extent** that **all** flashes are virtually upward and **downward** flashes are thereby **inhibited**, when the tower is very high. **say** 400 to 500 m.

Berger⁽⁵²⁾ found, for **example**, that about 84 per cent of his records were upward flashes and the **median** current magnitude was only about 250 A. By contrast, the 60 m tower has only sustained about 20 per cent upward flashes see Fig 20).

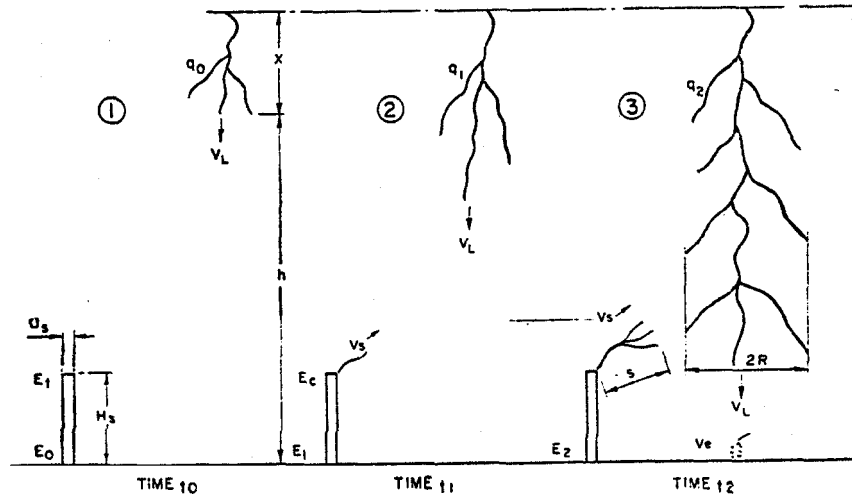


Fig 19 A hypothetical progression of a lightning leader to a tower with upward connecting streamers dependent upon propagation velocities after Anderson⁽²¹⁾.

The reason for this clearly arises from the effect of the tower on the electric field configuration whereby field intensification occurs at the top of the tower which is proportional to the so-called slenderness ratio (see Fig 13). This means that for a given field intensity at ground level due to an overhead thundercloud, the intensification at the top of a structure, depending on its dimensions and shape, will develop a critical field intensity to cause ionisation and breakdown of the air, and a corona discharge will ensue. If this discharge becomes more intense (ie, with an increasing field intensity) an upward leader will be initiated and having once started it would be capable of progressing over very large distances towards the cloud charge and frequently branching to other charge centres to discharge the cloud.

It follows also that such upward discharge could be initiated by a downward progressing leader which traverses only part of its way to earth, sufficiently to start the upward leader to meet it, probably within the cloud. Although the median current values are generally low in upward flashes, high impulse currents have been measured and even multiple strokes occur under these conditions.

However, there is still an unknown factor to be investigated regarding tall structures and that is the effect of space charge on the structure. Malan⁽⁵³⁾, for example, observed that the Strydom tower in Johannesburg was struck seven times in about 30 min when a very light storm cloud appeared above it. If, however, an obviously active and severe storm approached, flashes to ground would cease when about 2 km from the tower and recommence when the storm had passed over. During the intervening period overhead intra-cloud activity appeared to be enhanced. This could mean that excessive generation of space charge above a tower could in fact inhibit flashes to the tower. On the other hand, it has been suggested recently by Golde⁽⁵⁴⁾ that the space charge plumes emanating from a tower may in fact be used as an ionised pathway for lightning flashes to the structure over very large striking distances.

The other important parameter of lightning current

is its impulse shape which until recently has been measured oscillographically only by Berger⁽³⁶⁾. As a consequence of a collaborative effort with the CSIR his records were digitised and recorded on tape with the assistance of Kroninger in one year, and thereafter they were processed, resulting in the publication in an international journal⁽⁴⁷⁾ giving all pertinent results.

These records indicated the characteristic concave

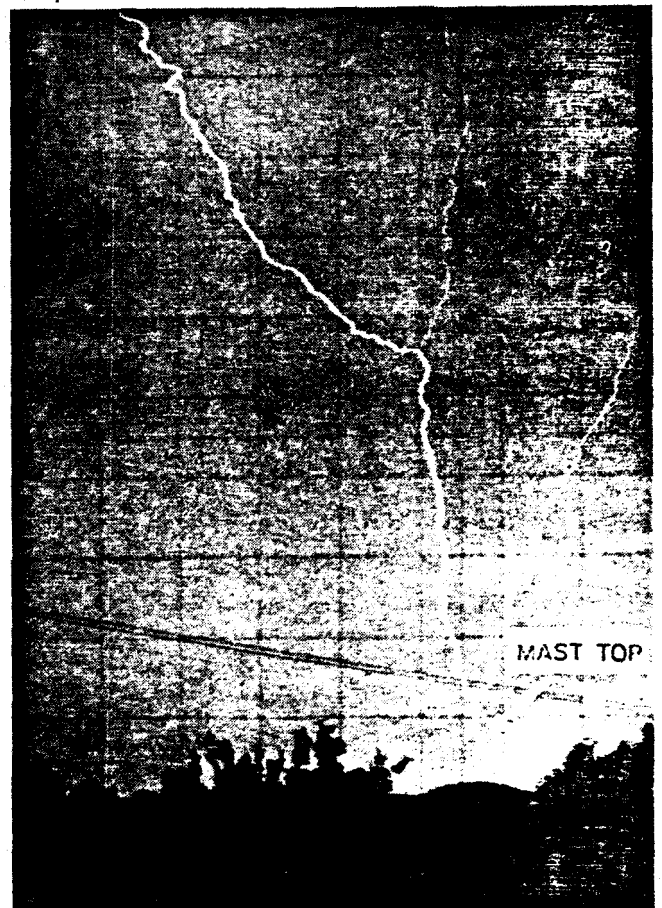


Fig 20 An upward lightning flash from the 60 m research mast in Pretoria after Eriksson⁽⁴⁹⁾.

shape of the front of the impulse for the first component of a flash having on average a **mean** front time of $8 \mu\text{s}$ while following strokes had front times of less than $1 \mu\text{s}$. The record of current, as obtained by Eriksson on the 60 m mast in Pretoria, has a **similar** shape of current (see Fig 16).

It has been thought that the difference between the shape of current impulses of first and subsequent strokes is due to the long upward leader photographed by Berger for the first stroke which was not repeated with following strokes. However, the maximum velocity of upward leaders observed is $1 \times 10^8 \text{ms}^{-1}$ so that the distance moved during a front time of, say, $10 \mu\text{s}$, could not be more than one metre, whereas upward leaders exceed 10 m and could be 100 m in length or more according to Berger⁽⁵²⁾. Hence, it must be supposed that the concave shape of the current is due to the mechanism of discharge of the leader which must therefore differ significantly for subsequent strokes. Furthermore, it appears that the height of a structure may therefore not have any significant effect upon the impulse shape of the current.

4.3 Polarity of lightning flashes

Schonland⁽⁵⁵⁾ originally found that negative lightning flashes, ie, originating from negative cloud charge, outnumbered positive discharges by 17 to 1 and Halliday⁽²⁰⁾ confirmed this; in Rhodesia, Anderson and Jenner⁽¹³⁾ obtained a ratio of 14 to 1 for flashes to a transmission line. Later the writer⁽³¹⁾ using field change data of flashes occurring within a defined range, obtained a figure of about 10 to 1; finally, Eriksson to date has not recorded a single positive flash in a sample of 15 flashes.

Berger *et al*⁽⁴⁷⁾, on the other hand, originally classified 26 measurements as downward positive discharges, against 103 negative, ie, about 4 to 1, but in a recent re-appraisal⁽⁵²⁾ he considers they were in fact upward flashes from his towers. This difficulty of definition arises because positive discharges have very long upward leaders compared to those of negative flashes to his towers. Since positive flashes have been observed by other investigators in Europe, however, the South African data may not be at variance.

It should be noted, however, that those positive discharges listed by Berger *et al*⁽⁴⁷⁾ were single stroke flashes and had extremely high values of charge and in particular 'prospective' energy or $\int i^2 dt$ values compared to negative flashes whereas the peak impulse currents were of the same order. If these flashes therefore were indeed downward, they would be capable of highly destructive and incendiary properties, consequently their occurrence and properties should also be confirmed in the Republic.

5 Lightning flash density

Traditionally, the acknowledged method of designating the thunderstorm and lightning activity of a country was by means of the isokeraunic level—the meteorological definition of which being the number of days per annum during which thunder was heard, namely, thunderstorm days (as illustrated in Fig 1 for the global situation and Fig 21 for South Africa).

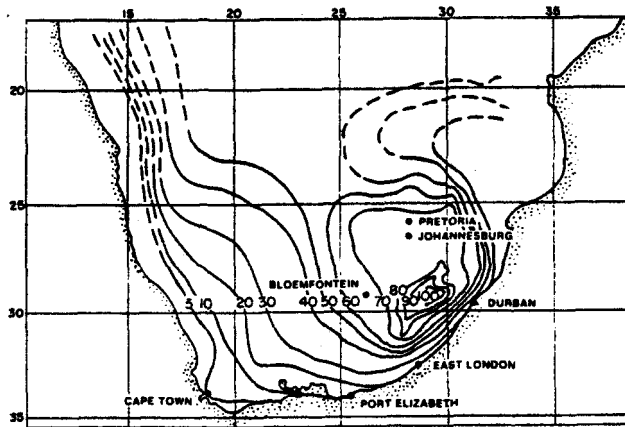


Fig 21 Isokeraunic levels in South Africa (Thunderstorm days).

In recent years, however, increased industrial expansion has led to an exponential increase in exposed transmission and distribution lines, in electrified railways and numbers of aircraft, and in communication circuits of many and various kinds, let alone the number of buildings, explosive factories and stores, some with attendant explosion hazards. Then, too, there have been corresponding population increases with greater risk of lightning fatalities out of doors. This, in turn, posed increased lightning problems in many countries; for example, Golde⁽⁶⁶⁾ reports that in a ten-year period over 8 000 power circuit interruptions per annum occurred in the UK with consequent disruption of industry. It was clear that a more exact measure of lightning conditions was needed in order that the probability of any piece of equipment, building or area being struck could be accurately determined; in this way rational protective measures could be undertaken according to the risk of damage; even the correct design of protective equipment itself was dependent upon the number of times it was expected to operate. Thus lightning activity had to be determined numerically, the unit chosen being its density — ie. the number of flashes occurring to ground per unit area, or in the clouds as well in order that aircraft flight safety could be considered.

Many instruments for counting lightning have accordingly been devised over the years. one of the earliest, in fact, being by Gane and Schonland⁽⁵⁷⁾ which they called the 'ceranometer' and which by counting low amplitude negative field changes (intra-cloud flashes) and high amplitude positive field changes (cloud to ground flashes) could with certain assumptions as to the range, derive values for these respective densities (hereinafter referred to as cloud or ground flash density).

Malan⁽⁵⁸⁾⁽⁵⁹⁾ also devised and tested a counter which was reported to differentiate between cloud and ground flashes by means of the radiation frequency from the two types — ground flashes emitted large amplitude radiation at 3-5 kHz which was about ten times the amplitude of 100 kHz radiation. Cloud flashes, on the other hand, radiated about an equal amplitude at these frequencies. Unfortunately, it was found that whilst these ratios of amplitudes at the frequencies were in general true over a continuous quanta of data, they did not in fact apply to individual flashes, and the project was discontinued.

Regarding overseas developments, Horner⁽⁶⁰⁾ proposed and used a certain counter to measure the total radio-frequency radiation from lightning in the global context without regard as to the type or range however. On the other hand, for measuring flash density, another counter proposed by Pierce and modified by Golde⁽⁶¹⁾ for measuring flash density was used extensively in Europe and in the then Central African Federation and a few were installed by ESCOM in the Republic. This was the forerunner of the transistorised version devised in Queensland by Barham⁽⁶²⁾ and finally adopted as the standard counter for CIGRÉ (International Conference on Large High Tension Electric Systems). (See Prentice⁽⁶³⁾).

It was in 1963 that a CIGRÉ task force was inaugurated with Dr Golde as Convenor, to foster the development and use of lightning flash counters internationally and the convenorship passed to the writer in 1970. Active research into lightning flash counters had begun at the CSIR five years previously in a project then known as the 'Hail-Lightning' project involving both the National Institute of Electrical Engineering (NEERI) and the National Physical Research Laboratory (NPRL). Serious difficulties had been encountered in attempts to differentiate between cloud and ground flashes and the CIGRÉ counter was no exception. This was probably inevitable since the counter had its maximum response centred on 500 Hz for electrostatic field changes, and many cloud flashes exhibited such slow field changes.

The characteristics of the CIGRÉ counters had to be experimentally determined — i.e., their response to and effective range for cloud and ground flashes. This was done by setting up a field calibration test ground consisting of a minimum of three recording stations (Fig 22) equipped with all-sky cameras (designed by the NPRL) for direction finding and identification of flashes.

In this way, data regarding the operational probability of the counter at each range could be accumulated separately for cloud and ground flashes and from which the effective ranges could be determined (see Fig 23).

Following the work by Malan⁽⁶⁶⁾ and others on the frequency spectra of lightning, counters responsive to 5 kHz and 10 kHz were constructed at the CSIR and tested in the same way. It was very soon discovered that these counters, especially the 10 kHz, were more discriminating against cloud flashes than the CIGRÉ counter. The initial result with the 10 kHz counter, named the RSA 10, was reported in the literature immediately) see Anderson⁽⁶⁴⁾ et al) but it took a few more years before substantial evidence regarding its full performance was available and from which it could be confirmed that 95 per cent of the counter's registration was due to ground flashes. Its corresponding probability functions are shown in Fig 24).

A further counter, named the RSA 5 was constructed using a standard CIGRÉ 500 Hz counter directly with a vertical aerial without changing the counter sensitivity. This turned out quite fortuitously and for no accountable reason to be much more responsive to cloud flashes than the CIGRÉ counter itself, and it can therefore, in conjunction with the RSA 10, be used to gauge the cloud flash density approximately.

The results of 10 years of research into counters is



Fig 22 Typical radio controlled lightning recording station showing all-sky camera on hut and RSA 10 lightning flash counter under test in foreground.

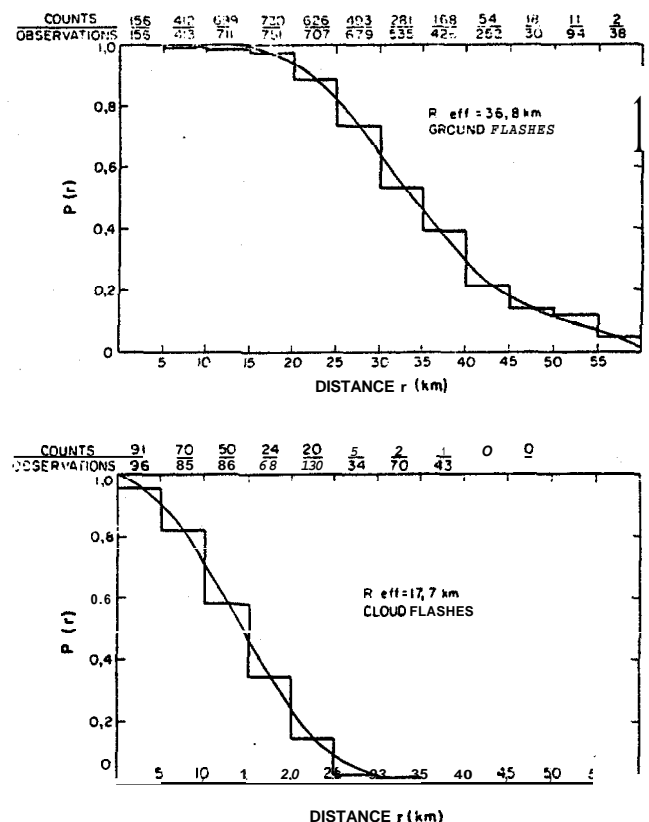


Fig 23 Probability functions for the CIGRÉ 500 Hz counter on ground and intra-cloud flashes respectively.

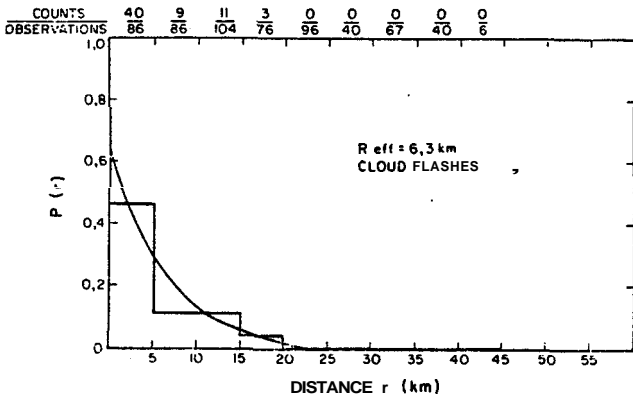
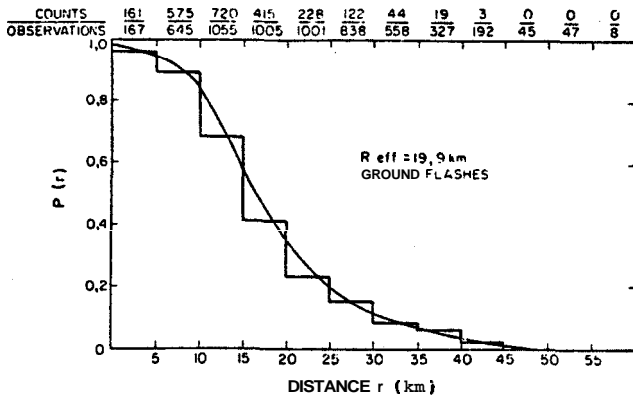


Fig 24 Probability functions for the RSA 10 counter on ground and inter-cloud flashes showing good discrimination against the latter.

given in the latest CSIR report⁽⁶⁵⁾ and pertinent characteristics are shown in Table 4.

The RSA 10 counter has since been approved⁽⁶⁶⁾ by the CIGRÉ Study Committee No 33 (Overvoltages and Insulation Co-ordination) as a counter (to be known as the CIGRÉ 10 kHz counter) for calibrating existing counters and also for use on its own in high lightning density situations provided some CIGRÉ 500 Hz counters are also used to maintain a correspondence with registrations reported from other countries using them.

The 10 kHz counter is currently being tested in a number of countries in Europe and the Far East and also in South America and about 20 of them are being evaluated in the USA.

More than three years ago it was decided to start a national programme for the measurement of ground flash density in the Republic and South West Africa, and

TABLE 4 Pertinent characteristics of three lightning flash counters

Parameters	Units	CIGRE	RSA 10	RSA 5
Response frequencies 3 db limits	lower		2	0.1
	centre	0.5	10	0.5
	upper	25	50	2.5
Effective ranges	ground flashes	36.8	19.9	15.7
	cloud flashes	16.7	6.9	7.6
*Correction factor Y_g	—	0.82	0.95	0.63

* Y_g is the proportion of total registration of counters which are ground flashes. The value for the RSA 10 counter was observed while the values for the CIGRÉ and RSA 5 counters were deduced from comparative measurements.

through the co-operation of major organisations including ESCOM and the General Post Office (GPO), the South African Railways and Harbours (SAR & H), the South African Broadcasting Corporation (SABC), and the CSIR, about 400 counters have been distributed and are being read mostly daily by these organisations with additional help from National Parks Boards, the Water Affairs Department, municipalities and private individuals.

A special computer programme was devised by Kroninger⁽⁶⁷⁾ in order that the results can be processed monthly at the CSIR and a map of flash density incorporating three years' data is shown in Fig 25. This shows a variation from less than 1 flash/km² on the western coast of South Africa, to over 10 in the eastern highveld area between the Transvaal and Natal, thus indicating a shift of the maximum activity from that shown on the thunderstorm-day map of Fig 21.

As a consequence of the results and observations carried out under the national programme, Eriksson⁽⁶⁰⁾ derived an approximate relationship between thunderstorm days and ground flash density N_g as follows:

$$N_g = 0,023 T_d^{(1,3)}$$

The variance is, however, considerable, as shown in Fig 26 and thus indicates the necessity to measure the ground flash density directly. It has furthermore been established that at least 5 per cent must be added to the flash densities measured to account for multiple terminations of lightning, ie, either so-called root branching or more than one simultaneous lightning flash to ground.

Apart from measuring the mean annual ground flash density, variations of the annual and monthly registrations can of course be undertaken and in the case of

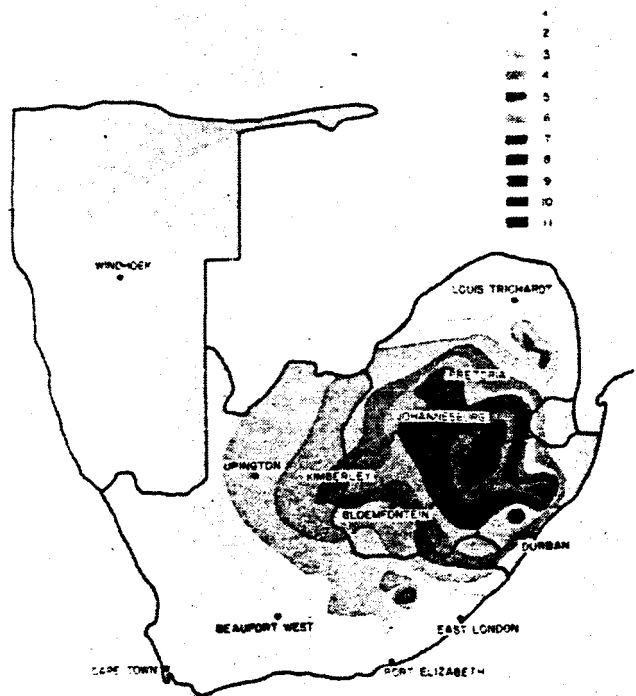


Fig 25 Mean lightning flash density for Southern Africa during the three year period July 1975 to June 1979.

Pretoria the **results** of individual months and years of accumulated data are shown in Figs 27 and 28 respectively **taken** from Ref⁽⁶⁵⁾.

This indicates the **very large variability** which **occurs**

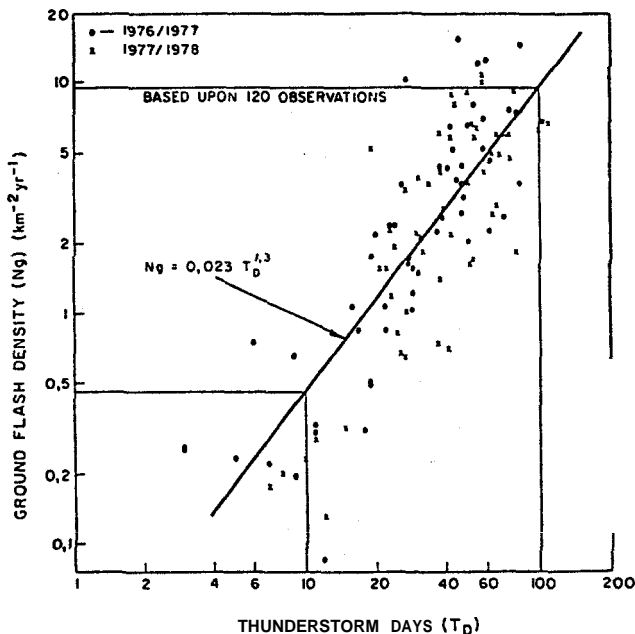


Fig 26 Correlation between the isokeraunic level (T_D) and the ground fluh density (N_g) after Eriksson⁽⁶⁴⁾.

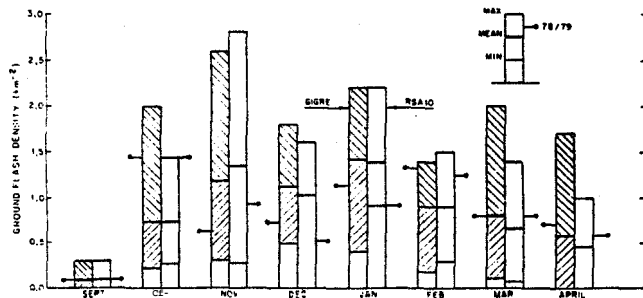


Fig 27 Monthly ground fluh density listed for Silverton, Pretoria determined from 11 years data from CIGRE counters and seven years data from RSA 10 counters after Anderson et al⁽⁶⁴⁾.

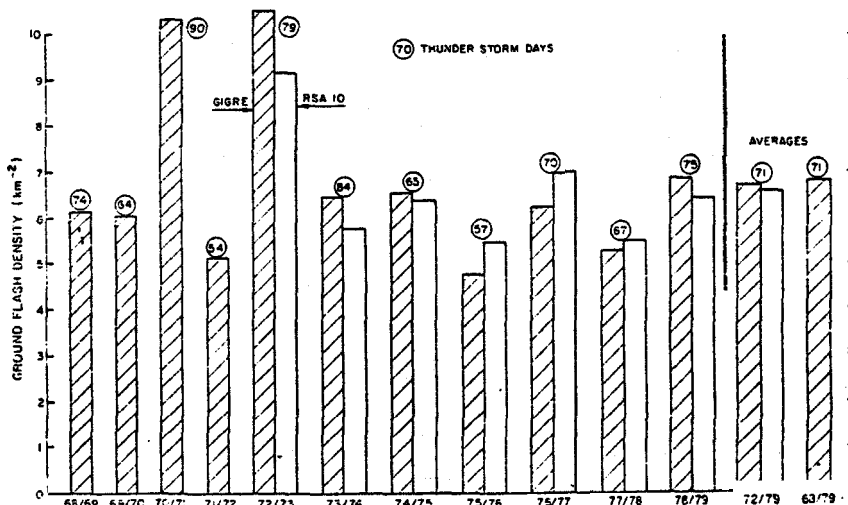


Fig 28 Annual ground flash density for Silverton, Pratorir from CIGRE and RSA 10 flash counter data after Anderson et al⁽⁶⁴⁾.

in the lightning density in any particular **month**, but strangely enough the accumulated data show that the lightning density has been within +10 per cent and -20 per cent of the **mean** value for eight years if two bumper years are excluded. In **these** bumper years, namely 1970/71 and 1972/73, lightning was as **much** as 80 per cent in **excess** of the **mean** for the other eight years, indicating perhaps support for some **unusual** instability **occurring** such as, for **example**, sun spot activity, as surmised by Eriksson⁽⁶⁸⁾.

Lightning flash **counters** have **also** been employed to measure some specific thunderstorm parameters. **such** as starting and finishing times, and **duration** of thunderstorms, shown by Eriksson⁽⁶⁹⁾ and depicted in Fig 29, indicating, for **example**, the predominance of afternoon thunderstorms in the Transvaal, with a most frequent starting **time** at about 15h00 and a **duration** of about 2 h. **That** thunderstorm conditions may **differ** on the **Natal coast**, however, is shown by referring to Fig 30.

In addition, the **mean** number of flashes per thunderstorm and the maximum flashing rates **can** be **determined** given a standardised counter and **such** data computed in **order** to compare thunderstorms from **season** to **season** and between different climatic **areas**.

In fact, this **theme** was **taken** up in a global **sense** by the **author** with Eriksson⁽⁷⁰⁾ which ultimately resulted in the formation by the International Commission on Atmospheric Electricity of an ad hoc **working group** on the Measurement of Comparative Lightning Parameters **under** their guidance.

6 Lightning protection

6.1 Lightning protection of electric power transmission and distribution systems

The question of safeguarding electric power supply from **damage** or interruption has undoubtedly been the **concern** of **electricity** supply **authorities** from the **erection** of the **first** power lines in South Africa — believed to have been before 1900, and it is **surely** remarkable that so **much** was achieved with so little knowledge of the phenomenon which was being dealt with.

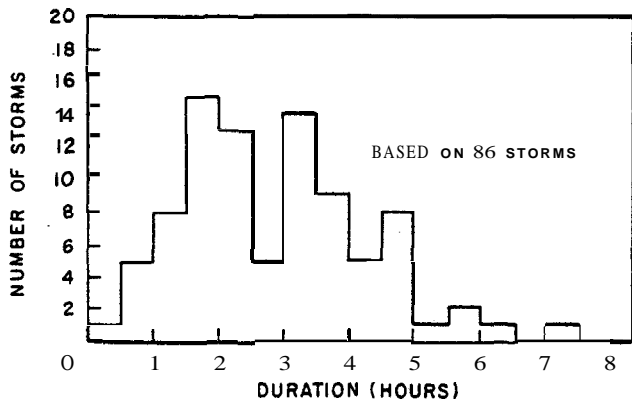
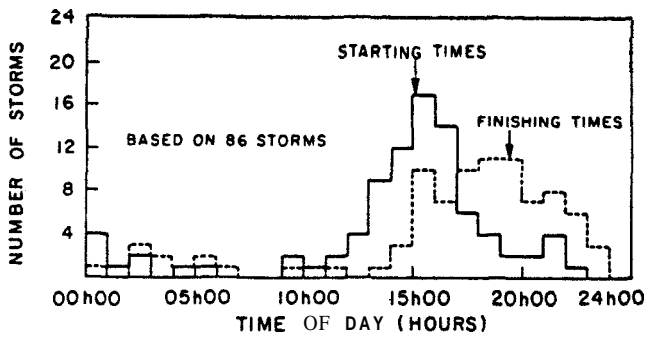
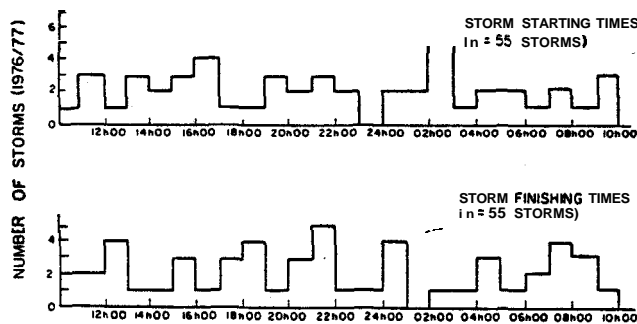
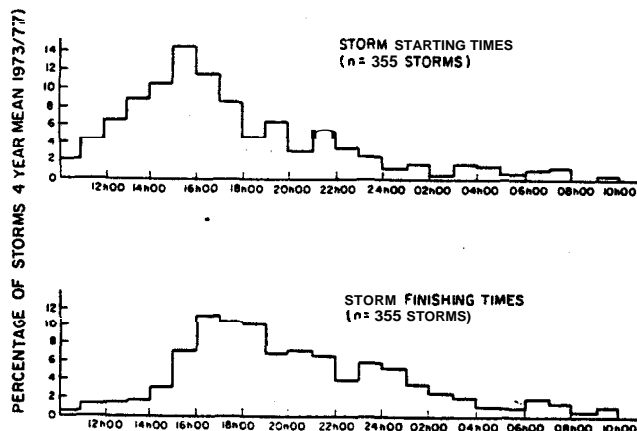


Fig 29 The time characteristics of thunderstorms in the Pretoria area during the 1977/78 season after Eriksson⁽¹²⁾.



(a) STORMS IN THE DURBAN AREA



(b) STORMS IN THE PRETORIA AREA

Fig 30 Variation of time characteristics of storms in Pretoria Transvaal compared with Durban Natal after Eriksson⁽¹²⁾.

For example, Adendorff⁽¹⁾, nearly 70 years ago, recommended the use of lightning conductors on each pole, especially if of wood, a well earthed overhead ground wire, horn and multigap arresters to limit the overvoltage, and earthing the neutral of transformers — hardly much different, in principle at least, from present day practice.

That the use of overhead ground wires was continued and that low earth resistance for towers was beneficial was acknowledged 22 years later by Rendell and Gaff⁽¹⁰⁾ in 1933 describing the lightning performance of the 132 kV system of the VFP over a 7-year period.

It is of interest also that they discovered a section of line which was apparently fault free over the 7-year period which could not, however, be attributed to low tower footing resistance. Anderson and Jenner reported also in a paper⁽¹³⁾ more than 20 years later, that several sections of 88 kV line in Rhodesia were not struck by lightning even once in eight years. In both cases storm paths were suggested as a possible cause but the effect of geological formations was discounted. However, at that time Golde suggested that the phenomenon was explicable in terms of Poisson's distribution assuming that lightning was distributed along the line entirely at random and this was not to be tested until much later when in a paper on the occasion of the diamond jubilee of the South African Institute of Electrical Engineers in 1969, Golde⁽¹⁴⁾ again drew attention to this question and quoted an example which is repeated in Table 5 which follows alongside the Rhodesian data given by the writer in his Vote of Thanks.

This intriguing probability distribution has since been demonstrated many times and is especially applicable to lightning protection problems so that it is pertinent here to repeat the basic Poisson statement, namely that the probability that an area A will sustain exactly 0, 1, 2, 3... n flashes in T years with an annual ground flash density of N_g is given by the expression

$$P_n = \frac{Z^n}{n!} \exp(-Z)$$

$$\text{where } Z = ATN_g$$

TABLE 5 Eight years of data on the frequency of lightning strikes to transmission towers

Number of times struck	Number of towers affected			
	210 kV line		kV lin.	
	Observed	Calculated	Observed	Calculated
Nor struck at all				172
Once only	163			137
Twice	106			55
Three times	71			15
Four times	15			3
Five times	5			0
Six times	2			0
Seven times	0	0	0	0
Total number of towers	477	477	382	382
Total number of strikes to towers	685		305	
Average strikes/tower	1		0,80	

In order to apply the above expression to a transmission line, however, it is first of all necessary to be able to estimate the number of lightning flashes which will make contact with the line given its prime dimensions and for this, knowledge of the striking distance (or equivalent attractive range) of lightning, is required.

Eriksson⁽⁵⁰⁾ has derived the following expression for the attractive radius obtained from data on lightning strikes to tall structures:

$$R_a = 16,3 H_e^{0,61} m$$

In this equation H_e is the effective height of a structure which in the case of a transmission line is the mean height of the earth wires or conductors above ground.

At a value of H_e of for instance 20 m, R_a is five times the effective height of the line but it is more if the effective height is less than 20 m.

On a purely geometric basis it would be expected that the attractive range of a structure would not exceed that of its own height so that the large increase observed could only be the result of upward leaders which effectively enlarge the collection area.

It is presumed that transmission lines will behave in a similar fashion to that of isolated structures as indeed other empirically derived expressions are seen to suggest, but it is clear that more field data are required in order to confirm these assumptions.

This is one of the objectives of a project being carried out by the CSIR in collaboration with ESCOM on the Cabora Bassa HVDC line; here cameras are arranged to photograph lightning strokes to or near the line (see Fig 31) whilst at the same time the voltage surges on the line are measured.

The voltage measurement technique employed, highlights yet another achievement in the use of a loose capacitance coupling to measure the voltage on the power system conductors by means of the voltage induced in a short parallel rod mounted on a caravan directly under the line as shown in Fig 32 and preliminary results have been reported⁽⁷¹⁾. The method was first developed at Apollo⁽⁷²⁾ on ESCOM's 400 kV system and is particularly suited to ad hoc measurements on the system without disruption of the supply. An oscillogram of surges on the three conductors of the 400 kV line is shown in Fig 33,

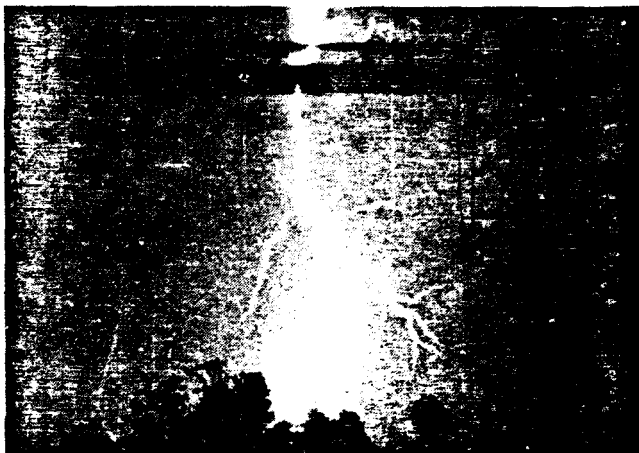


Fig 31 Lightning flash close to the Cabora Bassa HVDC line.

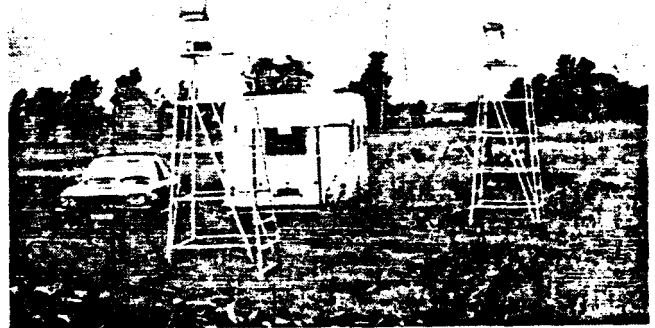


Fig 32 Surge recording station beneath the Cabora Bassa HVDC lin* (See voltage antenna on caravan roof and two cameras on stands).

and illustrates the possibility of a lightning stroke which penetrated between the two overhead earth wires which are 10 m apart and which may have resulted from an upward leader developing from this conductor during the approach of a lightning leader (see Eriksson⁽⁷³⁾).

The effects of lightning on extra-high-voltage systems are important and require to be studied in detail in order that these systems may be designed to operate in lightning areas with minimal interruption. In fact the 400 kV system in South Africa has an extremely good record. On the other hand at lower voltages the position begins to deteriorate as shown in Table 6.

Because of the necessity to keep the costs of low voltage distribution lines to a minimum, they are insulated only sufficiently to ensure satisfactory per-

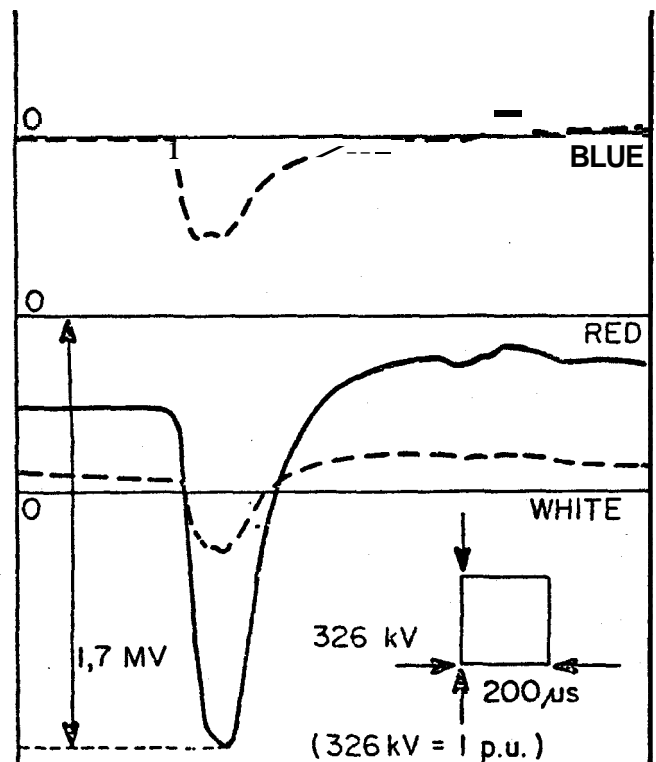


Fig 33 Record of oscillogram of a lightning surge on the 400 kV system at the ESCOM Apollo distribution station near Pretoria.

TABLE 6 Storm outage rates on the Rand Undertaking Electricity Supply System over period 1960/65

System voltage kV	Storm faults per 100 km/annum
11 to 22	20,3
42	21,9
98	11,9
132	8,0
275	1,9
*400	0,6

*400 kV performance during first year of operation 1975/76

formance at the normal operating voltage — say 11 kV — and the margin available for lightning overvoltages normally around 90 kV is thus insufficient to prevent flashover in the event of a direct stroke to the line. Even voltage induced by a nearby lightning strike is capable of overstressing the insulation or destroying the protective surge arresters.

In order to study the problem in detail a joint CSIR-ESCOM project was recently inaugurated which comprised the erection of a 10 km length of 11 kV distribution of standard construction some 30 km east of Pretoria.

The experiment is unique in that the line has been erected purely for research purposes and ESCOM and the CSIR have installed automatic recording stations on it for the purpose of measuring the overvoltages without the encumbrance of transformers and surge arresters on the line (see Figs 34 and 35). This will enable the basic effects of lightning to be determined first of all without

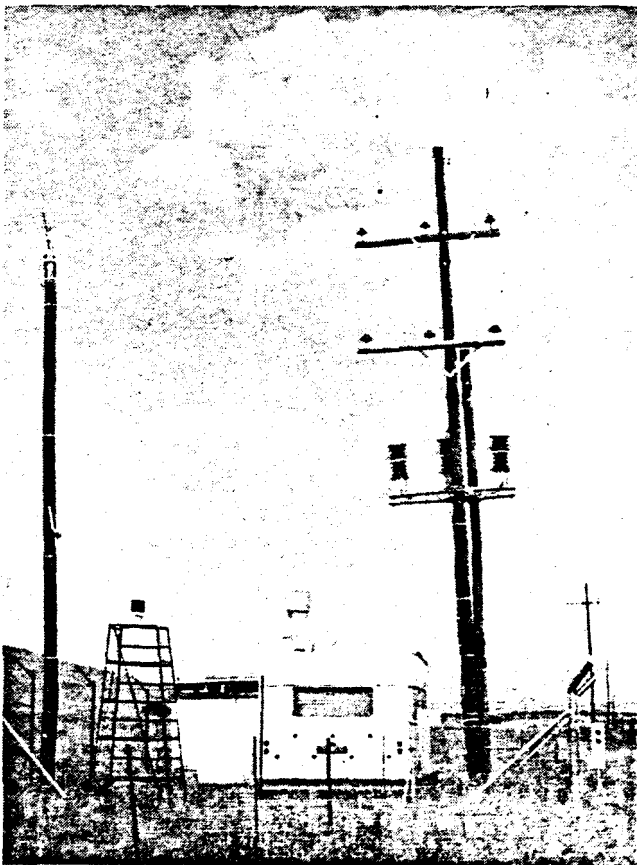


Fig 34 CSIR automatic surge recording station on 11 kV test line near Pretoria.

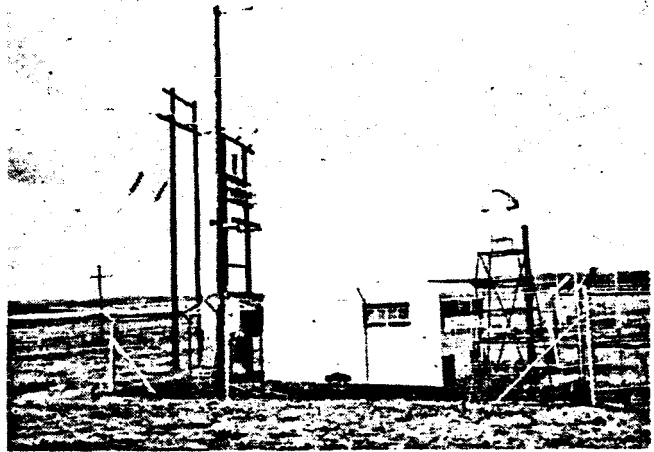


Fig 35 ESCOM automatic surge recording station at extremity of 11 kV test line near Pretoria.

an overhead earth wire, but later this will be added together with other equipment so that the effect of each stage can be carefully monitored.

The final objective is of course the optimisation of protective measures for these systems based on a more exact knowledge of the lightning parameters and consequent overvoltages induced to provide an improved service to rural consumers than formerly, commensurate with the economics of the supply.

One final aspect about 11 kV distribution is the high failure rate of distribution type surge arresters being experienced by electricity supply authorities operating in high lightning areas. According to type, between 2 per cent and 6 per cent per annum of the total number of installed arresters are being damaged and this is of serious concern in view of the high labour cost of replacement. Thus the whole situation is being re-examined and measurements undertaken by ESCOM and the CSIR on substations in service and also on the research test line referred to earlier. Furthermore, the SABS is examining the effect of multiple-stroke lightning which is believed to be one of the contributory causes to the high failure rates being experienced.

These and other problems of lightning research are being handled by a Task Force of the Lightning Working Group of the High Voltage Co-ordinating Committee under the auspices of the CSIR. This Task Force also collaborates with a sub-committee of the IEEE in the USA which is conducting a similar investigation in Florida and, incidentally, where ten RSA 10 lightning flash counters are also being evaluated.

Thus, despite the fact that some of the principles of lightning protection have been known for many years, a more detailed knowledge of lightning parameters is required for their application, due regard being paid to the economics of so doing, particularly in the case of low voltage lines where the cost to rural consumers is already a critical consideration.

6.2 Protection of communication systems

In the years following the 1930s the South African Posts and Telegraphs Engineering Department experienced tremendous expansion of its open wire

transmission system and as a consequence there was a considerable increase in exposure of the system to lightning. Being essentially very low voltage, the system was perhaps even more vulnerable to damage compared to electric power systems and presented a correspondingly more serious problem. This was tackled by an energetic group in the GPO Engineering Department headed by C F Boyce and by 1955 the basic problems had been isolated and reasonable solutions secured after considerable research and testing. Their results and recommendations were reported in the now classic monograph (Boyce *et al*)⁽⁷⁴⁾.

Later inter-city communication using multi-channel cable has developed and it was found that lightning could in fact still damage these cables. This was finally overcome by shielding the cable by means of parallel buried conductors or by enclosing the cable in a metallic duct.

Later came microwave transmission which whilst overcoming the line and cable problems, the exposure of the towers on high mountains to lightning still had to be contended with. This was coupled with the changeover from robust radio valve equipment to the use of much more complicated and delicate micro-circuits and latterly semi-conductor equipment which, because of its miniature size, is particularly vulnerable to even small overvoltages (or 'spikes' as they have been popularly called). Present day practice for the protection of telecommunication systems has recently been reviewed in detail by Boyce⁽⁷⁵⁾.

This protection practice has been extended to the field of computers particularly where these are serving numerous terminals situated some distance from the main computer. Special precautions are necessary to prevent spikes from entering and damaging the computer itself — usually by means of some form of isolation from external circuits, proper earthing and internal component protection, where necessary.

The introduction of television also introduced new problems — firstly with transmission towers on hilltops where fortunately experience had been gained on the existing microwave communication system and the radio broadcasting system. However, some unsolved problems still remain over the question of power supplies to these elevated towers where good earthing was not easily obtained due to the rocky nature in most situations.

Much has still to be learnt about the behaviour of such earths under lightning impulse conditions in order to obtain results and also improvements in the method of protecting the incoming electric power or communication lines from damage.

Secondly, the installation of domestic TV introduced further exposure to lightning through the TV aerial as well as the connection of a somewhat vulnerable and expensive receiver to a mains power supply which may in itself also be exposed to lightning spikes.

In general, the principles of lightning protection of radio, TV and communication systems are well established and are being steadily applied in these cases, but much has still to be learnt regarding more effective protective devices, screening practices, materials and earthing to optimise protection in the face of an ever

changing technology — and again a detailed knowledge of lightning parameters in the particular situation is necessary.

The possibility of either the TV aerial or the consumer-premises or mains power supply being struck by lightning is another issue and the question of the risk involved is discussed in the next section.

6.3 Lightning protection of buildings

As in most countries, South Africa has its Code of Practice for the lightning protection of buildings produced under the auspices of the South African Bureau of Standards⁽⁷⁶⁾. This is presently under revision since the last issue in 1951, and has undergone some change in view of the latest research findings. There are, however, one or two areas of uncertainty even now regarding the application of the Code.

The first and paramount is the question of the number of lightning strikes to be expected to a building or structure in a given lightning area and secondly, the degree to which protective measures should be applied.

Knowledge of the lightning ground flash density in terms of the number of flashes per km² per annum certainly provides a means to determine the average frequency of strokes to a particular building having a given area, over a long period — with certain assumptions to allow for additional strikes from fringe areas as a consequence of side flashes (ie, striking distance). Unfortunately, because the numbers are (statistically speaking) so small, it is necessary to assume a random distribution of the number of flashes over a period of years to a large number of equal small areas and to calculate the probability that such small areas will in fact be struck at least once in that period from Poisson's distribution namely that

$$P_1 = (1 - e^{-z}) \text{ where the } Z = N_g AT$$

where P₁ is the probability that the area A will be struck at least once in a period T years with an annual ground flash density N_g.

Fig 36 shows the result of such a calculation for areas varying between 100 and 10 000 m² and for periods from 10 to 30 years and illustrates that even under the highest lightning conditions attainable in the Republic — say 12 flashes per km² per annum, the number of areas struck at least once is less than four out of 100 when the area is less than 100 m² and less than 30 per 100 for an area of even 1 000 m². The lightning frequency only becomes significant when the area is of the size of a hectare or more. Fig 37 extends this calculation so that a more exact estimate of the risk can be made for any area up to 1 000 m² over 30 years, but of course any other figure can be calculated from the general expression given above.

The second point to decide is what the consequence of such a strike or strikes might be — and herein lies the key to the question of how much protection should be provided in a given situation.

In the case of a domestic house of some 100 m² in area, the probability of a strike is less than 1 out of 25 houses in 30 years even under the worst lightning conditions, so that unless the consequences could be

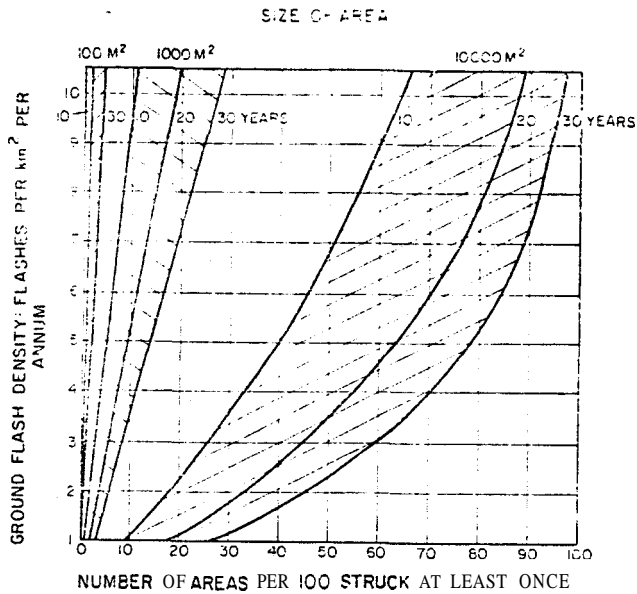


Fig 36 Probability of at least one lightning strike to various areas over ten to thirty years.

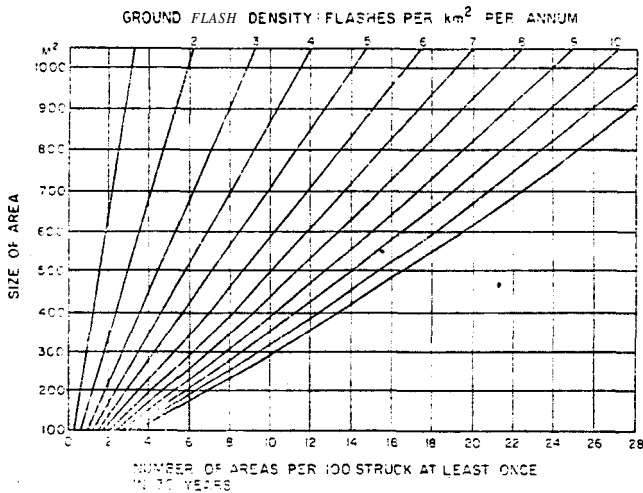


Fig 37 Probability of at least one lightning strike to small areas over 30 years.

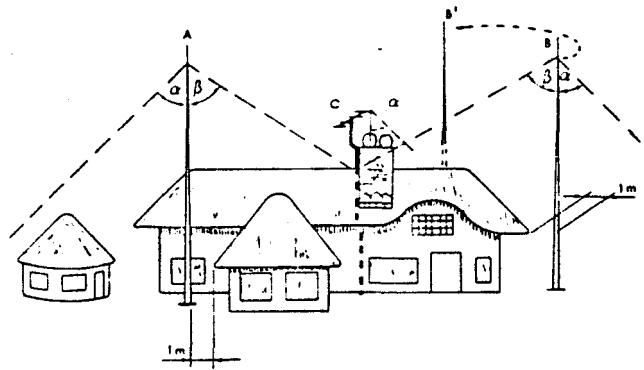


Fig 38 One method of the lightning protection of a dwelling house showing protective cones from SABS Code 03A 1975.

and this rule has served well over the past 30 years. This is probably because of the fact that upward leaders inevitably start from the protective mast or catenary during the approach of a flash of a lightning leader and make contact with it before it can strike ground anywhere within the distance from the mast or catenary at least equal to its height.

In the case of larger non-metallic buildings, protection by means of roof conductors laid at specified intervals across the roof area together with down conductors connected to a good earth was and still is accepted good practice: however, where such buildings are constructed of reinforced concrete, the use of the reinforcing to carry the lightning currents down the building is now considered permissible. It is still important to provide a top conducting system to connect with the reinforcing which can receive lightning hits without damage, and the provision of short finials is now recommended in addition, to facilitate the initiation of upward leaders from this system, i.e., they assist to determine where the strike points should occur.

Houses with metallic roofing are perfectly safe providing the roofing is well earthed. In a particular case a school building was erected without an electrical installation in which case there was no provision in the building regulations for earthing the metallic roof provided. The tragic consequence of this was that when lightning struck the roof and discharged down an internal wall of a class room, six school children were killed instantly.

The use of so-called radioactive lightning conductors is not at all effective because the rate of ion production from the isotope source is many orders of magnitude less than would be produced by the ordinary lightning rod or finial on the approach of a lightning leader, and the ionisation effect is correspondingly extremely limited. In this event, the protective area of 100 m radius claimed for such a device can almost certainly be expected to be violated at least once by lightning within 10 years if the lightning flash density exceeds 10 km⁻², according to the above referred to probability calculations. If the flash density is less than 1 km⁻² however, a period of more than 100 years would be required to attain the same certainty of a strike.

Lightning protection by means of barbed wire catenaries or cages having many sharp points for promoting

serious, no protection would seem to be necessary. Modern houses with their array of metallic water pipes, conduits and electric power cable etc in the ceiling areas provide a good protection for the inmates, but damage to masonry on the chimney and gable ends has occurred and these could be very simply and cheaply protected. On the other hand, thatched roofs are known to be a particular hazard because of the fire risk so that lightning protection is always recommended for these cases at least in the high lightning areas.

The usual method of protection in the latest code⁽⁷⁾ for the lightning protection of dwelling houses relies upon the use of metallic masts or catenaries which are high enough to shed a 45° cone of protection over the building and it is this protective angle which is based upon a given mechanism involving the striking distance of lightning (see Fig 38). The basis of the cone is that for all practical purposes the striking distances of lightning is assumed to be at least equal to the height of the structure

corona discharge may, for a similar reason, be discounted because the amount of ionisation is so small that the charge delivered into the atmosphere over several hours is less than a coulomb and could not therefore neutralise even a single average lightning flash of 20 coulombs. In any case, any useful amount of space charge released into the air above such an installation tends to reduce the electric field intensity thus inhibiting further discharge from the points.

Finally, a high rise building may certainly attract lightning to it for a distance probably of the order of its height above surrounding buildings and may even exhibit upward flashes if very high, for example the Empire State Building in New York. In such high structures side flashes to points below the top of the building have occurred and may be due to space charge effects which blanket the field on the top. In those cases, some conducting materials can be placed on the sides of the building to prevent damage.

The protection of explosives manufacturing plants and storage magazines requires special attention since it is not only the direct effects of lightning current flow which may detonate the explosive but also induced effects and sparks resulting from the current flow in the earth conductors or even in the earth itself. Adequate screening and earthing in a prescribed engineering manner has to be employed usually requiring professional advice.

Similarly lightning is a continuous hazard to blasting operations in open-cast working as well as in shallow mines and the necessary precautionary measures are under consideration whilst measurements on the lightning effects in coal mines have begun in a joint project under the auspices of the Coal Mining Research Controlling Council.

At the same time, the necessity for some form of reliable warning device for the approach of lightning storms is being investigated at the CSIR and a prototype is being used at a Transvaal Coal Mine. This consists of a sensitive lightning flash counter with provision for initiating an alarm if the rate of flashing exceeds a prescribed value. Such warning devices are, however, not infallible — for instance, no warning would be given of a flash starting from a cloud immediately above and a more sophisticated arrangement measuring also the electric field intensity and its variations is possibly required.

64 Lightning protection of people

Statistics of fatalities due to lightning in the Republic have been somewhat sparse but some records are available since 1933, with a break of nine years during and shortly after World War 2, covering 33 magisterial districts which contained, however, the bulk of the population.

The deaths among the White, Coloured and Asian population who might be regarded primarily as urban have amounted to an average of just less than 12 per annum over 37 years and this is equivalent to 1,85 per million per annum based on the 1970 population census.

Deaths from lightning reported among the Black people have amounted to 23 per annum on average and are thus 1,57 per million per annum. However, some

deaths in rural areas were possibly not recorded, since the cause of death was not always stipulated in the records. It is therefore reasonable to assume a figure at least equal to that of the other population group in which case the total number of deaths should average about 40 per annum — in fact, it has been 42 per annum during the last three years.

To put this in proper perspective, however, the average death rate due to road accidents during the last three years has been the enormous figure of about 7 500 per annum which is about 180 times higher than deaths due to lightning.

Thus, while the safest place during a thunderstorm is undoubtedly in an all metal motorcar, it must not be driven. However, lightning deaths being less common, and more spectacular perhaps, are given a large press coverage, from which more detailed statistics may be abstracted. For example, the following lists show some of the major categories reported in the last three years (See Table 7).

TABLE 7 Major categories of lightning fatalities

	Number	
	Killed	Injured
(1) In kraal hua struck by lightning and burnt down	42	34
(2) Inside buildings	20	53
(3) Sheltering under, or walking near, trees	7	10
(4) Working or caught in the open	7	13
(5) Drivin; tractors	3	1
(6) Playing or watching sport	3	28
(7) Fishing or rowin;	3	-
	85	141
	-	-

Regarding the fatalities inside buildings, six were the result of the strike to a metal roof of a school which was not earthed, while the remainder were to buildings with thatched roofs.

It is thus very clear that the application of the SABS Code of Practice for Lightning Protection to all buildings — and thatched huts or houses in particular — would reduce the bulk of the cases of fatalities, thereby limiting casualties to a very low level.

The other possibility of reducing fatalities is, as mentioned earlier, the possible introduction of lightning warning devices especially for work situations, but also for outdoor summer sporting activities involving large numbers of players and spectators who may not be under protective cover, and as stated above, such devices are in the course of investigation.

Finally, this review would not be completed without a reference to so-called ball lightning, one possible event having been recorded by Eriksson⁽⁷⁸⁾. Some experts claim it is purely an optical illusion and there is scant scientific evidence to prove its existence. However, reports over the years are so numerous that the subject cannot be ignored and the search for scientific observation and measurements must surely go on till fact replaces fancy and the myth is no more.

7 Acknowledgement

The author is indebted to the Council for Scientific and Industrial Research for its generous support of the lightning research programme in South Africa, which has enabled the considerable achievement referred to in the review, through the personal efforts of its staff and colleagues and the cooperation of the other organisations mentioned, which is also very much appreciated.

8 References

- ADENDORFF, G V: 'Atmospheric phenomena and their relation to the production of overvoltages in overhead electric transmission lines'. *Trans SAIEE Vol 2 p 154 (1911)*.
- PASK, T P: 'An approach to the study of lightning and allied phenomena'. *Trans SAIEE Vol 21 p 185 (1930)*.
- 'Annual Report of SAIEE for year ending 31 December 1930'. *Trans SAIEE Vol 22 p 6 (1931)*.
- HALLIDAY, E C: 'On the propagation of a lightning discharge through the atmosphere'. *Phil Mag S 7 Vol 15 No 98 Supp Feb (1933)*.
- SCHONLAND, B F J and COLLINS, H: 'Progressive Lightning'. *Nature London 132 p 407 (1933)*.
- SCHONLAND, B F J: 'The development of the Lightning Discharge'. *Trans SAIEE Vol 24 p 145 (1933)*.
- ALLIBONE, T E: 'Biographical Memoirs of Fellows of the Royal Society'. Vol 19 December 1973 B F J Schonland.
- HEWITT, F J: 'Study of lightning streamers with 50 cm radar'. *Proc Phys Soc Vol 66 Sect B Pt 10 pp 895-897 (1953)*.
- HEWITT, F J: 'Radar echoes from interstroke processes in lightning'. *Proc Phys Soc London B70 pp 961-979 (1957)*.
- RENDELL, E F and GAFF, H D: 'An analysis of lightning fault characteristics of the 132 kV lines of the VF and TP Co'. *Trans SAIEE Vol 24 Pt 11 p 258 (1933)*.
- BOYCE, C F, RAMSAY, I C and RETIEF, D P J: 'The protection of open-wire communication systems from lightning damage and interference with particular reference to South Africa'. *Trans SAIEE Vol 46 Pt 6 p 157 (1955) (Digest of Monograph)*.
- ANDERSON, R B and JENNER, R D: 'Lightning investigation on an 88kV line in Southern Rhodesia'. *Trans SAIEE Vol 39 Pt 8 p 217 Pt 9 p 257 (1948)*.
- ANDERSON, R B and JENNER, R D: 'A summary of eight years of lightning investigation in Southern Rhodesia'. *Trans SAIEE, Vol 45 Pt 7 p 215 and Pt 9 p 261 (1954)*.
- GOODLET, B L: 'Lightning'. *J Inst Elect Engineers Vol 81 No 487 pp 1-26 (1937) and Vol 82 No 494 (1938)*.
- BRUCE, C E R and GOLDE, R H: 'The lightning discharge'. *J Inst Elect Engineers 88 Pt II pp 487-520 (1941)*.
- GOLDE, R H: 'Lightning performance of high voltage systems'. *Trans SAIEE Vol 60 pp 269-282 (1969)*.
- WILSON, C T R: 'Some thundercloud problems'. *J Franklin Inst 208 pp 1-12 (1929)*.
- SIMPSON, G: 'On lightning'. *Proc Roy Soc A Vol III (1926)*.
- SCHONLAND, B F J and CRAIB, J: 'The electric field of South African thunderstorms'. *Proc Roy Soc London A Vol 114 p 229 (1927)*.
- HALLIDAY, E C: 'Polarity of thunderstorms'. *Proc Roy Soc A Vol 138 (1933)*.
- SCHONLAND, B F J and ALLIBONE, T E: 'Branching of lightning'. *Nature London 128, 794 (1931)*.
- MOJRE, C B and VONNEGUT, B: 'The thundercloud'. *Book Lightning edited by R H Golde Vol 1 Physics of Lightning Chap 3. Academic Press London New York San Francisco (1977)*.
- VONNEGUT, B: 'Some facts and speculations concerning the original role of thunderstorm electricity'. *Met Monogram 5 pp 224-241 (1963)*.
- HELD, G and CARTE, A E: 'Hail and lightning from Transvaal thunderstorms'. *Proc Intern Conf Cloud Physics London pp 65-66 (Aug 1972)*.
- PROCTOR, D: 'A hyperbolic system for obtaining VHF radio pictures of lightning'. *Jour Geophys Res Vol 76(6) pp 1478-1489 (1971)*.
- PROCTOR, D: 'A radio study of lightning'. *PhD Thesis submitted to the University of the Witwatersrand Johannesburg Vols 1 and 2 (1976)*.
- FEW, A A: 'Thunder'. *The Scientific American Vol 233 No 1 (July 1975)*.
- ERIKSSON, A J: 'The measurement of lightning and thunderstorm parameters: Results for the 1974/75 season'. *CSIR Special Report ELEK 75 Pretoria South Africa*.
- ANDERSON, R B: 'Lightning phenomena in the aerospace environment'. Part 1 *The lightning discharge Trans SAIEE Vol 66 Pt 8 p 166 (August 1975)*.
- GRIFFITHS, R F and LATHAM, J: 'Electrical corona from ice hydrometeors'. *Q. Journ Roy Met Soc 100 pp 163-180 (1974)*.
- ANDERSON, R B: 'The lightning discharge'. *PhD Thesis University of Cape Town South Africa CSIR Special Report ELEK 12 Pt II pp 6-12 (1971)*.
- ANDERSON, R B and KRONINGER, H: 'Lightning phenomena in the aerospace environment'. Part 2 *Lightning strikes to aircraft Trans SAIEE Vol 66 Pt 8 pp 172-175 (1975)*.
- KREHBIEL, P, McCrory, R A and Brook, M: 'The determination of lightning charge location from multistation electrostatic field change measurements'. *Conference on Cloud Physics Tucson Arizona American Meteor Soc Boston Mass October 21-24 (1974)*.
- SCHONLAND, B F J: 'Progressive lightning IV—The discharge mechanism'. *Proc Roy Soc London A 916 (164) pp 132-150 (1938)*.
- MALAN, D J and SCHONLAND, B F J: 'The electrical processes in the intervals between the strokes of lightning discharges'. *Proc Roy Soc London A206 p 145 (1951)*.
- BERGER, K: 'Oszillographische Messungen des Feldverlaufs in der Nähe des Blitz-einschlages auf den Monte San Salvatore'. *Bul SEV Bd 64 (1973) Nr 3 S120-136*.
- KRIDER, E P and LADD, C G: 'Upward streamers in lightning discharges to mountainous terrain'. *Weather Vol 30 No 3 pp 77-81 (1975)*.
- ANDERSON, R B: 'Measuring techniques'. *Book lightning edited by R H Golde Chap 13 p 437 Academic Press London New York San Francisco (1977)*.
- ANDERSON, R B, ERIKSSON, A J and KRONINGER, H: 'Lightning and tall structures: Some preliminary observations'. *4th Intern Conf on Gas Discharges IEE Conf Proc 143 pp 264-267 (1976)*.
- MALAN, D J: 'The relation between the number of strokes, stroke interval and the total durations of lightning discharges'. *Rev Geofisica Pura e Applicata Vol 34 pp 224-230 (1956)*.
- ANDERSON, R B: 'The lightning discharge'. *PhD Thesis University of Cape Town South Africa CSIR Special Report ELEK 12 Pt I pp 49-54*.
- PIERCE, E T: 'Electrostatic field changes due to lightning discharges'. *Quart Jour Roy Meteorol Soc 81 (348) pp 211-228 (1955)*.
- BERGER, K: 'Methoden und Resultate der Blitzforschung auf dem Monte San Salvatore 1963-71'. *Bul SEV 63 pp 1403-1422 (1972)*.
- CARTE, A E and JAGER, J D G: 'Multiple stroke flashes of lightning'. *Jour of Atmospheric and Terrestrial Physics Vol 41 pp 95-101 (1979)*.
- ERIKSSON, A J: 'Lightning ground flash multiple stroke discriminator'. *Proc IEE London Vol 125(6) June 1978*.
- SCHONLAND, B F J, MALAN, D J and COLLENS, H: 'Progressive Lightning II'. *Proc Roy Soc London A.152 p 595*.
- BERGER, K, ANDERSON, R B and KRONINGER, H: 'Parameters of lightning flashes'. *CIGRE Electra 41 pp 201-204 (1975)*.
- LEWIS, W W and FOUST, C M: 'Lightning investigation on transmission lines 8'. *Trans American IEE (1945)*.
- ERIKSSON, A J: 'Lightning and tall structures'. *Trans SAIEE Vol 69 Pt 8 pp 238-252 (1978)*.
- ERIKSSON, A J: 'Author's reply to discussion on his paper(49)'. *Trans SAIEE Vol 70 Pt 5 pp 121-125 (1979)*.
- ANDERSON, R B: 'Contribution to paper by A.J. Eriksson (49)'. *Trans SAIEE Vol 70 Pt 5 pp 114-118 (1979)*.
- BERGER, K: 'Lightning current parameters of upward strokes measured at Monte San Salvatore'. *C E Tram 7358 of Bul SEV/ISE 69 pp 353-359 (April 1978)*.
- MALAN, D J: 'Lightning and its effects on high structures'. *Trans SAIEE Vol 60 Pt II p 241 (Nov 1969)*.
- GOLDE, R H: 'Lightning and tall structures'. *Proc IEE (London) Vol 125 No 4 pp 347-351 (April 1978)*.
- SCHONLAND, B F J: 'The polarity of thunderclouds'. *Proc Roy Soc London A 118 p 233 (1928)*.
- GOLDE, R H: 'Lightning performance of British high voltage systems'. *Proc IEE London (113) No 4 p 601 (1966)*.
- GANE, P G and SCHONLAND, B F J: 'A lightning flash counter (the ceraunometer)'. *Trans SAIEE 38(4) 119 (1947) and Weather (June 1948)*.
- MALAN, D J: 'Radiation from lightning discharges and its relation to the discharge process in "Recent advances in atmospheric electricity"'. *Pergamon Press (1959)*.
- MALAN, D J: 'A lightning counter for flashes to ground'. *Proc Intern Conf Gas Discharges Burrenworrrh (1962)*.
- HORNER, F: 'The design and use of instruments for counting local lightning flashes'. *Proc IEE London Vol 107B pp 321-330 (1960)*.

- 61 GOLDE, R H: 'A lightning flash counter'. *Electronic Engineering* 38 p 164 (1966).
- 62 BARHAM, R A: 'A transistorised lightning flash counter'. *Electron Letters Tome 1*(6) Aug (1965).
- 63 PRENTICE, S A: 'CIGRE Lightning flash counter'. Pt 1 and II *Electra* 22 pp 149-171 (May 1972).
- 64 ANDERSON, R B, VAN NIEKERK, H R and GERTENBACH, J J: 'Improved lightning - earth flash counier'. *Electron Letters Vol 9 No 17* (Aug 1973).
- 65 ANDERSON, R B, VAN NIEKERK, H R, MEAL D V and SMITH, M A: 'Tenth progress report on the development and testing of lightning flash counters in the Republic of South Africa during 1977/78'. *CSIR Special Report ELEK 148 Pretoria* (July 1978).
- 66 ANDERSON, R B, VAN NIEKERK, H R, PRENTICE, S A and MACKERAS, D: 'Improved lightning flash counters'. *CIGRE Journ Electra No 66* pp 85-98 (1979).
- 67 KRONINGER, H: 'Newsletter—National lightning recording scheme No 3'. *CSIR Special Reort ELEK 181*(Sept 1979).
- 68 ERIKSSON, A J: 'Thunderstorm incidence in South Africa'. *Proc 21 Annual Conf SA Inst Phys R ELEK 108*(July 1976).
- 69 ERIKSSON, A J: 'The measurement of lightning and thunderstorm parameters: Results for the 1977/78 season'. *CSIR Special Report ELEK 149* (July 1978).
- 70 ANDERSON, R B and ERIKSSON, A J: 'The measurement of lightning and thunderstorm parameters including the application of lightning flash counters'. *Proc 5th Int Conf Atm Elect Sept 1974. Electrical processes in atmospheres Editors H Dolezalek, R Reiter* pp 724-727.
- 71 ERIKSSON, A J and MEAL, D V: 'Progress report on the Cabora Bassa surge recording station 1977/78'. *CSIR Special Report ELEK 147* (July 1978).
- 72 ANDERSON, R B, ERIKSSON, A J and KRONINGER, H: 'The measurement of voltages on transmission lines by remote electrostatic field sensing'. *Submitted for publication to the SAIEE*(July 1975).
- 73 ERIKSSON, A J: 'Lightning overvoltages on high voltage transmission lines—Investigation of waveshape characteristics'. *CIGRE Journ Electra No 47* pp 87-110 (July 1976).
- 74 BOYCE, C F, RAMSAY, I C and RETIEF, D P J: 'Digest of Monograph: The protection of open-wire communication systems from lightning damage and interference with particular reference to South Africa'. Published by the SAIEE June 1955 *Trans SAIEE Vol 46 Pt 6* p 157 (1955).
- 75 BOYCE, C F: 'Protection of Telecommunication Systems'. Lightning book edited by R H Golde. Chap 25 pp 793-829 *Academic Press London New York San Francisco* (1977).
- 76 SABS 'Code of Practice 03/1951 for the Protection of buildings against lightning' (under revision).
- 77 SABS 'Code of Practice 03A/1975. The protection of dwelling houses against lightning'.
- 78 ERIKSSON, A J: 'Video tape recording of a possible ball-lightning event'. *Nature Vol 268 No 5615* pp 35-36 (July 7, 1977).

Vote of Thanks

F J Hewitt I regard it as a considerable privilege to have been invited to propose the Vote of Thanks to Dr Anderson our new President.

I regard it as a privilege firstly in that Dr Anderson and I are colleagues in the same organisation — the CSIR, and I feel thus I can associate myself in some way with some of the work described tonight. I know that the Council — the governing body of the organisation commonly known as the CSIR — would wish me to convey their congratulations, the first of many, to Dr Anderson, on his address and this I now do.

Secondly, it is a privilege in that the work described by Dr Anderson is one in which I personally for a short time and in one very restricted area — operated. He was gracious enough to mention it this evening. I still find it a subject of great interest — and leading as it must to a better knowledge of thunderstorms — the process by which we get the greater part of what little rain we do get nowadays — it may well be now a subject of even greater practical importance than

when the protection of electricity distribution systems was the practical incentive.

Thirdly, I regard it as a privilege in that lightning research was the main personal scientific interest of one who I regard as amongst the most distinguished members of this Institute — Sir Basil Schonland. Sir Basil made lightning research synonymous with South Africa. It is very gratifying that lightning research is alive and well today, in South Africa — for which to a considerable extent we are indebted to Dr Anderson, and fourthly I am privileged in that the field of research is one in which I believe this Institute took one of its most constructive and farsighted decisions. In December 1930 the SAIEE set up a Lightning Investigations Committee. This arose from a paper presented to the Institute in April 1930 entitled 'An approach to the study of the Lightning and allied phenomena', in which the author proposed the establishment of a Lightning Research Laboratory fully equipped for both field and laboratory work — the author added however 'it is impossible for the Institute to embark on extensive research, but one could initiate a scheme which may develop into a semi-national organisation'. How better to describe the CSIR.

From these words in an Institute paper may have sprung the germ of the idea from which the Bernard Price Institute developed five years later.

It is interesting too to note the remarks of His Excellency, the Governor-General of the Union of South Africa, the Earl of Athlone, on the occasion of the Banquet to celebrate the coming of age of the SAIEE on 16 October 1930. He said 'To its loss, South Africa can claim a painful intimacy with lightning — we who live in this country have quite peculiar opportunities of observing its behaviour and who knows, but a lightning observatory may at some time be established from which the most valuable knowledge will result...'. I feel the Institute will have a large say in the matter.

It was at the Annual General Meeting of the SAIEE in 1932 that the then Mr Bernard Price drew the attention of the Institute to Schonland's work at Cape Town University and as a result Schonland was invited on to the Institute's Sub-Committee.

The SAIEE made an appeal for funds and was supported by the Chamber of Mines, the Electricity Supply Commission, the Victoria Falls and Transvaal Power Company and the AS & TS. As a result of this, field work in the Witwatersrand commenced in the summer of 1932/33, and I quote 'in the course of two storms eleven good photographs of flashes were captured'. I feel that the Annual General Meeting of 1932 must have been of quite exceptional interest. I wonder if it was a matter raised under 'general'.

It is highly appropriate that an incoming President is himself personally continuing these studies today — with Parliamentary funds I might add — he might not be so pleased with a £500 grant which was the amount that made the summer 1932/33 season's observations possible.

I would now like to refer briefly to Dr Anderson's prestige in the international scientific scene. He is at the present time the official South African representative

on **Study Committee** No. 33 of CIGRÉ (international Conference on Large High Voltage Electric Systems) the **subject** of Study Committee No. 33 being 'Over-voltages and **insulation** co-ordination'.

His contribution to the work of this Committee has been recognised by his **appointment**, as the **Chairman** of the Committee's Working Group on Lightning and he is the Convenor of its Task Force on Lightning Counters. He has in fact played an important personal role in influencing the development of lightning flash counters internationally — their calibration — and their use in determining lightning flash density. His research group has also provided unique input on surges on transmission lines to another CIGRÉ Committee.

Dr Anderson is also active in the International Commission on Atmospheric **Electricity (ICAE)**, and a member of Working **Groups** of the I triple E (IEEE) — on the lightning protection of distribution systems and prediction of the lightning performance of transmission lines.

He **is thus** well-known in lightning research in international circles and South Africa's international **image** in science **is** enhanced thereby.

I have not **said** anything in **detail** about Dr Anderson's **personal** contribution to knowledge of lightning. His

address 'Lightning research in Southern Africa' gives us some **idea** of his work as **such** a review would **be totally** inadequate without frequent **reference** to it, however modest he may have been about its inclusion. **It is** perhaps somewhat **sobering** that after some 47 summer seasons and **despite much** ingenuity and many many interesting discoveries there **still** remains **much** to be explained in the lightning process and in **its** relation to the **thunderstorm** as a whole. **Such** a situation is not unique to lightning — it is **surely** true that in **every** field of science the more one probes and the more one understands, the **further does** the horizon of the complete understanding recede. In this lies the challenge for the scientist of the future. The engineer in his daily tasks must **operate** within the **existing** state of knowledge. **To** the scientist or the engineer **such** as Dr Anderson extending the boundaries of knowledge, there is the ever present challenge of the unknown.

We have been privileged to listen tonight to a most lucid account of how this **challenge** has been met to date in the field of lightning research in South Africa — it **is** a record in which Dr Anderson's **personal** contribution has been considerable and on which we would **all** now like to congratulate **him**. I now **formally** propose a hearty Vote of Thanks to Dr Anderson.

CSIR

Council for Scientific and Industrial Research

In association with the British Science Research Council



South African Astronomical Observatory

PO Box 9, Observatory, 7935 South Africa

Telex 57-20309, Telegrams Astronomie;

Telephone National (021) 55 1341

International 272155 1341

Our ref.

Your ref.

12 July 1982

Dr F Louange
9 rue Sainte-Anastase
75003 PARIS
France

Dear Dr Louange

Thank you for your letter of 21/5/82. The work carried out at this Observatory is purely of an astronomical and astrophysical nature using various telescopes with advanced electronic instrumentation.

I enclose the latest Annual Report for your information.

Yours sincerely

M W Feast

BELGIQUE



AMBASSADE
de
BELGIQUE

Paris, le 23 avril 1982

P 10-90

N^o 13749

Monsieur,

Comme suite à votre lettre du 19 avril dernier, j'ai l'honneur de vous faire connaître ci-dessous quelques adresses d'institutions scientifiques belges susceptibles de pouvoir **VOUS** communiquer les renseignements que vous souhaitez :

- ⊗ - Observatoire royal de Belgique
avenue Circulaire 3
Bruxelles - (Tél. 374.38.01)
- ⊗ - Institut d'aéronomie spatiale de Belgiaue
avenue circulaire 3
1180 - Bruxelles (Tél. 374.27.28)
- ⊗ - Observatoire MIRA (station météorologique didactiaue)
1850 GRIMBERGEN (Tél. 02/269.12.80)
- Société Belge d'Etude des Phénomènes Spatiaux (SOBEPS)
26, Boulevard Aristide Briand
Anderlecht.

Veillez agréer, Monsieur, l'expression
de mes sentiments distingués.

Baron Alain Guillaume
Ministre - Conseiller

Monsieur LOUANGE François,
Ingénieur - Conseil
9, rue Sainte-Anastase
75003 - PARIS

Volcanic material from Mount St Helens in the stratosphere over Europe

M. Ackerman, C. Lippens & M. Lechevallier*

Institut d'Aéronomie Spatiale de Belgique, 3, Avenue Circulaire,
 B-1180 Brussels, Belgium

*E.T.C.A., 16 bis, Avenue Prieur de la Côte d'Or,
 F-94114 Arcueil, France

The **two** most recent balloon flights devoted to **studying** the stratospheric aerosol vertical structure by **comparison** with winds, temperature and ozone **vertical** structures took place on 7 May and on 5 June 1980. At 15.23 h GMT on **18** May Mount St Helens volcano (**46°N, 122°W**) erupted with a tremendous explosion, **projecting** ash into the stratosphere. An explosion of this **size occurs** only about once a **decade**¹. This **sudden** introduction of **material** into the atmosphere **offers** the opportunity to study air motions both **horizontally** and **vertically**. The **last such large-scale** opportunity **was** offered by the Mount **Fuego** eruption which took place in 1974. In **this** latter **case**, the enhancement of stratospheric aerosols was observed by **means** of ground-based **lidars** and of balloon-borne **particle counters**. The time development of the aerosol event in 1974 and 1975 has been described **elsewhere**²⁻⁴. Mount St Helens **material can** now also be traced by **various satellite-borne** instruments. This new stratospheric aerosol event appears to be spectacular. As **shown** by the **photographs discussed here**, it **leads in its** early stage of **development** to an **increase** by a **factor** of three of the Earth limb **reflectivity at 15-km altitude** after a period of **several** years of low stratospheric aerosol content.

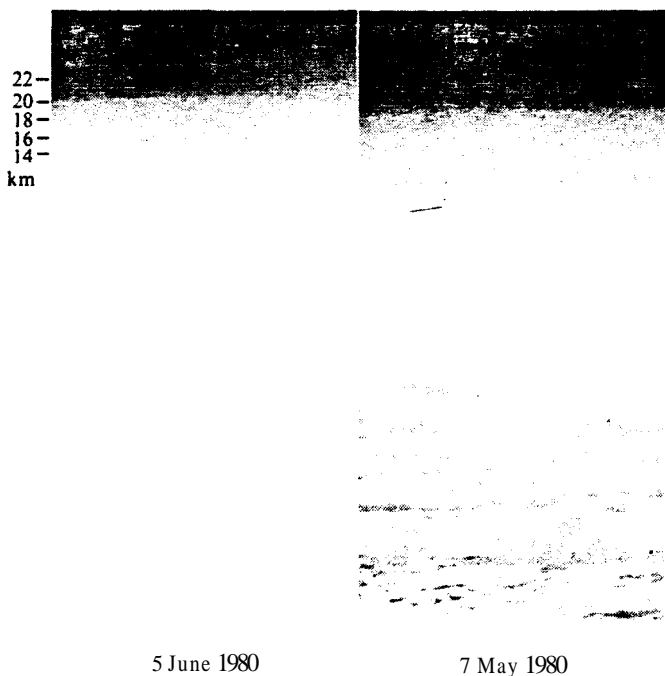


Fig. 1 Photographs of the Earth limb taken with identical exposure settings in the azimuth of the Sun at low solar elevation angles from balloon gondolas on 7 May and on 5 June 1980. The gondolas were at 37- and 35-km altitude respectively. An altitude scale of the grazing line of sight is shown in kilometres. Below the dark blue sky horizontally stratified aerosol layers are revealed by scattered sunlight. In the 5 June case, material from the Mount St Helens volcano has spread in the low stratosphere over a large horizontal extent. It enhances the brightness of the limb so that the cloud cover in the foreground can hardly be seen through the whitish veil. In contrast, the cloud cover is well visible on 7 May. Note that the grazing point at 16-km altitude is some 500 km away from the camera. An altitude difference of 1 km at that altitude corresponds to 7 arc min.

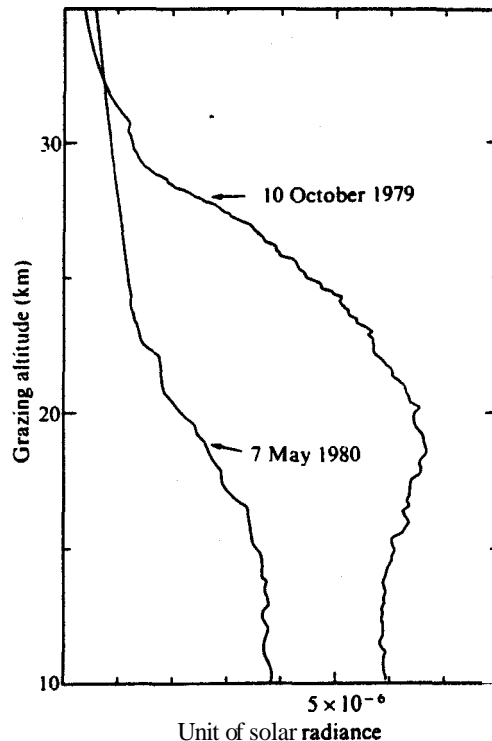


Fig. 2 Earth limb radiance in the azimuth of the Sun versus grazing altitude of the line of sight. The solar elevation angles were respectively 6.18° and 69.4° on 10 October 1979 and on 7 May 1980. The variation of the limb radiance versus altitude is relatively smooth in both cases. As most of the radiance observed is due to scattering by particles, their amount in the low stratosphere appears larger in October than in May where a low aerosol background had been reached. The situation at higher altitudes seems to be reversed. However, these aspects require confirmation from other flights and further interpretation of these raw data where ozone and air absorption should be taken into account. The uncertainties due to difficulties of the photographic photometry have also to be considered.

The new method⁵ is based on the photographic observation from balloon altitude of the Earth limb in the azimuthal direction of the Sun at low solar elevation angles. Aerosols are known to scatter light mostly at small angles whereas, comparatively, Rayleigh scattering by air molecules occurs almost evenly at all angles. Our observational geometry favours aerosol detection.

At balloon altitude the camera lenses view the Earth limb below the horizontal line directly and the Sun above it through a neutral optical density ($D \approx 4$) screen which serves several purposes. It avoids penetration of straylight in the optics to obtain clean pictures of the Sun at various elevation angles providing an angular scale. It puts both the Sun and the Earth limb in the sensitive dynamic range of the film calibrated in relative units by means of a step wedge photographed before flight. The solar images provide the absolute scale. The gondola is Sun oriented so that the cameras have the Sun in the middle of the horizontal field of view. Colour (Kodak EPR 475) and black and white (Kodak Plus X Pan) 70-mm films are used. The results reported here were obtained in the red using Wratten filters nr. 25 set in front of the 80-mm focal length lenses of the Hasselblad EL500 cameras and without filter. The cameras are remotely operated from the ground. The telemetry return signal allows us to check their operation.

Three flights are considered here. The first two took place on the afternoons of 10 October 1979 and 7 May 1980 from Aire sur l'Adour in south-west France. To determine the geographical coordinates as accurately as possible, the tracking was performed by the CNES telemetry station and by radars located at the Centre d'Essais des Landes (Biscarosse). The altitude, longitude and latitude of the gondola at the time that the picture

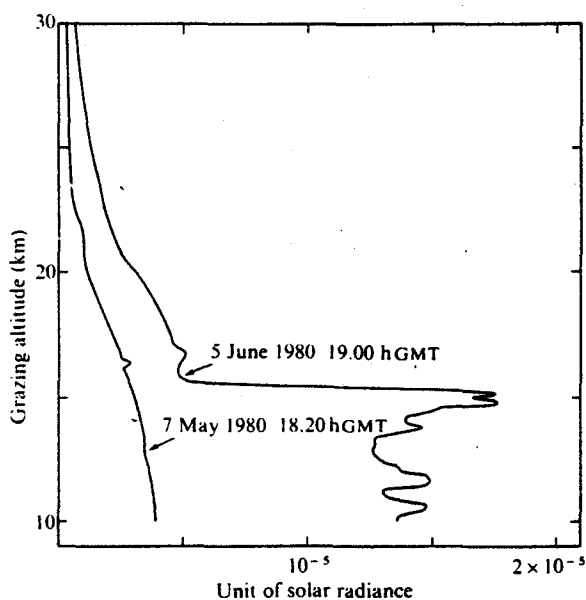


Fig. 3 Earth limb radiance in the azimuth of the Sun and in units of solar radiance versus altitude of the grazing line of sight. The solar elevation angles were respectively 6.94° and 6.26° on 7 May and on 5 June. The large and sharply cut radiance increase between 15.6 and 15.2 km is due to the stratospheric loading of volcanic material. The radiance increase at higher altitudes is thought to be partly due to the illumination increase of the upper levels by the lower levels. The thin layers (some 300-m thick) at some 16.5-km altitude seems to be a frequent feature of the mid-latitude stratosphere and is thought to be related with the height of the tropical tropopause.

was taken were respectively 37 km, 1° E and 44° N. The third flight took place on 5 June 1980 from the other CNES range in the Alps. Radar tracking was performed in this case from Ile du Levant on the edge of the French Riviera. The coordinates were 35.2 km, 2° E and 44° N.

Inspection of limb pictures such as those shown in Fig. 1 reveals the presence of aerosol layers with a thickness ranging from 100 metres to several kilometres. The latter layers extend

horizontally over the whole field of view whereas the thinner layers may have a smaller extension. The black and white photographs are analysed using a Jarrell-Ash densitometer. Grazing altitudes in the stratosphere are determined using the tables of Link and Neuzil⁶, taking refraction into account.

The Earth limb radiance is deduced from the densitometric measurements. The radiance vertical profiles observed on 10 October 1979 and on 7 May 1980 in white light are compared in Fig. 2. These profiles are similar showing mostly smooth vertical structure. Figure 3 shows the vertical radiance profiles observed in red light on 7 May and on 5 June 1980. The abrupt radiance increase observed on 5 June between 15- and 16-km altitude is similar to the increase of particle amount observed shortly after the Fuego eruption²⁻⁴. The very sharp cutoff at the upper boundary of the layer is typical.

On the other hand, satellite-borne instruments have tracked at 16-km altitude material from the volcano crossing the east coast of the US on 23 May and moving towards Europe above the Atlantic Ocean on 27 May (M. P. McCormick, personal communication). The observation reported here is likely to have occurred shortly after the arrival over Europe.

Theory^{7,8} predicts that a stratospheric aerosol increase reduces the amount of solar energy reaching the troposphere and the ground. Two main processes are involved: absorption in the aerosol layer and reflection to space of solar energy flux leading to small average temperature decreases in the troposphere^{4,9}. The reflectivity data reported here will be augmented by further flights and together with other absorption data will hopefully improve the understanding of the problem and help to evaluate more precisely the possible impact of stratospheric aerosol events.

We thank the French Centre National d'Etudes Spatiales balloon launching range for launches, tracking and recovery of the gondolas.

Received 9 July; accepted 14 August 1980.

1. EOS 61 (1980).
2. Hoffman, D. J. & Rosen, J. M. *J. geophys. Res.* **82**, 1435-1440 (1977).
3. McCormick, M. P., Swisler, T. J., Chu, W. P. & Fuller, W. H. Jr. *J. Atmos. Sci.* **35**, 1296-1303 (1978).
4. Russell, P. B. & Hake, R. D. Jr. *J. Atmos. Sci.* **34**, 163-177 (1977).
5. Ackerman, M. & Lippens, C. *Aeronom. Acta C n° 54* (1979).
6. Link, F. & Neuzil, L. *Tables of Light Trajectories in the Terrestrial Atmosphere* (Hermann, Paris, 1969).
7. *CIAP Monogr.* (US Department of Transportation, Springfield, 1975).
8. Pollack, J. B. et al. *J. geophys. Res.* **81**, 1071-1083 (1976).
9. Mass, C. & Schneider, S. H. *J. Atmos. Sci.* **34**, 1995-2004 (1977).

Stratospheric aerosols properties from Earth limb photography

M. Ackerman, C. Lippens & C. Muller

Belgian Institute for Space Astronomy, Circular Avenue, 3, B-1180-Brussels, Belgium

Balloon-borne observation at three wavelenghts of visible sunlight scattered by the Earth limb allows the determination of aerosols abundances and size distributions at various altitudes in the stratosphere. The stratospheric aerosols are apparently still under the influence of the Mount St Helens volcanic eruption five months after its occurrence on 18 May 1980.

IT is only relatively recently that detailed studies of the stratospheric aerosols have been initiated. They are of importance because nucleating and catalytic agents are central in determining the radiation balance of the atmosphere. A survey of light scattering techniques used in the remote monitoring of atmospheric aerosols has been published recently¹. Twilight phenomena have been used both from the ground^{2,3} and from satellites, and Earth-limb observation from space has been based on sunlight scattering observed directly^{4,5} or through its absorption⁶. *Zn situ* sampling initiated 20 years ago⁷ has also provided much information on the composition of aerosols⁵.

We have previously reported⁹ the photographic observation, from a balloon gondola floating in the upper stratosphere, of the enhancement of stratospheric aerosols over Europe 23 days after the Mount St Helens volcanic eruption. Several other reports have now appeared¹⁰⁻¹³ while details have been provided on the air trajectories which have caused the volcanic plume to move at various altitudes in various directions¹⁴ at the beginning of their many cumbersome revolutions around the Earth. Much information has been collected on the properties of the ejecta in relation to atmospheric effects¹⁵. On 15 October 1980, five months after the eruption, another photographic balloon flight took place. One of the first observations was finding that the enhancement of stratospheric aerosols below 20 km altitude has become very horizontally homogeneous. This means that it is now possible to determine the basic properties of volcanically influenced aerosols and of natural aerosols which seem to differ in several respects in the stratosphere.

Observation method

Photographic cameras onboard a balloon gondola simultaneously record at various wavelengths the light from the Earth limb below the horizontal line-of-sight while the solar elevation is low. This light is scattered direct sunlight with a contribution from the Earth albedo which is minimized when the Sun is low. The observation geometry is shown in Fig. 1. The limb radiance, R , can be expressed directly in solar radiance units because solar images are recorded simultaneously with a known attenuation factor. The solar elevation is calculated from the time that the picture was taken and from the geographical position. An angular scale is constructed from several consecutive shots. The depression angles at which radiances are measured are related to the line-of-sight altitude of closest approach to the Earth surface taking into account refraction effects¹⁶. The measured integrated radiances can be inverted taking into account absorption by ozone and air along the line of sight by the 'onion peeling' method to yield the *in situ* radiance, R^* , per unit length versus altitude.

The Sun-oriented gondola can be rotated about its vertical axis so that pictures can be taken at various azimuth angles, A , relative to the Sun's position. The scattering angle θ of direct

solar radiation can be computed from the relationship

$$\cos \theta = -\sin D \sin h_{\odot} + \cos D \cos h_{\odot} \cos A \quad (1)$$

where D is the depression angle at which the atmospheric radiance is measured and h_{\odot} is the solar elevation angle at the time of measurement. As expected from their strong forward scattering properties, aerosols re-emit little light at an azimuth angle 180° away from the direction of the Sun. The limb radiance observed in this case is used to subtract Rayleigh scattering and to isolate aerosols scattering at all azimuths taking into account the Rayleigh phase function¹⁷.

If direct solar radiation only is considered, an *in situ* monodisperse aerosol radiance R_i^* per cm of pathlength is related to the average solar radiance R_{\odot} by

$$R_i^* = R_{\odot} \pi a^2 Q_s \sigma \varphi_{\theta} n / 4\pi \quad (2)$$

where a is the angular radius of the Sun's disk, 2.16×10^{-5} rad, φ the properly normalized particulate phase function, Q_s the scattering efficiency factor, σ the particulate scattering geometrical cross-section in cm^2 if the number density, n , of the particles is expressed in cm^{-3} .

In practice, our data confirm the previous observation¹⁸ according to which the phase function can, within experimental uncertainties, be represented by the Henyey-Greenstein function. The asymmetry factor g of the phase function and the total scattering efficiency can then be determined. The variation

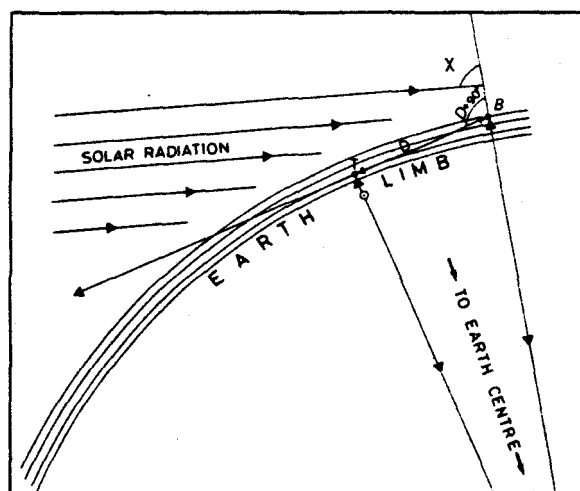


Fig. 1 Observational geometry: quasi parallel light falls on the atmosphere at a solar zenith angle X , the atmosphere is seen at various depression angles D ; through the rotation of the gondola, photographs are taken at various azimuth angles A from the Sun direction.

of these parameters with wavelength can be fitted to their theoretical variations using the effective size parameter of Hansen and Travis¹⁹. This procedure, which uses the Mie scattering computation programme of Wiscombe²⁰, leads to an evaluation of the effective particle size and provides information on other properties. From these two quantities and from the product nu obtained directly from equation (2) the value of n can be deduced.

The aerosol particle size is usually treated in terms of the wavelength, λ , of the interacting light through the Mie size parameter

$$x = 2\pi a/\lambda \quad (3)$$

where a is the radius of the spherical particle in a monodisperse aerosol. In a polydisperse aerosol the number of particles of radius r is expressed¹⁹ by

$$n_r = Ar^{(1-3b)/b} e^{-r/ah} \quad (4)$$

where a becomes the effective radius while b is a measure of the width of the size distribution; A is a constant related to the total number of particles.

Comparing R_s^* with θ , the scattering angle, at various wavelengths provides information about the asymmetry factor, g . A knowledge of g and its variation with the wavelength of the interacting light leads to the unique determination of a and b . How the scattering efficiency Q , varies with size parameter can then be determined. The behaviour of these quantities is known from the Mie scattering theory.

Experimental details

The balloon flight took place on 15 October 1980. The tropopause height being 11.4 km. The gondola floated at 37.6 km altitude and was equipped with seven Hasselblad EL500 cameras with 80-mm focal length lenses and 70-mm films. Four of them were pointing forwards, one being loaded with colour EPR 475 Kodak film, and three in the opposite direction.

Each camera was paired with the one opposite: Wratten filters 47 (440 nm) and 25 (650 nm) with Plus X Kodak film and filters 87 with Kodak aerographic 2424 film (860 nm). To ensure that the Sun images were in the dynamic range of the film, neutral density screens made of exposed and processed sheet films were placed 60 cm from the lenses with their lower edge placed a few centimetres above the optical axis. Before flight, step wedges, inconel filters and samples of the neutral density screens illuminated in parallel light were recorded by each camera in the laboratory. After the flight, the Plus X films were processed using the Kodak D76 developer ($\gamma = 1$) and the IR-sensitive film was processed in the Kodak D19 developer ($\gamma = 2.3$). The dynamic range of this last film was too small to record usefully simultaneous Sun and limb images so that its absolute calibration was derived from the comparison of optical densities due to quasi-pure Rayleigh scattering observed 180° from the Sun in the three colours above 30 km altitude. The absolute calibration in blue and red light was based directly on solar images. The colour, blue, red and IR camera settings (aperture, speed) were respectively: $f/11$, $1/125$ s; $f/8$, $1/250$ s; $f/8$, $1/250$ s; $f/8$, $1/125$ s. As soon as the gondola could be Sun oriented, pictures were taken during ascent and later during the float period. With its Sun sensor remaining locked on the Sun, the gondola was then rotated about its vertical axis so that the cameras could record Earth limb images 65°, 115°, 180°, 245° and 295° from the solar azimuth. The whole horizon scan took place between 16.08 and 16.18 h GMT, during which atmospheric illumination conditions changed very little. The latitude and longitude were respectively 1° E and 44° N. The average solar azimuth and elevation angles were 248° and 9.3° respectively. The optical densities were measured on three tracks per frame normally to the horizon by means of a Jarrell-Ash micro-densitometer and subsequently converted into radiance, in units of solar radiance, versus altitude of the grazing line of sight every 200 m. Each photograph allows an angular coverage of about 34°.

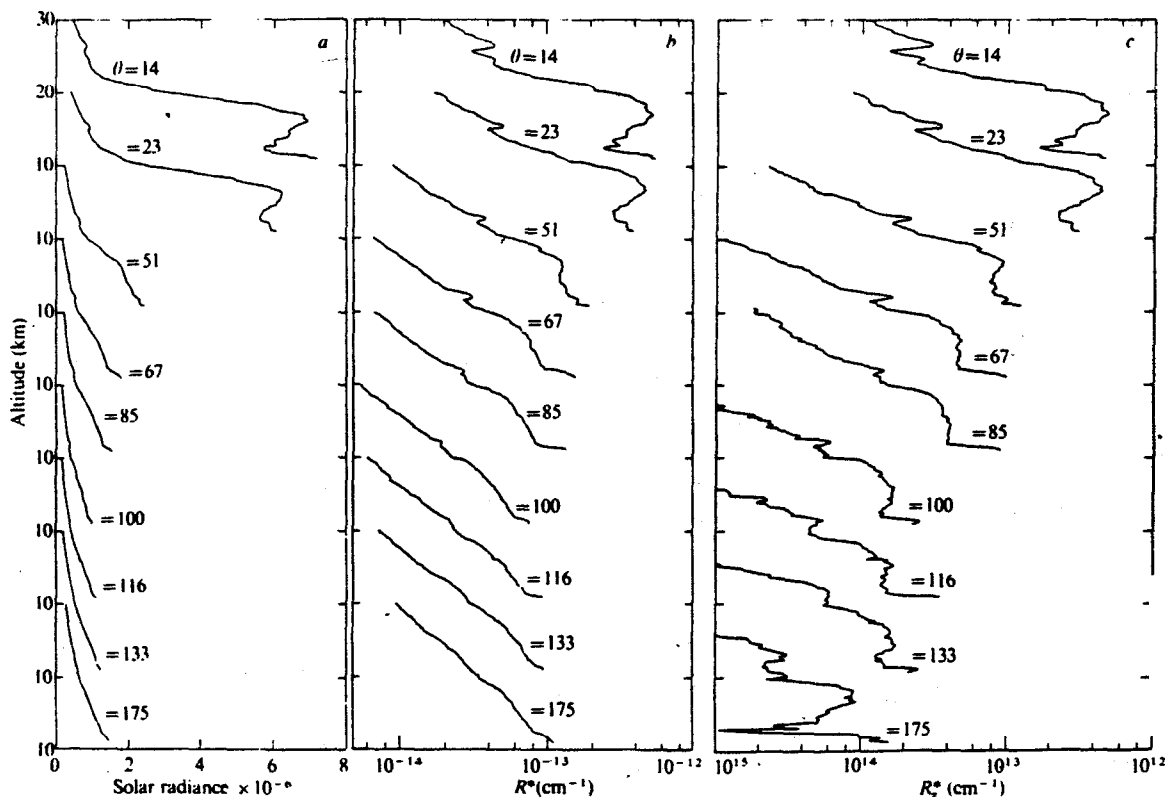


Fig. 2 Data at 650 nm versus altitude for various scattering angles, 8: a. integrated radiances, R , along the lines of sight; b. inversed radiances, R^* ; c. inverted radiances due to aerosols, R_1^* . Each successive lower curve is displaced by 10 km altitude from the one above. R^* and R_1^* are expressed in units of solar radiance.

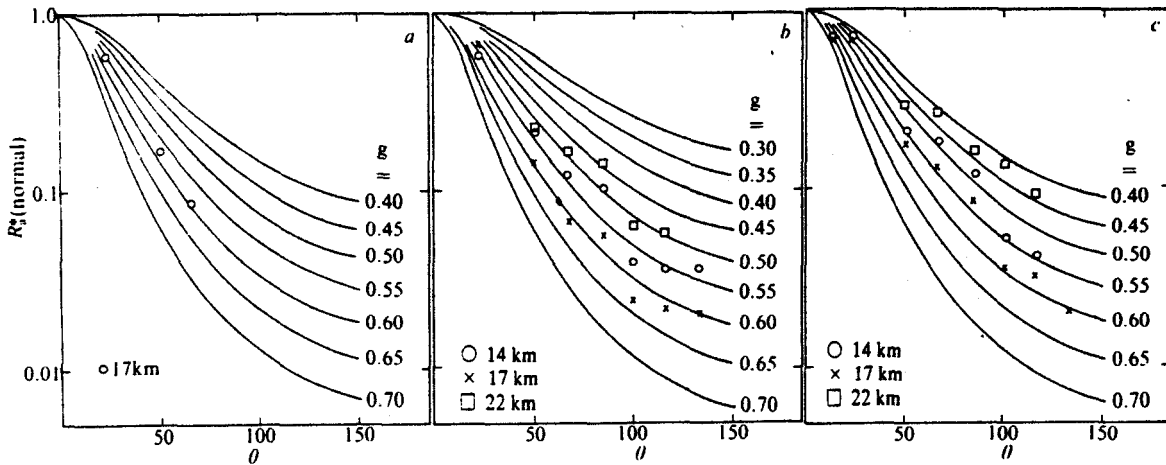


Fig. 3 Henyey-Greenstein phase functions of the radiance versus scattering angles, normalized at $\theta = 0^\circ$ for various values of the asymmetry factor, g . The experimental data points are shown at the three altitudes studied and for the three wavelengths: a, 440 nm; b, 650 nm; c, 860 nm.

Results

As an example, the observed limb radiance values are presented versus the altitude of closest approach of the line of sight to the Earth surface (sea level) for 650 nm and for various scattering angles in Fig. 2a.

The comparison of the vertical radiance profiles observed at small scattering angles in red light 11 days before, less than 1 month⁹ and five months after the Mount St Helen's eruption shows several characteristics. A radiance enhancement peaking at 17 km altitude still exists on 15 October 1980, by a factor of almost three relative to the pre-eruption value. Above 22 km altitude the radiance has returned to values close to what it was on 7 May 1980. This suggests that the heavy layer observed over England on 6 and 7 June¹⁰ and on 5 June⁹ over France constituted the main body of the material injected in the stratosphere by the volcano. Over 5 months, that layer would then have spread in altitude and its centre of gravity would have moved upwards by ~ 2 km, this being perhaps related to air heating through sunlight absorption by the aerosols.

The various photographs taken around the vertical axis of the gondola reveal the 17 km layer at all azimuth angles; above 20 km altitude a well defined 1-km thick layer is readily seen. Such thin, well separated features have been observed on each of our previous flights and most probably have no relationship with volcanic activity. They belong to the 'natural' stratospheric aerosol. In this particular case the layer is present towards the south from the gondola and absent towards the north. Its altitude is at 22 km from 125° azimuth counted clockwise from the geographical north to $\sim 220^\circ$ where it begins to rise up to ~ 25 km at 250° where it splits and becomes invisible. Particulate matter is also present above, what we call here, the 22 km layer. With respect to the horizontal homogeneity, the comparison of the aerosol direct sunlight scattering with the scattering angles is safe for the 17-km layer; for higher altitudes care must be taken.

For the angular study, along the lines-of-sight integrated radiances are inverted using standard ozone and air distributions²¹ and their respective absorption cross-sections²². The *in-situ* radiance values, R^* , in units of solar radiance and per cm along the line-of-sight at the tangent altitude, are presented in Fig. 2b. The R^* values at 650 nm (Fig. 2b) show at $\theta = 175^\circ$ an exponential dependence versus altitude, as expected, on which some structure and noise is superimposed. At 860 nm in the backward hemisphere where aerosols are expected to bring a small contribution and particularly at 30 km altitude, the variation of R^* with θ fits well the Rayleigh phase function, giving confidence to the very low contribution from the Earth albedo to the observed signal. This is not surprising as the average cloud deck radiance measured at depression angles from 5 to 15° ranges from 7×10^{-7} to 6×10^{-7} of the solar

radiance at respective azimuths from 0 to 180° from the Sun. At $8 = 14^\circ$ and 17 km altitude the aerosol contribution is about 14 times the Rayleigh contribution.

At 650 nm (Fig. 2b) the Rayleigh phase function can be fitted to the radiance variation observed in the backward hemisphere at 30 km altitude. In this case, however, the average cloud radiance varies from 6×10^{-6} near the Sun's azimuth to 6×10^{-7} elsewhere. In the forward direction the aerosol contribution to the radiance is 10.8 times the Rayleigh contribution at 17 km. At 440 nm, Rayleigh scattering dominates even if at $8 = 14^\circ$ it still seems to be five times smaller than aerosol scattering at 17 km. At $\theta = 175^\circ$, R^* grows faster than exponentially at altitudes below 20 km. Multiple scattering here has an important role because the Rayleigh optical thickness on the tangent line of sight reaches unity at 20 km. This occurs at 9 km and at ground level for 650 and 860 nm respectively. In addition the average cloud deck radiance is very high in blue light varying from 1.6×10^{-5} near the Sun to 10^{-6} of the solar radiance elsewhere. The data obtained in blue light can then only be used

Table 1 Summary of balloon-borne results for three characteristic altitudes

Altitude	14 km	17 km	22 km
g_{440}	—	0.6	—
g_{650}	0.55	0.60	0.50
g_{860}	0.52	0.56	0.45
$\sum Q_s n \sigma_{440} (\text{cm}^{-1})$	—	3.2×10^{-8}	—
$(\sum Q_s n \sigma_{440})_{AM} (\text{cm}^{-1})$	—	1.5×10^{-8}	—
$\sum Q_s n \sigma_{650} (\text{cm}^{-1})$	9.4×10^{-9}	1.0×10^{-8}	2.9×10^{-9}
$(\sum Q_s n \sigma_{650})_{AM} (\text{cm}^{-1})$	6.0×10^{-9}	5.8×10^{-9}	1.5×10^{-9}
$\sum Q_s n \sigma_{860} (\text{cm}^{-1})$	1.9×10^{-9}	2.7×10^{-9}	9.3×10^{-10}
$(\sum Q_s n \sigma_{860})_{AM} (\text{cm}^{-1})$	2.4×10^{-9}	3.1×10^{-9}	9.2×10^{-10}
Q_{440}	—	0.8	—
Q_{650}	0.14	0.52	0.1
Q_{860}	0.10	0.35	0.05
$\sum n \sigma_{440} (\text{cm}^{-1})$	—	4×10^{-8}	—
$(\sum n \sigma_{440})_{AM} (\text{cm}^{-1})$	—	1.9×10^{-8}	—
$\sum n \sigma_{650} (\text{cm}^{-1})$	6.7×10^{-8}	1.9×10^{-8}	2.9×10^{-8}
$(\sum n \sigma_{650})_{AM} (\text{cm}^{-1})$	4.3×10^{-8}	1.1×10^{-8}	1.5×10^{-8}
$\sum n \sigma_{860} (\text{cm}^{-1})$	1.9×10^{-8}	7.7×10^{-9}	8.9×10^{-9}
$(\sum n \sigma_{860})_{AM} (\text{cm}^{-1})$	2.4×10^{-8}	8.9×10^{-9}	8.8×10^{-9}
a (μm)	0.042	0.15	0.045
b	3.6	0.6	1.8
V (cm^3)	1.8×10^{-13}	1.5×10^{-13}	7.0×10^{-14}

g , The asymmetry factor of the phase function; $\sum Q_s n \sigma$, the optical aerosol scattering extinction deduced from observed radiances; $(\sum Q_s n \sigma)_{AM}$, the optical aerosol scattering extinction deduced from comparison with the molecular scattering extinction; Q_s , the scattering efficiency factor; $\sum n \sigma$ and $(\sum n \sigma)_{AM}$, the geometric scattering extinctions; a , b , the size distributions parameters; V , the total volume of particles per cm^3 of air at the respective altitudes.

with caution and at small scattering angle. The situation here is different from that in the balloon-borne aureole observation²¹ due to the low solar elevation used.

Figure 2c presents the *in situ* radiance due to aerosols R^* obtained by subtracting the Rayleigh scattering R_M^* , due to air. R_M^* is evaluated from R^* at $\theta = 175^\circ$ following the 'clean air' procedure currently used in lidar work²⁴. R_M^* is then adapted for the various scattering angles considered according to the molecular phase function¹⁷.

Interpretation

The angular dependance of R^* has been fitted to the variation of the scattered light intensity with θ computed for various values of the asymmetry factor g of the Henyey-Greenstein function as shown for three wavelengths in Fig. 3. In blue light a few values of θ give useful results. For the reasons discussed above values for the 22-km layer have only been considered for θ between 51° and 116° .

The asymmetry factors so determined are listed in Table 1 with the optical scattering extinction coefficients $Q_s n \sigma$. The values at 440 nm have not been used because a model taking into account the measured cloud radiances indicates a non-negligible contribution of the albedo to the limb radiance. But this contribution is negligible at the larger wavelengths. The observed g values, taking into account that it is probably slightly higher than 0.6 and 440 nm, tend to indicate that a value of the real index of refraction equal to 1.55 (see ref. 25) is observed here. This value will then be used to deduce the size parameter x , and its variation with λ from 650 to 860 nm leads to the values of a and b characterizing the size distribution listed in Table 1. Eventually, the scattering efficiency Q_s can be deduced from a and b following the Mie scattering theory¹⁹.

With the data available, there is, of course, another method of determining $\sum Q_s n \sigma$. From the air σ values¹¹ and from the air number density n_{air} taken from a model²¹ (mid-latitude, spring-
autumn) (n_{air}), can be evaluated. The R_M^* values determined at $\theta = 175^\circ$ by the 'clean air' method²⁴ are compared with the R^* measured and by taking into account the air and aerosols phase

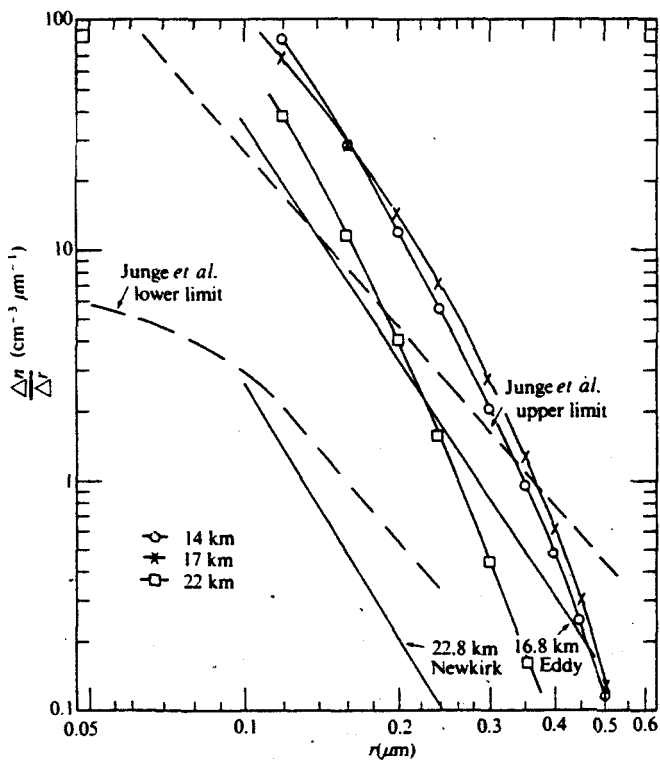


Fig. 4 Number of particles per cm^{-3} versus their radii and per micrometre size interval for three characteristic altitudes: 14, 17 and 22 km. Two previous data sets^{7,23} are shown for comparison.

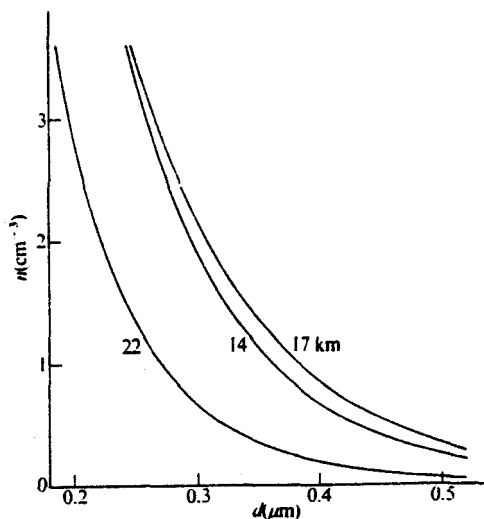


Fig. 5 Total numbers of particles with diameters larger than given values. The ratio of the number of particles with diameters (d) $> 0.3 \mu\text{m}$ to the number of particles with diameters $> 0.5 \mu\text{m}$ is larger for the layer at 22 km altitude than for 17 and 14 km altitudes indicating the volcanic influence in these two latter cases²⁹.

functions the values of $(\sum Q_s n \sigma)_{AM}$ for the aerosols are deduced. They are also listed in Table 1.

The absolute particle distribution shown in Fig. 4 for the three altitudes considered is based only on the geometrical extinction coefficient $\sum n \sigma$ at 860 nm for two reasons. In IR light, the albedo contribution to the measurement is negligible while it is a maximum in blue light and in the inversion of R leading to R^* the correction for the absorption by O_3 , of which a standard vertical distribution had to be used, is the largest in red light. This is supported by the discrepancy observed at shorter wavelength between the extinctions determined from the observed radiances and those determined by comparison with the molecular scattering. The agreement is very good at 860 nm. The Mie scattering theory also had the best chance to be valid, even if the particles do not exhibit a perfectly spherical and smooth shape, at small values of the size parameter.

Discussion

Our particle distributions are compared in Fig. 4 with the upper and lower limits deduced from *in situ* sampling⁷ and with two extreme values resulting from solar aureole measurements²³. The present results fall within the range of those data except for particles $< 0.2 \mu\text{m}$ radius where the upper limit given by Junge et al.⁷ is exceeded. As mentioned above the aerosols below 20 km are still in volcanically perturbed conditions. On the other hand, the collection efficiency of an *in situ* sampler might be reduced for small particles. Note also that our distributions are steeper especially at large radii. This effect is less pronounced in the comparison with the aureole data. This effect seems to be due to the small values of effective radii obtained here.

Another comparison of our data, shown in Fig. 5, can be made for the total number of particles with a radius $> 0.15 \mu\text{m}$ obtained by balloon-borne optical particle counters²⁶. The number densities of these particles are $0.4\text{--}1.3 \text{ particle cm}^{-3}$ in the 14–17 km altitude region and $0.1\text{--}0.9 \text{ particle cm}^{-3}$ at 22 km. The data presented here for 22 km correspond to a low aerosol content above 20 km and lead to $0.7 \text{ particle cm}^{-3}$ above $0.15 \mu\text{m}$. At 14 and 17 km altitude the values presented in Fig. 5 respectively imply 1.9 and $2.1 \text{ particle cm}^{-3}$ of particles with radii $> 0.15 \mu\text{m}$. A comparison between the two methods would be required to define a possible discrepancy as the aerosols are volcanically enhanced in the present case.

The optical extinction coefficient $Q_s n \sigma$ measured at $1 \mu\text{m}$ wavelength by the SAM II Satellite-borne instrument at low

aerosol load in July 1979²⁷ exhibits an almost constant value at altitudes from 14 to 20 km of 10^{-9} cm⁻¹. This compares very favourably with our 860 nm value at 22 km. At 17 and 14 km altitude, the extinction in the present case is 3 and 2 times larger. This can be expected from the volcanic influence which may also explain the larger effective particle radius a at 17 km altitude.

A value of the asymmetry factor g of 0.4910.7 has been measured recently at 633 nm, a wavelength close 650 nm used here, from 10.7 to 12.8 km altitude in the stratosphere¹⁸. This value corresponds to our measurement at 22 km where the aerosol is considered to be purely 'natural'. Because g is larger in the present case at 14 and particularly at 17 km, one of the volcanic influences must then be to increase the g value and if the Mie theory is applicable to increase the particle size as we observe it at 17 km altitude.

Received 27 April; accepted 25 June 1981.

1. Deirmendjian, D. *Rev. Geophys. Space Phys.* **18**, 341-360 (1980).
2. Bigg, E. K. *Tellus* **16**, 76-83 (1964).
3. Volz, F. E. & Goody, R. M. *J. Atmos. Sci.* **19**, 384-406 (1962).
4. Giovane, F., Schuerman, D. W. & Creenberg, J. M. *J. geophys. Res.* **81**, 5383-5388 (1976).
5. Garriott, O. K. *J. opt. Soc. Am.* **69**, 1064-1068 (1979).
6. Rozenberg, G. V. & Nikolaeva-Tereshkova, V. V. *Izv. Atmos. Oceanic Phys.* **1**, 228-232 (1965).
7. Junge, C. E., Chagnon, C. W. & Manson, J. E. *J. Mer.* **18**, 81-108 (1961).
8. Cadie, R. D. & Grams, G. W. *Rev. Geophys. Space Phys.* **13**, 475-501 (1975).
9. Ackerman, M., Lippens, C. & Lechevallier, M. *Nature* **287**, 614-615 (1980).
10. Thomas, L., Chaloner, C. P. & Bhattacharyya, S. K. *Nature* **289**, 473 (1981).
11. Reiter, R., Jäger, H., Carnuth, W. & Funk, W. *Geophys. Res. Lett.* **7**, 1099-1101 (1980).
12. D'Altorio, A., Visconti, G. & Fiocco, G. *Geophys. Res. Lett.* **8**, 63-65 (1981).
13. Meixner, F. X., Georgii, H. W., Ockelman, G., Jäger, H. & Reiter, R. *Geophys. Res. Lett.* **8**, 163-166 (1981).
14. Danielsen, E. F. *Science* **211**, 819-821 (1981).
15. Pollack, J. B. *Science* **211**, 815-816 (1981).
16. Link, F. & Neuzil, L. *Tables of Light Trajectories in the Terrestrial Atmosphere* (Hermann, Paris, 1969).
17. Penndorf, R. *J. opt. Soc. Am.* **47**, 176-183 (1957).
18. Grams, G. W. *Geophys. Res. Lett.* **8**, 13-14 (1981).
19. Hansen, J. E. & Travis, L. D. *Space Sci. Rev.* **16**, 527-610 (1974).
20. Wiscombe, W. J. *Appl. Opt.* **19**, 1505-1509 (1980).
21. *U.S. Standard Atmosphere, 1976* (U.S. Government Printing Office, Washington DC, 1976).
22. Ackerman, M. in *Mesospheric Models and Related Experiments* (ed. Fiocco, G.) (Reidel, Dordrecht, 1971).
23. Newkirk, G. Jr & Eddy, J. A. *J. Atmos. Sci.* **21**, 35-60 (1964).
24. Grams, G. & Fiocco, G. *J. geophys. Res.* **72**, 3523-3542 (1967).
25. Toon, O. B. & Pollack, J. B. *J. appl. Met.* **15**, 225-246 (1976).
26. Hofmann, D. G., Rosen, J. M., Pepin, T. J. & Pinnick, R. G. *J. Atmos. Sci.* **32**, 1446-1456 (1975).
27. McCormick, M. P. *et al. Geophys. Res. Lett.* **8**, 3-4 (1981).
28. Whitten, R. C., Toon, D. B. & Turco, R. P. *Pageophysic* **118**, 86-127 (1980).
29. Hofmann, D. J. & Rosen, J. M. *J. Atmos. Sci.* **38**, 168-181 (1981).

Annexe

TÉLÉPHONES :

DIRECTION : 374 43 00

AUTRES SERVICES	}	374 67 87
		374 02 79
		374 09 41
		374 02 48

1180 Bruxelles, le 9 juin 1982
AVENUE CIRCULAIRE. 3

Monsieur François LOUANGE
Rue Sainte-Anastase 9
FR-75003 PARIS

Monsieur,

En réponse à votre lettre du 21.5.1982, nous avons l'honneur de vous communiquer que L'IRM effectue des observations dans le domaine des décharges d'électricité atmosphérique,

Les observations consistent d'une part, du comptage du nombre d'éclairs et d'autre part de l'enregistrement des transitoires électriques émis par les éclairs.

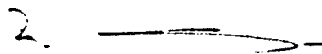
Les comptages sont effectués à l'aide de compteurs du type "CIGRE", installés à Maldegem, Bornem, St.Katelijne-Waver, Deurne et Mol. La mise au point d'un compteur permettant de déterminer l'heure exacte des décharges est en cours à L'IRM.

Les signaux électriques transitoires émis entre 1 kHz et 600 kHz sont enregistrés à l'aide d'une mémoire digitale ; une résolution de 0,5 µs peut-être obtenue.

En annexe vous trouverez les schémas blocks des différents appareils et nous sommes à votre disposition pour des renseignements complémentaires.

Je vous prie d'agréer, Monsieur, l'assurance de ma considération distinguées.

Le Directeur,



Dr. R.SNEYERS

DESCRIPTION DES CIRCUITS

2.1 LE FILTRE F 0779.I

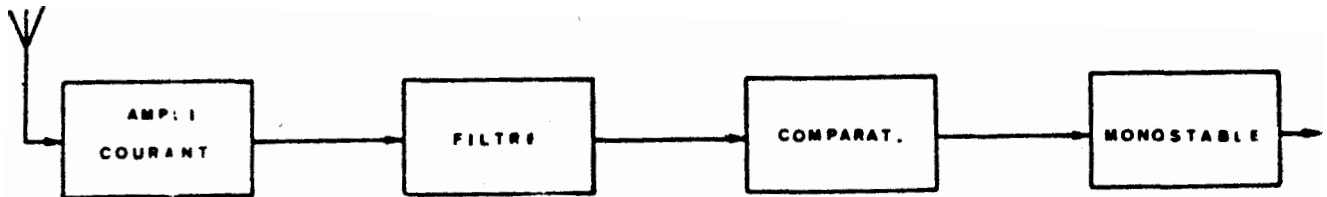


Fig. 1

Cette plaquette se compose, primo d'un ampli en courant ceci afin d'assurer une grande impédance d'entrée, puis d'un filtre actif passe bande dont les fréquences de coupure sont de 180 Hz et 500 Hz et le gain unitaire.

L'élément suivant est un comparateur dont le seuil peut être réglé avec une grande précision grâce au potentiomètre se trouvant sur la face avant.

(un tour représente un seuil de 500mV).

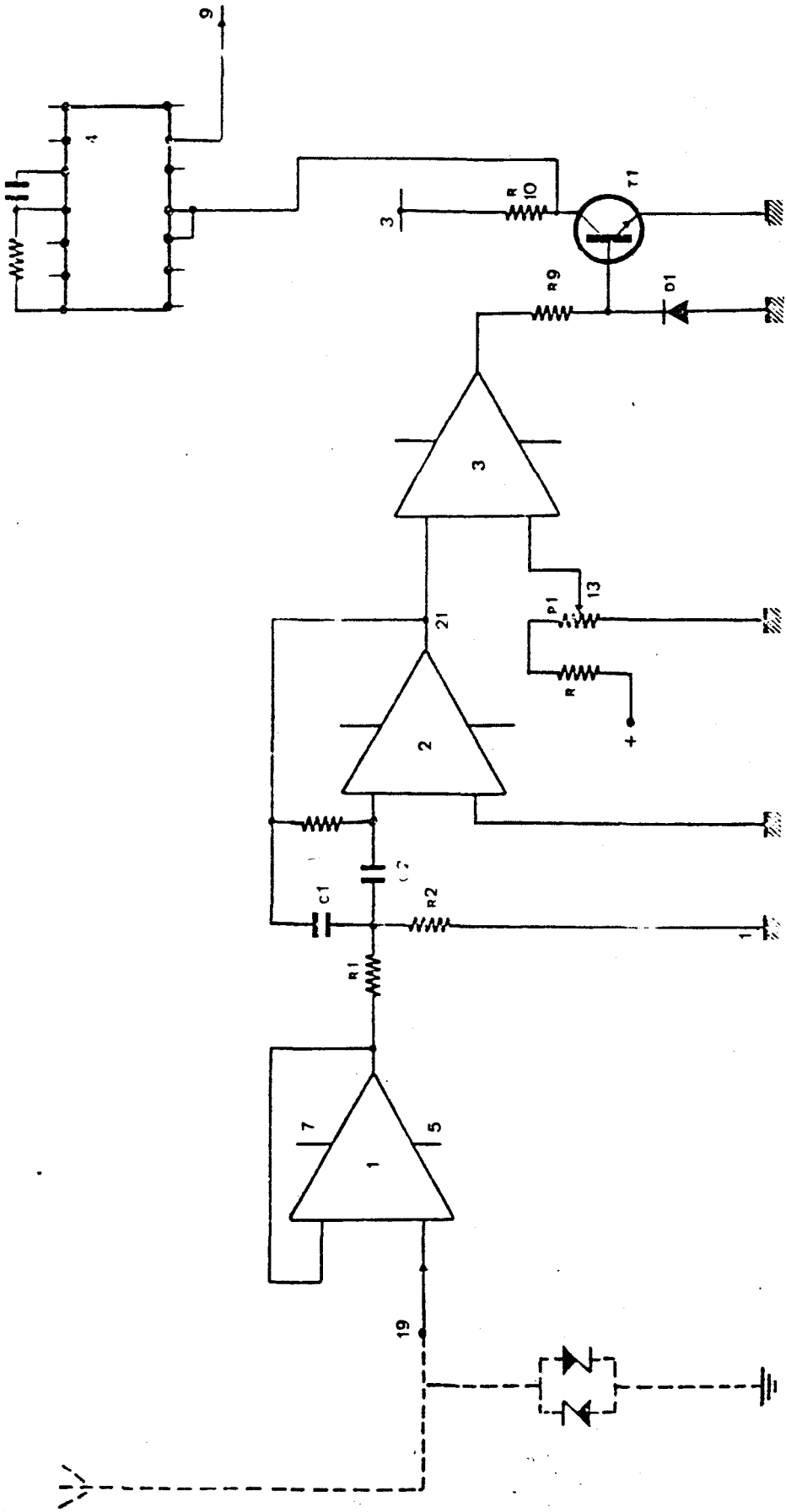
La position de ce potentiomètre sera déterminée par l'expérience.

En fermant la petite manette sur le bouton, on assure la constance du niveau de détection.

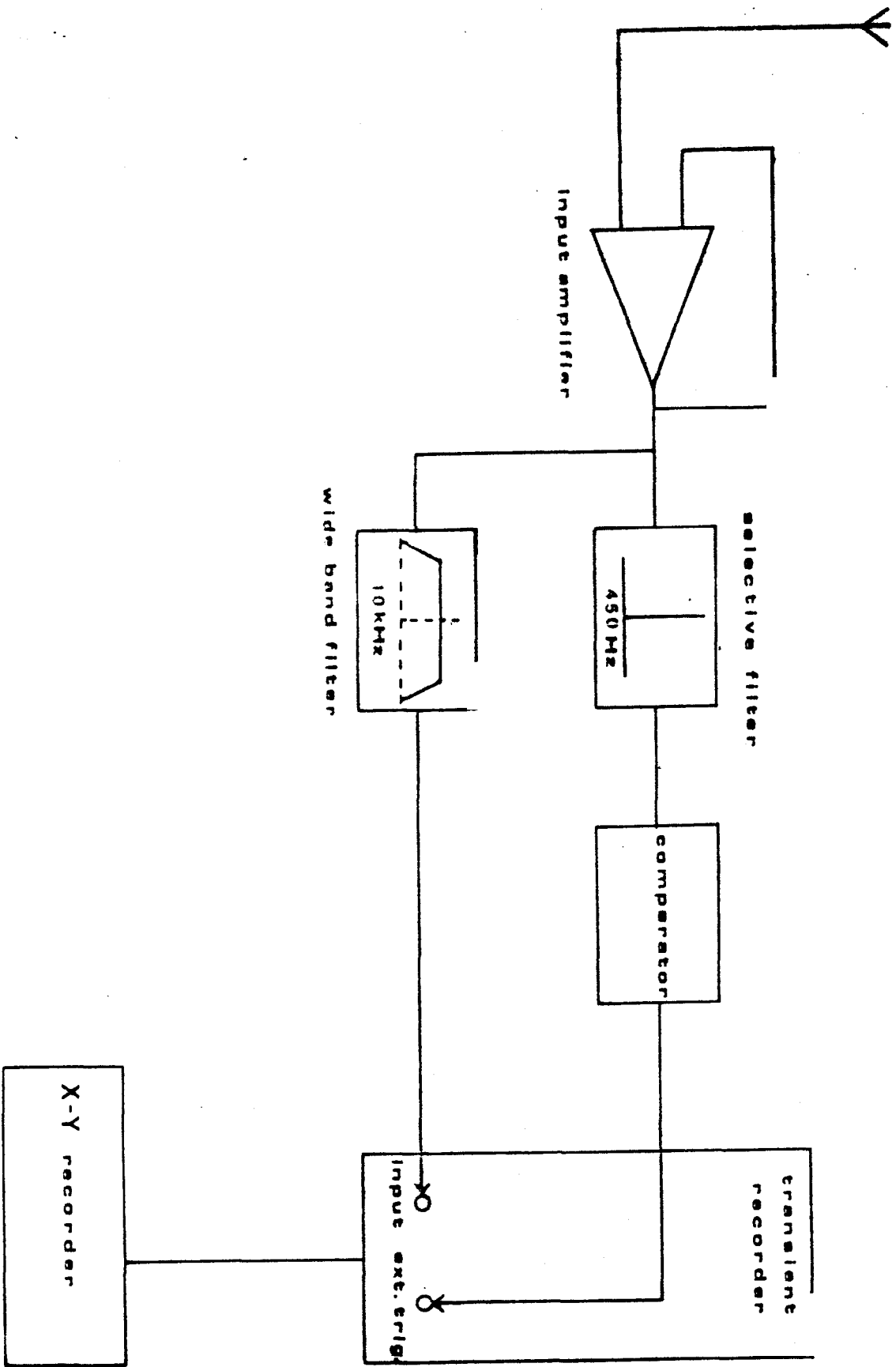
Après ce comparateur, se trouve un transistor qui adapte la tension de sortie au niveau TTL.

Enfin c'est un monostable qui termine le circuit de détection dont le temps est réglé sur 2 mS, ce qui a pour but d'éliminer tout rebondissement afin d'avoir une seule impulsion.

Voir fig. 2



F 0770



B R E S I L

AMBASSADE DU BRÉSIL

34. COURS ALBERT 1^{er}
75008 PARIS

Paris, le 7 juin 1982

Monsieur François Louange
9 rue Saint-Anastase
75003 Paris

Monsieur,

En réponse à votre lettre du 19 avril, j'ai le plaisir de vous faire parvenir les adresses des institutions suivantes:

- ⊗ - Observatório Nacional
Rua General Bruce, 586
20.921 Rio de Janeiro - R.J.
- ⊗ - Instituto Nacional de Pesquisas Espaciais
Avenida dos Astronautas, 1758
12.200 São José dos Campos, S.P.
- ⊗ - Instituto Astronômico e Geofísico
Universidade de São Paulo
Av. Miguel Stefano, s/n
São Paulo- S.P.

2. Dans le cas où d'autres institutions s'intéressent à la détection des phénomènes aérospatiaux rares au Brésil me seraient signalées, je vous le communiquerai ultérieurement.

Veillez agréer, Monsieur, l'assurance de mes salutations distinguées.

Georges Lamazière
(Georges Lamazière)
Chef du Service de
Science et Technologie



Cq

CONSELHO NACIONAL
DE DESENVOLVIMENTO
CIENTÍFICO E TECNOLÓGICO

São José dos Campos, July 9, 1982.

REF: 30.100.000.1070/82Mr. François Louange
Ingénieur Conseil
9, rue Sainte Anastase
75003 Paris
FranceDear *Mr.* Louange:

Thank you for your letter of June 6, 1982 relating to your appointment to undertake a survey on rare aerospace phenomena.

I would like to inform you that INPE which is responsible for Brazilian space research, has no involvement in the mentioned area of your interest.

As far as I know there is no detection system established in Brazil.

Sincerely yours

Nelson de Jesus Parada
Director General

ASC/ta.

INPE - INSTITUTO DE PESQUISAS ESPACIAIS

CONSELHO NACIONAL DE DESENVOLVIMENTO CIENTÍFICO E TECNOLÓGICO - INSTITUTO DE PESQUISAS ESPACIAIS
SÃO JOSÉ DOS CAMPOS, SP - AV. DOS ASTRONAUTAS Nº 1758 - CX. POSTAL 514 - FONE (0123) 229977 - TELEX (011) 31570 - CEP 12.200
SÃO CARLOS, SP - RUA PAULISTA - FIM - ROD. PRES. DUTRA, Km 40,0 - CX. POSTAL 01 - FONE (025) 61377 - TELEX (022) 1160 - CEP 12.630
CUIABÁ, MT - MORRO DA CONCEIÇÃO S/N - CX. POSTAL 714 - FONE (065) 301-904 - TELEX (0652) 114 - CEP 76.000
MIRASSOL, SP - LT. SAUGADO FILHO Nº 3000 - CX. POSTAL 130 - FONE (064) 23 - 284 - TELEX (0842) 1185 - CEP 13.500
MATALEZOS, CE - DISTRITO DE EUZÉBIO - CX. POSTAL 1281 - FONE (085) 224-4900 - CEP 60.000
SÃO PAULO, SP - RUA TATIANA Nº 65 - FONE (011) 257-9755 - TELEX (011) 3400 - CEP 01239

C A N A D A



National Research Council
Canada

Conseil national de recherches
Canada

Herzberg Institute
of Astrophysics

Institut Herzberg
d'astrophysique

Ottawa, Canada
K1A 0R6

File Référence 4712-3

October 8, 1982.

M. François Louange,
9, rue Sainte-Anastase,
75003 Paris,
France.

Dear Mr. Louange:

Please excuse the delay in replying to your letter of July 20 which arrived shortly before I left on a trip to Europe.

We operate a camera network of 12 stations in western Canada for the photography of bright fireballs. The enclosed reprint describes the general properties of the system and we would be happy to provide any other details that might be of interest.

Yours sincerely,

Ian Halliday,
Planetary Sciences Section.

IH:vp

Encl.

Telex 053-3715
Télex 053-3715

Canada

THE INNISFREE METEORITE AND THE CANADIAN CAMERA NETWORK

BY IAN HALLIDAY, ALAN T. BLACKWELL AND ARTHUR A. GRIFFIN
*Herzberg Institute of Astrophysics, National Research Council of Canada
Ottawa and Saskatoon*

ABSTRACT

The events which led to the establishment of the camera network in western Canada known as the **Meteorite Observation and Recovery Project (MORP)** are described. The network consists of 12 small **observatories**, each equipped with **five cameras**, a **meteor detector** and **exposure control** systems. A bright **fireball** was **observed in Alberta** and from an **aircraft above** clouds in Saskatchewan on **February 5, 1977**, at **19^h 17^m 38 M.S.T.** Two MORP stations in Alberta photographed the event from which a predicted impact point was calculated, **leading** to the **recovery** of a 2-kg meteorite near Innisfree, Alberta, on **February 17**. **Five smaller pieces** were **located after** the disappearance of snow in April. Measurements of the weak radio-activity **produced** by cosmic-ray activity were made on the main **piece shortly** after recovery at a laboratory in the United States. The results from this meteorite are of **special interest because** the **meteor** photographs **provide a reliable orbit** for the **object** before impact. **Innisfree is** only the third meteorite for which **such a well-defined orbit is** available. The **low-inclination, direct orbit** appears normal for asteroidal fragments which **collide** with the **earth**.

Introduction. **Meteorite** research in Canada received a great stimulus as a result of events which began with the **fall** of the Bruderheim meteorite near Edmonton, Alberta, on March 4, 1960. One recent consequence of the Bruderheim event was the **photographic** recording and prompt recovery of the Innisfree meteorite, which **fell** in Alberta on February 5, 1977, only 116 km from the **much** larger Bruderheim **fall**.

The **fall** and recovery of the large shower of stone meteorites **north** of the small town of Bruderheim has been described by Folinsbee and Bayrock (1961). Many fragments, totalling **over 300 kg**, of this typical hypersthene chondrite (petrologic type L6) **were** recovered within an **elliptic** area nearly 4×6 km in extent. This **abundant** supply has made possible a **very** extensive study of the meteorite and has provided **exchange material** for the improvement of the meteorite collections in Canada. The total **recovered** mass for Bruderheim is the largest for any **Canadian** meteorite.

The experience gained in field **searches** and laboratory study of Bruderheim was put to good use when three other **meteorite** falls occurred within **500 km** of Edmonton in the next seven **years**. **These** meteorites were Peace River in **1963** (Folinsbee and Bayrock 1964); Revelstoke in **1965** (Folinsbee *et al.* **1967**) and Vilna in **1967** (Folinsbee *et al.* **1969**). **These** four events **brought** to ten the number of **Canadian** meteorite falls for which the

date of fall was known and suggested that several falls per decade might be expected if reports of bright fireballs were pursued intensively. By coincidence, the next fall in Canada, the Innisfree meteorite, occurred ten years to the day (almost to the hour) after the Vilna event. Several other meteorites classified as "finds" rather than "falls" were recovered during the decade but information on the date of fall is not available in these cases.

The Bruderheim event had other, less obvious results. The collection of the fallen meteorites and their acquisition for scientific study had been handled efficiently because of the presence and interest of amateur astronomers within the Edmonton Centre of the Royal Astronomical Society of Canada and geologists at the University of Alberta and the Research Council of Alberta. In many parts of Canada the event might have gone unnoticed. This realization led directly to the establishment in 1960 of the Associate Committee on Meteorites by the National Research Council of Canada to stimulate interest in all aspects of meteorite research. The Committee consists of about fifteen members chosen to give broad geographic coverage across Canada. One of the Committee's first actions was to organize a national system for the prompt reporting of fireballs to the regional representatives and the central office in Ottawa, a system which worked well for Innisfree.

Another early action of the Associate Committee was to recommend the creation of a network of photographic stations in western Canada to record bright fireballs. The aim of such networks is to provide accurate data on the atmospheric trajectory, from which the probable impact point of meteorites on the ground can be calculated with more confidence and less delay than by the collection and analysis of eyewitness reports. Secondly, the data from the upper end of the luminous path can be used to calculate the orbit of the meteoroid around the sun before it collided with the earth. The observational data may also be used for statistical studies of the rate of occurrence of bright meteors, orbital statistics of large meteoroids in the solar system, etc.

Photographs of the atmospheric flight of the Pribram meteorite in Czechoslovakia had been secured in 1959 with conventional meteor cameras (Ceplecha 1961). In 1961 the International Astronomical Union approved a resolution calling for the construction of photographic fireball networks and the first two networks were established about 1964 in Czechoslovakia (Ceplecha and Rajchl 1965) and the central plains of the United States (McCrosky and Boeschstein 1965). The Czechoslovakian network soon expanded in cooperation with West Germany and is known as the European Network. The Canadian Meteorite Observation and Recovery Project (MORP) became the third such project (Halliday 1973).

followed more recently by networks in the United Kingdom (Hindley 1975) and in the U.S.S.R. (Zotkin et al. 1976).

The Meteorite Observation and Recovery Project.

History of the Project. Since the purpose of meteorite networks is to recover meteorites for which the astronomical data have been secured, networks should be located to provide a large amount of clear night-sky conditions over a terrain which is suitable for a meteorite search. Although Canada has a very large land area, the only region of adequate size which meets the second requirement is the agricultural region of the three prairie provinces. Clear weather is expected to be as frequent here as elsewhere in Canada and one of the by-products of the project is data on clear night-sky conditions. Preliminary data on these conditions are presented at the end of this section.

The planning and construction of the MORP network were accomplished in the late 1960s within the Astronomy Division of the Dominion Observatory, then a Branch of the Department of Energy, Mines and Resources. Some preliminary site searches began in the summer of 1966 with eight of the final observatory sites selected in 1967 and the remaining four in the spring of 1968. One potential site was later shifted ten kilometres when it was found the land would not support a loaded cement truck. The network was planned to keep all stations away from the glare of large cities and sites were selected to be near existing power lines and away from roads with heavy traffic. Where possible, however, they were chosen to be not far from major highways and local habitation, the latter in order to derive some protection against potential vandalism. Figure 1 shows the location of the twelve observatories where the station names refer to nearby towns, usually within 10 km of the station. Table I lists the geographic locations and elevations of the stations; the elevations include a height of 4 m above ground for the cameras.

The MORP network is operated from a field headquarters on the campus of the University of Saskatchewan in Saskatoon, near the geographic centre of the network. The Asquith observatory, west of Saskatoon, was chosen as the first station and its small building was erected during the summer of 1968. Some modifications were introduced into the building design before two more observatories were built the following winter, then seven stations in the summer of 1969 and, finally, the two Manitoba observatories during the winter of 1969-70. The first cameras were installed at Asquith late in 1968 but the network was not effectively operational on a routine basis until 1971.

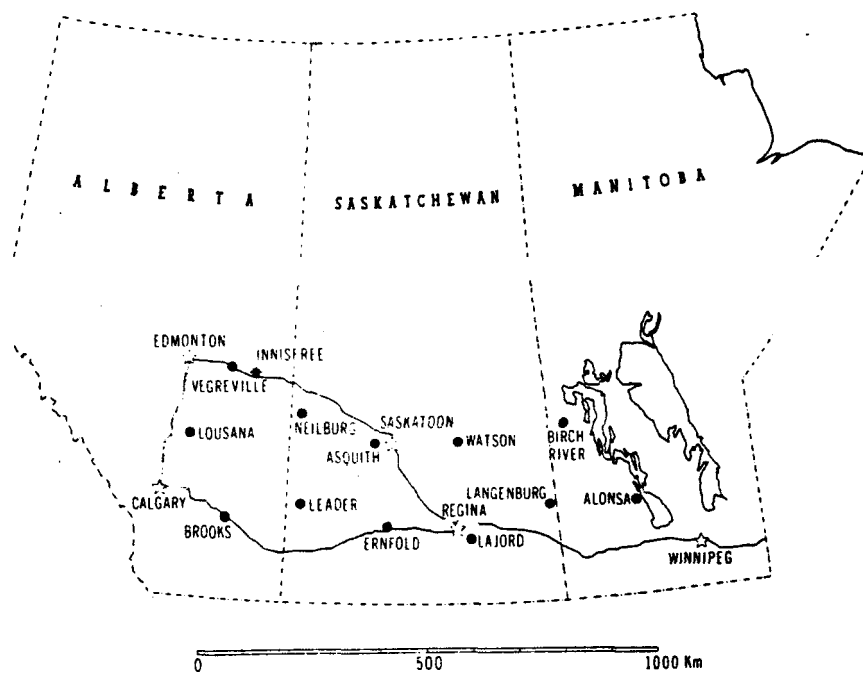


FIG. 1.—Map of the MORP network showing the location of the twelve stations (filled circles) and the site of the Innisfree meteorite fall relative to some major cities (open stars) and highways in western Canada. The effective search area for meteorites is about 700,000 km².

TABLE I
LOCATIONS OF THE MORP STATIONS

Station	Latitude	Longitude	Elevation (metres)
A Asquith	52° 12' 04" N	107° 07' 04" W	527
B Neilburg	52 41 25	109 36 11	651
C Vegreville	53 32 03	112 06 45	640
D Lousana	52 07 42	113 11 48	929
E Brooks	50 29 53	111 53 15	774
F Leader	50 54 01	109 37 01	677
G Ernfold	50 31 18	106 51 04	710
H Lajord	50 16 21	104 09 28	600
I Langenburg	50 44 51	101 43 08	512
J Alonsa	50 44 36	99 03 31	287
K Birch River	52 24 06	101 00 49	277
L Watson	52 01 29	104 34 21	533

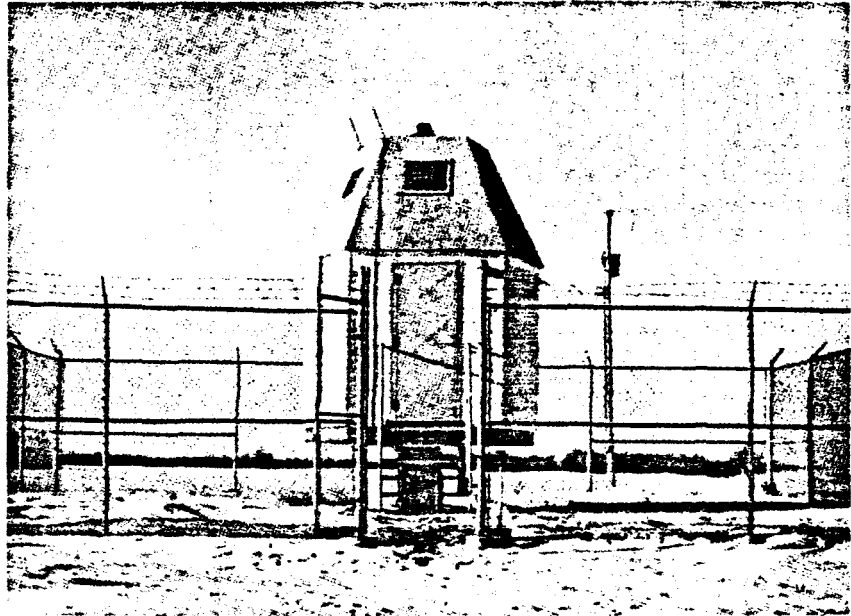


FIG. 2—The exterior of the MORP observatory near Langenburg, Saskatchewan. Note the meteor detector mounted on the roof of the building.

Observatories. Consideration of the area of sky covered by one camera led to a **decision** to use five **cameras** per station, each covering about **54°** of azimuth near the horizon. The **cameras** are positioned with the lower edges of their fields of view only **1°** or **2°** **above** the horizon and the upper edges near a **mean** elevation of **55°**. The unobserved zenith area of each station **is** surveyed by neighbouring stations, but **small triangular areas between** the fields of adjacent **cameras** and the horizon are not covered. The protective buildings were **chosen** to be pentagons in **spite** of some **slight** concern that local contractors might not be familiar with **72°** and **108°** combinations. Figure 2 shows the exterior of one of the observatories **under typical** winter conditions with a modest snow cover on the ground.

The observatory floor area **is** only **6.5 m²**. The roof has an almost **flat** central section, on which is mounted the **meteor** detector described below, and five **sides** which **slope** at **23°** to the vertical. Each window has an area of **1900 cm²** and is coated with a transparent but conductive coating which **carries** a **few** amperes of low-voltage **a.c.** power to keep the surface free of ice and dew. The building **is** heated or cooled, as necessary, by a **combina-**

tion heater and air conditioner. A security fence encloses the building and it has been a great relief that during the eight years of their existence, problems of vandalism and intrusion have been negligible at the observatories.

The cameras are mounted on a steel frame which is bolted to a concrete pedestal about 2.5 m above the floor. The pedestal goes down into the ground about 2 m and there opens into a flat base. This structure provides a very stable mounting for the cameras, independent of building vibrations. The floor is an integral part of the concrete pedestal about 1.5 m above ground: one result of this is that the building stands fairly high above the ground surface and turbulent dust- or snow-laden winds flow more easily past the building and cause less obscuration of the sky. Another result is that snowdrifts almost never block the door.

Cameras. The MORP cameras were specially manufactured by the Charles A. Hulcher Company of Hampton, Virginia, and use wide-angle Super-Komura 50-mm lenses. The film used is Kodak 70-mm Plus-X Pan in 100-foot rolls on the dimensionally stable Estar base. Each picture has, in the margin between frames, a camera identifier (station letter A to L and camera number 1 to 5) and three fiducial marks (see figure 3). Each fiducial mark consists of a 60-micron dot surrounded by four radial arms calling attention to it and the marks can be used to interrelate the measurements of two pictures from the same camera. This is useful if a meteor is photographed adequately itself but the picture lacks sufficient stars because of thin clouds or haze. One camera at each station records in one corner of the frame the time of the end of each exposure. Originally, time was recorded by a Bulova "accutron" clock with a 24-hour dial and a 999-day calendar, but a conversion to digital time displays is now in progress.

Each camera has been tested to determine the distortion in the pictures, since each lens has its own unique distortion pattern. The test setup in a gymnasium involved a horizontal array of forty precisely spaced lights, sufficiently distant from the camera to leave the focus at infinity. By tilting the camera, about thirty successive superimposed exposures were made until the entire frame of film was covered with a matrix of dots. Measurements of the dots were used to construct a contour map of the distortion, from which by interpolation a set of 841 pairs of numbers was extracted, representing displacement in X and Y co-ordinates all over the field. The computer program which calculates orbits and impact points looks up the distortion file of the relevant camera and adjusts all measurements to allow for this effect of the lens.

The cameras have a "sun shutter" in front of the lens to protect the lens

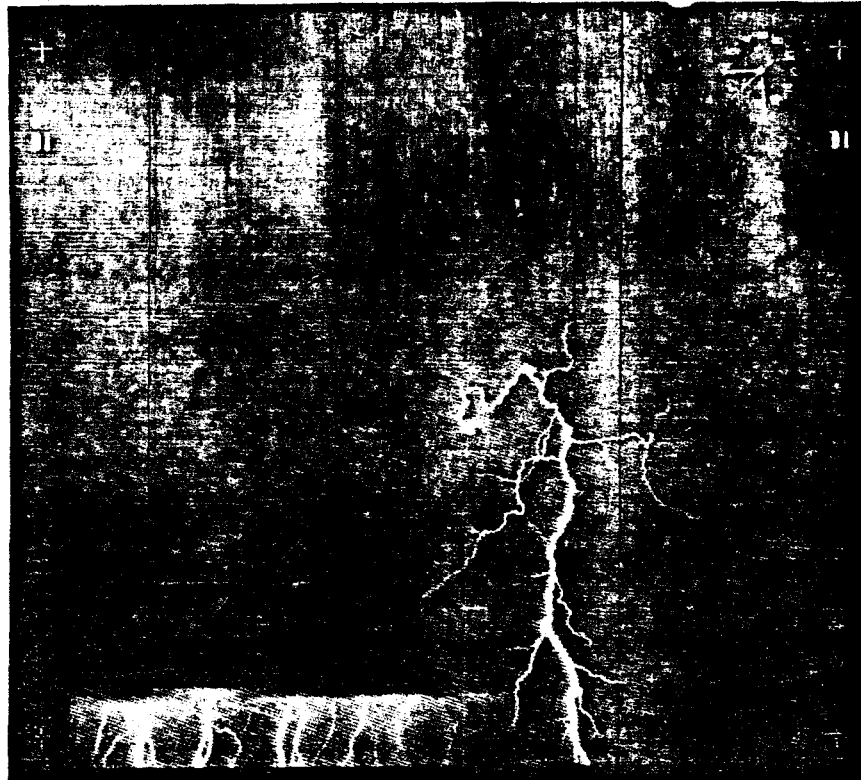


FIG. 3—Photograph taken during a thunderstorm, looking north from Lousana, Alberta. One nearby lightning flash contrasts with the numerous cloud-to-earth flashes in the background. This photo is from camera DI (camera 1 at station Di the same camera that later secured one of the photos of the Innisfree meteorite. The clock image records the time of the end of the exposure.

during daytime and a "masking shutter" which is normally open and closes only during film advances to prevent star images appearing dragged across the picture. The cameras also have a "chopping shutter", as is usual in meteor cameras, to break the meteor trail four times each second in order to give timed intervals on the trail photograph for use in determining velocity. The chopping shutter in the MORP cameras is a rotating wheel driven by a synchronous motor, but it is unique in having three equal sectors of different opacities. One sector is completely transparent and this is the only one that transmits significant starlight. Another sector is made of

filter material of density 5.0 (and supposedly neutral as to colour) which blocks out **all** but a most **unusually bright meteor** and has **blocked** out every **meteor seen** to date by the MORP cameras. The third sector has neutral density 2.0 (a reduction, in astronomical terms, of 5 mag) and will transmit enough light from a **very bright meteor** to make an image that may be more **suitable** for measurement **than** the overexposed image that came through the transparent sector. The **masking** shutter and the chopping shutter are both near the focal plane.

Meteor Detector. It is desirable to know the time of occurrence of each photographed **meteor since** the time is required in an exact **calculation** of the **orbit**. The problem is how to detect the occurrence. The **meteors** of **interest** are **bright**, but not in **comparison** to the sum of **all light coming** from the sky. Most **meteors** move **within** a limited range of angular velocities and this motion **is** their most distinctive characteristic. The MORP "**meteor detector**", designed by Spar Aerospace Products Limited of Toronto, looks for this motion. It consists of a light-sensitive photomultiplier tube (abbreviated PMT, model RCA 2067) **above** which are two coaxial **cones** of perforated **metal**, one larger and completely covering the other. The PMT **produces** a **current** proportional to the incident light. Any light that reaches the PMT must pass through **holes** in both **cones** and light from a **moving** source **such** as a **meteor** will find different combinations of **holes** in quick succession. The output of the PMT **will then** have a rapidly **varying** component. The PMT **is** connected to an electronic **filter** that passes only the range of frequencies from 1 to 10 Hz which has been deemed **appropriate**, based on typical **meteor** velocities and the geometry of the **meteor detector**. Therefore, provided only that the **meteor** has enough **brightness** to stand out **above** the integrated background **level**, the system **can detect it** and respond by printing the time of the event and advancing the film **after** a delay to **ensure** the **meteor** is not **still** in flight. This **should** protect what **is** expected to be a **valuable** picture. **All** pictures show the time at which the **exposure** ended, the only difference in the case of there having been a **meteor** signal is the appearance of a large marker at the edge of the frame (**to** upper left of the clock image in figure 3).

The **meteor detector is** tested about once a **month** by the station operator, who shoots up a **small rocket** flare of the type used for **distress signals**. The test is not a **perfect** simulation of a **meteor**, **because** at a distance sufficient to properly diminish the brightness the **entire** flight of the flare **would** be below the field of view of the **meteor detector (since** the detector **does** not look down to the horizon in **order** to avoid vehicle **lights**). The **operator** gets an indication that the system **is** working from a brief flash of the building **entrance** light.

Exposure Control. The electronics which control the camera operation were designed and produced by SED Systems Limited of Saskatoon. It is desirable to get as **much** exposure time on each frame as possible, but not to the point where a **meteor** image already on the film, or one about to arrive, would be obscured by **overall fogging**. An exposure control system **determines** the time at which each picture will end. Light from the **northern** sky (to avoid moonlight) **falls** on a **silicon** photodiode, but **first** the light has been **interrupted** at a **100-Hz** frequency by a driven-tuning-fork type of **beam** chopper. The current through the photodiode **is** proportional to the light brightness and **because** of the chopper **it is** an **alternating** current, which **is** convenient to amplify. After amplification, the signal **is** rectified by a synchronous transistor switch and the **resulting half-wave is** integrated by an operational amplifier. The output of the op-amp **is** a voltage which increases at a rate proportional to the area of the half-wave. When this voltage reaches a certain level it **triggers** a pulse of current from another op-amp. The **result is** that the **interval** between **these** pulses **is** proportional to the sky **brightness**. The pulses are counted and when a preset number of the **order** of a few hundred is reached, the film **is** advanced. Except for inaccuracies due to non-linearity of circuit responses, the time to reach a certain number of pulses will be proportional to the total accumulation of exposure on the film.

The pulses from the exposure control circuit are also used to determine when **cameras** should **start** and stop each day. As long as the rate of pulses exceeds a certain limit (about one pulse per second) the light level is so high that the resulting short exposures are uneconomical. **i.e.** less **than** 10 to 15 minutes in length. As the light decreases after sunset, the **cameras** are turned on when the pulse rate **is** slow enough; conversely, before **sunrise** the pulse rate increases and at the shut-down point the **cameras**, the **meteor** detector and the **exposure-control** circuit are de-activated for the **day**. **The** length of exposures will normally **vary** from about 10 minutes to **3** hours. To **minimize loss** of data due to electronic **failures**, there are safeguard circuits which prevent film-advance rates of more **than** two pictures in **20** minutes and limit the **duration** of any exposure to a maximum of 200 minutes.

Routine Procedures. Each observatory **is** visited about twice a week by an **operator** who lives **near** the station. Local residents were trained for this in a **few** hours and with the aid of a **manual** that covers routine and extraordinary procedures, **these** operators do an excellent job. In the **entire** history of the project only one **operator resigned** (he was transferred by **his regular** employer) and **one** passed the job to **his** son.

The operators push certain switches to elicit responses from the system

that indicate correct or improper functioning. They tune to WWV radio time signals and at a precise minute they push a switch to expose the clock on the film. In this way, when their reports are compared with the times read on the film, a continuous monitoring of clock errors is possible.

The 100-foot rolls of film last from three to six weeks, depending on the length of the nights at various seasons. The operators change the film when necessary and mail it to the Saskatoon headquarters of MORP in reusable aluminum cylinders. If a meteor of interest is reported by eyewitnesses, the exposed film may be removed prematurely and rushed to Saskatoon for prompt examination. The film is processed in an automatic processor that handles three rolls of film at a time, requiring three hours to a batch. After processing, the film is mounted on a five-film viewer especially built for this purpose. The five rolls that were exposed at one station at the same time are synchronized on this machine, since the time that applies to all five is recorded on only one of the films.

Each frame is examined for meteors and for data on sky conditions with the information entered directly at a computer terminal. The picture is considered to be subdivided into four parts, upper and lower portions of both left and right sides. The upper fields are that portion above 20° elevation while the lower fields are the portion between 8° and 20° in elevation. The criterion for classifying sky as clear is good visibility of star trails and the data are divided into half-hour intervals in the computer analysis with the predominant characteristic of an interval ascribed to the whole interval. The twenty areas of sky thus recorded for each station are used by the computer to calculate the total area of atmosphere, at an assumed height of 70 km, under observation by the network at any time. This data will eventually be combined with data on the distribution of observed meteors in order to derive meteor flux values.

Incidental Observations. A photographic monitoring of the sky will inevitably garner pictures of more than just meteors. The MORP cameras have provided some useful pre-discovery observations of a nova (Blackwell et al. 1975). The films have been searched for bursts of light that were at one time predicted to be associated with gamma-ray bursts (to no avail and the suspected association has now been virtually abandoned). They have never seen what is usually called an Unidentified Flying Object and surely this negative evidence should be considered in any discussion about the reality of UFOs. They have recorded some rather interesting – in fact, beautiful – pictures of lightning such as the example reproduced in figure 3.

The MORP cameras have also shown that, contrary to a widely-held belief, the sky in western Canada is not particularly clear and cloud-free.

As data began to accumulate, it became evident that the number of **hours of good** observing was less **than** expected. An analysis **is** now available for about 1000 days from March **1974** to December **1976**. The numbers derived are the number of half-hour intervals during which the sky was clear or cloudy at each of twelve typical locations in the **agricultural** area of western Canada. The **following** information has been extracted from about 64,000 **station-hours** of observing. The distribution by **categories** of sky condition is:

Category A - **virtually no clouds above 8°** elevation during a half-hour interval. 13%

Category B - **partly cloudy**, but in **at** least one of ten **azimuthal sectors** there is a patch of clear sky **above 20°** elevation lasting at least one-half hour. This category **includes** observations that would have been in category **A** except that some instrumental problem prevented a complete observation. Experience leads to the opinion that **such** problems should transfer about **4** percentage points from category B to category **A**. 22%

Category C - **completely cloudy** so that there was not even one sector that was clear for one-half hour. **Instrumental** problems enter to a small **extent** - if the sky had been clear in one **small** part which **happened** to be missed by a faulty **camera**, **then an interval** that should have just barely qualified as category B would have been reported as category C. We believe this situation should transfer less **than 2** percentage points from category C to B. 65%

The revised statistics, based on **these** adjustments for instrumental **problems** are:

Category A - virtually no clouds	17%
Category B - partly cloudy	20%
Category C - completely cloudy	63%

Before MORP was established, information about cloudiness was obtained from Environment Canada, as **it** is now known. The data at the available locations nearest to the MORP stations indicated the percentages of conditions as **follows**:

Category 1 - completely clear to 29% cloudy	42%
Category 2 - from 30% to 79% cloudy	16%
Category 3 - from 80% to 100% cloudy	42%

The MORP categories do not **coincide** with the Meteorological Branch's

categories, but one way to compare the two is by noting that category 3 is less frequent **than** category C, even though the former **is much** less **restrictive than** the latter (up to 20% **of the** sky may be clear for category 3 but sky better **than** about 3% clear would be **taken** into category B rather **than C**). In looking for explanations of the discrepancy, we note that the Environment Canada observations are made at **2300** and **0500** hours. Perhaps there **is** a systematic tendency for the sky to cloud over **after 2300** hours or clear before 0500 hours. Another possibility is that the years **1974** to **1977** were **cloudier than** the years 1951 to **1960**. Cloud statistics are **merely a peripheral interest** of MORP but **these** observations are noted here in case they may be of **interest** to meteorologists. More data are available on request.

The Fall of the Innisfree Meteorite.

Visual Observations. Camera networks **provide** more **accurate** data on the paths of bright **meteors than** do even a large number of **visual** observers but reports from eyewitnesses may be **crucial** in **initiating prompt** action. In the MORP system an unreported bright **meteor** might not be found on the films for over a **month**, so it is important to **learn** quickly that an interesting fireball has been **seen**. A **bright** fireball may be **seen** over **such** a large area that reports of it **may follow** a variety of routes before reaching interested scientists. **Such** was the case with the Innisfree fireball.

Among the groups of Canadians whose help in **reporting** bright **meteors** has been requested by the Associate Committee on Meteorites are **airline pilots** and crew. Obviously **pilots** are in a position to see the night sky **above** clouds and away from city **lights**. The crew of Air Canada's flight **167** from Winnipeg to Vancouver on **February 5, 1977**, observed the Innisfree **fireball above** clouds near **Swift Current**, Saskatchewan, about 470 km from the **meteor**. **They** gave a description of the event by radio to the control tower in Regina, which was promptly **relayed** to Mr. John Hodges of that city, a member of the Associate Committee for many years. He telephoned the **staff** of the MORP office in Saskatoon who immediately **took** action to **call** in the films from a few stations expected to **be** the **ones of interest** for the event. **Since** weather conditions in Saskatchewan were **generally cloudy**, local observations from the Saskatoon area would not have alerted the staff as quickly.

In Alberta the sky was clear and reports from observers near Edmonton were directed to **Professor** R. E. Folinsbee, initially as a **result** of interviews by the **Fort Saskatchewan Detachment** of the Royal **Canadian Mounted Police**. Rural police forces are another **valuable** source of **infor-**

mation on spectacular events and the Associate Committee has routinely sought their help. An appeal over local radio stations for observations produced more than a hundred responses of which seventeen with some possible value have been generously made available to us by Professor Folinsbee. Two other reports, one being the observation from the aircraft, were received in Ottawa through the reporting system.

Anticipating knowledge of the actual meteor path derived from the photographs we find that these visual reports come from distances varying between 2 and 304 km from the sub-meteor point at the time of maximum light. Six observers at four different locations were within 30 km of the ground path and an additional six were between 50 and 100 km distant.

One of the more lengthy reports is the result of an interview by the R.C.M.P. with Miss Brendalee Walker, age 13, who lives on a farm near Chipman, Alberta, about 77 km from the ground point beneath maximum meteor light. The report was made within an hour or two of the observation and is given here in full.

It was approximately 7:15 p.m. 5 February, 1977. and I was standing outside of the farmhouse. near the woodbox. Our farm is 1½ miles north. 2 miles east and 1½ miles north of Chipman, Alberta. I was looking north and I saw what appeared to be car lights shining off our gas tank. and when I looked up the whole east sky was lit up. There was a large spark and about six little ones trailing. They were heading east. They were all pure white and very bright. The large one was about the size of a large car and the rest were only small, about the size of basketballs. They were all in a straight line, going east and appeared to be only about 50 feet over the top of the trees. I don't have any idea how fast they were going. I saw them for at least 30 seconds and they were still moving when I got to the house. The sparks appeared to be falling pretty rapidly and were something like a plane landing. The sparks appeared to be travelling about 40 miles per hour.

Although it is not part of the verbatim report the accompanying police report quotes Miss Walker as also saying a swishing sound accompanied the lights but there was no large sonic boom. She did, however, run into her home long before these latter sounds would have had time to reach her. From the photographic record it is clear that the duration has been greatly overestimated in this report, which is a very common tendency. At the location of the observer the path would have appeared steeply inclined to the horizon with maximum light at an elevation near 24° in a direction 16° south of the easterly direction described. The similarity to an aircraft landing is enhanced by the low angular velocity (about 6° s⁻¹) for this observer.

Two other youthful observers of the Innisfree meteorite fall, Lyell and Martin Ferguson, ages about 10 and 8 years, were much the closest of any in the group of witnesses to the actual meteor path. They were walking

south on a road about 14 km north-northeast of Innisfree when the sky lit up behind **them**. One of them turned around to look for an **approaching** car but the fireball was so nearly overhead he did not see it **until** he was **again** facing **south**, when he observed fragments descending **high** in the sky in front of **him**. From the **photographic** record it is deduced they were within 2 km of the sub-meteor path, almost **under** the brightest point on the trail. There **is** some discrepancy in their estimates of just where the **light** disappeared but their favorable location minimizes the uncertainty involved. Both boys described a sonic boom "like distant **shooting** dying away to the southeast about 1½ minutes after the fireball".

The only other convincing report of sounds was an observation by Mr. Ken **McGillivray** who was located somewhat northeast of the town of Innisfree, about 11 km from the **late** portions of the sub-meteor path. He described two large fragments plus six to **eight** small **ones**, and after **going** in the farmhouse to describe the **meteor** to members of the **family**, he **again** went **outside**. By repeating his actions an **interval** of 1 minute 45 seconds was found between the **meteor** and the sound, **described** as "a **rumble**, then a **sharp rumble**, mellowed **rumbling** for 15 seconds, loud, then 5 seconds dying away". Another witness, in a schoolyard only a kilometre more distant from the path, heard no sounds.

The report of "swishing" sounds by Miss Walker may be a **valid** observation of the anomalous sounds which sometimes accompany the **luminous** phenomenon (Lamar and Romig 1964). Without confirmation from other observers this must remain **doubtful**. The more usual sounds of **rumbling** or distant explosions were definitely heard but apparently only in a small area near the end of the trail. It appears that the sounds were **much less** impressive **than those** recorded for many other **meteoritic** events. Reports of colour were few, with the "pure white" of Miss Walker's report, "a large red **ball**" by one of the **nearby** observers and finally a blue flash described by a **person** who was **indoors** with a window facing away from the **actual meteor**.

An analysis of **all** the **visual** observations would **certainly** have led searchers to the right area, due in considerable measure to a fortunate spacing of a few observers very close to the end-point and on opposite **sides** of the path. The **visual** end-point would appear to be defined within a **circle** of radius about 10 km, centred close to the actual location of the **fallen** meteorites. This is **several** kilometres beyond the point where the photographic **trails** end, but it **is** reasonable to suppose a nearby **visual** observer would have followed fragments to a lower luminosity **than** the **MORP cameras**.

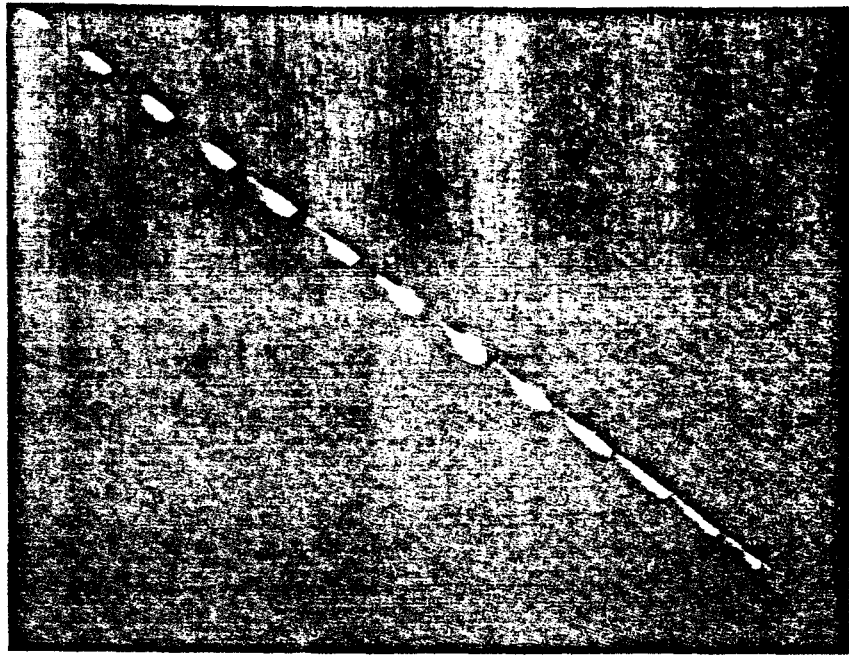


FIG. 4—The Innisfree meteorite in flight, from upper left to lower right, photographed from the MORP station at Vegreville. The rotating filter wheel produces 4 segments of trail per second. The bright stars crossing the meteor trail near the middle are Castor and Pollux. Note the evidence of separate fragments low on the path. The meteor entered the field at a height of 59 km and was observed over a path length of 37.8' in 3.82 seconds.

Photographic Observations. As a result of the visual report from the Air Canada-aircraft, the films from the four stations Watson, Asquith, Neilburg and Vegreville (see figure 1) were called in for immediate processing. The weather at the three Saskatchewan stations had been cloudy but the Vegreville films produced the bright meteor shown in figure 4. The early portion of the trail was lost in the station's blind spot above altitudes of 55° but nearly four seconds duration of trail was recorded. Near the bottom, several distinct fragments are visible and a significant decrease in angular velocity suggests a similar decrease in the linear velocity, an essential requirement for the survival of fragments as meteorites. The meteor detector at Vegreville had been activated by the fireball, establishing the exact time of some early portion of the bright part of the trail as 1977.6 February, 02^h 17^m 38^s U.T.

The main hope of obtaining a photograph from a second station now shifted to the Lousana station with some chance that the Brooks station might also have recorded it. **Since** it was known that the **operator** at Lousana was temporarily absent, **Eldon** Hubbs from the MORP office in Saskatoon made the long **drive** to Lousana and back on the **same day to retrieve** the films. When they were processed, a faint **meteor** image was found on the first exposure of the evening. Unfortunately this exposure suffered so severely from twilight sky fog that the only star image on the frame was a short trail of Polaris. Careful transposition of star **trails** from the next frame via the **fiducial** marks provided an adequate reference background for measurement of the **meteor** position. The **meteor** as **seen** from Brooks would have been lost in one of the small **triangular areas** between two camera fields and the horizon; however, **it** might not have been bright **enough** to be recorded **at** this station in any case, if conditions were not **ideal**. No other stations secured photographs so we are left with the minimum coverage for a complete reduction, **i.e.** two stations.

The two **meteor** photographs were measured in Saskatoon and the measures relayed to Ottawa by telephone. Due to **minor** modifications to the computer **program** it was temporarily not possible to **run** the **program** in Saskatoon. On February **14th**, computations on the N.R.C. computer in Ottawa indicated an end-point for the **longest surviving** fragment near a height of 20 km and a terminal velocity well below 4 km s^{-1} . **These** values are very **similar to** the terminal values for the Lost City meteorite, **19-km** height and 3.5 km s^{-1} (**McCrosky et al. 1971**), and **thus** provided the first evidence that a meteorite **fall** was probable. **Programs** of fireball **photography** have shown that many spectacularly bright **meteors** end at heights and **velocities** which are so high that the survival of any **material larger than** dust **particles is unlikely**. **Until** the height and velocity values were **available** on February 14 the **fireball** of February 5 was **merely** one of a group of **several interesting** fireballs **photographed** by the **network**, but the survival of this object to **such** a great depth in the atmosphere made an immediate search desirable.

Meteorite Search. **Before initiating** the field search, solutions of the dark-flight portion of the **trajectory** (below 20 km) were performed for three hypothetical meteorite **sizes**. The data on the atmospheric wind profile recorded at Edmonton about three **hours** before the **meteor** were used. The solution employs **these** data together with the known gravity and rotational values for the **earth** and calculates step by step the displacement due to **these** effects plus the ballistic drag for a spherical object **falling** through air

of known density at each height. The body size is represented by a **mass-to-area** ratio and values appropriate for stone **meteorites** of masses **10**, **4** and **0.5** kg were **chosen**, in the belief that **pieces** in this range **might** have survived and be in **observable** locations. Owing to two favorable aspects of the event, namely that the wind was **essentially a tail wind** which tends to keep **smaller pieces** from drifting far behind **larger ones**, combined with a steep path for the fireball (elevation of the apparent radiant 68°), the spread between the three hypothetical fragments was only 2 km on the ground. The predicted area of fall was in **farming** country about 13 km northeast of the small town of **Innisfree** which is situated on the main highway from Edmonton to Saskatoon.

On February 16 two of the **authors**, **Halliday** and **Giffin**, flew from Ottawa to Edmonton and proceeded to Vegreville by car **while Blackwell** and **Eldon Hubbs** drove from Saskatoon, **stopping** en route to assess the snow conditions in the predicted fall **area**. The fields were covered with 20 to 40 cm of moderately packed snow except on exposed **knolls** where the wind had reduced the snow cover and recent sunshine had **begun** to expose rocks and clumps of soil. Conditions appeared **suitable** for a search by snowmobile so that evening arrangements were made with young snowmobilers from Vegreville to **begin** a search the **following** morning.

The search began at **10:30 a.m.** on February 17, **using** four machines, three of them driven by local youths with the **authors** of this paper as passengers while the **fourth** was **driven** by **Eldon Hubbs**. Weather conditions were **quite** mild with daytime temperatures **near $+5^\circ\text{C}$** which **caused** some concern about overheating the **engines** and required minimum **cruising** speeds near **25 km hr^{-1}** . Traverses were run with spacings varying from 12 to 18 metres between successive runs, depending on the **amount** of **stubble** or other **material** breaking **the** snow surface.

The normal unit of **agricultural** area in western Canada is a quarter section, a square **0.5** mile on a **side** (805 metres), **so individual traverses** were **generally** of this length **unless blocked** by obstacles **such** as small patches of deciduous bush. With four machines **it** required an hour to cover each quarter section. Frequent stops were made to examine field **stones**, clumps of **soil** which appeared **quite** black due to the absorption of melted snow, and disturbances caused by the burrows of small **animals**. **At 4 p.m.** Halliday spotted a dark **object** some 5 or 6 metres to one **side** of the snowmobile track which, on **circling** back to examine **it**, proved to be the main **piece** of the meteorite resting on the snow, surrounded by **0.5** metre of dirty snow (**see** figure 5). Evidently the meteorite had penetrated the 30 cm of snow to the **frozen soil** and rebounded to the surface, bringing up some



FIG. 5—The main mass of the Innisfree meteorite is shown held just above the spot where it came to rest on the snow. Some dirt and meteorite chips are scattered around the spot as a result of bouncing off the field beneath the snow.

soil and knocking a few small chips off the meteorite. The meteorite was buried about half its own depth in the snow and would probably soon have been buried more deeply due to warming of the black exterior in sunshine.

The discovery of a meteorite in the field is a more concrete event than most scientific discoveries. The feeling of elation which accompanied the event may have been partially due to this effect but was more directly related to the fact that after nearly eleven years of planning, construction and operation of the camera network, a meteorite had now been observed and recovered very much according to the original plans. The meteorite was found during the search of the fourth quarter section after only four hours of actual searching, slightly less than twelve days after its fall. Figure 6 shows the search team at the site of the find.

The following day an agreement was signed with Mr. William Fedechko, owner of the land on which the meteorite was found, for the purchase of the meteorite "for a fair price to be determined after preliminary study of the meteorite". Accurate measurements were made of the location of the meteorite fall and the search was continued, with particular attention given to areas further along the path where somewhat larger pieces would be



FIG. 6—Six of the seven members of the search team shown with the four snowmobiles used in the search. From left to right, E. Hubbs, V. Kuzz, A. T. Blackwell, K. Fred. I. Halliday and M. Freed. with the photo taken by A. A. Griffin. The meteorite is seen in front of the third snowmobile from left, a small haversack used to protect the camera and maps lies to the left of the meteorite.

expected if they existed. The weight of the first specimen was 2.07 kg which, at the time, left doubt as to whether it was the largest surviving fragment. Nine quarter sections (5.8 km²) were searched by snowmobile but no other pieces were found. Professor Folinsbee and his students made a particular effort to locate areas where very small fragments (0.1 to 1-g range) might have been carried by the wind, but none was found. In consultation with Dr. Folinsbee it was agreed to propose the name "Innisfree" for the meteorite, in accord with the usual practice of choosing the name of a nearby town or village not previously used for naming another meteorite.

Careful study of the Vegreville photograph during March showed that at least five fragments had survived below an altitude of 25 km and probably something had reached the ground from each of these pieces, in addition to smaller pieces which would not appear individually on the photograph. The search effort was renewed in April once the snow had disappeared. A group of students led by Professor Folinsbee searched on April 9 and located a

small piece of total mass **33** grams. **although** it was fractured **into** many **pieces**. Its location was 600 metres back up the path from the original find, on land owned by a neighbour of Mr. Fedechko. Three days **later** Mr. Fedechko notified the MORP office in Saskatoon that three **pieces** with a combined weight in excess of a **kilogram** had been found by his family and **some** visitors. **all** on the **same** quarter section as the original find. **It** appears that two **of these** were found on **April 10** and the largest **of the** three on April 11. The MORP staff from Saskatoon returned to Innisfree the **following** week and a **sixth piece** of the meteorite was found by Blackwell on **April 21**. It was in numerous fragments, apparently the **result** of having been **run** over by a farm implement used in plowing a firebreak. The first **piece** found by the Fedechkos was in two fragments and the smaller of **these** was distributed as souvenirs, so the total weight of this **piece**, estimated as **120** grams, is **uncertain**. **Pieces** 4.5 and 6, in **order** of discovery, **weighed** 345, 894 and **330** grams. The total recovered mass is 3.79 kg and the **mean** coordinates of the fall are $111^{\circ} 20' 15''$ W, $53^{\circ} 24' 54''$ N. Major portions of the Innisfree fall will be located in the National Meteorite Collection at the Geological Survey of Canada, Ottawa, and in the collection of the University of Alberta, Edmonton.

Detailed study of the relationship between the **pieces** and the individual trails on the Vegreville **photograph** will be reported elsewhere. **It is** believed the five main **pieces** can be identified **individually** with the five trails observed on the photograph. The "ellipse of fall" is small, an area 400 by 500 metres can enclose the location of all the finds. The centre of this area is **only** 300 metres from the point predicted on February 14 for a 4-kg **piece**, the point which was used as a **rough** centre of interest in the original search.

The experience **gained** in the Innisfree search leads us to certain conclusions. Frozen soil is **obviously** a great advantage in keeping kilogram-size meteorites from burying **themselves** in the ground. The dark-flight **compu-**tation indicates the large **piece** struck the ground with a velocity near 70 m s^{-1} (**157 m.p.h.**) and required **130** seconds to fall after the light went out. The rebound phenomenon was especially **helpful** for this 2-kg specimen. If the smaller **pieces** also rebounded, **then** they were subsequently obscured by the snow before the search in **February**. **A similar** rebound effect was observed for some of the Bruderheim stones and also in at least one witnessed fall in the U.S.S.R. (**A. N. Simonenko**, **personal** communication). Meteorite searches on foot may be effective, as in the case of the **later pieces** of Lost City (**McCrosky et al.** 1971) but the **time** required to search an area of **several** square kilometres is very large. For winter searches we **believe** snowmobiles **offer** a great advantage in **agricultural** areas, **espe-**

cially if the location can be determined before fresh snowfalls occur. The sixth piece of Innisfree was found by an observer on the roof of a station wagon which was cruising slowly across the field. The added height for the observer above the ground is beneficial, even for quite small meteorites and we recommend this method where possible for searches on grazing areas or plowed fields.

It may be of interest to speculate on the role played by winter conditions on meteorite recovery in Canada. Innisfree is the eleventh Canadian "fall" for which the exact date of the event is known, as opposed to "finds" in which a meteorite is discovered by accident. If we ignore the three early falls before 1905 when population patterns were much different from the present, then the modern falls are: Dresden, Ontario, July 1939; Benton, New Brunswick, January 1949; Abee, Alberta, June 1952; Bruderheim, Alberta, March 1960; Peace River, Alberta, March 1963; Revelstoke, British Columbia, March 1965; Vilna, Alberta, February 1967; Innisfree, Alberta, February 1977. Six of these eight events were winter falls on snow-covered terrain. For Bruderheim, Revelstoke and Vilna, some or all of the meteoritic material was recovered from the ice on lakes or rivers. Two other Canadian meteorites, Great Bear Lake (June 1936) and Holman Island (March 1951) were recovered from seasonal ice surfaces so, although they are finds rather than falls, the ice conditions were a vital factor in their recovery and establish the dates of the fall within a few months. A survey of worldwide dates of meteorite falls shows no preference for northern hemisphere winter months so the apparent preponderance of winter events among Canadian falls is attributed to a better chance of recovery when frozen soil and ice leave the meteorites in a more visible situation.

The Innisfree Meteorite.

Description. The Innisfree meteorite is a rather normal stone meteorite of the low-iron (1.-type) or hypersthene chondrite group. Detailed classification is not yet complete and the final designation may be L4 or L5 although it may prove not to be typical of any one subclass. The individual pieces were covered with the usual thin, black fusion crust, about 0.3 mm in thickness. Most pieces were of a chunky shape with rather flat sides and angular corners. There is no obvious indication that the pieces fit together and they would not be expected to fit, since study of the meteor photograph indicates they separated at a variety of heights while ablation was still very active. One face of the main piece shows an area of partial fusion crust

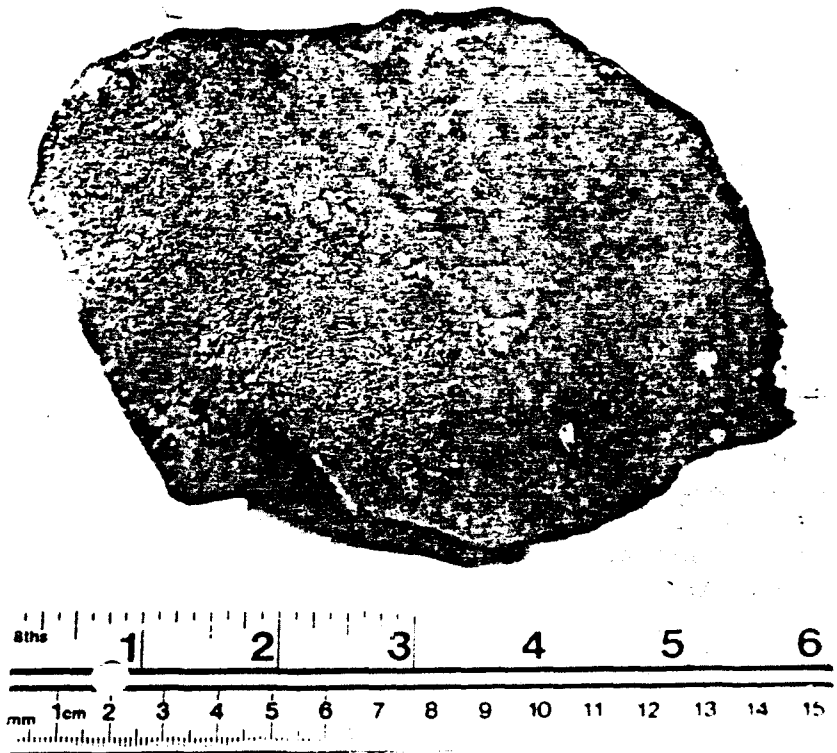


FIG. 7—The 2-kg piece of the meteorite photographed seven hours after recovery. The dark fusion crust exhibits a fine pebbled texture on the vertical face, a network of hairline cracks on the upper surface and a potential fracture near the corner in the right background. The scale shows inches (upper) and cm (lower).

where a **thin** layer may have broken off when the **velocity** was **just too** low to generate a fresh **crust**. Figure 7 shows a view of the main **piece** photographed late on **February 17, 1977**, about seven hours after it was found.

Various types of technical studies have been undertaken on samples of the Innisfree **meteorite** at different laboratories in **several** countries and the results **will** appear in technical journals. One important class of study is the

TABLE II
ORBIT OF INNISFREE METEORITE

Semi-major axis	<i>a</i>	1.872 AU
Eccentricity	<i>e</i>	0.4732
Inclination	<i>i</i>	12.27°
Argument of perihelion	<i>ω</i>	177.97°
Longitude of asc. node	<i>θ</i>	316.80°
Perihelion distance	<i>q</i>	0.986 AU
Aphelion distance	<i>q'</i>	2.758 AU
Period	<i>P</i>	2.561 yr

measurement of the weak radioactivity produced in the meteorite in space by the bombardment of cosmic rays. There is a very wide range of half-lives for the isotopes which may be produced so it is important to have such measures made as soon as possible after a fresh meteorite is recovered. For this reason the main mass of the meteorite was taken by Halliday to the Battelle Pacific Northwest Laboratories in Richland, Washington, on February 19 and measures of the radiation began exactly two weeks after the fall of the meteorite. These measures have revealed at least one interesting anomaly in Innisfree, indicating it has been subjected to a high level of cosmic radiation in the relatively recent past (Rancitelli and Laul 1977).

The Orbit. Pribram, Lost City and Innisfree are the three meteorites for which two-station photography provides a reliable orbit and much of the interest in Innisfree depends on this fact. The cosmic-ray effects mentioned in the previous section are of much greater interest when the recent orbit of the meteorite is known and the same is true for studies of thermal effects to which the meteorite has been subjected in space.

The Innisfree meteorite entered the atmosphere with a velocity of 14.5 km s⁻¹ from a geocentric radiant, corrected for earth rotation and gravity, at $\alpha_{1950} = 6.66^{\circ}$, $\delta_{1950} = 66.21^{\circ}$. The orbital elements derived from these data are listed in Table II and the orbit is shown in figure 8 relative to the orbits of the inner planets. The orbits of Pribram and Lost City are also shown, neglecting the modest inclinations of the meteorite orbits. Innisfree had a low-inclination, direct orbit with perihelion very close to the earth's orbit and aphelion well beyond Mars, in the asteroid belt. It is typical of the orbits believed to pertain to meteorites in general, for which an asteroidal origin is increasingly supported by current research.

Many of the numerical quantities relating to the fireball and the fragments of the Innisfree meteorite are collected together in Table III for convenience.

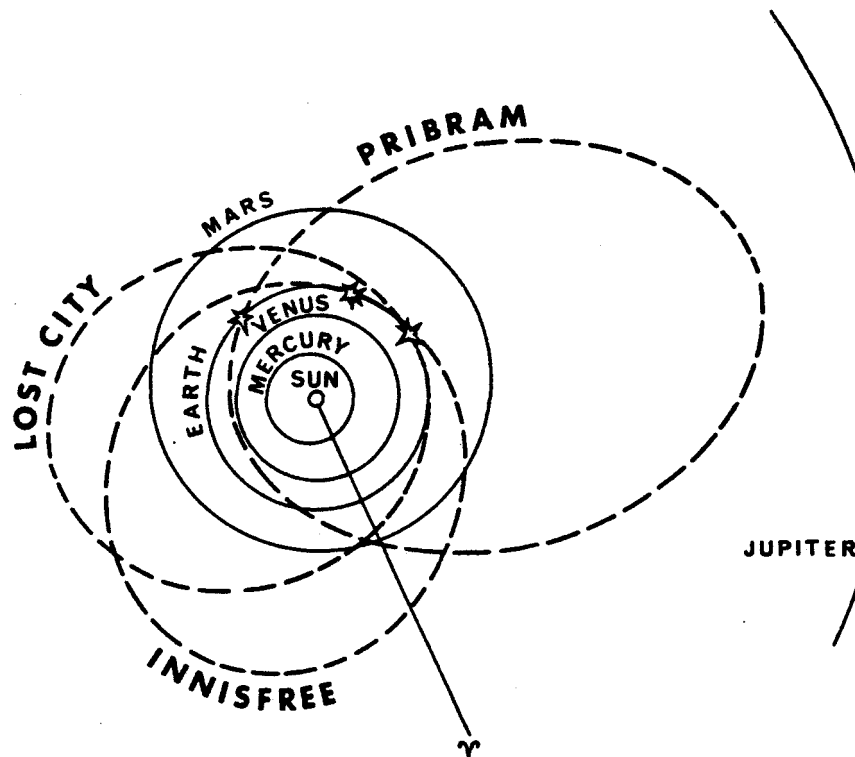


FIG. 8—The orbits of the Pribram, Lost City and Innisfree meteorites are shown projected on the ecliptic plane relative to the orbits of the five inner planets. The direction to the first point of Aries is also indicated.

TABLE III
SUMMARY OF DATA ON INNISFREE METEORITE

Time of meteor	1977, February 6, 02 ^h 17 ^m 38 ^s U.T.
Recovery of first piece	1977, February 17, 23 ^h U.T.
Mean co-ordinates of fall	$\phi = 53^{\circ}24'54''$ N; $\lambda = 111^{\circ}20'15''$ W
Masses of fragments	2.07; 0.033; 0.120; 0.345; 0.894; 0.330 kg
Total mass recovered	3.79 kg
Pre-atmospheric velocity	14.54 km s ⁻¹
Terminal velocities from photos (five fragments)	2.7 to 4.7 km s ⁻¹
Beginning height (Lousana)	62.4 km
End height (Vegreville)	19.9 km
Duration of photographed trail	4.09 s
Corrected geocentric radiant (1950)	$\alpha = 6.66^{\circ}$; $\delta = 66.21^{\circ}$
Elevation of apparent radiant	67.8°

Acknowledgements. The authors are indebted to many groups and individuals for their **co-operation** and interest. The **friendly advice** and encouragement received from Dr. Richard E. McCrosky of the Smithsonian Astrophysical Observatory, Cambridge, Massachusetts and Dr. Zdenek Ceplecha of the **Ondrejov** Observatory, Czechoslovakia, were of **great** value at **all** stages of the project. We particularly wish to commend the local operators of the **MORP** stations for their loyal service to the **program** over the years and also the two technicians involved with the **project**, Mr. Norman Dyrvik and Mr. **Eldon** Hubbs, for their numerous contributions. **The** assistance of **all those** who contributed **visual** observations was **much** appreciated and **our** thanks are extended to the chauffeurs of the **snow-**mobiles used in the search. We congratulate Mr. Fedechko and his family on their **proficiency** in **finding** meteorite fragments and thank him for his co-operation with **all** aspects of the search. It was a pleasure to continue a longstanding association with Professor Folinsbee and we are indebted **to** him and his students for the **visual** observations collected by them and placed at **our** disposal. The assistance and **advice** of Dr. A. G. Plant, Dr. R. J. **Traill** and Mr. H. R. Steacy of the Geological **Survey** of Canada **is** also **gratefully** acknowledged.

REFERENCES

- Blackwell, A. T., Feldman, P. A., Griffin, A. A.** and Halliday, I. 1975. *J. Roy. Astron. Soc. Can.*, 69.241.
- Ceplecha, Z. 1961, *Bull. Astron. Inst. Czech.*, 12.21.
- Ceplecha, Z. and **Rajchl, J.** 1965, *ibid.*, 16. 15.
- Folinsbee, R. E. and Bayrock, L. A. 1961, *J. Roy. Astron. Soc. Can.*, 55.218.
- Folinsbee, R. E. and Bayrock, L. A. 1964, *ibid.*, 58. 109.
- Folinsbee, R. E., Bayrock, L. A., Cumming, G. L. and Smith, D. G. W. 1969, *ibid.*, 63.61.
- Folinsbee, R. E., **Douglas, J. A. V.** and Maxwell, J. A. 1967, *Geochim. Cosmochim. Acta*, 31, 1625.
- Halliday, I. 1973 in *Evolutionary and Physical Properties of Meteoroids*, ed. C. L. Hemenway, P. M. **Millman** and A. F. Cook. NASA SP-319. Washington. p. 1.
- Hindley, K. B. 1975, *J. Brit. Astron. Assoc.*, 85, 150.
- Lamar, D. L. and **Romig, M. F.** 1964, *Meteoritics*, 2. 127.
- McCrosky, R. E. and Boeschstein, H. Jr. 1965, *Smithsonian Astrophys. Obs. Spec. Rept.*, no. 173.
- McCrosky, R. E., Posen, A., Schwartz, G. and Shao, C.-Y. 1971.1. *Geophys. Res.*, 76.4090.
- Rancitelli, L. A.** and **Laul, J. C.** 1977. *Meteoritics*, 12.346.
- Zotkin, I. T., Simonenko, A. N., Fedynsky, V. V., Khotinok, R. L.** and **Kramer, E. N.** 1976. *Meteoritica*, no. 35, 3 (in Russian).

COLOMBIE

Paris, le 20 Avril 1982

No 403

Monsieur François LOUANGE
Ingénieur-Conseil
9, Rue Sainte-Anastase
75003 PARIS

Monsieur,

En réponse à votre lettre du 19 Courant,
je me permets de vous conseiller de vous mettre en
rapport directement avec l'Organisme :

⊗ " COLCIENCIAS "
FONDO COLOMBIANO DE INVESTIGACIONES
CIENTIFICAS
Transversal 9A No 133-28 BOGOTA
Rép. de Colombie

En ce qui concerne la protection de l'environne-
ment, vous pouvez écrire à

⊗ INSTITUTO NACIONAL DE LOS RECURSOS NATURALES
RENOVABLES Y DEL AMBIENTE " INDERENA "
Apartado Aéreo 13458
BOGOTA

distinguées.

Hernán Tovar
Hernán Tovar
Ministre Plénipotentiaire

22, Rue de l'Elysée 75008 Paris

Paris, le 21 Avril 1982

No 491


Monsieur François LOUANGE
Ingénieur-Conseil
9, Rue Sainte-Anastase
75003 PARIS

Monsieur,

Je vous confirme la lettre que je vous ai adressé hier et vous engage à vous mettre également en rapport avec l'Organisme :

⊗ INSTITUTO DE ASUNTOS NUCLEARES
Avenida El Dorado Carrera 50
BOGOTA

Veillez agréer, Monsieur, mes salutations
empressées.


Hernán Tobar
Ministre Plénipotentiaire



El presidente del Comité Científico de la Organización Europea de Investigación Espacial, Eduardo Amaldi, asistió a la inauguración del Taller de Ondas Gravitacionales organizado por la Asociación del Centro Internacional de Física. El certamen se desarrolla en el Instituto de Asuntos Nucleares. En la gráfica se aprecia a los científicos Galileo Violines, Ernesto Villarreal y Eduardo Posada. (Foto de Jaime Niño).

Comenzo Taller sobre ondas gravitacionales

Comenzo en Bogotá el Taller sobre Ondas Gravitacionales, organizado por Acif, Asociación Pro-Centro Internacional de Física, en el cual participa un grupo de profesores italianos especialistas en este campo.

El Taller, que durará hasta el 7 de abril, estará centrado en los métodos experimentales para detectar las ondas gravitacionales, cuya existencia esta prevista por la teoría pero no ha podido ser confirmada hasta la fecha. „Las ondas gravitacionales son el equivalente a las electromagnéticas pero referente al campo gravitacional. La teoría de la relatividad las ha previsto, pero no se han detectado en la tierra.

El curso esta dirigido a los estudiantes de post-grado de diferentes universidades de Colombia y de República Dominicana y se desarrollará en la sede del Instituto de Asuntos Nucleares.

El Grupo de Investigación de Ondas Gravitacionales de Roma participara activamente y actuaran como confe-

rencistas los físicos italianos Amaldi, Pallotino, Ricci, Pizzella y Galileo Violini.

El Taller es la primera actividad que desarrolla este año Acif y cuenta con el apoyo de Colciencias, el Icfes, IAN y la Universidad de Roma.

La creación de un Centro Internacional de Física en Colombia fue acordada a principios del año pasado como resultado del Encuentro Mundial de Físicos, organizado por la Universidad de Los Andes y la Sociedad Colombiana de Física.

Los objetivos de Acif son: promover la investigación científica en los países en vía de desarrollo y en particular de la Región Andina, de Centro América y del Caribe; establecer un foro internacional para fomentar los contactos entre científicos de los países desarrollados y en vía de desarrollo, y colaborar con la comunidad científica para que logre su entrenamiento y la consecución de los elementos adecuados para la investigación.



INSTITUTO DE ASUNTOS NUCLEARES

ADSCRITO AL MINISTERIO DE MINAS Y ENERGIA

Apartado Aéreo 8595

BOGOTÁ, D. E. COLOMBIA

Oficio D-1672

1° de julio de 1982


Señor
FRANCOIS LOUANGE
Ingénieur - Conseil
9, rue Sainte-Anastase
75003 - PARIS
FRANCIA

Estimado señor Louange:

En atención a su nota del 21 de mayo quiero manifestarle que no tenemos conocimiento sobre sistemas de **detección de fenómenos aeroespaciales raros** en el Instituto de Asuntos Nucleares de Colombia.

Le sugiero escribir al Departamento Administrativo de Aeronautica Civil o al Instituto Geofísico de los Andes, en las siguientes direcciones: **Aeropuerto Internacional Eldorado y carrera 7a. N° 40-62, respectivamente.**

Atentamente,


ERNESTO VILLARREAL SILVA
Director General

EVS/idel



REPUBLICA DE COLOMBIA.

Departamento Administrativo de Aeronáutica Civil

AEROPUERTO EL DORADO - BOGOTÁ, D.E. - COLOMBIA

DE-0605-82

BOGOTÁ D.E. 04 DE AGOSTO DE 1982

Señor
FRANCOIS LOUANGE
9, rue Sainte-Anastase
75003 Park

REF: Su carta 11/07/82.-

Atendiendo a su solicitud realizada para que le sea suministrada información técnica sobre los sistemas de detección utilizados en Colombia por la Aeronáutica Civil, muy comedidamente le informo lo siguiente:

El país cuenta con sistemas de radar tipo LP23 y TA10B de origen francés y cuyas características son:

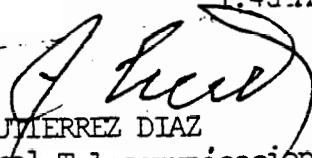
- Sistema TA10 B

Banda de frecuencia	S
Alcance	6 ^o MN
Ancho de pulso	$\tau = 0.75$ Mseg.
Período de repetición	$T = 1$ Mseg
Potencia pico	550 KW
Quantum de tratamiento	0.36 Ms

- Sistema LP23

Banda de frecuencia	L
Alcance	200 MN
Ancho de pulso	3 Mseg.
Período de repetición	$T = 330$ MS
Potencia pico	2 MW
Quantum de tratamiento	1.45 MS

Atentamente,


ALIRIO GUTIÉRREZ DÍAZ
Director General Telecomunicaciones
y Ayudas a la Navegación Aérea

D A N E M A R K

KONGELIG DANSK AMBASSADE
AMBASSADE ROYALE DE DANEMARK
PARIS

Monsieur François LOUANGE
9 rue Sainte-Anastase
75003 PARIS

77, AVENUE MARCEAU. 75116 PARIS
TELEPHONE: 723.54.20
ADR. TELEGR.: AMBADANE
TELEX: 620172

gennemsiag
copie(s)

bilag
annexe(s)

J. nr.:
Réf.: 46. Dan. 6/5

Dato
Le 28 Avril 1982

Monsieur,

En réponse à votre lettre du 19 courant au sujet d'une étude sur la détection des phénomènes aérospatiaux rares, nous vous proposons de vous adresser aux organismes danois cités ci-dessous:

DANSK RUMFØRSKNINGSINSTITUT

⊗
Lundtoftevej 7
2800 Lyngby

(Centre danois d'Etudes spatiales)

FORSØGSANLÆGGET RISØ

⊗
4000 Roskilde

(Institut de Recherches scientifiques Risø)

Dans l'espoir que vous obtiendrez les renseignements souhaités et en vous conseillant de rédiger votre demande de préférence en anglais, nous vous prions d'agréer, Monsieur, l'assurance de notre considération très distinguée.



Elisabeth MANFORD-HANSEN
Déléguée Commerciale

RISO



Riso National Laboratory

Postbox 49
DK-4000 Roskilde, Denmark
Phone +45 2 37 12 12, Telex 43 116
Cable address: Risatom

Date June 3, 1982
Your ref. .
Our ref. **SEL/BSJ**
Dept. 06-Physics

Mr. **Francois** Louange
9, Rue Sante-Anastase
75003 Paris
France.

Dear Mr. Louange,

Thank you for your **letter** requesting information on instruments, used for detecting rare aerospace phenomena.

I only know of one organization engaged in **such** studies in Denmark: The **Scandinavia** UFO Information. They **sell to** their **members** a simple **instrument** used to detect changes in the **magnetic** field. I do not know if your are interested in contact with **such** organizations. If so the **name** and address of the **chairman** is:

Mr. Flenning **Ahrenkiel**
Holmevangenget 5
DK-2970 Hørsholm
Denmark

Sincerely yours,


Søren E. Larsen

E Q U A T E U R



EMBAJADA DEL ECUADOR EN FRANCIA

N°4-8-95/82

Paris, le 7 Juin 1982

Monsieur François LOUANGE
Ingénieur Conseil
9, rue Saint Anastase
75003 PARIS

Monsieur,

J'ai le plaisir d'accuser réception de votre lettre du 19 Avril 1982, concernant la détection des phénomènes aérospatiaux rares en Equateur.

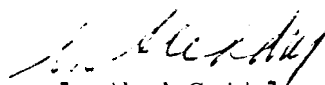
Je regrette de ne pouvoir vous donner d'indications à ce sujet et vous conseille de vous adresser directement à :



Señor Secretario Ejecutivo del
Consejo Nacional de Ciencia y Tecnología (CONACYT)
Arenas y Larrea
Edificio Consejo Provincial
Apartado C 0028
QUITO EQUATEUR

en lui exposant votre intérêt pour cette question.

Je vous prie de croire, Monsieur, à l'assurance de mes sentiments les meilleurs.


Gonzalo Abad Grijalva
Ambassadeur

ESPAGNE



AM mjb

Embajada de España

No 385

Paris, le 27 avril 1982

Monsieur François LOUANGE
Ingénieur - Conseil
9, rue Sainte Anastase
75003 Paris

Monsieur,

J'accuse réception de votre lettre du 19 courant et j'ai le plaisir de vous informer que je n'ai pas manqué de transmettre son contenu aux autorités espagnoles compétentes à Madrid.

Dès qu'une réponse me sera parvenue, je m'empresserai de vous la communiquer.

Dans cette attente, je vous prie de croire, Monsieur, à l'expression de mes sentiments distingués.

Arturo Morales

Ministre Chargé des Affaires Culturelles

E T A T S - U N I S

NASA European Representative

The American Embassy
2 Ave. Gabriel
75008 Paris. France



Reply to Attn of **AMP**

Mr. Francois Louange
Ingénieur-Conseil
9 rue Sainte Anastase
75003 - Paris

Paris, Le 29 Mai 1982

Monsieur,

En espérant que vous voudrez bien nous pardonner le retard avec lequel nous répondons à votre lettre du 19 avril, retard dû à une erreur d'acheminement du courrier, je vous envoie l'adresse d'un organisme aux États-Unis qui s'occupe de la détection des phénomènes aérospatiaux:

SCIENTIFIC EVENT ALERT NETWORK (SEAN)
National Museum of Natural History
MRC 129
10th St. & Constitution Ave., N.W.
Washington D.C. 20560
(David R. Squires, Operations Officer)

Tel: (202) 381 - 4174

Cet organisme a été fondé en 1975. Il fait partie du Musée National d'Histoire Naturelle. SEAN rassemble des éléments d'information sur ces phénomènes qui sont ensuite transmis à des savants, qu'il s'agisse d'éruptions volcaniques, de tremblements de terre importants ou inhabituels, de chutes de météorites, ou de tout autre événement de cette nature.

J'espère que l'adresse ci-dessus vous sera utile, et je vous prie d'agréer, Monsieur, mes salutations distinguées.

Anne M. Pérouse
Bureau du Représentant Européen de La NASA

Tel: 296-1202 Poste 2641



National Museum of Natural History • Smithsonian Institution

WASHINGTON, D.C. 20560 • TEL. 202-357-1511

Mail Stop 129

June 23, 1982

Francois Louange, Ingenieur-Conseil
9, rue Sainte-Anastase
75003 Paris, France

Dear Mr. Louange,

Thank you for your **letter** of June 1, seeking information for the GEPAN study on the detection of rare aerospace phenomena. On June 3, I met with Dr. **Alain Esterle**, the manager of GEPAN. We discussed the study and I provided him with detailed information on detection systems and other matters relevant to GEPAN's work, including **names**, addresses, and telephone **numbers** of system managers and other sources of information. Fortunately, we had plenty of time (about 2 hours) and we were able to complete **our** discussion. Therefore, I do not now have any more information that I think would be **useful** to you.

The GEPAN study is clearly a **valuable** project and I hope that I have been of some help.

Sincerely,

Lindsay McClelland

GRANDE - BRETAGNE



Ambassade de Grande-Bretagne

35 rue du Faubourg Saint-Honoré - 75383 Paris Cedex 08

Tdrx 650264 (indicatif INFORM 650264) -- Téléphone : 266.9142

M. François Louange,
Ingénieur - Conseil,
9, rue Sainte-Anastase,
75003 Paris.

Votre référence

Notre référence Sc 274/2

Date le 1 juillet, 1982

Monsieur,

Suite à votre lettre du 19 avril au sujet des **phénomènes** aérospatiaux, j'ai pris contact avec le 'Science and Engineering Research Council' en Angleterre pour essayer de vous mettre en rapport avec les personnes que travaillent dans le domaine de l'espace en Grande-Bretagne.

Je vous prie de bien vouloir trouver ci-joint la liste des noms et adresses de ces personnes, établie par le Dr Payne du SERC.

Le Dr Payne a également indiqué, dans chaque cas, la spécialité précise en expliquant brièvement les activités de ces spécialistes.

Surtout n'hésitez pas à me contacter pour tous renseignements complémentaires. Dans l'espoir que ces quelques informations vous seront utiles, je vous prie de croire, Monsieur, à l'assurance de ma considération distinguée.

Cathy James

P.P. A G Owen
(Premier secrétaire Technologie)

10.dit 1982/13

DR B R MARTIN —

**DETECTION OF RARE SPACE PHENOMENA: LETTER FROM MR A G OWEN -
BRITISH EMBASSY, PARIS**

In reply to the query from M **Francois** Louange, we **can** point out that:

1. Meteorites

Dr **R** Hutchison, British Museum (**Natural History**) is curator of the National Meteoritic Collection, one of the two major collections in the world. As curator, Dr Hutchison keeps extensive (and **historic**) documentation of observed **falls**. He **can** also probably **advise** M Louange as to how to contact Home Office **records** on sightings of other **unusual** phenomena.

2. Comets

These are rare space phenomena on a **visual** scale. In the **UK**, **comet** watches are **organised** by **Dr K Waterfield** from his **private** observatory in Wiltshire, and also by **Mr Miles** of the British Astronomy Association - part of the BA.

3. Detection Systems

Amateur **observers**, **organised** through the Royal Society by **M** Wigley, play a special role in **optical tracking** of near Earth spacecraft. **These** observations are technically managed by Dr C Brookes of Aston University. In addition **to** satellite predictions, Dr Brookes is responsible for two, 1 metre Schmidt **photographic tracking cameras**, one in UK, the other for **S Hemisphere** observations from Siding Spring, Australia. Aston also **receives** non-classified NATO radar observations of spacecraft (**NORAD**).

4. RGO

Like the Royal Society, the Royal Greenwich Observatory **is** a treasure house of information on rare sightings of **all** kinds: Dr Wilkins **of** RGO **can** **advise**.

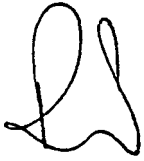
5. Sightings of Unusual Electrical Phenomena

Dr T E Allibone, FRS (now **retired**) **is** a world authority on sightings of unusual **electrical phenomena** - ball lightning etc. He **can** **advise** on where **such** sightings are documented.

6. Names and Addresses

Dr **R** Hutchison; British Museum, Cromwell Road, **SW7** 5BD
 Dr **K** Waterfield, **Woolston Observatory**, North Cadbury, Yeovil, Somerset
 Mr **H G** Miles, Coventry Polytechnic, Priory St, Coventry **CV1** 5FB
 Mr **P** Wigley, The Royal Society, 6 **Carlton House Terrace**, London **SW1Y** 5
 Dr **C** Brookes; **St Peters** College, College Road, Saltley, **Birmingham**
 Dr Wilkins, RGO, **Herstmoncuex** Castle, Hailsham, East Sussex
 Dr **T E** Allibone, York Cottage, **Lovel** Road, Winkfield, Windsor

7. I suggest that Dr Atkinson briefly replies to Mr Owen, appending this minute by way of explanation.



DR R M PAYNE
Secretary, SSC
15 June 1982

H O N G R I E

INSTITUT HONGROIS

7, RUE DE TALLEYRAND

75007 PARIS

TÉL. 333-23-82 à 333-23-86

Paris, le 22 avril 1982.

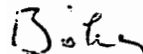
M. François LOUANGE
ingénieur - conseil
9 rue Sainte-Anastase
75003 Paris

Monsieur,

J'ai bien reçu votre lettre du 19 ct. concernant
une demande d'information au sujet de la détection
des phénomènes aérospatiaux rares.

Ne connaissant pas le sujet, **j'ai** transmis votre
courrier aux autorités hongroises pour obtenir une
réponse valable. Je vous **communiquerai** celle-ci
dès que **possible**;

Veuillez agréer, Monsieur, l'expression de mes
sincères salutations .



András BÓKA
attaché scientifique

I N D O N E S I E

AMBASSADE D'INDONÉSIE
49, RUE CORTAMBERT - 75016 PARIS
TEL : 503-07-60

Service Pédagogique et Culturel
No.: 0636/DIKBUD/IV/82.

Paris, le 23 avril 1982.

Monsieur François LOUANGE
9, Rue Sainte-Anastase
75003 P A R I S

Monsieur,

En réponse à votre lettre du 19 avril 1982,
j'ai le plaisir de vous communiquer l'adresse de :

L A P A N (Lembaga Antariksa dan Penerbangan
Nasional)
(= Institut d'Aérospatial et d'Aéronautique
National)

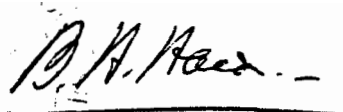
Jalan Pemuda

JAKARTA - TIMUR I N D O N E S I A

où vous pourrez, à mon avis, avoir des informations concer-
nant la détection des phénomènes aérospatiaux rares. Et il
serait souhaitable que vous exposiez vos désirs en anglais.

En vous remerciant de votre attention, je vous
prie de bien vouloir agréer, Monsieur, l'expression de mes
sentiments distingués.

Pour l'Ambassadeur,
Le Chef du Service Pédagogique et Culturel,


Benny Hoedoro HOED
Conseiller Pédagogique et Culturel.-

NOUVELLE ZELANDE



41/7/1

NEW ZEALAND EMBASSY
7^{ème}, RUE LEONARD DE VINCI
75116 PARIS

Paris, le 30 avril 1982

Monsieur,

Je vous remercie de votre lettre du 19 avril concernant l'étude que vous êtes chargé à effectuer sur l'état actuel des recherches dans la détection des phénomènes aérospatiaux rares.

J'ai transmis votre lettre aux **autorités** compétentes en Nouvelle-Zélande, et dès que j'aurai reçu leur réponse, je vous en ferai part.

Je vous prie d'agréer, **Monsieur**, l'expression de ma considération distinguée.

Diane Wilderspin

(Diane Wilderspin)
Premier Secrétaire

Monsieur François LOUANGE,
Ingénieur - Conseil,
9, rue Sainte Anastase,
75003 PARIS.

P A Y S - 3 A S

AMBASSADE VAN HET KONINKRIJK DER NEDERLANDEN

AMBASSADE ROYALE
DES PAYS-BAS

No. 54.7.4....

Paris, le 4 .mai 1982.....
7, rue Eblé (75007)
tél. 306.61.88

Monsieur,

En réponse à votre lettre du 19 avril dernier je vous suggère de vous mettre en rapport avec les associations suivantes:

- ⊗ - L'association Terre et Cosmos:
Aarde en Kosmos
Postbus 108
1270 AC Huizen (N.H.)
- ⊗ - Association néerlandaise aérospatiale
Nederlandse Vereniging voor Ruimtevaart
Nachtegaalstraat 82 bis
3581 AN Utrecht

ainsi qu'avec les observatoires planétaires néerlandais dont je vous cite les adresses ci-après:

- ⊗ - Radiosterrenwacht Westerbork
Schattenberg 1
Zwiggel
Westerbork
- ⊗ - Sterrenwacht Kapteyn
Mensingeweg 20
9301 KA Roden.

Je vous signale également la Commission interdépartementale pour les Etudes et la Technologie Spatiales:

- ⊗ - Interdepartementale Commissie voor
Ruimteonderzoek en Ruimtetehnologie
Postbus 20101
2500 EC 's-Gravenhage.

'Veillez agréer, Monsieur, l'expression de mes sentiments distingués.

M. François Louange
, rue Sainte-Anastase
75003 Paris


C.J. Huijbregts
Chef du Service d'Information



Kapteyn Sterrenwacht

der Rijksuniversiteit te Groningen
Mensingheweg 20 - 9301 KA Roden - Nederland
Telefoon (0)5908-19631

June 11, 1982

Mr. **François** Louange
9, rue Sainte-Anastase
75003 PARIS
France

Dear Sir,

With **interest** I have read your **letter** of May 21 about the detection of rare aerospace phenomena.

Unfortunately, the techniques employed at **our** observatory are designed exclusively for the study of pointsources or of very small fields (up to a **few** minutes of arc). Moreover, **our** work lies mainly in the infrared **domain**, which is not the most convenient part of the spectrum for the type of phenomena that you try to study.

More interesting **information** for your **project** might **come from** institutes where wide-field photography of the sky, or airglow and aurora **measure-**ments are carried out, but to my knowledge no astronomical institutes in the Netherlands are involved in research of this kind. I am afraid therefore, that I cannot give you any relevant information.

Hoping that you will find more helpful reactions elsewhere, I remain,

Yours sincerely,

Dr. J.W. Pel.



RADIOSTERRENWACHT DWINGELOO
Oude Hoogeveensedijk 4
7991 PD Dwingeloo
tel.: 05219-7244
telex: 42043 SRZM NL

RADIOSTERRENWACHT WESTERBORK
Schattenberg 4
9433 TA Zwiggelte
tel.: 05939-421
telex: 53621 RAOBS NL

F. Louange, Ingénieur-Conseil,
9, Rue Sainte-Anastase,
75003 Paris.
France.

onze referentie:

uw referentie:

Dwingeloo, 17 June 1982.

Dear Sir,

Your letter of 21 May has been passed on to me. I am not sure whether our instrumentation would be of interest to you but here is a summary of what we have. The Netherlands Foundation for Radio Astronomy operates instruments for the passive exploration of radio emission from extra-terrestrial bodies. The major facilities are a large array for super-synthesis observations at the principal radio wavelengths of 6, 21, 49 and (in about a year) 18 and 92 cm. This is located at the Westerbork Radiosterrenwacht. At Dwingeloo we operate a 25 m parabolic reflector at wavelengths ranging from 6 m to several metres, as well as several smaller telescopes devoted to solar research. A copy of our latest annual report which may be of use is being sent to you separately.

In addition I believe that the Department of Geodetics at Delft Technical University operates wide-field cameras for various satellite studies.

You should probably also contact the Dutch Meteorological Institute (KNMI) at De Bilt, who have a variety of relevant research programs.

Yours sincerely,

Richard G. Strom.



•
Dr. F. Louange
9 Rue Sainte-Anastase
75003 Paris
France

your letter of:

de bilt, September 8, 1982

your reference:

our reference: 22919

subject:

enclosure(s):

Dear Dr. Louange,

In answer to your request we can inform you about the following equipment used by the Royal Netherlands Meteorological Institute:

- 2 Weather radars, operating at 5.5 an wavelength, with a peak power of about 200 KW and a 1^o.5 deg. beamwidth. These radars are located in De Bilt and Schiphol Airport. In normal operation every hour a sketch is made of the precipitation echoes.
- About 18 lightning detectors, regularly distributed over the Netherlands to form a network. These detectors are essentially long wave radio receivers counting voltage pulses above a preset threshold. The counters provide 10 min. totals of the number of cloud to earth lightning flashes.
- A wide-angle cloud camera is used (daytime only) during rather infrequent special measuring campaigns.

I hope this information is useful for your work.

Sincerely,

(H.R.A. Wessels).

p.p. box 201
3730 AE de bilt
the netherlands

wilhelminalaan 10
tel.: +31 30 76 69 11
telex 47096

R . F . A .

Botschaft
der Bundesrepublik Deutschland
Ambassade
de la République fédérale d'Allemagne
Wiss. SE

75008 Paris, le 22 avril 1982
13/15 Av. Franklin D. Roosevelt
Fernsprecher/Téléphone: 3593351 et 2561790
Fernschreiber/Télex: AA Paris 28136 F
Telegrammanschrift/
Adresse télégraphique: Diplogerma Paris

Monsieur François LOUANGE
9, rue Sainte-Anastase
75003 Paris

Monsieur,

J'ai l'honneur de vous informer que votre lettre en date du 19-04-82 a été transmise, pour attribution, au service compétent en Allemagne qui vous répondra directement, ce qui - toutefois - pourra demander un certain temps.

Veillez agréer, Monsieur, l'expression de mes sentiments distingués.

P.o.



Claus von Kameke
Conseiller (Affaires scientifiques)

Der Bundesminister für Forschung und Technologie

513 - 8700

Tel. (0228)

Datum

59- 3104

30.07.1982

Geschäftszeichen

oder 59-1

M. **Francois** Louange
9, rue Sainte-Anastase

75003 Paris
Frankreich

Sehr geehrter Herr Louange,

von der Deutschen Botschaft erhielt ich Ihre **Anfrage bezüglich** seltener Weltraumphänomene.

In der **Bundesrepublik** Deutschland befassen sich die folgende Institute mit Teilaspekten, der von Ihnen angesprochenen Thematik:

Professor Hans Volland (**Blitzforschung**)

⊗ **Astronomische** Institute der Universität Bonn
53 Bonn 1
Auf dem **Hügel** 71

Professor T. Kirsten (**Meteorite**)

⊗ Max Planck Institut für Kernphysik
Abteilung Kosmophysik
Sanpfercheckweg 1
69 Heidelberg 1

Ferner möchte ich Sie auf die Veröffentlichung "**Offizielle** Untersuchungsberichte der **Russen** und der Amerikaner über unidentifizierbare Himmelserscheinungen"

Herausgeber: **Mutual** (UFO Network-Central European
Section (MUFON-CES)
Dipl.-Phys. I. Brand
Gerhart-Hauptmannstr. 5
8152 Feldkirch-Westerham

hinweisen, die eine **Zusammenstellung** zu diesem Thema darstellt.

Ich hoffe, Ihnen mit **diesen** Informationen gedient zu haben.

Im Auftrag.

Beglaubigt:

M. Otterbein

M. Otterbein
Angestellte



H. Volland, J. Schafer
Radioastronomical Institute
University of Bonn
Auf dem Hügel 71
5300 Bonn

West Germany
Phone 0228-733674 or 733393
Telex 0886440 astro d

THE AUTOMATIC VLF-ATMOSPHERICS STATION VLFAA/79

1. Configuration of the system

This new Vlf-atmospherics station allows completely automatic receiving, **analysing** and recording of atmospherics data. The **mean** azimuth and distance (or the **coordinates**) as well as the strength and spread of each thunderstorm activity center (more accurate: center of maximum activity of lightning discharges from which the **atmospherics** originate) are calculated within each measuring period of **20** minutes by a desktop computer and they are immediately (in real time) printed out and stored on the **magnetic** tape cassette. Additionally, a small **plotter** draws the thunderstorm **centers** onto a **map**. Except from changing, when desired, the drawing paper of the **plotter**, and from changing the data cassette approximately once each **month**, no maintenance is required.

The equipment consists of five parts (see Figs. 1 and 2): the antenna, the **receiver/analyser** and the computer with a **plotter** connected to it. A crossed loop antenna plus a whip antenna is used for the detection of the **electro-magnetic** field. While the loop antennas are **tuned** to a frequency of 9 kHz, the vertical electric antenna receives at 5, 7 and 9 kHz. The whole antenna is a passive **device** with an **optional** heating possibility (for extreme low temperatures) in the antenna head. It can be set up on a flat roof, on open field or even aboard a ship. The antenna **cables** (length, if necessary, up to 100 m) are connected to the **receiver/analyser** which can be placed upon a desk together with the computer and the **plotter**.

2. Operation of the system

Each atmospheric impulse is analysed whose spectral amplitude (SA) at 5 kHz surmounts the discriminator level (noise). The time resolution is ca. 50 msec (1200 pulses/min). The analyser transfers the following four digitized parameters of each received atmospheric impulse to the computer: the angle of incidence (azimuth), the group delay time difference (6-8kHz) GDD, the **spectral** amplitude ratio (9/5 kHz) SAR and the spectral amplitude (5kHz) SA. **These** values are also given to the **oscilloscope** plugs at the front of the analyser. Additionally, a **meter** shows the total number of incoming pulses per second (Fig.2). After a power interrupt, the **calculator** loads automatically the whole **program** and runs it anew.

Within a measuring period of 18 min (changeable) the calculator collects the data of **all** incoming sferics. **During** the next two minutes, four histograms are calculated **from** the received parameters and Gaussian fits to the **peaks** are made, so that for each thunderstorm activity center the azimuth, GDD, SAR and SA are determined which are then printed out and stored on tape cassette. Furtheron, a **propagation model** for VLF-Atmospherics is incorporated in the **operation program**. Using the spectral parameters as input, the **distances** of the activity **centers** are determined.

The characteristics of each thunderstorm activity center are printed out and plotted onto a map in real time, so that an immediate overview of the behaviour of the lightning and thunderstorm activity in a wide environment around the station is made possible.

The accuracy of the system depends on several influences. Constant deviations of the azimuth, eg. due to inexact alignment of the loop antennas or to other constant environmental influences can be eliminated by a deviation table. However, this was not necessary with the presently existing stations. Further deflections due to random disturbances of the electro-magnetic signal are not critical, because they are canceled out by the statistical fitting process. The arithmetical determination of the azimuth is in general accurate to 0.50, depending on the stationarity and the form of the activity center. The determination of the spectral parameters, and, consequently, the determination of the distance of an activity center by employing a suitable VLF-propagation model, is possible with deviations which are generally around 5%. Further improvement is expected with an increasing number of stations which, by means of cross-bearing, allows the development of optimal models. The range within which thunderstorms can be located reaches from a maximum distance of between ca. 4000 km for eastern centers at daytime and ca. 12000 km for signals from west during nighttime to a minimum distance of ca. 200 km.

3. Measurement examples

Up till now, two stations of this new kind are operating continuously since more than one year at Pretoria and Tel-Aviv. Figs. 3 and 4 show examples of the realtime recordings at Tel-Aviv. This version of representing activity centers is especially suitable for synoptical purposes: the small triangle marks the location of maximum activity, the length of the pointer is proportional to the strength (pulses per minute) and the orientation gives the time (GMT) like a clock. So it can be noticed easily that, e. g., the activity center in the north Adriatic area in Fig. 3 (23. June 1981, 3:00 - 14:0 GMT) weakens between 5 and 12 GMT, whereas the center over the north part of the Caspian Sea is strongest developed around 12 GMT. The thunderstorm activity can be verified on a synoptical maps, which, however, is available only every 6 hours and which gives no information on strength and development of the activity centers. Fig. 4 shows the cumulative activity centers within the period from 23. June 14.50 to 24. June 2.30 GMT (normally, with this representation, the sheet should be changed every 6 or at most 12 hours) in order to demonstrate the range during nighttime. For example, the South American activity is recorded during the weakening of the previously very strong West African centers around 2.00 GMT. An activity center in the western Atlantic is prominent between 1.00 and 2.00 GMT. The development of the centers of lightning discharges can be traced quite easily and shows generally a very close connection to the synoptical thunderstorm observations, though these are mostly rather fragmentary in time and space.

4. Availability of the system

The VLF-atmospherics receiver / analyser is built by an electronics company at Berlin. The complete price (including antenna, cables etc.) is ca. 19 000 Dollar. Term of delivery is approximately 3 months.

The desktop calculator Hewlett-Packard HP 9825 and the plotter HP 7225 cost ca. 8000 and 3500 Dollar, resp., and can be obtained worldwide.

The software is provided and maintained (at no costs) by the Radioastronomical Institute of the University of Bonn, West Germany.

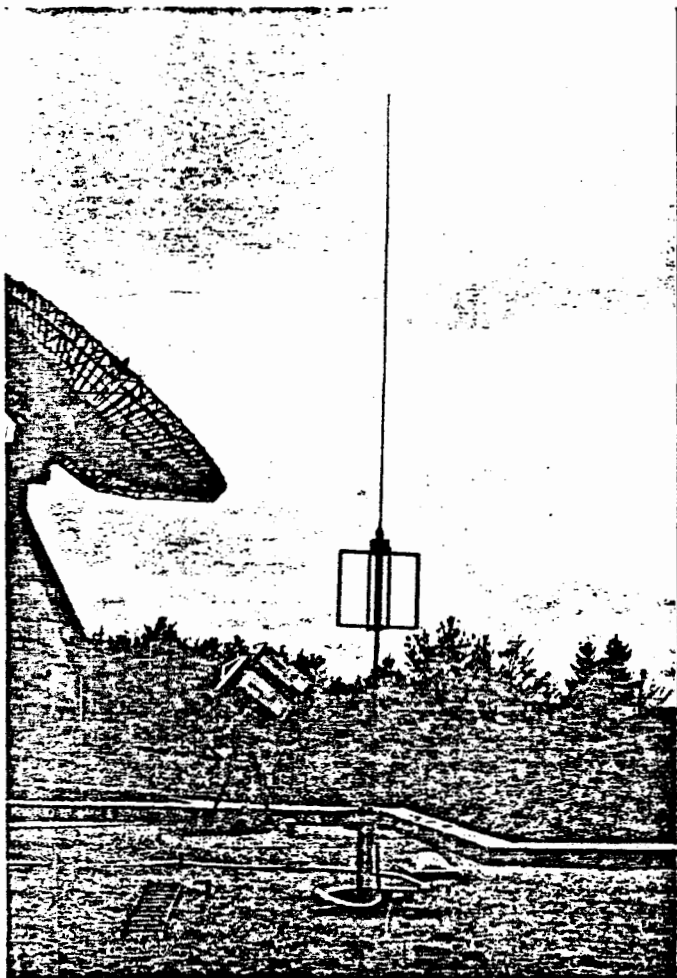


Fig.1 VLF - Antenna

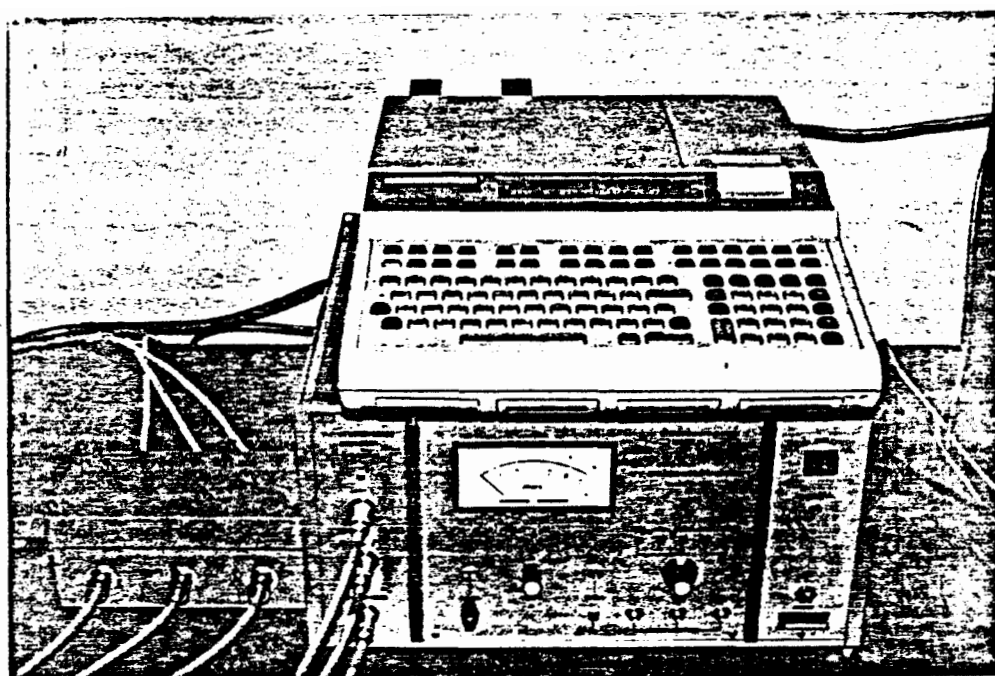


Fig. 2 VLF-Atmospherics Receiver/Analyser with desktop computer

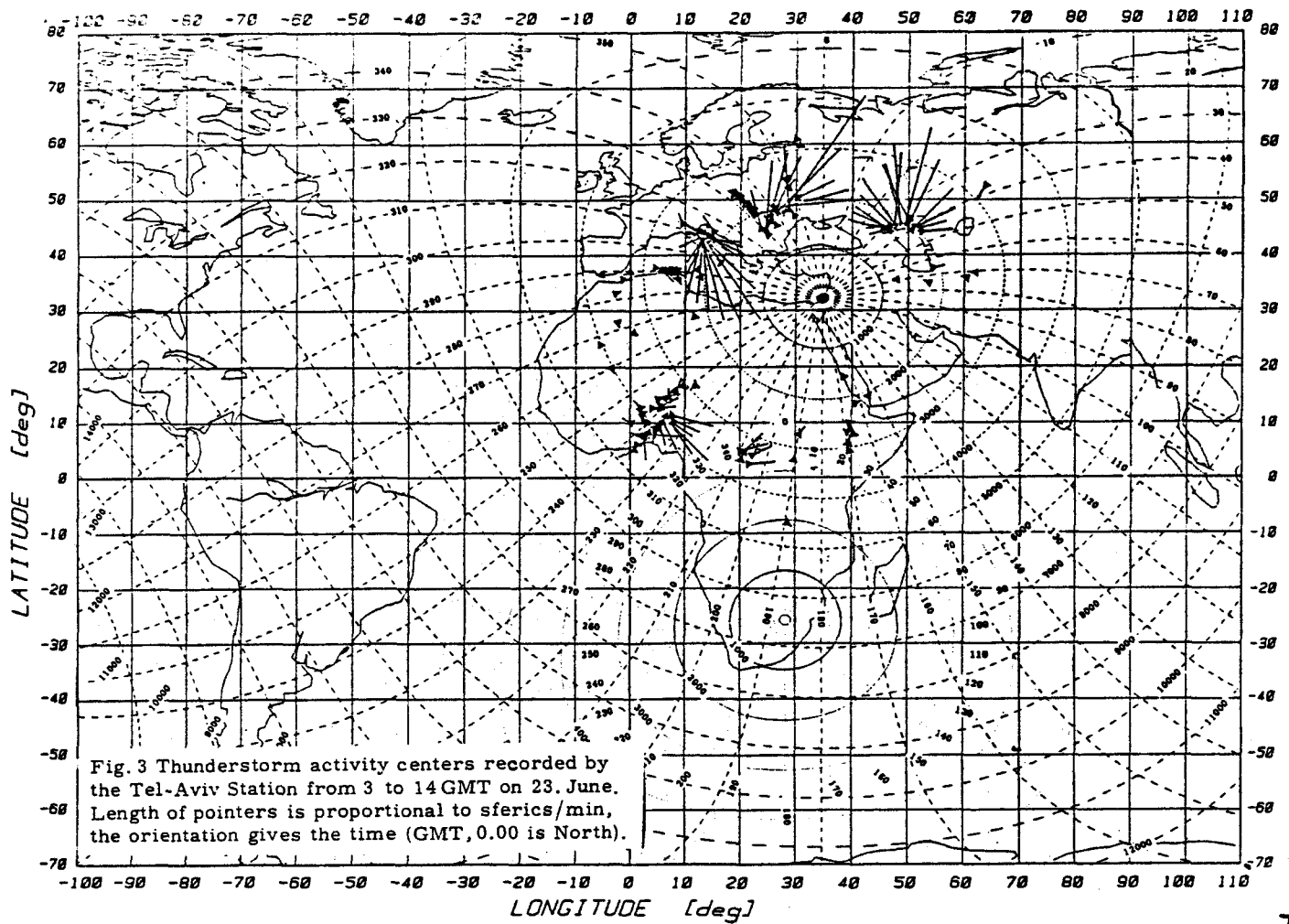


Fig. 3

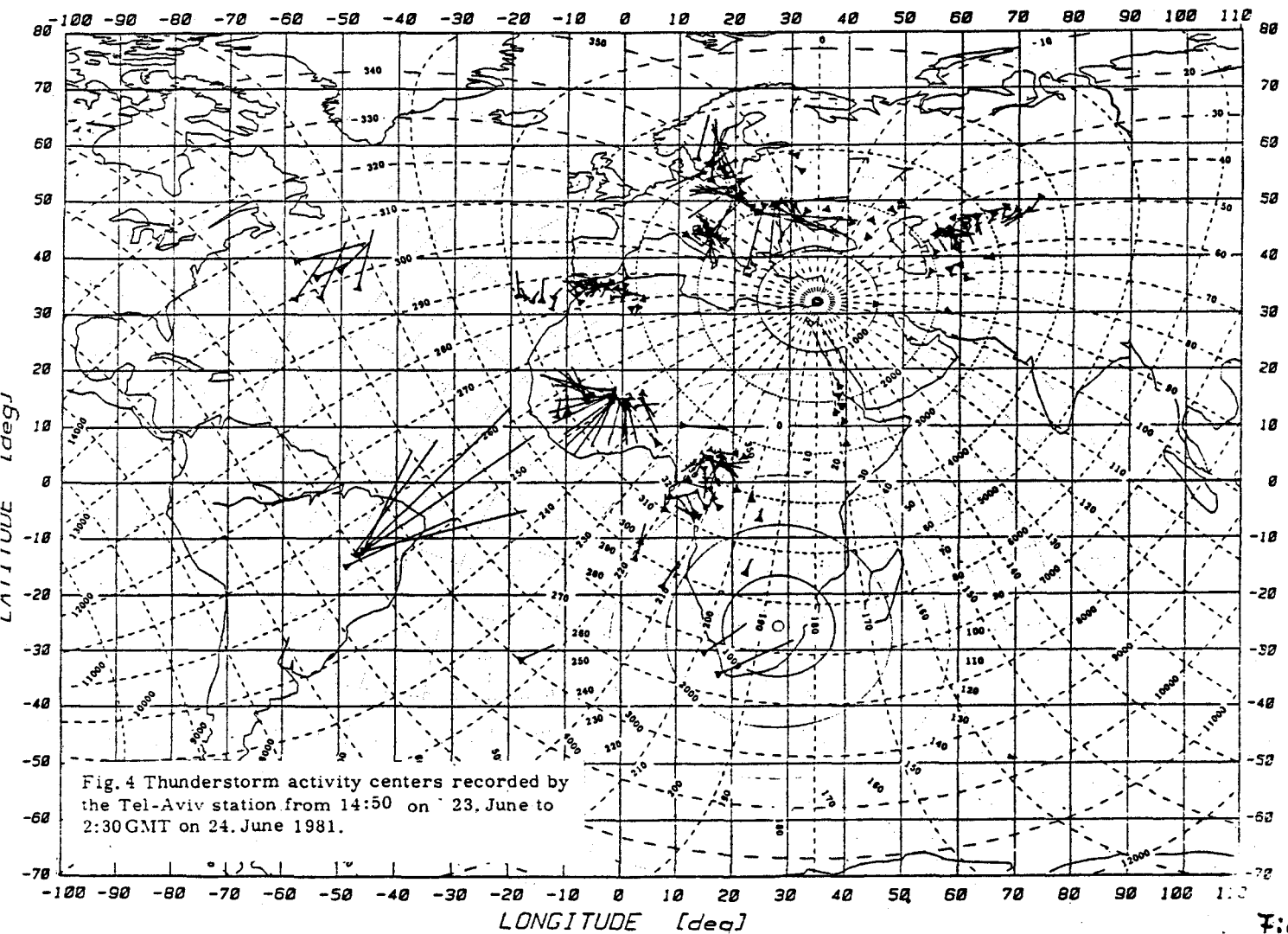


Fig. 4

REGISTRATION OF THUNDERSTORM CENTERS BY AUTOMATIC ATMOSPHERICS STATIONS

H. Volland, J. Schäfer and P. Ingmann
Radioastronomical Institute, University of Bonn

W. Harth
Max-Planck-Institut für Radioastronomie, Bonn

G. Heydt
Heinrich-Hertz-Institut für Nachrichtentechnik (HHI), Berlin

A. J. Eriksson
National Electrical Engineering Institute, Pretoria

A. Manes
Israel Meteorological Service, Bet Dagan

SUMMARY

A new generation of VLF-atmospherics receivers and analysers is presented which operates completely automatically and allows the real-time identification of thunderstorm activity centers. The mean azimuth and angular spread of each thunderstorm center within the detection range as well as the mean statistical properties of three measured spectral parameters of the atmospherics originating at that center are determined within each measuring period (20 min) by a desktop computer. Using a suitable statistical procedure for determining the mean angular and spectral parameters and applying a new extended model for VLF-propagation as a function of the solar zenith angle and of the magnetic field component along the propagation path, the operation program determines in real time the distances and the strengths (strokes per min) of the activity centers so that all data can be immediately printed out and stored on the internal magnetic tape cartridge. Additionally, an external plotter is used for marking the thunderstorm centers on a map. No maintenance is required apart from changing the data tape cartridge once every month. At present, two systems of this new kind are installed at Pretoria (South Africa), Tel Aviv (Israel) and a somewhat older one at Berlin. Three more stations are planned to be established toward the end of this year. First results show the characteristics of the method, the short and long range capability and resolution and the reliability of the thunderstorm localisations.

INTRODUCTION

VLF-atmospherics measurements have been carried out for many years now using the VLF-atmospherics analyser developed by the HHI, Berlin, (e.g. Heydt and Volland, 1964). In this earlier version of the equipment, the parameters of interest for each atmospheric impulse exceeding the input threshold of the receiver were successively displayed according to their angle of incidence as points on an oscillograph screen. A photographic picture of the screen was usually taken every five minutes. The point clusters in these pictures provided an estimate of the mean direction of incidence and the mean values of the spectral parameters for each center of activity. Results of the data analysis applying this method and further references can be found in the papers of Frisius et al. (1970) or Harth (1972a and b). The disadvantage of this version was the necessity to determine the parameters by individual inspection of each picture and to punch the data in order to make them accessible to a computer. Thus, the procedure for an a posteriori determination of the distances of the activity centers by applying a model for the spectral parameters was too circumstantial and costly. Furthermore, the independent variables of the VLF-propagation model had to be estimated externally with a relatively large uncertainty.

The new version of the atmospheric analyser allows completely automatic receiving and analysing of the atmospheric waveforms as well as a real-time determination of the activity centers using a built-in propagation model so that the data can be printed out, plotted and stored on magnetic tape. The equipment consists mainly of four parts: The antennas, the receiver/analyser, the desktop computer and the (optional) plotter. The antennas (double crossed loops plus a whip) are passive devices needing no maintenance and can be set up easily on a flat roof, in an open field or aboard a ship. The loop antennas for the determination of the azimuth (angle of incidence) are tuned to a frequency of 9kHz, the whip antenna delivers signals to small band receivers tuned to 5, 7 and 9kHz.

In the receiver/analyser, an atmospheric waveform is analysed whenever its spectral amplitude at 5kHz exceeds the input threshold lying just above the internal and external noise disturbances. The time resolution is ca. 45ms. The analyser transfers the following four parameters of each analysed atmospheric to the desktop computer (HP9825) :

the angle of incidence (azimuth) α ,
the Group Delay time Difference (6-8kHz) GDD ,
the Spectral Amplitude Ratio (9/5kHz) SAR ,
the Spectral Amplitude (5kHz) SA .

These values are also given to the oscillograph terminals at the front of the analyser and a meter displays the total number of incoming atmospheric waveforms per second.

The desktop computer collects all data within one measuring period (e.g. 20 min), fits a Gaussian to the GDD, SAR and SA data of each thunderstorm center, determines its azimuth and stores the appropriate parameters on the internal magnetic tape cartridge. Applying a VLF-propagation model and using the fact that three independent spectral parameters (GDD, SAR and SA) are measured, the distances of the activity centers are estimated in real time so that the data can be printed out and stored and the centers can be plotted immediately on a map by means of a desktop plotter. If the system is interrupted due to power failure or some other error, the calculator automatically loads the entire operation program and runs it anew.

METHOD OF MEASUREMENTS

A cloud-to-ground lightning (return stroke, R-stroke) can be approximated by a vertical electric dipole located on the ground. Above a perfectly conducting earth, the electromagnetic radiation field consists of a vertical E_z -component and a horizontal B_ϕ -component perpendicular to the propagation path of the wave. Describing the characteristics of the earth-ionosphere wave guide by a transmission function (normalized to the value of free propagation over a perfectly conducting earth)

$$W(\rho, \omega) \equiv |W| e^{i\Phi} , \quad (1)$$

the vertical component of the electric field E_z of a single atmospheric at distance ρ from a receiver can be expressed by a Fourier integral

$$E_z(\rho, t) = \frac{1}{2\pi} \int_{-\infty}^{+\infty} W(\rho, \omega) \hat{E}_z(\rho, \omega) e^{-i\omega t} d\omega, \quad (2)$$

where

$$\hat{E}_z(\rho, \omega) = |\hat{E}_z| e^{i\Phi} = \int_{-\infty}^{+\infty} E_z(\rho, t) e^{i\omega t} dt \quad (3)$$

is the Fourier transform of the atmospheric waveform above a perfectly conducting earth (Volland, 1982).

The atmospheric receiver/analyser measures the magnitude of the Fourier transform in (2) (spectral amplitude):

$$SA \equiv |W(\rho, \omega) \hat{E}_z(\rho, \omega)| \quad (4)$$

of each atmospheric arriving at an angle of incidence ψ at two frequencies (5 and 9 kHz) by narrow band receivers.

It furthermore determines the ratio of the SA at the two frequencies for each atmospheric (spectral amplitude ratio):

$$SAR \equiv \frac{|W(\rho, \omega_1) \hat{E}_z(\rho, \omega_1)|}{|W(\rho, \omega_2) \hat{E}_z(\rho, \omega_2)|} \quad (5)$$

and finally the instrument determines the differences in the arrival times of two spectral groups using the second derivative of the phase of the Fourier transform in (2) (Volland, 1968) (group delay time difference):

$$GDD \equiv \Delta t_{gr} \approx \frac{\partial^2 \theta}{\partial \omega^2} \Delta \omega, \quad (6)$$

where

$$\theta(\rho, \omega) = \Xi(\rho, \omega) + \Phi(\rho, \omega) \quad (7)$$

is the sum of the phases of W and \hat{E} in (2). In terms of the measured finite differences this may be written

$$GDD \equiv \Delta t_{gr} \approx \frac{\theta_2 - \theta_m}{\omega_2 - \omega_m} - \frac{\theta_m - \theta_1}{\omega_m - \omega_1} = \frac{\theta_2 - 2\theta_m + \theta_1}{\Delta\omega} \quad (8)$$

The phases $\theta_i(p, \omega)$ are measured at the frequencies $\omega_1 = 5$ kHz, $\omega_2 = 9$ kHz and at the mid-frequency $\omega_m = 7$ kHz. Therefore the first derivatives (finite differences between 5/7 kHz and 7/9 kHz resp.) in (8) correspond to the arrival times of the spectral groups at 6 and 8 kHz, and their difference gives the time delay between these spectral groups. GDD, like SAR, is a measure of the dispersion characteristics of the wave guide.

Besides these three spectral parameters or the E_z -field, the angle of incidence ψ of each atmospheric is determined by conventional direction finding techniques, using a crossed loop antenna for the B_θ -field and the phase ξ in (7) for an unambiguous identification of the right hemisphere. The four parameters of each atmospheric are sent in a digitized form to the computer. The azimuth is partitioned into 240 classes, the GDD into 250 classes (-62.5 to 437.5 μ sec), the logarithm of SA into 192 classes (from -6 to 42 dB) and the logarithm of CAR into 192 classes (from -12 to 36 dB).

DATA ANALYSIS AND PROPAGATION MODEL

The probability distribution of the spectral amplitudes SA follows rather closely a logarithmic normal distribution (Volland, 1968)

$$N = \frac{0.174}{\sigma} N_0 \int_S^{\infty} \exp\left(-\frac{(\log y - \log \bar{y})^2}{2\sigma^2}\right) \frac{dy}{y} \quad (9)$$

where N is the number of atmospherics exceeding the threshold S , N_0 is the total number within the time interval considered, σ is the root mean square value and

$$\bar{y} = \pi * e^{-2.65 \sigma^2} ; \quad \pi = A * |W(p, \omega) \hat{E}_0(p, \omega)|. \quad (10)$$

A is an amplification factor depending on the receiver characteristics, and \hat{E}_0 is the statistical mean of $|\hat{E}_z|$. Knowledge of A allows us to determine the transmission function if \hat{E}_z is known, or \hat{E}_0 can be determined if $|W|$ is known. Applying mode theory for VLF propagation, model values for the transmission function W can be calculated (Harth, 1972a).

SAR follows a log-normal distribution like SA (Equ.9). However, because the SA- and the SAR-histograms are established on a logarithmic axis (measurment in dB), they can be fitted with normal distributions, as it is done with the GDD- and the azimuth(point source)-histograms. In the fitting procedure, the minimum of a weighted sum of the squares of the logarithmic ratios between the fit-function values Y_i and the measured histogram values y_i is determined (not the usual linear least squares sum), i.e. using the condition

$$\sum_i w_i (\ln \frac{y_i}{Y_i})^2 = \min \quad (11)$$

or

$$\frac{\partial}{\partial p_j} \sum_{i=1}^{i_{\max}} w_i (p_0 + p_1 y_i + p_2 y_i^2 - \ln(y_i))^2 = 0 \quad (j=1,2,3) \quad (12)$$

the quantities p_j and consequently the parameters N_0 , \bar{Y} and σ of the normal distribution

$$N_i = \frac{N_0}{\sigma \sqrt{2\pi}} * e^{-\frac{(Y_i - \bar{Y})^2}{2\sigma^2}} \quad (13)$$

can be calculated:

$$\begin{aligned} \sigma &= \sqrt{-2/p_2} \quad , \\ \bar{Y} &= p_2 * \sigma^2 \quad , \\ N_0 &= (p_0 + \bar{Y}^2 / 2\sigma^2) * \sqrt{2\pi} \sigma \quad . \end{aligned} \quad (14)$$

Setting the weights $w_i = y_i$, the formulation (11) has the advantage that very large values as well as very small values (the noisy surrounding outside the main peak) of y have less influence as compared to the usual linear least square fit.

From the fact that all measured parameters show generally a smooth normal distribution it is obvious that the parameters obey a well defined dependence on the propagation conditions, which is however disturbed randomly due to the noisy characteristic of emitter, wave guide and receiver. Therefore, in the following model calculations the mean values \bar{Y} of the parameters are used as measurement input.

In the case of the first mode approximation, it follows from the theoretical model calculations that SAR and GDD are linear functions of the distance ρ

$$\text{GDD} = a_1 + b_1 \rho \quad ; \quad \text{SAR} = a_2 + b_2 \rho \quad . \quad (15)$$

The source terms a_i are approximated by constant values whereas the propagation terms b_i depend on the geographic locations of source and receiver, times of day and season and the structure of the lower ionosphere. If the propagation conditions are known, the distance between source and receiver can be determined directly from the SAR or the GDD measurements, where again the center values of the normal distributions are taken. Usually, however, the propagation conditions are known only approximately, so that considerable inaccuracies could occur. The advantage of this method is that most of these ambiguities can be ruled out by applying those model conditions which give the same distance from the SAR as well as from the GDD measurements.

Relatively close to the source, some additional ambiguities in the interpretation of the data occur due to the interference of several higher modes in the propagation of VLF waves. This nonuniqueness can be reduced considerably if again both the SAR and the GDD data are used, because the deviations of SAR and GDD from linearity (due to higher modes) are to a large degree opposite to each other (Harth, 1982) so that the effect is canceled out if one includes these deviations in the models for b_i . At this stage of development, the model of Harth (1972) for b_1 and b_2 of the far field are used. The independent variables are the ionospheric reference height z and the so-called "anisotropy factor" Ω (Wait and Spies, 1964). In Fig. 1 (Schäfer and Volland, 1982), this model is reproduced in the region between $\Omega = -1$ and $\Omega = +1$ for the ionospheric reference heights $z = 70 \text{ km}$ (daytime model) and $z = 85 \text{ km}$ (nighttime model). The parameter Ω describes the influence of the earth's magnetic field on the propagation model. It is the horizontal component of the gyrofrequency of the electrons, orthogonal to the propagation path of the atmospheric (parallel to the H-vector of the wave) and normalized to the electron-neutral collision frequency at the ionospheric reference height. Normally, Ω varies between

$\Omega \approx -1$ for West-East propagation and
 $\Omega \approx +1$ for East-West propagation.

Values beyond ± 1.5 are unlikely. Here, however, the range of Ω is extended beyond -1.8 and $+1.8$ with an artificial sharp bend in the model values. This behaviour simulates well the near field characteristics calculated by Harth (1982). Furthermore, the daytime and nighttime models can be interpolated for arbitrary reference heights using a height dependence for GDD and SAR given by Volland (1968). Then one obtains

$$b_1(z, \Omega) = \frac{\alpha_1}{z^2} + \frac{\beta_1}{z}, \quad (\mu\text{sec/Mm}) \quad (16)$$

with

$$\alpha_1 = b_1(85, \Omega) * 1.27 * 10^3 + 1.61 * 10^5,$$

$$\beta_1 = b_1(85, \Omega) * 70 + 1.89 * 10^5,$$

$$b_1(85, \Omega) = 29.3 - 3.3\Omega^2 - 7.6 + \exp(-5\Omega-7) - \exp(5\Omega-7)$$

and

$$b_2(z, \Omega) = \frac{\alpha_2}{z^3} + \frac{\beta_2}{z}, \quad (\text{dB/Mm}) \quad (17)$$

with

$$\alpha_2 = b_2(85, \Omega) * 4.67 * 10^4 + 2.77 * 10^6,$$

$$\beta_2 = b_2(85, \Omega) * 78.3 + 3.84 * 10^2,$$

$$b_2(85, \Omega) = 4.8 + 2\Omega - \exp(-9\Omega-20).$$

The constants a_i consist of the source parts which represent the typical mean values of the spectral parameters GDD and SAR of the lightning emitter itself and of the portions which are due to the individual phase and amplitude characteristics of the receiver. The source terms of GDD and SAR are estimated to 10 μ sec and -7dB (cf. Harth and Pelz, 1973; Volland, 1982), respectively, whereas the receiver terms are different for each atmospheric station and can be found by comparison with synoptic thunderstorm reports and by cross-bearings with another station (as an example, the values are approximately 40 μ sec and -6dB, resp., for the Tel Aviv station).

The propagation models for GDD and SAR given by (15) - (17) depend on three independent variables

- (a) the distance p ,
- (b) the anisotropy factor Ω
- (c) the ionospheric reference height z .

After the statistical analysis of each single activity center detected within one measuring period has provided the peak values of the three spectral parameters GDD, SAR and SA, one can in principle determine all of the three independent variables of the propagation models. Due to the more complex statistical distribution of the third spectral parameter SA (see next chapter), only GDD and SAR are used for the modelling at this stage. One therefore has to independently specify one of these independent variables. The variable chosen is the reference height z of the lower ionosphere. The mean reference height along the propagation path of the atmospheric is calculated by the operation program as a function of the solar zenith angle ζ along the path. The applied formula for the height z' at a single source point is given by

$$z' = 77.5 - 7.5 \frac{\cos(\zeta)}{\sqrt{\epsilon + \cos^2 \zeta}} \quad (\text{km}) \quad (18)$$

The "steepness" parameter a , which determines the transition gradient of the reference height from daytime to nighttime values, is set to $\epsilon = 0.15$. For a given universal time (GMT), the solar zenith angle ζ at the source point can be expressed as a function of the solar angle ζ' at the receiving station, the distance x between source and receiver and the angle λ between source point and subsolar point on the global sphere as seen from the receiver:

$$\cos(\zeta) = A \cos(x+B) \quad (19)$$

with

$$A^2 = \cos^2(\zeta') - \sin^2(\zeta') \cos^2(\lambda) \quad ,$$

$$\tan(B) = -\tan(\zeta') \cos(\lambda) \quad .$$

The solar zenith angle ζ' and the angle λ at the receiver location can be easily calculated for a given universal time. It has turned out that an artificial asymmetry which simulates a more nighttime-like situation near sunrise and sunset at the receiving station fits the measurements best. Therefore the local time LT at the receiver is modified according to

$$LT' = LT - \tau \sin(LT \cdot \pi / 12) \quad , \quad (20)$$

where τ is preliminarily set to $\pi/9$. The advantage of the formulation (18) for the height z' is that it can be analytically integrated along x up to a distance p (given in radians) when the expression (19) is inserted (A and B are constants) to obtain the mean reference height z :

$$z = \frac{1}{p} \int_0^p z' dx = 77.5 - 7.5 \frac{\sqrt{\epsilon+1}}{p} \left(a \sin\left(\frac{\sin(p+B)}{\sqrt{\epsilon/A^2+1}}\right) - a \sin\left(\frac{\sin(2)}{\sqrt{\epsilon/A^2+1}}\right) \right) \quad (21)$$

The remaining two independent variables p and Q can now be calculated using an iterative algorithm in order to find those unique values of p and Q (with the mean z -value given by (21)), for which the models of GDD and SAR in (15) derive exactly the measured values of these parameters.

The calculated parameters z , Q and the distance p of the activity centers can then be printed out and symbols indicating time (GMT) and strength (atmospherics per minute) can be plotted at the locations of the thunderstorm centers on a map with a desktop plotter. Furthermore, the analysed azimuth and spectral parameters (statistical mean, standard deviation/width, intensity/number of pulses within the normal distribution) are stored on the magnetic tape cassette of the computer. With an average number of four to six activity centers detected per measurement cycle (20 minutes) in the reception area of an atmospheric station, the tapes have a storage capacity of one month and more. The cassettes are collected at Bonn, where the data are copied to normal computer tapes, so that they are available for an a posteriori detailed study of the global lightning activity.

During the course of the measurements, when a sufficient number of synoptic coincident reports and simultaneous recordings from different stations are available, the coefficients in (16), (17) and (18) will be optimized. Of course, even after optimizing the propagation model, there will be some remaining deviations from model conditions. On the whole, an accuracy of direction finding of up to 0.5° and of distance determination of up to 5% is expected. The minimum distance, where an unambiguous determination becomes impossible due to the higher order modes propagation and the near field influences, is around 200km. The maximum distance reaches to more than 10000km for signals from the west during nighttime propagation conditions. However, a quantitative real time analysis is possible only up to distances of approximately 4000km because the number of atmospheric in the large amplitude tail of weak centers will not surmount a minimum number (set to 25) which is required for the statistical analysis. A possible blocking of activity regions by closer thunderstorm centers (normally, only the closest center in one direction is seen) can be taken into consideration for long-term (monthly, yearly) statistical models of the lightning density per area and time.

MEASUREMENTS

A first example of the measurements during one 20 minute interval between 8:20 and 8:40GMT on 23.June 1981 (18min for data collecting, 2 min for the evaluation) at the Tel Aviv station is shown in Fig.2. In the lower panel, a histogram of the number of atmospheric arriving per minute is plotted as a function of the angle of incidence (azimuth) ψ (solid line). Five centers of activity can be clearly distinguished. It is noticed that their shapes are generally quite well normally distributed. Starting with the largest peak at 304.5° , labeled "1", the operation program determines first the statistical parameters (center value, height, width) of all the activity centers, using (11)-(14). The fitted normal curves are shown as dashed lines in Fig.2. It can be generally assumed that the sources are point-like, or at least confined to a few degrees in azimuth, so that the width of the angular distribution must be predominantly due to random signal distortions along the propagation path. These deflections, which

can reach values of 10° and more are obviously normally distributed (as resulting from random noise influences), so that the accuracy of the direction finding is not influenced by this. Another point concerns so called 'site' errors of the azimuth bearing which may be due to metal constructions near the receiving antennas. These constant azimuth deflections can reach several degrees and are eliminated (after some calibration measurements) automatically by the operation program using an elliptical deviation of the angle of incidence. At the Tel Aviv site, for example, an elliptic distortion with an axis ratio of 0.8 (maximum distortion = 6.4°) and a 80° rotation of the large axis against North is found. It can be concluded from Fig.2 and from other data showing persistent activity centers for a larger time period that a typical activity center can be localized to within $\pm 0.5^\circ$.

The next step of computation is the construction of histograms of the spectral parameters GDD, SAR and SA for each single center of activity. Starting again with the largest one (labeled "1" in Fig.2), all atmospheric originating from that specific center (all pulses below the fitted curve "1") are extracted, the resulting spectral histograms are formed and the optimum normal distributions are fitted from (11) - (14). These histograms are shown in the upper panels of Fig.2 for the three largest activity centers during this measurement interval. The real-time printer output of the computer is inserted in the lower panel. For each activity center, numbered 1 to 5, it shows first the statistical parameters (in one line: center value, width and number of pulses per minute of the normal distribution) of the azimuth (ϕ), the GDD (Δ), the SAR (r) and the SA (a). Though the pulse rates are relatively low in this particular case (around 20 per minute; large activity centers can easily show 200 atmospherics and more per minute), the distributions are remarkably well represented by Gaussians. The spread of the spectral distributions arises from the random disturbances on the propagation path and additionally from the internal spread of the parameters in the source. Nevertheless, the center values are very well defined and can be confidently entered into the propagation models (15), (16) and (17). As already mentioned, the distributions of the SA are generally more complicated and more disturbed than those of GDD and SAR. Whereas the GDD and SAR are formed from two or three neighbouring frequencies, so that disturbances are partly cancelled out, the SA is measured at one frequency (5kHz). Furthermore, the peak of the SA-distribution cannot always be recorded because the source may be so far away that the peak of the SA-distribution shifts below the receiver threshold. This is almost the case for the example at the top of Fig.2. It can be deduced from the indicated double-peak structure of the GDD and SAR and from the broader azimuth distribution, that this activity region actually includes another weaker and more distant center of activity.

Using the procedure described in the last section, the distances p of each activity center and the appropriate propagation model parameters (reference height z and anisotropy factor Q) are calculated, using the center values of the GDD and SAR distributions as input. The results are then printed out in real time (insert to Fig.2, elliptic angle distortion included).

The detected activity centers are marked directly on a world map by means of a small desktop plotter. Fig.3 shows all the activity centers detected by the Tel Aviv station between 3:00 and 14:20 GMT on 23. June 1981, including the measuring period discussed in detail in Fig.2. In this representation, the locations of the centers are marked by small triangles,

the strength of th2 activity is indicated by the length of the pointers (10° length \approx 50 atmospherics/min) and the orientation of the vectors designates the time (GMT) like a normal clock (one turn within 12 hours).

One observes four larger activity centers which are prominent over a longer time period. The first one over the northern parts of Italy, labeled "1" in Fig.2, remains nearly constant in place and is strongest developed near 5:00GMT. Similarly, the bright activity center at the Caspian Sea is stationary with its maximum near noon. At 8:30GMT it was relatively weak and a second, still weaker center could be detected nearly behind this one, which explains the outlined double structure in the distributions of the parameters in Fig.2. There are two other prominent centers, the first one over West Africa, decaying during the morning hours, and the second one over Eastern Europe developing around noon.

In order to compare the atmospherics measurements with synoptical reports, the time period of the afternoon on 22. June and the night of 22. /23. June have been investigated. The complete list of all synoptical reports north of 15° N which were related to thunderstorms was available for this period. Fig.4 shows the centers of the atmospherics activity between 14:40 and 2:40GMT in the same manner as before. in Fig.5, the stations reporting thunderstorms are marked by crosses for 12:00GMT and by stars for 24:00GMT on 22.June 1981. Direct thunderstorm reports are marked by large symbols, indirect reports (e.g. cumulonimbus clouds) by smaller ones. For all prominent activity regions (West Africa, Spain, Italy, North-East Europe, Caspian Sea), the bulk of reporting stations coincide well with the dominating atmospherics localizations. Contrary to the atmospherics measurements, however, the strength and the development as well as th3 movement of a specific activity center cannot be estimated from the synoptical maps which are available only every six hours.

An example shall now be presented, which shows the recordings of all three stations as compared with pictures taken by the METEOSAT II satellite (continuously operating only since September 1981). The only date available for this comparison was the 30. September / 1. October 1981, because before that date the Pretoria station had an operational shut down for some weeks and after it the (older) Berlin station broke down due to a hardware failure. Although this fortuitous example may not be overwhelming, it does show some typical features of the measurements. Figs.6, 7 and 8 show the recordings of the Berlin, Tel Aviv and Pretoria stations, respectively, for the time period from 6:00GMT on 30. September 1981 to 6:00GMT on 1. October 1981. In their 24 hour representation, the pointers turn once within one day so that at 0:00GMT they point to North, at 6:00 to East, at 12:00 to South and at 18:00 to West. Looking first at Figs.6 and 7, one notices two prominent activity centers, one over Italy and the Adriatic Sea, the other over the Eastern Balkans which become bright mainly during the daytime hours (12:00GMT = southward pointer) and are observed by both the Berlin (52.62° N/ 13.13° E) and the Tel Aviv stations with little differences in appearance. Comparing these with the cloud pictures (visible image) of the Meteosat II satellite at 11:25GMT (Fig.9), it becomes obvious that the lightning activity within the cloud complex over the Adriatic and Balkans is not equally distributed but is concentrated essentially in these two centers of activity. The exact determination of the storm's locations is influenced somewhat by the different directions of observation. For example, the North-East Adriatic area is emphasized for the Berlin station. It should be noted that the angular and spectral resolution of the older equipment at the Berlin sta-

tion is worse than the new version by a factor between 3 and 5. It is interesting that the cloud spur reaching up to the Baltic area and the frontal cloud bands west of the Bay of Biscay (see Fig.9) do not contain any lightning activity during daytime. In the evening after 18:00GMT, however, the Biscayan front becomes active while another activity region over the North Sea (which is blocked out for the Tel Aviv station by the nearer activity) weakens at that time. Obviously, these features cannot be deduced definitely from the satellite cloud pictures, although the infrared (IR) and water vapor (WV) images are somewhat better indicators of thunderstorm activity than the visible image. In the infrared image at 17:55GMT in Fig.10, high reaching convective clouds appear brighter than low level layered clouds. The developments of the cloud and frontal structures can be estimated comparing both satellite images. Obviously, one cannot deduce a reliable "activity" estimation (in the sense of strokes per time) from the images: The cloud formation over Northwest Africa, reaching from the Atlantic ocean to Spain and appearing quite bright in Fig.10, in fact produces very little lightning activity (cf. Figs. 6 and 7). Still, the most prominent activity centers in central Africa should certainly be expected near the very bright cloud complexes in Fig.10.

The effect of mutually blocking or overlapping activity centers, as deduced from atmospheric measurements, is exemplified by the moderate thunderstorm activity west of the Caspian Sea, which was hardly visible at Berlin (Fig.6), or by the activity region in the Bay of Biscay which is seen from Tel Aviv starting at ca. 18:00GMT (Fig.7) with a certain admixture of the decaying Italian activity within nearly the same angular domain. Additionally, local disturbances of the ionosphere seen to influence the measurements at Tel Aviv around midnight where the distances in the northwest direction are probably overestimated.

The amplitudes of the atmospheric are damped out with increasing range so that the portion of their distribution which exceeds the input threshold of the receivers eventually becomes too small and the activity center can no longer be identified. For good propagation conditions during night along Mes?-East paths, this limit lies around 10000km. The bright activity region north of South America, which is seen during nighttime at a distance of ca. 7500km from Berlin, thus lies close to the maximum range for the Tel Aviv station in the azimuthal direction of about 285° and a distance of 9000km. Unfortunately, Tel Aviv again receives a certain admixture of a closer (ca. 5.5Mm) but much fainter activity region around $30^\circ\text{N}/25^\circ\text{W}$ (compare Fig.10), so that the distances appear partly too short. A second activity center in that region, seen at an azimuth of ca. 277° from Tel Aviv (again with an admixture of the closer activity) cannot be seen so clearly from Berlin because of the blocking influence of the activity in the Bay of Biscay. On the other hand, the measurements of the third station in Pretoria (Fig.9) exhibit nearly the same direction of 288° for both centers. The corresponding locations, around $15^\circ\text{N}/57^\circ\text{W}$ and $12^\circ\text{N}/40^\circ\text{W}$, estimated from these measurements, agree quite well with the locations of the bright infrared (=cold) cloud clusters on the satellite picture in Fig.10. At Berlin, an admixture of the activity cluster close to the South American coast is seen. It is worth noting that the prominent hurricane near $40^\circ\text{N}/40^\circ\text{W}$ (called "IRENE"), which appears just as bright as the active thunderstorm regions on the satellite images (Figs.9 and 10), does not produce any significant lightning activity during this time (cf. Turman and Edgar, 1982, who find the same behaviour with typhoon "GILDA" in 1977).

Looking now to the other prominent activity regions detected by the Pretoria station, one finds a correspondence between the atmospheric locations in South America (near $12^{\circ}\text{S}/40^{\circ}\text{W}$) and southeast or Madagascar and the satellite pictures. The South American activity is not recorded by the Tel Aviv and Berlin stations because of the blocking and disturbing influence of the activity in West Africa. As this activity is seen by the Tel Aviv station quite frequently, observation of activity in South America is somewhat rare. It is noticed in Figs. 8 and 7 that another very bright visible cloud cluster east of Pretoria on the African continent is not active at all. This is also suggested, however, by the IR-Image (in Fig. 10, 6 hours later, an area northwest of that cluster becomes active), which does not exhibit a very cold cloud temperature there.

A very peculiar behaviour of the VLF-propagation shall be discussed now as deduced from atmospheric measurements of the thunderstorm activity in Central Africa. Obviously, the activity distribution there looks substantially different as seen from each of the three receiving stations. Some qualitative correspondence can be observed, for example, between the Berlin and Tel Aviv data near sunset in west Africa (with a combination of two centers to a single large one seen from Tel Aviv), or between the Tel Aviv and the Pretoria measurements in central Africa near noon (pointers to South) and near midnight (pointers to North) with somewhat different distances and intensities in each case. It is noticed, that the relatively high lightning activity near the equator is often not, or only with too low strengths, detected by the Tel Aviv station (registrations by the Berlin station are very rare), and that the locations of maximum activities, as seen from Pretoria, are usually south of the equator. This is a quite typical behaviour of the registrations in central Africa. Though the relatively small distances to Tel Aviv and Pretoria (around 4Mm) should guarantee a moderate damping according to the propagation model in Fig. 1, activity centers beyond and close to the magnetic equator (near 10°N on the African continent) and at angles close to north-south or south-north directions ($\Omega \approx 0$) can hardly be detected. Therefore one has to draw the conclusion that the usual Wait/Harth model for VLF-propagation, even in its extended version in Fig. 1, is insufficient to describe these trans-equatorial, nearly meridional propagation behaviour. The implication of the model, that a pure horizontal and parallel (relative to the propagation path) magnetic field corresponds to isotropic conditions without a magnetic field must be revised and a much higher damping must be introduced under these circumstances. Starting point to a more realistic propagation model for this specific conditions (very small magnetic dip angle, NS or SN propagation, medium distances) is a full wave calculation which shows that the reflection coefficients become very small for meridional propagation, very small dip angles and near grazing incidence at the Brewster angle (e.g. Tsuruaa, 1972). This would imply the introduction of two more independent parameters - the vertical and parallel Ω -components - into the propagation model.

Another very interesting feature of the trans-equatorial propagation can be occasionally manifested in the measurements of the station at Tel Aviv, less frequently at Pretoria. This effect is also visible in Fig. 7, where the recorded pulse rates of the equatorial activity region around 23°E and the separate center behind this one near $17^{\circ}\text{E}/15^{\circ}\text{S}$ (as seen from Pretoria and confirmed by the satellite cloud picture, Fig. 10) are extremely small or vanish completely for some time, until suddenly the pulse rates increase and the distances seem to jump by a factor of two and more (two locations near $53^{\circ}\text{S}/2^{\circ}\text{E}$ at 0:10 and 0:30 GMT). This beha-

viour, which is occasionally much more dramatic than in this case, can be observed especially during the few hours around midnight. After such an event, the values fall back to the previous conditions. This behaviour is essentially caused by an abrupt and considerable increase of the group velocity difference between 5 and 9 kHz, partly accompanied by an excess damping of the 5kHz component. The reason for these distortions of the spectral parameters may be a whistler-like ducting of the atmospherics along low latitude field lines in combination with equatorially confined E-layer irregularities which would allow the VLF-waves to penetrate into the ionosphere and to come out again. Similar considerations with regard to low latitude whistlers have been presented by Hayakawa and Tanaka (1978).

A final example demonstrating the short range capability of the system and the VLF-propagation model (15) should also be noted. Fig.11 shows the recordings of the station at Pretoria between 12:00 on 2.10.81 and 12:00GMT on 3.10.1981. One observes a clustering of activity centers around the station within a radius of less than 500km, including the immediate vicinity of the station. This location corresponds exactly to the bright cloud complex in the infrared satellite image, Fig.12 (11:55GMT on 2.10.1981). The activity regions near 20°E/10°S and near the west coast of Madagascar are already visible in this picture, although they display their strongest activity during nighttime. On the other hand, the activity region southwest of Madagascar, which becomes strong only after 3:00 GMT on 3.10.1981 (Fig.11), can not be observed in Fig.12, but is extremely bright on the corresponding image for 3.10.1981 (not shown). This demonstrates the frequently observed very rapid development of activity regions. As already indicated, atmospherics activity at and beyond the magnetic equator is hardly detectable.

CONCLUSIONS

The new development in the field of VLF-atmospherics research and technology described here is characterized by the following central aspects:

- (a) A completely automatic receiving and analysing system allows a real time determination of lightning activity parameters. The data are stored on magnetic tape cassettes for an a posteriori analysis and are also used to mark the thunderstorm centers on a map by means of an on-line desktop plotter. Easy accessibility to these data recordings is necessary for the development of global models of the lightning density and for detailed a posteriori investigations of the VLF-propagation conditions.
- (b) A statistical program for recording and collecting VLF-atmospherics has been developed which yields a reliable estimate of the angular shape of an activity center as well as the shape and location of the spectral parameters GDD, SAR and SA of those atmospherics originating at a specific center of activity.

(c) A new analytical VLF-propagation model has been introduced which is based on the usual models of Wait (Wait and Spies, 1964) or Harth (1972a), but is extended to be applicable for arbitrary ionospheric reflection heights and takes into account the higher mode influences at closer distances (near field range). This model uses the mutually independent spectral parameters (statistic mean values of all atmospherics from a specific activity center) in an iterative algorithm to determine the distance to the activity center and the appropriate values of the ionospheric reflection height and the anisotropy factor Ω .

At present, the receiving network consists of two new stations at Pretoria and Tel Aviv and an older one at Berlin. It will be expanded in the near future with new stations at the German Antarctic station and in India and Switzerland. The coverage of the existing stations comprises Europe and Africa and parts of Asia and America, with some regions of partial overlapping.

The existing measurements and analyses, from which examples have been presented, show that reliable information is obtained on the locations and the strengths (strokes per minute) of thunderstorm activity centers. Comparisons between the atmospheric measurements and a large number of single thunderstorm reports on synoptic charts showed that whenever some or the bulk of weather stations in a certain area report thunderstorm activity, a local lightning source is confirmed by the atmospheric method in this area or close to it. On the other hand, centers of atmospheric activity, especially on the oceans, are not necessarily detected by the synoptical network, usually because of sparse station coverage (thunder can be heard only up to ca. 30 km), which demonstrates the usefulness of this system for weather forecasts and thunderstorm warnings. Areas of atmospheric activity can be confirmed as cloud complexes in satellite images (METEOSAT), especially infrared and water vapor images, but not all cloud clusters, even if they show bright features (cold temperatures) in these two channels, produce a significant amount of lightning activity.

Contrary to other methods, an atmospheric network is capable of continuously detecting (in 20-minute intervals) not only the locations of the lightning activity centers, but also their strength (in absolute number of strokes per minute) and their evolution. The detection range of atmospheric activity is limited due to the specific VLF-propagation conditions. Although the maximum range is up to 10000 km for the development of lightning density models, the limit for a quantitative real time analysis is near 4000 km. Theoretically, a complete model coverage of the globe could thus be achieved with ca. 10 optimally located stations.

Applications of the atmospheric system and its real time data are possible in the fields of thunderstorm warning and forecasting. For the weather services, atmospheric measurements can be a valuable additional parameter (like satellite images). It is intended to include the atmospheric information in the routine forecasting procedures. Tests have been already started at the Israel Weather Service. A first survey of the frequency and the strength of the lightning activity in different areas within the detection range of the existing network reveals not only the well-known activity regions on the continents (cf. the thunderstorm day maps published by WMO, 1956; or U.S.A.F., Handbook of Geophys., 1960),

but also considerable activity above the Atlantic and Indian oceans, even southward of 50°S. Such features can also be observed in the global lightning distribution charts of Orville (1981) and Turman and Edgar (1982) who analysed the DMSP-satellite lightning recordings of the high altitude internal cloud discharges at dawn, dusk and midnight. Comparable analyses using the atmospheric measurements of the cloud-to-ground component of the lightning activity on a continuous time basis, even with regard to a possible connection with planetary waves (cf. Harth et al, 1982), are in preparation.

Acknowledgement. This work is being supported within the scope of a cooperative project by the Deutsche Forschungsgemeinschaft (DFG), Bonn, by the Center for Scientific and Industrial Research (CSIR), Pretoria, and by the Israel Weather Service, Tel Aviv. We thank Dr.M.Bird for the critical reading of the manuscript.

REFERENCES

- Frisius, J., Heydt, G., and Harth, W. : Observations of Parameters Characterizing the VLF-Atmospheric Activity as Function of the Azimuth. *J.Atmos.Terr.Phys.*, 32, 1404-1422, 1970.
- Harth, W. : VLF Atmospheric Parameters Described by the Wait and Walters Model. *J.Geophys.*, 38, 153-167, 1972a.
- Harth, W. : VLF Atmospheric: Their Measurement and Interpretation. *J.Geophys.*, 38, 815-849, 1972b.
- Harth, W. : Theory of Low Frequency Wave Propagation. Handbook of Atmospheric, H.Volland (ed.), CRC-Press, Boca Raton, FL., 1982.
- Harth, W., Steffen, P., Hofmann, C.A., and Falcos, H. : The Day-to-Day Variation of Atmospheric Activity over the South American Continent. *J.Atmos.Terr.Phys.*, 44, 123-129, 1982.
- Hayakawa, M., and Tanaka, Y. : On the Propagation of Low-Latitude Whistlers. *Rev.Geophys.Space Phys.*, 16, 111-123, 1978.
- Heydt, G., and Volland, H. : A New Method for Locating Thunderstorms and Counting their Lightning Discharges from a Single Observing Station. *J.Atmos.Terr.Phys.*, 26, 780-782, 1964.
- Ingmann, P., Volland, H. and Heydt, G. : Observation of the Thunderstorm Activity during July/August 1975 in the European-North American Area by a Groundbased Single-Station Technique. *Meteorol.Rdsch.*, 34, 151-160, 1981.
- Orville, R.E. : Global Distribution of Midnight Lightning - September to November 1977. *Mon.Wea.Rev.*, 109, No.2, 391-395, 1981.
- Schäfer, J., Volland, H., Ingmann, P., Eriksson, A., and Heydt, G. : A Network of Automatic Atmospheric Analysators. NASA Conference Publication 2128 (Proceedings of the Symposium on Lightning Technology), FAA-RD-80-30, 215-225, 1980.

- Schäfer, J., and Volland, H.: VLF-Atmospherics as a Tool for Probing VLF-Propagation Conditions. Proceedings of the AGARD-Conference on Medium, Long and Very Long Wave Propagation. AGARD-CPP-305, 6.1-6.12, 1982.
- Tsuruda, K.: Penetration and Reflection of VLF Waves through the Ionosphere: Full Wave Calculations with Ground Effect. J.Atmos.Terr.Phys., 35, 1377-1405, 1973.
- Turman, B.N., and Edgar, B.C.: Global Lightning Distributions at Dawn and Dusk. J.Geophys.Res., 87, 1191-1206, 1982.
- United States Airforce Handbook of Geophysics. The Macmillan Company, New York, pp9.14-9.30, 1960.
- Volland, H.: Die Ausbreitung langer Wellen, Verlag Fried.Vieweg&Sohn, Braunschweig, 1968.
- Volland, H.: Low Frequency Radio Noise. Handbook of Atmospheric, H.Volland (ed.), CRC-Press, Boca Raton, FL., 1982.
- Wait, J.R., and Spies, K.P.: Characteristics of the Earth-Ionosphere Waveguide for VLF Radio Waves. Technical Note, NBS, No.300, 1964.
- World Meteorological Organisation: World distribution of thunders storm days, Report TP.21,II, Geneva, 1956.

FIGURE CAPTIONS

- Fig.1 VLF-Propagation model for the spectral parameters CDD (Delay time Difference between spectral Groups at 6 and 8kHz) and SAR (Ratio between spectral Amplitudes at 7 and 5 kHz) as a function of the anisotropy factor Q for different ionospheric reference heights between 65 and 85 km.
- Fig.2 Example of the atmospheric recordings of the station at Tel Aviv in the measurement cycle 8:20-8:40 on 23.June 1981. In the lower panel, the histogram of all recorded atmospheric is shown as a function of the angle of incidence (azimuth) with the centers of activity numbered consecutively. The histograms of the three spectral parameters GDD, SAR and SA (Spectral Amplitude at 5kHz) for the three most intense activity centers are given in the upper panel. Gaussian fits to the distributions are plotted as dashed curves. The insert to the lower panel shows the real time printer output giving center value, width and area (pulses per min) of the distributions for azimuth ($\bar{\alpha}$), GDD (Δ), SAR (r) and SA (a) and the calculated values of Q , ionospheric height Z_{ref} and distance p of each activity center.
- Fig.3 Real time plotter chart of the Tel Aviv station for the measuring period 3:00 to 14:20 on 23.June 1981. Locations of activity centers are marked by small triangles, their intensities are indicated by the length of the pointers ($10^\circ \approx 53$ strokes/min), the time (GMT) is given by the orientation of the pointers (12:00GMT = northward, one full clockwise turn within 12 hours).
- Fig.4 Same as Fig.3 for the measuring period 14:40 on 22.June to 2:40 on 23. June 1981.
- Fig.5 Locations of all synoptical stations north of $15^\circ N$ reporting direct or indirect (cumulo-nimbus clouds etc.) thunderstorm activity, marked by large and small symbols, respectively. Crosses are Cor 12:00GMT on 22. June, stars for 0:00GMT on 23.June 1981.
- Fig.6 Activity centers recorded by the Berlin station for the measuring period 6:00GMT on 30.August to 6:00 on 1.October 1981. Pointers rotate once every 24 hours with 0:00GMT northward.
- Fig.7 Same as Fig.6 for the station at Tel Aviv
- Fig.8 Same as Fig.6 for the station at Pretoria
- Fig.9 METEOSAT II image of the visible channel at 11:25GMT on 30.September 1981. (Supplied by the European Space Agency)
- Fig.10 METEOSAT II image of the infrared channel at 17:55GMT on 30.September 1981. (Supplied by the European Space Agency)
- Fig.11 Activity centers recorded by the station at Pretoria in the measuring period 12:00 on 2.October 1981 to 12:00 on 3.October 1981.
- Fig.12 METEOSAT II image of the infrared channel at 11:55GMT on 2.October 1981. (Supplied by the European Space Agency)

Propagation Model for GDD and SAR

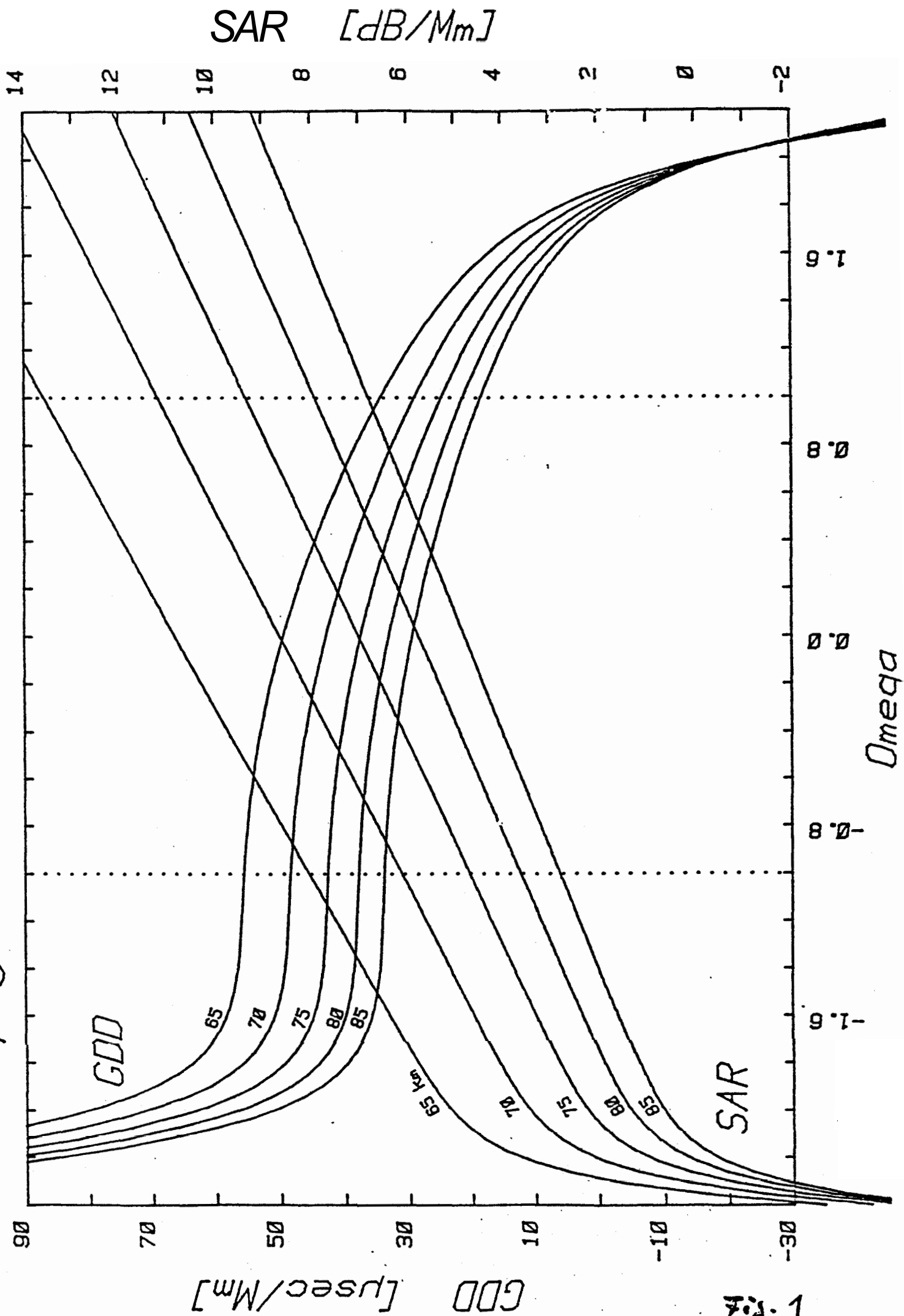


Fig. 1

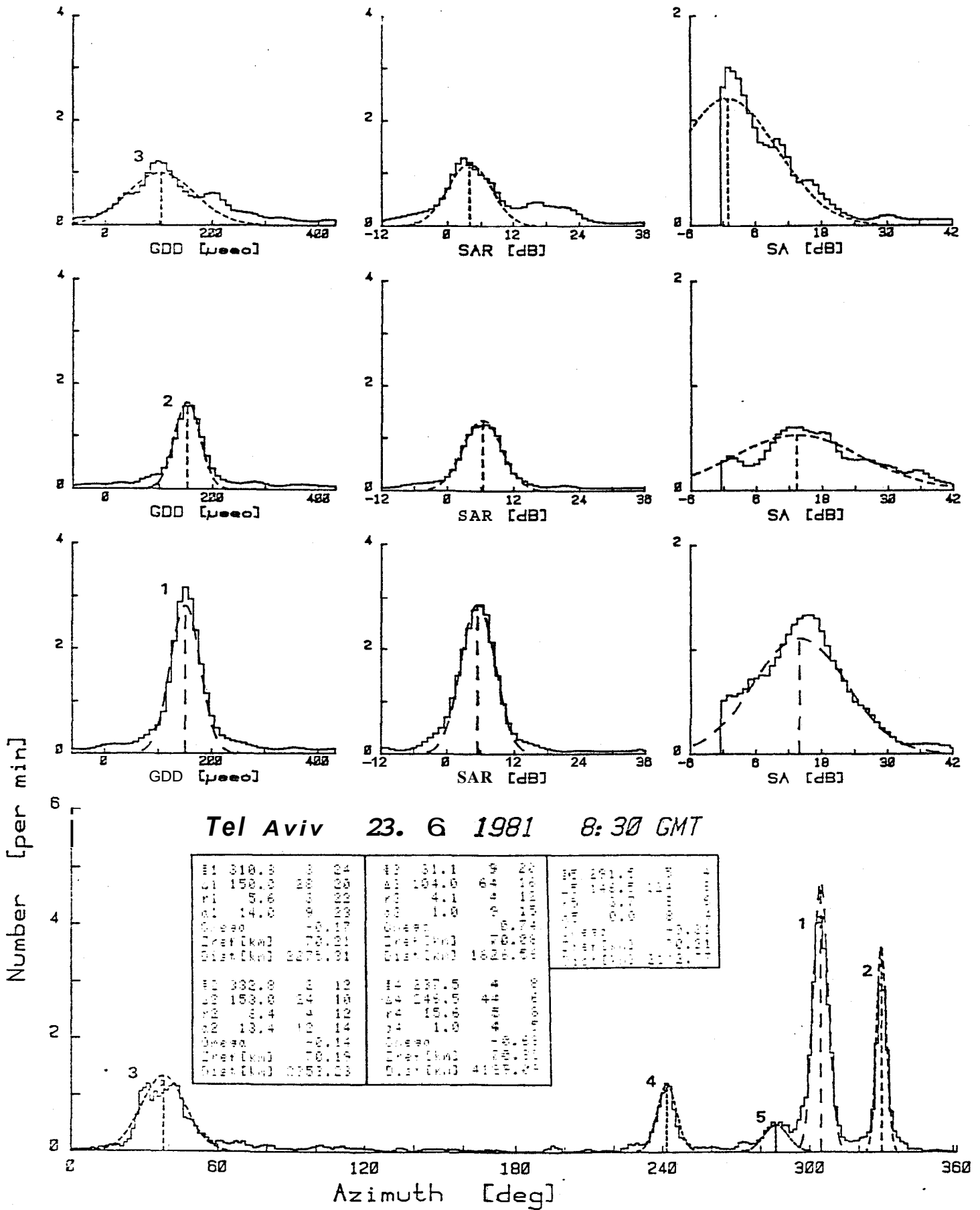


Fig. 2

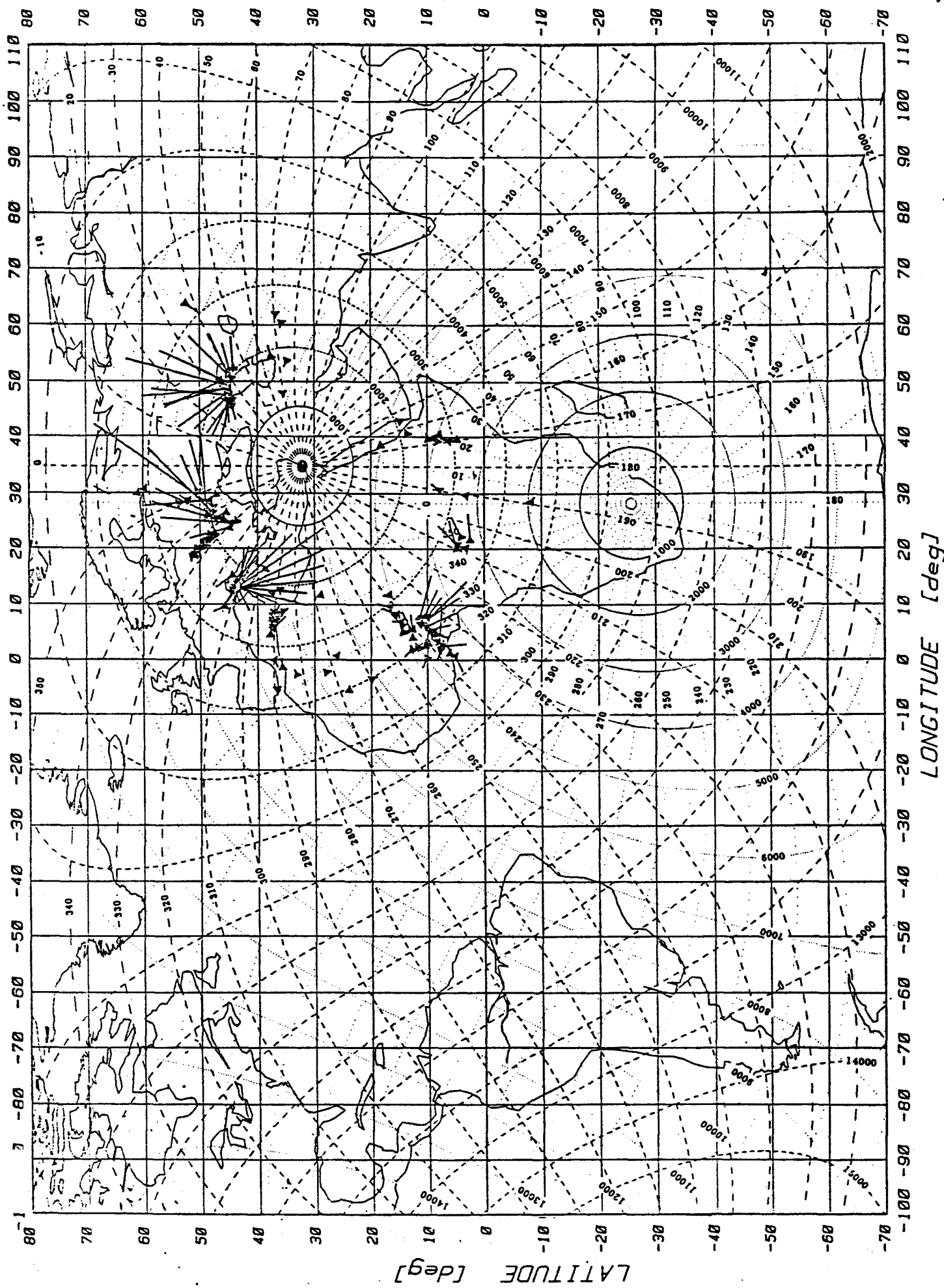
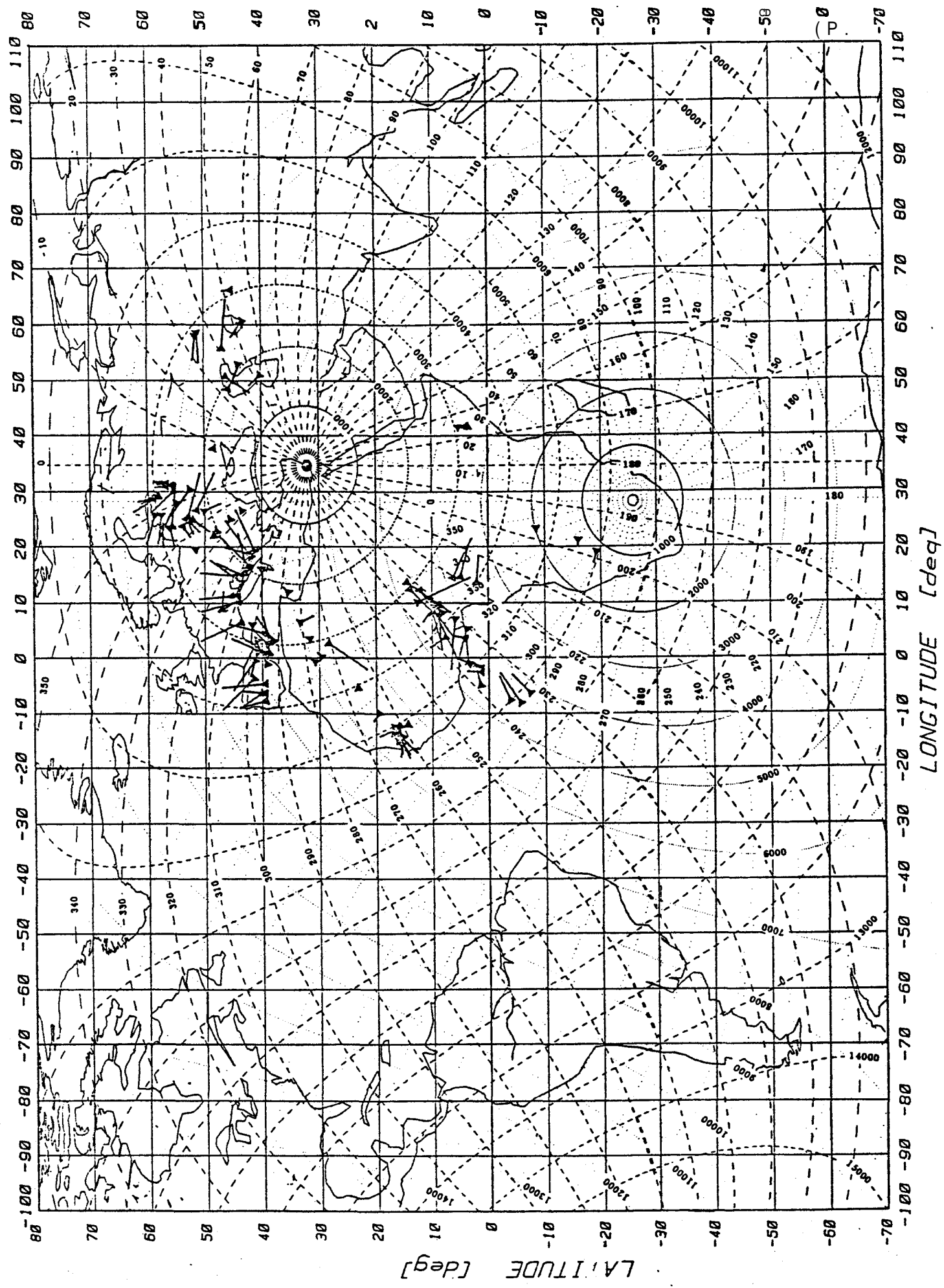
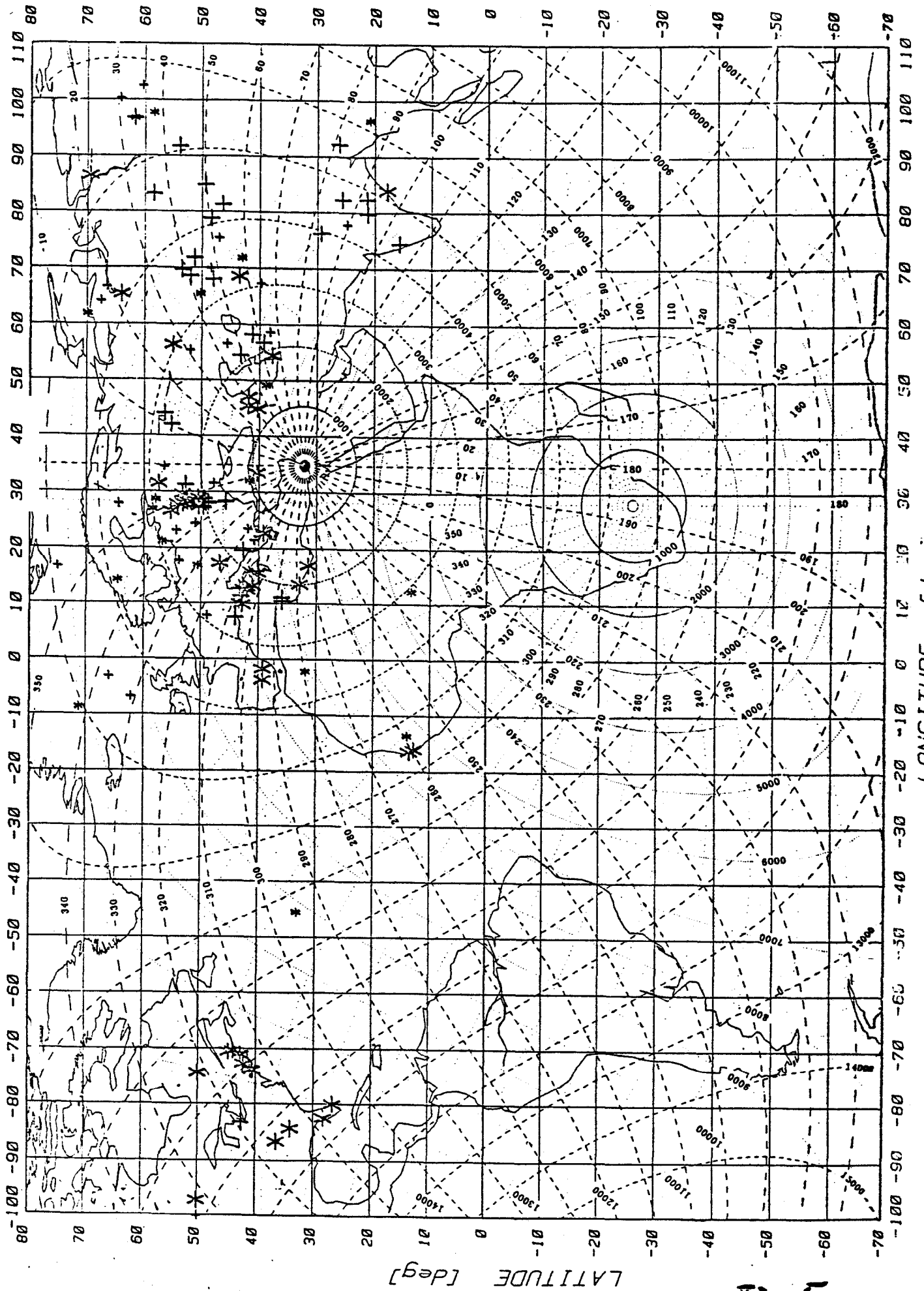


Fig. 3

H. W.



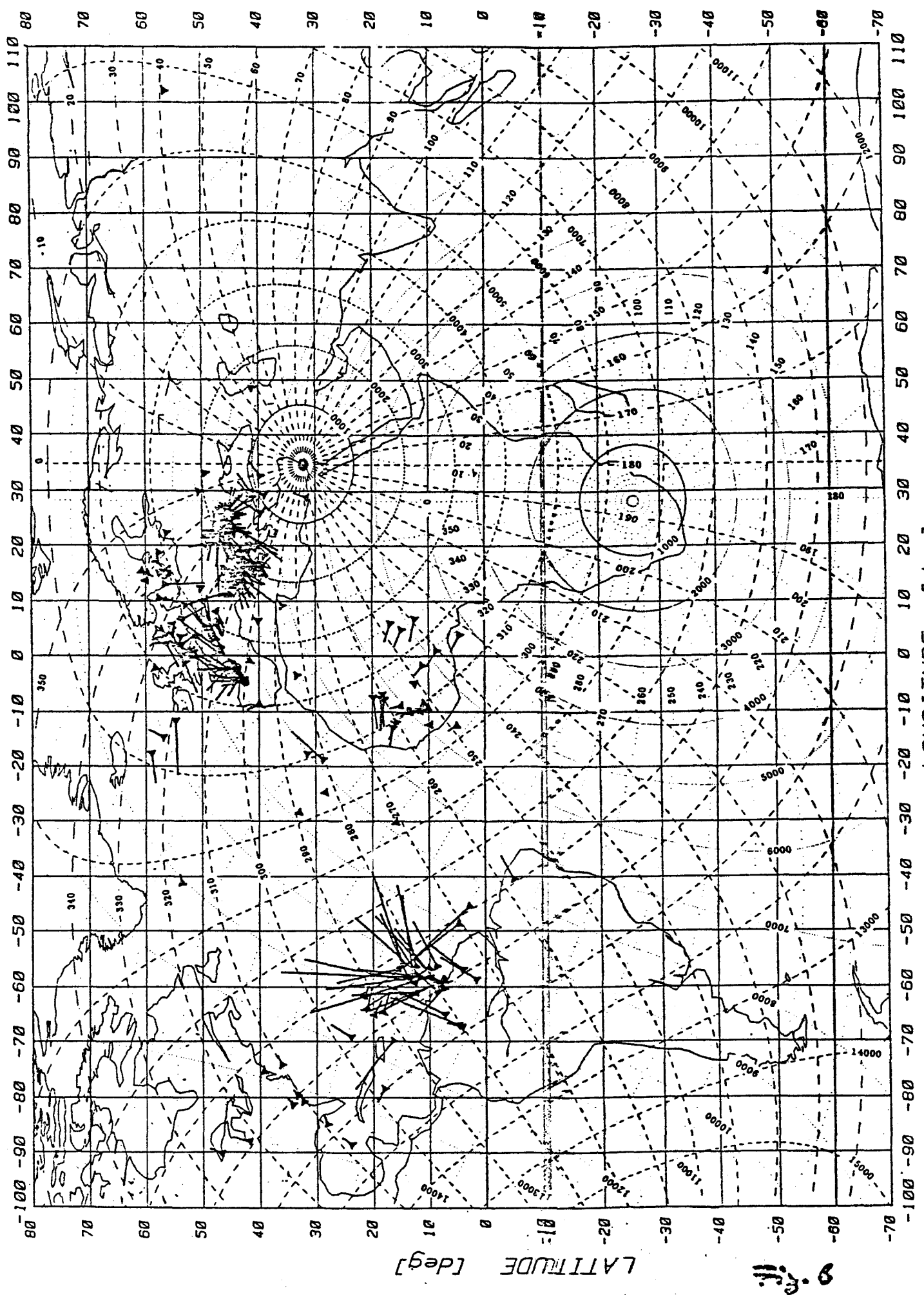
5-21-5



LONGITUDE [deg]

LATITUDE [deg]

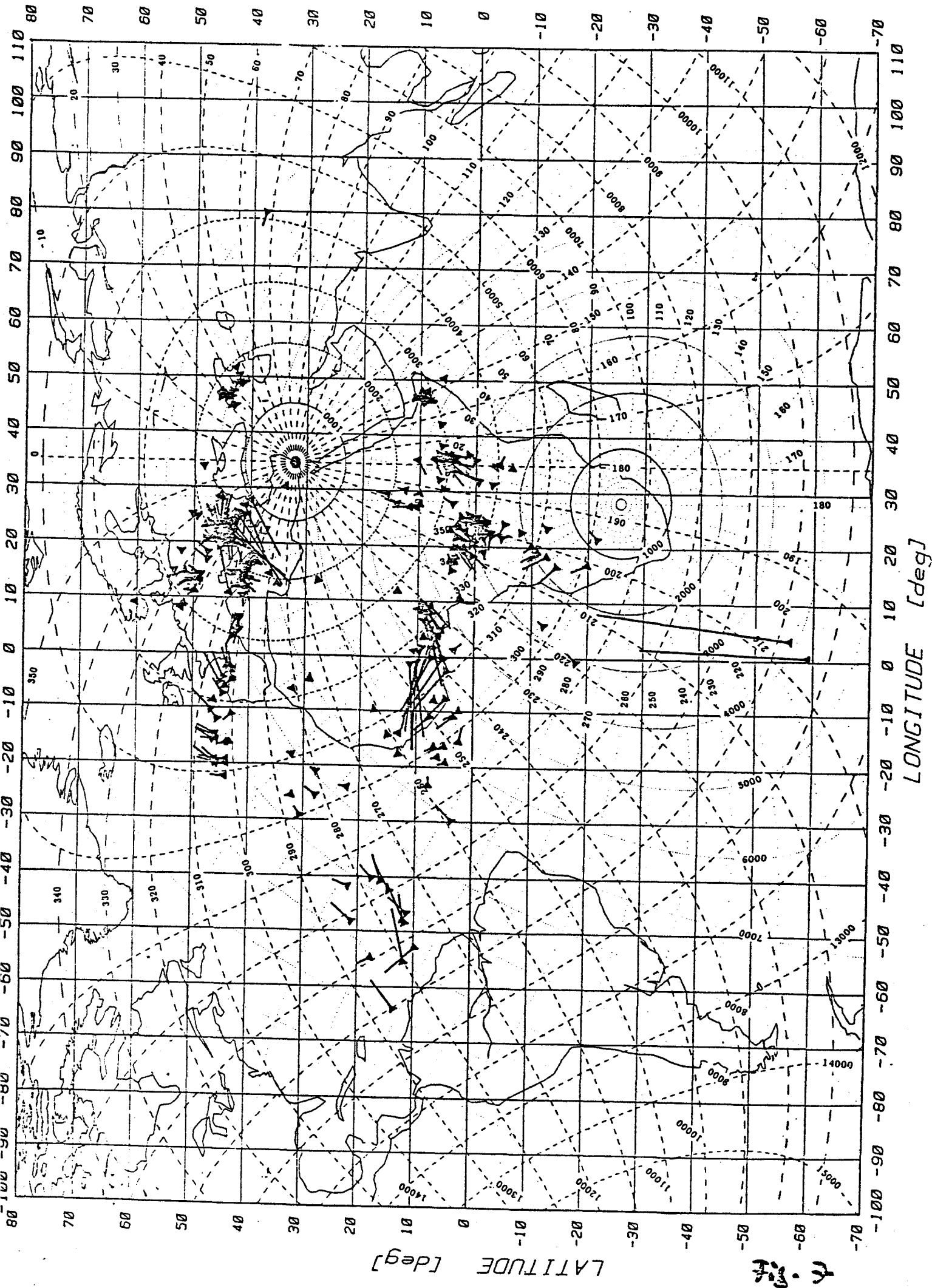
L. 5. 14.



LATITUDE [deg]

0.75

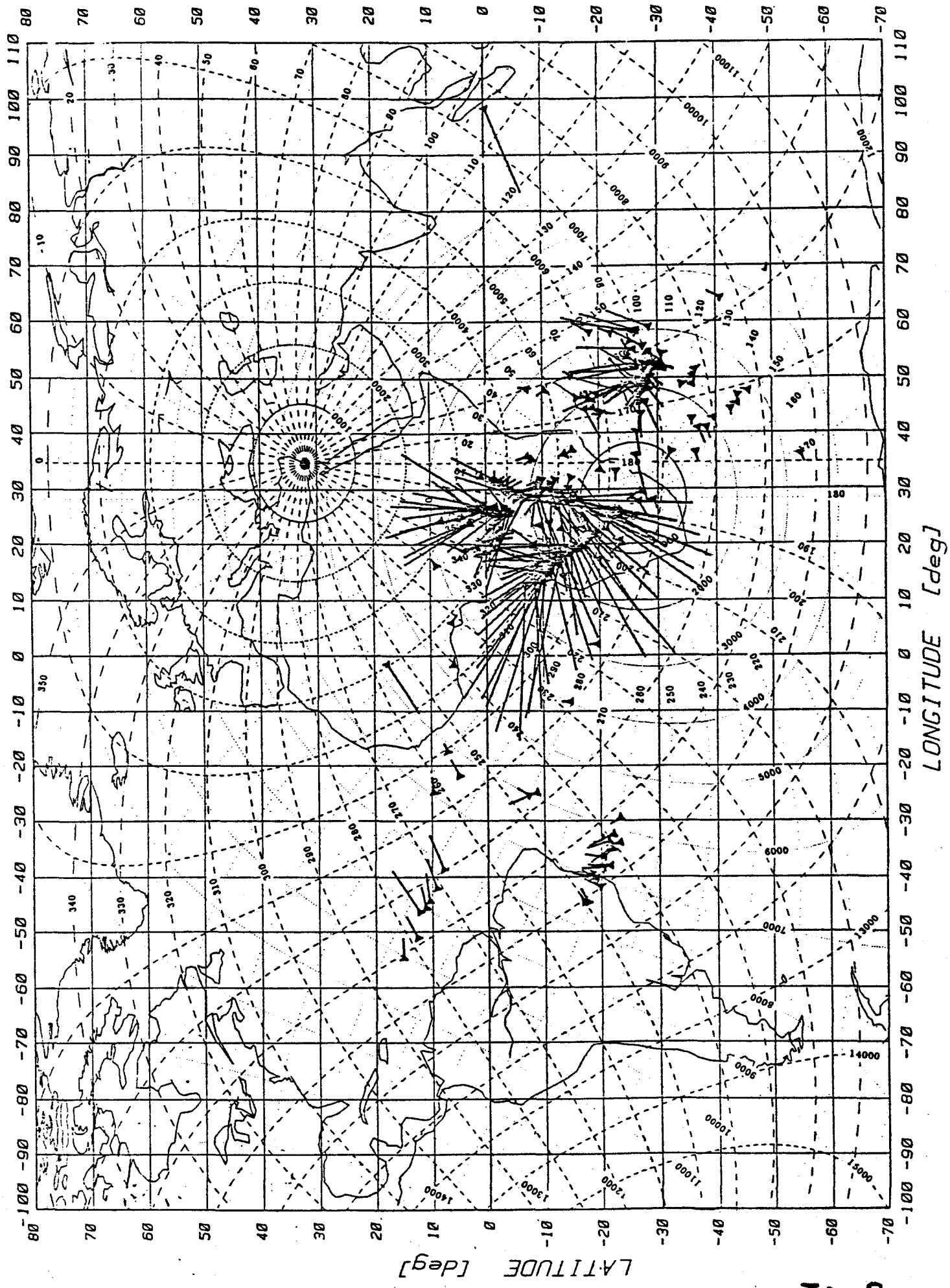
1.00 1.10 1.20 1.30 1.40 1.50 1.60 1.70 1.80 1.90 2.00 2.10 2.20 2.30 2.40 2.50 2.60 2.70 2.80 2.90 3.00 3.10 3.20 3.30 3.40 3.50



LATITUDE [deg]

LONGITUDE [deg]

天. 2



Dr. P. H.



METEOSAT

1981 MONTH 9 DAY 30 TIME 1125 GMT (NORTH) CH. VIS 2
NOMINAL SCAN/RAW DATA SLOT 23 CATALOGUE 1034520124

Fig. 9



METEOSAT

1981 MONTH 9 DAY 30 TIME 1755 GMT (NORTH) CH. IR 2
NOMINAL SCAN/RAW DATA SLOT 36 CATALOGUE 1034520073

Fig. 10

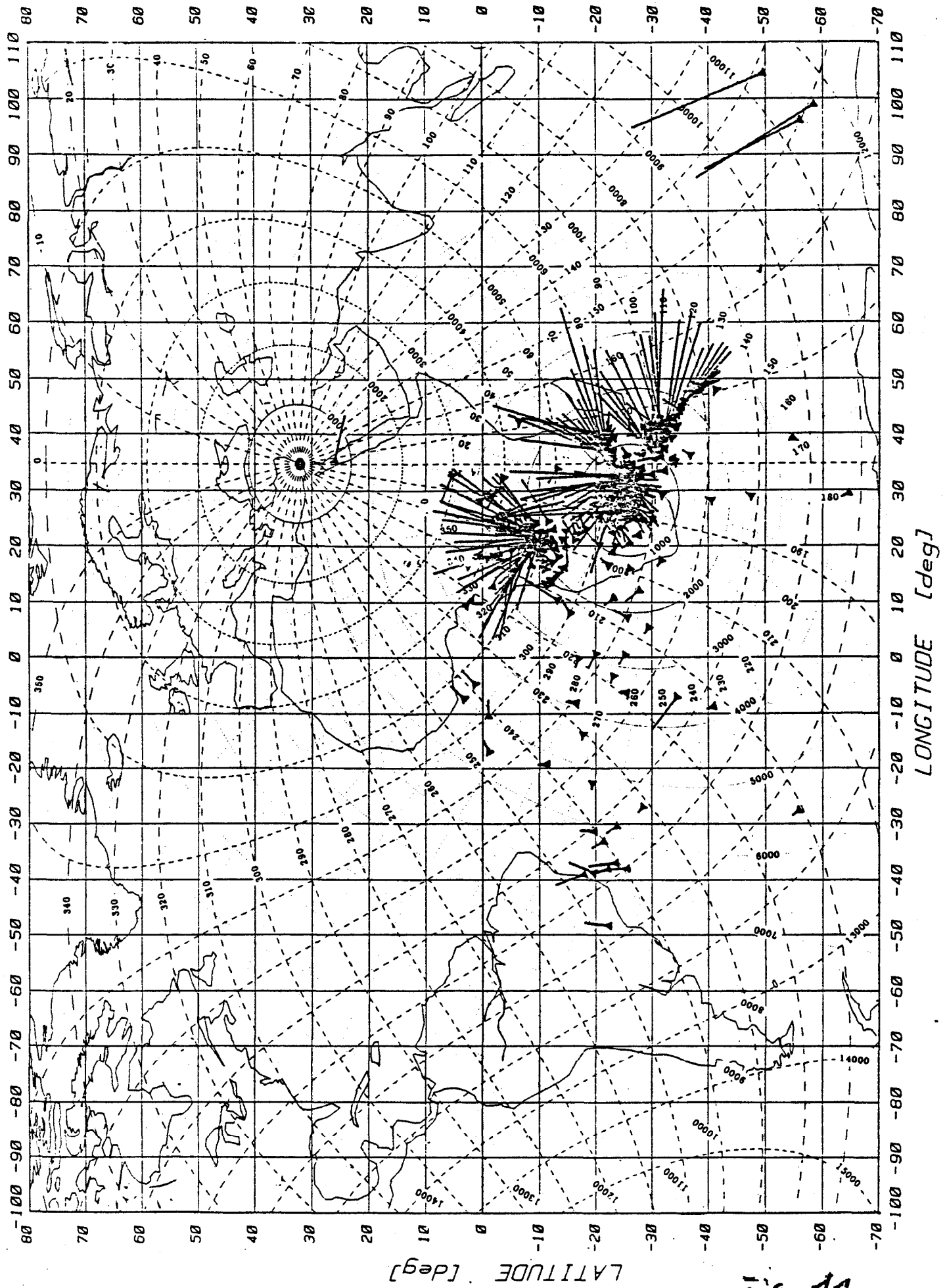


Fig. 11



METEOSAT

1981 MONTH 10 DAY 2 TIME 1155 GNT (NORTH) CH. IR 1
NOMINAL SCAN/RAW DATA SLOT 24 CATALOGUE 1034520093

Fig. 12

AGARD

ADVISORY GROUP FOR AEROSPACE RESEARCH & DEVELOPMENT

7 RUE ANCELLE 92200 NEUILLY SUR SEINE FRANCE

Paper Reprinted from
Conference Proceedings No. 305

**MEDIUM, LONG AND VERY LONG
WAVE PROPAGATION
(AT FREQUENCIES LESS THAN 3000kHz)**

NORTH ATLANTIC TREATY ORGANIZATION



VLF-ATMOSPHERICS AS A TOOL FOR PROBING VLF-PROPAGATION CONDITIONS

J. Schafer and H. Volland
Radioastronomical institute, University of Bonn
Auf dem **Hügel 71**, D 5300 BOM 1, West Germany

SUMMARY

This paper presents a new technique for receiving and analysing atmospheric **signals** and for deriving the VLF-propagation conditions. The equipment consists mainly of a **receiver/analyser** with an **on-line** desktop computer. The computer controls the observations and analyses the received parameters in real time, so that the results, e. g. the reference height of the lower ionosphere or the strengths and locations of the thunderstorm activity **centers**, **can** be printed out immediately or displayed on a world map with a small desktop **plotter**. The data are also stored on **magnetic** tape cassettes.

At present, two stations of this kind are operating continuously at Pretoria (South Africa) and Tel Aviv (**Israel**). A somewhat **earlier** version is used at Berlin. Further stations are being projected to complete a global network (among **these** a station in **the** Antarctic). At the moment, Europe and Africa and parts of South and North America and Asia are covered. **These** measurements are used to investigate the short and long-term as well as the local and global behaviour of the lightning activity and the VLF-propagation conditions and to elucidate **their** correlation to atmospheric electric and possibly also external (e. g. **solar**) parameters. Some **results** of the measurements, **including** statistical analyses of the received parameters and **typical** real time plot **charts** are shown to demonstrate the methods and capabilities of the present system.

1. INTRODUCTION

Lightning strokes are **known** to **produce** a wide band of electromagnetic radiation, the VLF-impulsive part of which is called atmospheric. **Because** of the large antenna **lengths** and current densities of **these natural** transmitters and **because** of the good transmission characteristics of the terrestrial waveguide **between** earth and ionosphere for VLF-waves, the radiated VLF-impulses **can** be traced at distances of global scale. The permanent presence of atmospheric (**ca.** 100 strokes per second over the **entire** globe) allows one to continuously survey the atmospheric activity and the propagation conditions for **VLF**-waves, and especially the state of the lower ionosphere, with relatively few recording stations **around** the world.

The theoretical background of **these** analyses is a propagation model for VLF-waves depending **mainly** on (a) the **mean** reference height of the lower ionosphere along the propagation path, and (b) the **mean anisotropy** factor, which describes the influence of the geomagnetic field and the plasma collision frequency. Basic calculations on the characteristics of **such** models have been carried out e. g. by Wait and **Spies** (1964). Using wave guide mode theory, Volland (1968) has shown the pronounced dispersive behaviour of the spectral parameters of VLF-atmospherics in the frequency band **ca.** 3 and 10 kHz, which makes this band **suitable** for experimental investigations. Based on **these** theoretical results, a **VLF**-atmospherics analyser has been developed at the **Heinrich-Hertz-institut**, Berlin, (Heydt and Volland, 1968), and subsequently improved in **several** versions. Besides the direction of incidence (azimuth) of each atmospheric, this receiver determines the spectral amplitudes at two **suitable** frequencies in the VLF-band as well as the difference in the **arrival** times between two spectral groups. Extensive model calculations of **these** spectral parameters for **various** ionospheric conditions are due to Harth (1972). The main drawback of this first generation of VLF-analysers was the method of data processing. For each atmospheric, one of the spectral parameters could be displayed against the azimuth on an oscillograph screen as a point. **Taking** a **photographic** picture of all atmospheric within a time period of e. g. 5 minutes, one could **estimate** the **mean** azimuth and the corresponding **mean** value of the spectral parameter from the clusters on the picture by **visual** inspection. This **complicated** and time consuming process and the inefficiency in the recording of the spectral parameters (**only** one at a time together with the azimuth) inspired the development of a new generation of VLF-atmospherics receivers. This new atmospheric station includes a desktop computer for controlling and analysing the measurements so that it **can** be **operated** completely automatically. The calculator collects the spectral parameters and the azimuths of **all** incoming atmospheric over a time period of 20 minutes. The operation **program** then performs a **statistical** analysis of **all** atmospheric data from each single **center** of activity. Furthermore, it **contains** an optimized VLF-propagation model, which is used to directly determine the distance to the thunderstorm **centers** and the applicable propagation conditions for VLF-waves. A desktop **plotter** is then enacted to **denote** the locations and strengths of the activity **centers** on a **map**. The received and analysed **atmospherics** data are printed out in real time and also stored on the **internal** tape cartridge of the computer for possible a posteriori analysis:

Two of **these** new stations have been operating **continuously** for more **than** one year at Pretoria and Tel Aviv (**Schafer et al.**, 1980), an older one is installed in Berlin, and another new station **will** be **established** in the Antarctic next year. **The** small **size** of the equipment its easy **handling** and its **insensibility** to **external** influences allow it to be installed almost **everywhere**, with its **antenna** placed on a roof, in an open field or aboard a ship.

2. PROPAGATION OF VLF-ATMOSPHERICS IN THE TERRESTRIAL WAVE GUIDE

VLF-atmospherics originate **mainly** from cloud-to-ground **lightning strokes** which can be well approximated by vertical electrical dipoles on the ground. The transmitted impulses travel through the atmospheric wave guide between earth and ionosphere, see Fig. 1 (Ingmann et al., 1981), and are transformed on this way according to the propagation conditions, which **depend predominantly** on the location and the state of the lower ionosphere. The vertical electric field component of an atmospheric at distance P from the source over a perfectly conducting earth

$$E(\rho, t)$$

with its complex Fourier transform

$$\hat{E}(\rho, \omega) = |\hat{E}| e^{i\phi} = \int_{-\infty}^{+\infty} E(\rho, t) e^{i\omega t} dt \tag{1}$$

is transformed by the complex transmission function

$$\hat{W}(\rho, \omega, p_1, p_2, \dots) \equiv |\hat{W}| e^{i\Phi} \tag{2}$$

to yield the spectral amplitude

$$\hat{E}(\rho, \omega) \cdot \hat{W}(\rho, \omega, p_1, p_2, \dots) = |\hat{E}| \cdot |\hat{W}| \cdot e^{i(\phi+\Phi)} \equiv \hat{A} \cdot e^{i\Theta} \tag{3}$$

Here, p_i are all the terrestrial parameters which influence the transmission function. **Since** the earth can be **regarded** to a very good approximation as perfectly conducting in the far field (more than some 100 km), the parameters p_i **describe** the state of the lower ionosphere. Simple exponential models for the electron density and the collision number profiles in the lower ionosphere are sufficient for **VLF-reflection** calculations, **because** the main reflection takes place at electron densities of only a **few hundred** electrons/cm³. The electron density profile

$$N(z) = N(z_0) \exp(b(z-z_0)) \tag{4}$$

and the electron - neutral particle collision frequency profile

$$\nu(z) = \nu(z_0) \exp(-a(z-z_0)) \tag{5}$$

can be combined in the model calculations to form the ratio of the squared plasma frequency ω_p^2 to the collision frequency ν

$$\omega_p^2(z) / \nu(z) \equiv \omega_r(z) = \omega_r(z_0) \exp(\beta(z-z_0)) \tag{6}$$

with

$$\omega_r(z_0) = \omega_p^2(z_0) / \nu(z_0) = 3.18 \cdot 10^9 N(z_0) / \nu(z_0) \quad (N(z) \text{ in cm}^{-3}) \tag{7}$$

and $\beta = a+b$. z_0 is the ionospheric reference height. ω_r is called the "conductivity parameter"; it is the only relevant parameter for a pure isotropic plasma r (no magnetic field). If the terrestrial magnetic field is included, the gyrofrequency ω_T of the electrons has to be regarded as the second important parameter, which can also be normalized to the collision frequency at z_0 to yield the so called "anisotropy factor"

$$\zeta = \omega_T / \nu(z_0) \tag{8}$$

Although ω_T is actually a 3-component vector for arbitrary directions of propagation, it is the trans-

verse component of the **earth's magnetic** field that is the most decisive (Wait, 1962). **so** that the **anisotropy** factor is related only to that component.

3. THE DEPENDENCE OF VLF-ATMOSPHERICS PARAMETERS ON THE PROPAGATION CONDITIONS

The **highly** dispersive character of the transmission function (2) in the VLF-band **offers** the opportunity for **model** calculations of the amplitude and phase relationship between at least two **suitable** spectral groups in this band. The atmospherics **receiver/analyser** uses three narrow band receivers at 5, 7 and 9 kHz. The first atmospherics parameter is the Spectral Amplitude "SA" at 5 kHz

$$SA \equiv \hat{A}(\rho, \omega_1, p_1, p_2, \dots) \quad (9)$$

Secondly, the ratio of the amplitudes at 9 and 5 kHz is formed

$$SAR \equiv \hat{A}(\rho, \omega_1, p_1, p_2, \dots) / \hat{A}(\rho, \omega_2, p_1, p_2, \dots) \quad (10)$$

This parameter is called the Spectral Amplitude Ratio (SAR). The third measured parameter is the time difference in the **arrival times** of the spectral groups at 6 and 8 kHz. called the Group Delay **Time Difference** (GDD). It is deduced from the second derivative of the phase θ in (3) with respect to frequency (Volland, 1968)

$$GDD \equiv \Delta t_{gr} \approx - \frac{\partial^2 \theta(\rho, \omega, p_1, p_2, \dots)}{\partial \omega^2} \cdot \Delta \omega \quad (11)$$

In terms of **finite differences** this may be written

$$GDD = \Delta t_{gr} \approx \frac{\theta_2 - \theta_m}{\omega_2 - \omega_m} - \frac{\theta_m - \theta_1}{\omega_m - \omega_1} \quad (12)$$

$$= \frac{\theta_2 - 2\theta_m + \theta_1}{\Delta \omega} \quad (13)$$

with $\theta_i = \theta(\rho, \omega_i, p_1, p_2, \dots)$ and $\omega_2 - \omega_1 = \omega_m - \omega_1 = \Delta \omega$. Measuring the phases θ_i at 5, 7 and 9 kHz, the first derivatives in (12) refer to 6 and 8 kHz, resp., so that their difference gives the time delay **between these** spectral groups.

Models of **these** three spectral parameters **showing** their dependence on the conductivity parameter (6) and the anisotropy factor (8) have been calculated **by** Harth (1972) at the **above** mentioned frequencies. He used values of

$$N(z_0) = 300 \text{ cm}^{-3}, \quad \nu(z_0) = 5 \cdot 10^6 \text{ s}^{-1}$$

and

$$\begin{aligned} z_0 &= 70 \text{ km}, \quad \beta = 0.3 && \text{for daytime and} \\ z_0 &= 85 \text{ km}, \quad \beta = 0.5 && \text{for nighttime propagation conditions.} \end{aligned} \quad (14)$$

The anisotropy factor β varies at middle latitudes between **ca.** -1 for west-east, and **ca.** +1 for **east-west** propagation. In Fig. 2, the daytime and **nighttime** models for GDD and SAR (denoted by their **reference** heights of 70 and 85 km, resp.) are plotted as function of Ω in the range between the dotted lines. **These** parts of the **curves** are based on a **linear** dependence of the parameters on distance (Mm = 1000 km). Unfortunately, this is only **accurate** at large distances from the source (**beyond ca.** 2000 km) where the first mode approximation is sufficient. The higher modes have to be included for consideration at **closer** distances. This leads to a more complicated non-linear behaviour of the spectral parameters (Harth, 1981 a. b).

In **order** to **account** for **these** deviations from linearity, **which** are nearly **antiparallel** for GDD and SAR, the normal range of Ω (-1 to +1) has been **artificially** extended, and exponential **tails** have been added

to the models. **Interpolating** between the daytime and nighttime models by **means** of the height dependence given by **Volland** (1968) and including the exponential extensions one obtains the following functions for **GDD** and **SAR**, depending on the anisotropy factor Ω and the reference height z (in km), see Fig. 2,

$$\text{GDD}(z, \Omega) = \frac{a}{z^2} + \frac{b}{z} \quad (\text{usec} / \text{Mm}) , \quad (15)$$

with

$$\begin{aligned} a &= \text{GDD}(85, \Omega) \cdot 1.27 \cdot 10^3 + 1.61 \cdot 10^5 , \\ b &= \text{GDD}(85, \Omega) \cdot 70 + 1.89 \cdot 10^5 , \\ \text{GDD}(85, \Omega) &= 29.3 - 3.3 \Omega^2 - 7.6 + \exp(-5\Omega - 7) - \exp(5\Omega - 7) \end{aligned}$$

and

$$\text{SAR}(z, \Omega) = \frac{e}{z^3} + \frac{f}{z} \quad (\text{dB} / \text{Mm}) , \quad (16)$$

with

$$\begin{aligned} e &= \text{SAR}(85, \Omega) \cdot 4.87 \cdot 10^4 + 2.77 \cdot 10^6 , \\ f &= \text{SAR}(85, \Omega) \cdot 78.3 + 3.84 \cdot 10^2 , \\ \text{SAR}(85, \Omega) &= 4.8 + 2\Omega - \exp(-9\Omega - 20) . \end{aligned}$$

Because of the greater sensitivity of SA to **disturbances** and its more complicated statistical distribution, **only** GDD and SAR are used for the modelling at this stage.

Besides **these** propagation effects of GDD and SAR of an atmospheric impulse, the source terms (**originating** in the lightning stroke itself) of **these parameters** have to be considered. **During** the course of the measurements, the values of

$$\begin{aligned} 7\text{dB} &\text{ for SAR} && \text{and} && (17) \\ -5\text{usec} &\text{ for GDD} \end{aligned}$$

have turned out to fit well. **These** quantities are in satisfactory agreement with **those** deduced theoretically by Volland (1981) using a wave guide lightning model.

4. METHOD OF MEASUREMENTS AND DATA EVALUATION

The computer collects the data of all atmospheric **within** a measuring period of 20 minutes. Subsequently, a histogram of the **number** of atmospheric per **azimuth-interval** (1.5°) is **calculated**. A **typical** example of **such** a histogram, recorded at the atmospheric station at Tel Aviv, is shown in Fig. 3 (**lower** panel). Five **centers** of activity **can** be clearly discerned. **All** activity **centers** are fitted by normal distributions using a fitting routine **included** in the operations **program** of the computer. The fact that activity **centers can** normally be fitted **quite** well by normal distributions indicates that they **can** be regarded as point sources. **Theoretically**, the horizontal **magnetic** vector of an atmospheric should be exactly orthogonal to the direction of incidence, so that a very narrow peak should be measured (conventional direction finding with double crossed loops is used here). **However**, a certain disturbance of the **signals** is always present which **can lead** to deflections of **up to** 10° and more for a single atmospheric impulse. Due to the **random** character of **these** disturbances, a statistical **analysis** of an activity center yields the exact position and the strength (atmospherics/min) of that **center**, even if the rate per minute is very **low** (**down to ca.** 2/min).

Having determined all significant activity **centers** in the azimuth histogram, the spectral parameters of each of **these centers** are evaluated using the **same fitting** procedure with normal distributions. The **histograms** of GDD, SAR and SA of the three largest activity **centers** are shown in the upper panel of Fig. 3. The statistical **parameters** of the spectral and angular measurements are **listed** in the **real time printer output** (see **inset** to azimuth histogram - lower panel). For each parameter $\{\phi = \text{azimuth}, \Delta = \text{GDD}, r = \text{SAR} \text{ and } a = \text{SA}\}$ are **printed** the peak value, the width ($1a$) and the total **number** of impulses (**per** minute) of the corresponding normal distribution. One notices that the **assumption** of a normal distribu-

tion **again** fits **quite** well for the GDD (in usec) and SAR (in dB) parameters. **especially** when the pulse rate is high enough (large **centers** of activity often show pulse rates ten times larger **than these, up to** 200 per minute and more). This is **again** due to the unavoidable disturbances of the **signals along** their propagation paths, and to the internal spread of the values in the sources, but this obviously **does** not affect the location of the peak values. A more difficult situation arises for the SA parameter. Although its **histogram** normally follows a logarithmic normal distribution (**Volland, 1968**), the statistical **parameters can** sometimes be evaluated only with **quite** large uncertainties. This happens **particularly** for very distant sources, when only the large amplitude wing of the distribution **can** be recorded **because** the left part is below the receiver threshold. This threshold **is** defined in the receiver as **0 dB**. It corresponds to a spectral field strength of **ca. $0.8 \mu\text{V} \cdot \text{m}^{-1} \cdot \text{Hz}^{-1}$** . Measuring SA in DB **above** this threshold **again** implies a normal distribution of this parameter.

5. DETERMINATION OF THE VLF-PROPAGATION CONDITIONS AND THE DISTANCES OF THE ACTIVITY CENTERS

In **order** to determine the model values of the spectral parameters at the receiving station, one has **to** know three independent variables (see Fig. 2):

- (a) the reference height z_0 of the lower ionosphere,
- (b) the anisotropy factor, Ω
- (c) the distance of the activity center.

Therefore, by measuring the three independent spectral parameters GDD, SAR and SA, one **should** theoretically be able to determine the variables. Due to the more complicated distribution of SA, **only** GDD and SAR are used at this stage of development of the system. An extension of the model including the SA parameter is in progress. For the present, however, one of the independent variables has to be inserted externally into the model. The variable **chosen** is the reference height of the lower ionosphere. **It** is determined by the operations **program** simply as a function of the zenith angle of the sun for any given point on the globe. The universal time (GMT), available in the computer, and a fundamental spherical **analysis** is used for this task. Now the computer uses an iterative **algorithm** to determine that unique value of Ω , for which the distances, deduced from the measured GDD and SAR **values** with the aid of the models in Fig. 2, become equal. Additionally, the **mean** ionospheric reference height along the propagation path (depending on the **mean** zenith angle of the sun) is **taken** into account. By this method, the appropriate Ω -value **is** determined **internally** together with the distance. The parameters Ω , z_0 and the distance are **printed** out immediately. Fig. 3 and Fig. 4, which was **taken** one hour **later**, clearly demonstrate the efficiency of the calculation method. As an **example**, one notices that the two largest activity **centers** near 38° and 304° azimuth remain nearly constant in direction and distance (this **will** be **shown** in more **detail later**). Though the GDD and SAR values for **these centers** change **during** this time (in a **antiparallel** manner), the distances are **accurate** within 0.25% and **2%**, resp.. The appropriate Ω -value for **these** directions has shifted according to the propagation model (Fig. 2). Generally, the distances are **correct to within** about 5%. An exception to this **rule** are **those** cases, where the propagation direction traverses the terminator at very **small** angles and where the terminator is very close to the receiver. An optimization of the model for **these** conditions is being developed.

6. MEASUREMENT EXAMPLES

The measured and evaluated atmospheric data are not only printed out, but also stored on the **magnetic** tape cassette of the computer with a capacity of approximately one **month** of data recording. The system includes a small desktop **plotter** (DIN A4) for **real** time use of the data, which marks the strengths and the locations of the recorded thunderstorm **centers** directly on a **map**. Figs. 5 and 6 show **two examples** of **such** recordings. Activity **centers** are marked by a small triangle with a pointer, whose length is proportional to the strength of the center- (atmospherics/min) and whose direction gives the time (**GMT**) like a clock. In Fig. 5, the plot **sheet** has **been** in the **plotter** for 5 hours (**8:00-13:00** GMT on 23. June 1981), i. e. **during** 15 measuring periods. The activity **centers** at **8:30** and **9:30** GMT, shown in **detail** in Figs. 3 and 4, **can** be clearly identified. As already mentioned, the locations of the largest **centers** in Figs. 3 and 4, near 38° and 304° , remain nearly constant. The first one is a stationary activity center east of the **Caspian** Sea, which begins to develop at **8:00** GMT and strengthens considerably **up to 12:00** GMT. This development is also evident from Figs. 3 and 4. The second **example** is also a stationary center in the western Mediterranean, which **gradually** decays **during** this **measuring** period. Furthermore, a large activity **region** develops at **around noon** in eastern Europe, which **exhibits** a **shift** in the location of the peak intensity. This overall picture agrees well with the meteorological condition and frontal **system** of that day, as verified on the synoptical charts. **These** weather **maps**, however, are available only

every 6 hours and **give** no information on the strength and development of the activity **centers**.

Fig. 6 shows a **similar** picture of the recorded thunderstorm activity **during** 16.5 hours (therefore some overlapping pointers occur), **mainly** at nighttime propagation conditions. **During those times** when the strong West African sources are weak (in this case around 2:00 GMT), strong activity **centers can be detected** in South America. This gives some indication of the range of the system: activity **centers** in the western direction **can be recorded during** nighttime at distances of up to 12 000 km, whereas sources in the **east** are visible only at distances of **up to** about 7 000 km (**during** nighttime). Atmospheric sources **can** generally be detected **during** the day at distances of only **up to** 60% of the nighttime values.

The strong sources over the African continent are **always** detectable at Tel Aviv **during** nighttime and partly also at daytime. Sources in South America and in the western Atlantic (**see** Fig. 6) are also often recorded. Together with the station at Pretoria, which records the **same** sources over the African continent and in South America, and with the station at Berlin, **these** continuous sets of data are used for optimizing the propagation models of the atmospheric parameters and for **investigations** of the general characteristics of the propagation conditions and the (**half**) global lightning activity.

7. CONCLUSIONS

A new method of evaluating **atmospherics** data, **including** the strength and locations of lightning activity **centers and** the appropriate VLF-propagation conditions, is presented. The new VLF-atmospherics receiving station is controlled completely automatically **by** a desktop computer (HP9825), which also makes a statistical analysis of the received atmospheric data and applies a sophisticated VLF-propagation model for **evaluating** the parameters of the propagation model as **well as** the distances and strengths of the activity **centers** in real time. In **order** to have an immediate overview, the detected atmospheric sources are plotted directly on a **map** by **means of** a **small desktop plotter**, and the data are **additionally stored** on **magnetic** tape cassettes.

The accuracy of direction finding is in general **accurate to** 0.5° , **depending** on the stationarity and form of the activity center. The determination of the spectral parameters, as **well as** the subsequent **determination** of the distance of an activity **center** by **employing** a **suitable** VLF-propagation model, is possible to an accuracy of around 5%. Further improvement is expected with an increasing **number** of stations, which, by **means of** cross-bearings, **will** assist in the development of optimal models. The maximum range within which thunderstorm **can be located extends** from **ca.** 4000 km for eastern **centers at day-**time to **ca.** 12 000 km for sources in the western direction **during** nighttime. The **minimum range** is around 200 km, at which an unambiguous determination of the distance becomes **difficult** due to the **over-**whelming influence of the higher modes.

8. REFERENCES

- Harth, W., 1972, "VLF Atmospheric Parameters Described by the Wait and Walters Model", *Z. Geophys.*, 38, 153.
- Harth, W., 1981a, "Theory of Low Frequency Wave Propagation", Handbook of Atmospheric, H. Volland (ed.), CRC Press, Boca Raton, FL.
- Harth, W., 1981b, "The Higher Order Mode in the Lower VLF-Range Measured at Medium Distances", *Current Proceedings*.
- Heydt, G., and Volland, H., 1964, "A New Method for Locating Thunderstorms and Counting their Lightning Discharges from a Single Observing Station", *J. Atmos. Terr. Phys.*, 26, 780.
- Ingmann, P., Volland, H., Heydt, G., 1981, "Observations of the Thunderstorm Activity during July / August 1975 in the European-North American Area by Groundbased Single-Station Technique", *Meteorol. Rdsch.*, (in print).
- Schäfer, J., Volland, H., Ingmann, P., Eriksson, A.J., Heydt, G., 1980, "A Network of Automatic Atmospheric Analysators", Proceedings of the symposium on Lightning Technology, NASA Conference Publication 2128, FAA-RD-80-30.
- Volland, H., 1968, "Die Ausbreitung langer Wellen", Vieweg Verlag, Braunschweig
- Volland, H., 1981, "Low Frequency Radio Noise", Handbook of Atmospheric, H. Volland (ed.), CRC Press, Boca Raton, FL.
- Wait, J. R., 1962, "Electromagnetic Waves in Stratified Media", Pergamon Press, Oxford, New York.
- Wait, J. R., and Spies, K. P., 1964, "Characteristics of the Earth-Ionosphere Waveguide for VLF Radio Waves", Technical Note, NBS. No. 300.

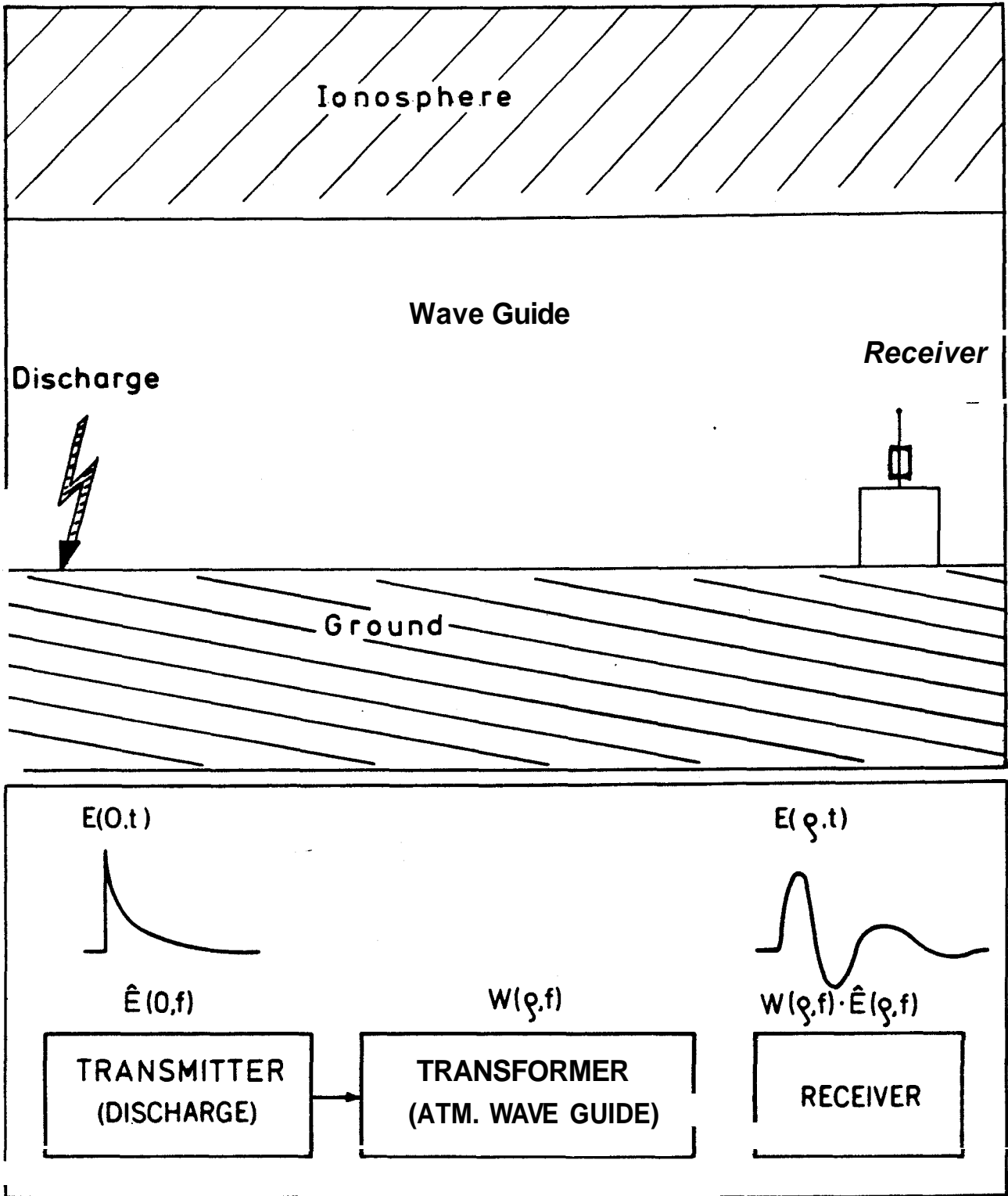


Fig. 1 Schematic diagram of the propagation of VLF-atmospherics through the terrestrial waveguide between earth and ionosphere.

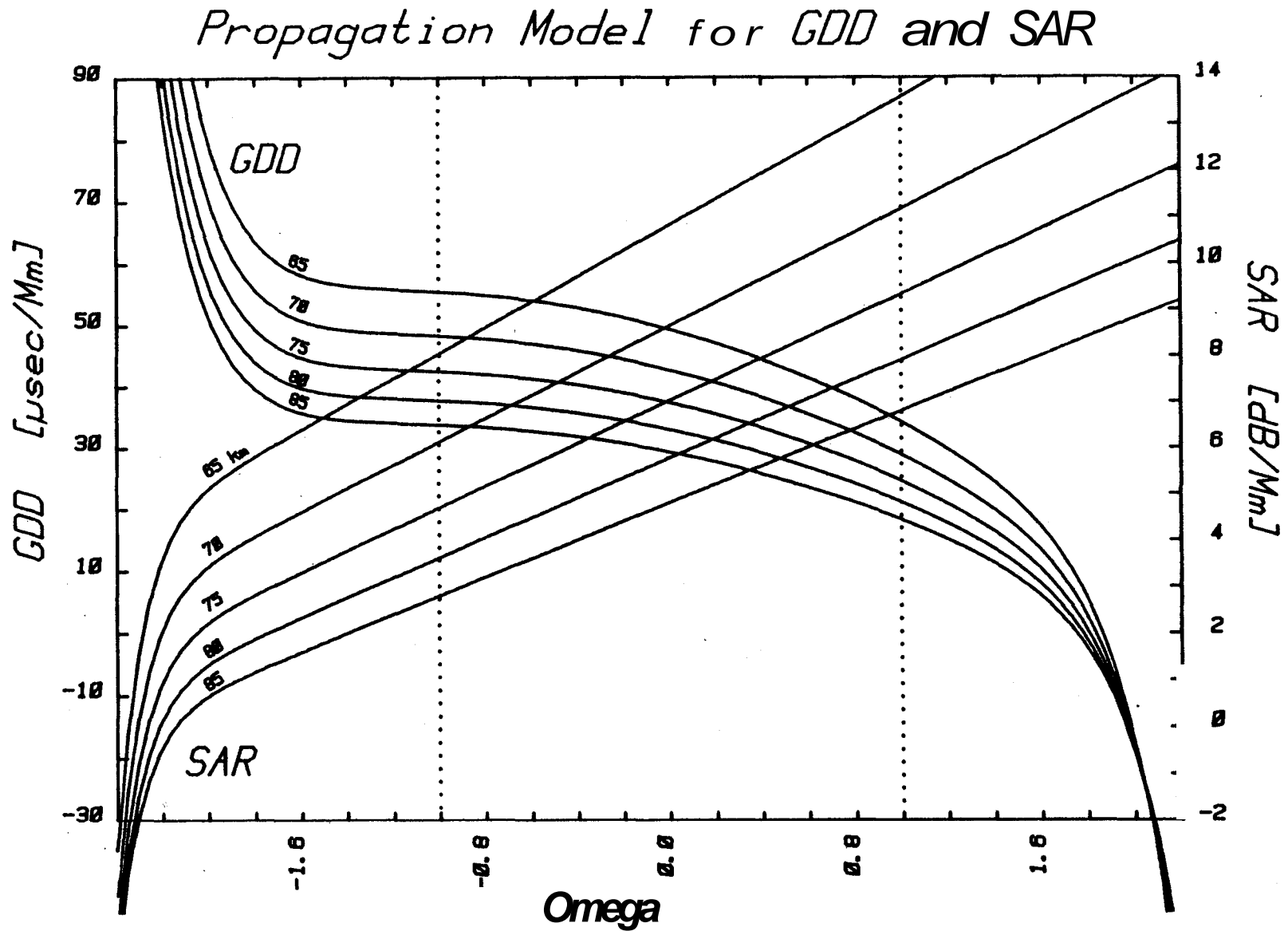


Fig. 2 Propagation models for the atmospheric parameters GDD (Group Delay time Difference, 6 - 8 kHz) and SAR (Spectral Amplitude Ratio, 9 / 5 kHz) as function of the anisotropy factor Omega (Ω , see text) for various ionospheric reference heights z_0 (km).

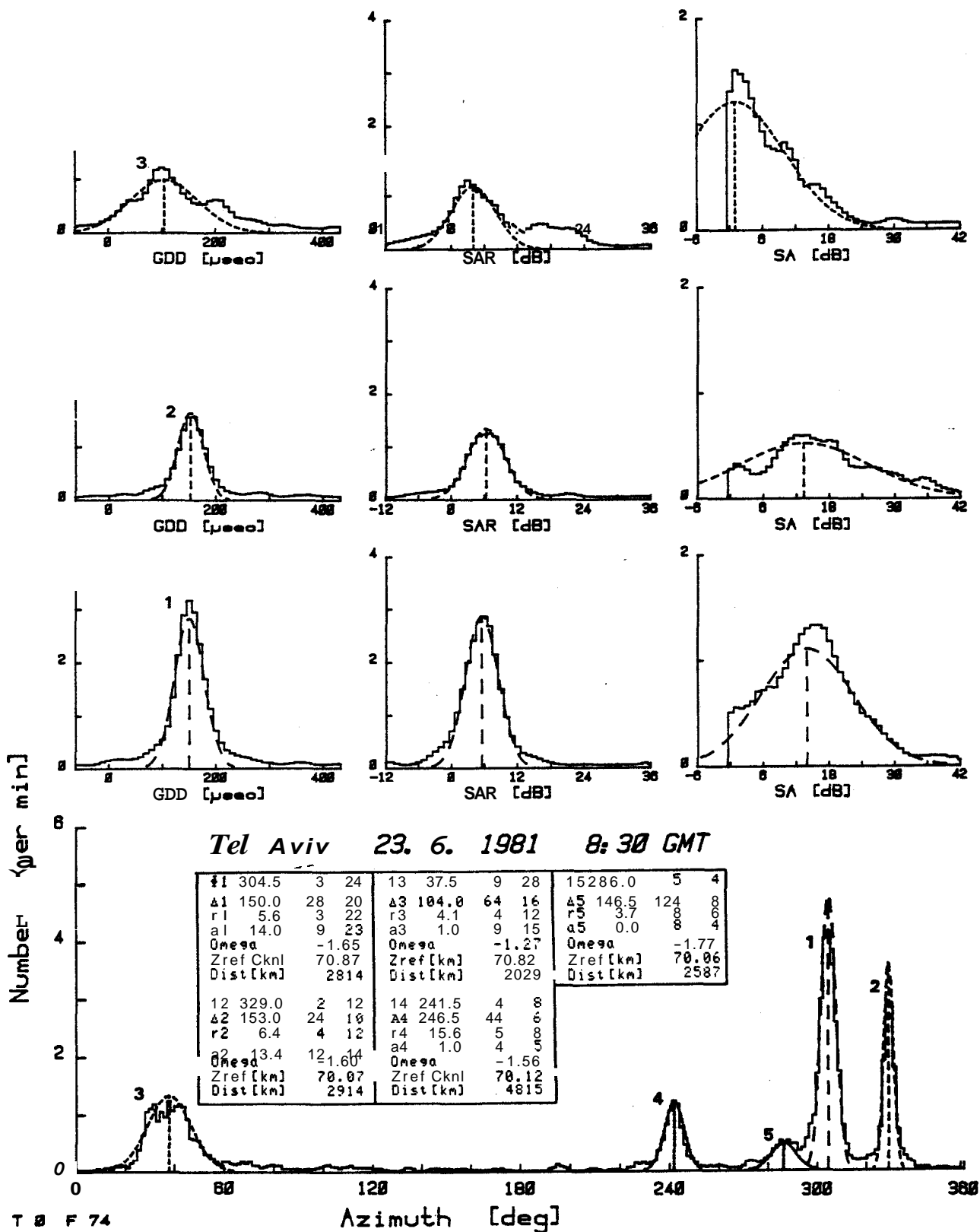


Fig. 3 Histograms of the azimuth and the spectral parameters GDD, SAR and SA (of the three largest activity centers) recorded at Tel Aviv in the measuring period 8:20 - 8:40 GMT on 23 June 1981. The inset in the lower panel is the real time printer output of the computer (HP 9825).

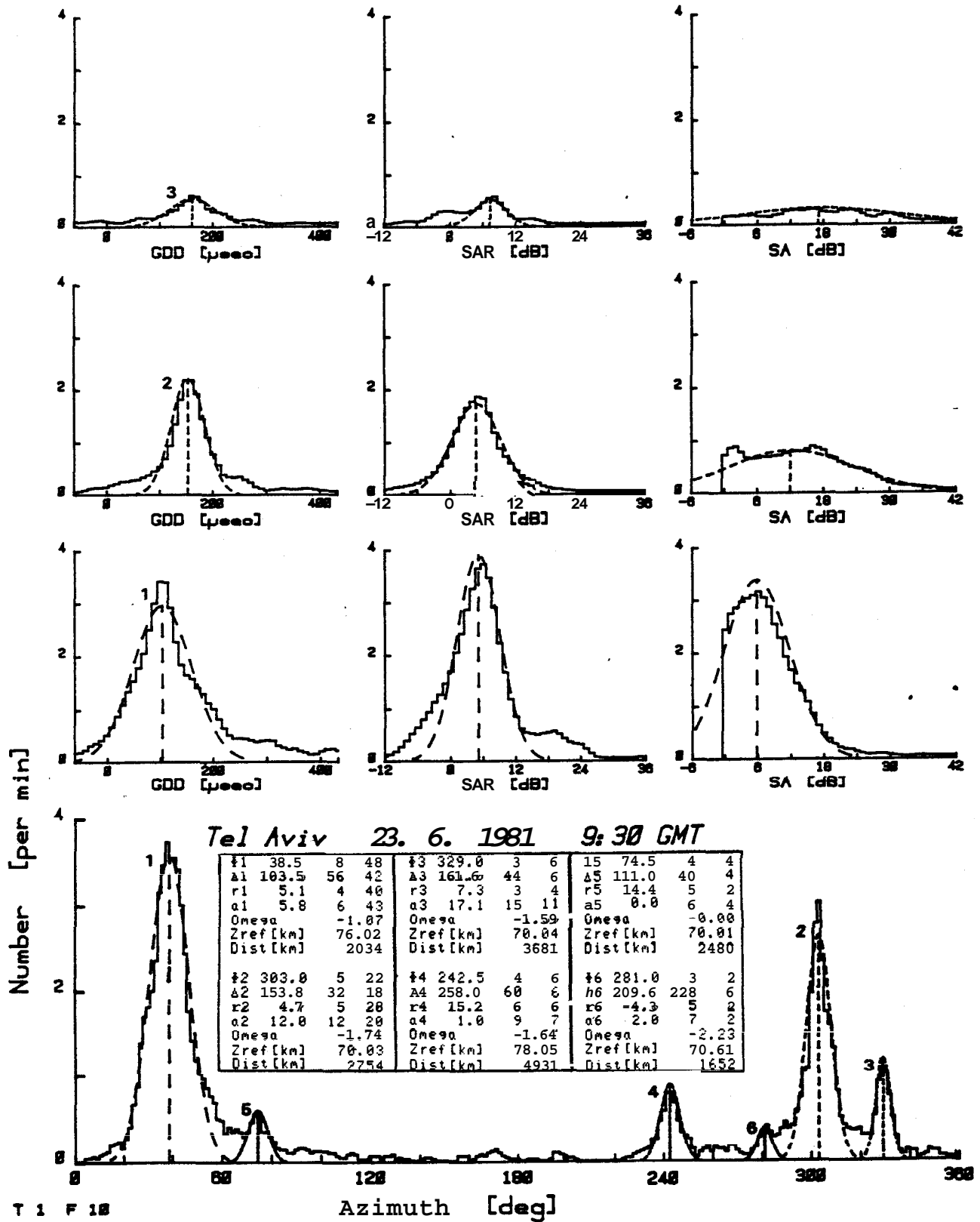


Fig. 4 As Fig. 3; for the measuring period 9:20 - 9:40 GMT on 23. June 1981.

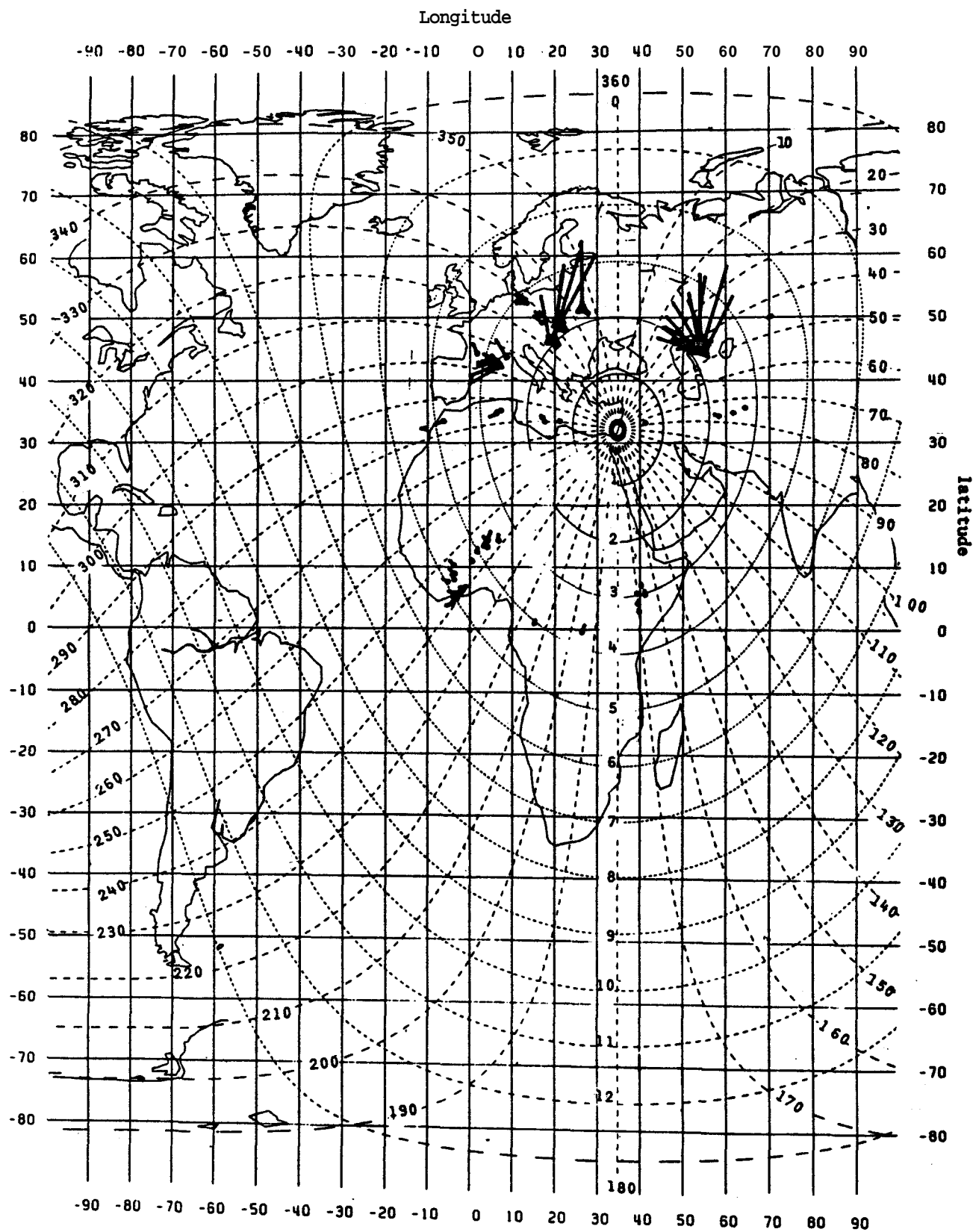


Fig. 5 Thunderstorm activity centers recorded by the Tel Aviv station from 8:00 to 13:00 GMT on 23 June 1981. The length of the pointers is proportional to atmospheres/min, the orientation gives the time (0:00 and 12:00 GMT is North).

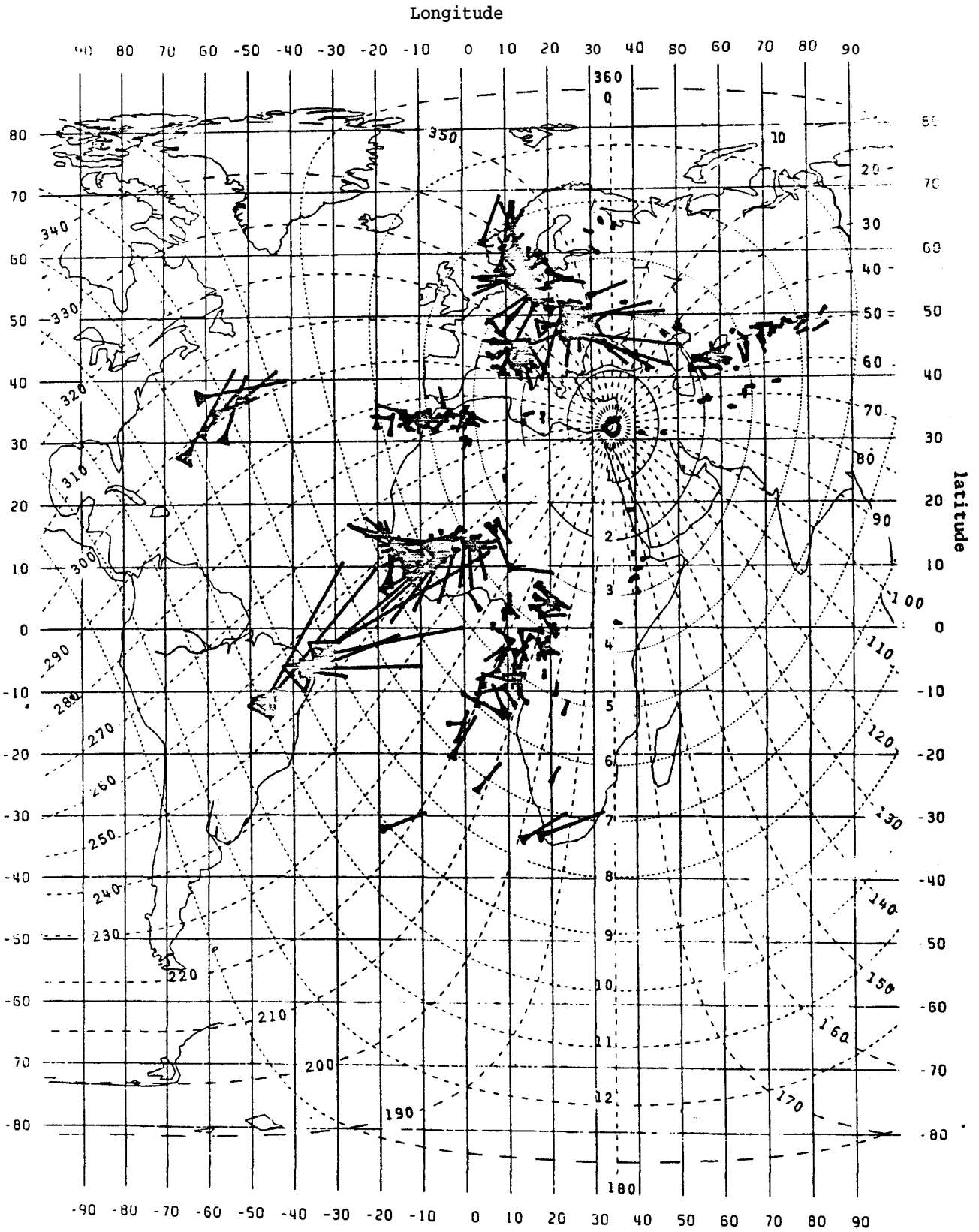


Fig. 6 Thunderstorm activity centers recorded by the Tel Aviv station from 14:00 GMT on 23. June to 6:30 GMT on 24. June 1981. See Fig. 5.

MAX-PLANCK-INSTITUT FÜR KERNPHYSIK

Dr. J. Kiko

Monsieur
Francois Louange
Ingénieur-Conseil
9, rue Sainte-Anastase

F-75003 Paris

D-6900 HEIDELBERG 1

Postfach 103980

Saupercheckweg 1 (beim Bierhelder Hof)

Telefon Sammel-Nr. (062 21) 5161

Durchwahl (062 21) 516 **287**

Telex 461 666

20 August 1982

Dear Mr Louange,

The aims of GEPAN are of **interest** also to us **under** the aspect of fireball observation. The Max-Planck-Institut für Kernphysik in Heidelberg **operates** the German part of the European Network of fireball observation. This **is done** in the German part by using 24 **cameras** photographing the sky by **night** via parabolic mirrors as described in the attached paper.

The European Network covers in **Germany** the area **south** of a line approximately given by the cities of Cologne and Kassel, the whole of **CSSR** and a **minor** part of **Austria**.

The contact addresses are in **CSSR**:

Dr. Zdenek Ceplecha
Astronomický Ústav
Ceskoslovenské Akademie Věd
Observatoř Ondřejov

O n d ř e j o v, CSSR

in Austria:

Dr. Gerd Polnitzky
Universitäts-Sternwarte
Türkenschanzstr. 17

A-1180 Wien

/2

May be, **our** observation network **will** fit in your detection **system** of rare aerospace phenomena rather **well**.

With best regards
yours sincerely

A handwritten signature in cursive script, appearing to read "J. Kiko".

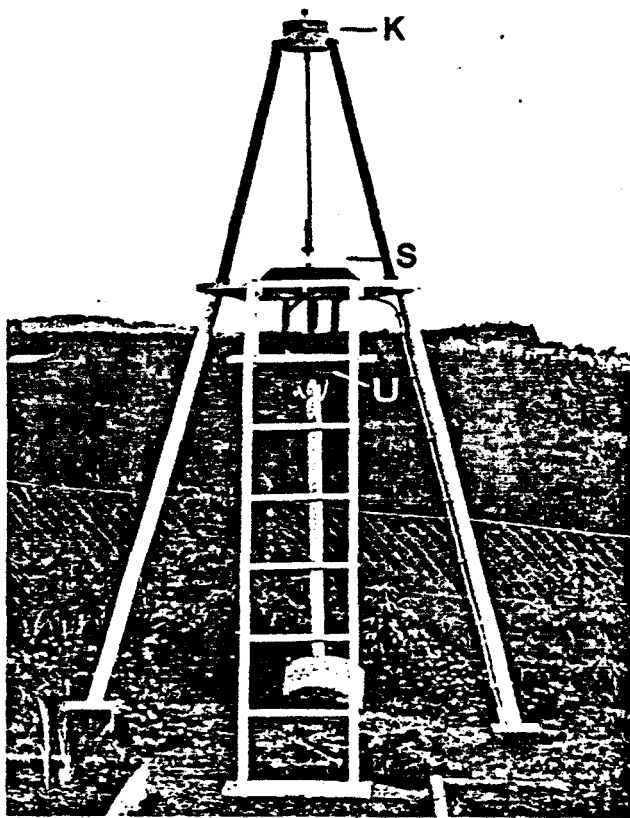
J. KIKO

encl.

Meteoritenortung in Süddeutschland

Die Untersuchungen an Meteoriten **haben** gezeigt, **daß alleine** aus den mineralogischen, chemischen und massenspektrometrischen Analysen die Herkunft dieser **Materie nicht** ermittelt werden kann. Es wird **immer** deutlicher, **daß** unbedingt die Bahndaten **erforderlich** sind, um zusammen mit den Laboruntersuchungen die bestehenden Hypothesen **bestätigen** oder widerlegen zu können. Dies hat mehrere Forschungsinstitute **veranlaßt**, Meteoriten-Ortungssysteme aufzustellen, die die Leuchtspuren von **Meteoriten** und Meteoriten an verschiedenen **Orten** photographieren.

Der **erste Versuch** wurde von Dr. Cepelcha, Astronomisches Institut **Ondrejov** in der **Tschechoslowakei** unternommen, der zwei 180°-Kameras aufstellte und das **Glück** hatte, **nach** kurzer



Ansicht einer 180°-Meteoriten-Kamera, wie sie in Marienberg Westerwald aufgestellt ist (K = Kamera, S = Spiegel, U = Schaltuhr).

Zeit am 7. April 1959 den Meteoriten Pribram aufzufinden und die Bahnelemente berechnen konnte. Dies ist der **erste** und einzige Meteorit dieser Art, den wir **haben**. **Inzwischen** wurde das Netz in der Tschechoslowakei erweitert und **auch** ein **solches** in den USA aufgestellt. Wenn **auch** in den ersten Jahren kein so **großartiger Erfolg** erzielt wurde, so haben wir **dennoch** entschieden, im süddeutschen Raum solche Meteor-Kameras **aufzustellen** und sie an das tschechische Netz **anzuschließen**. **Durch** zusammenhängende Gebiete erzielt man eine **größere** Ausbeute. Auch im **anderen Teil** Deutschlands ist man mit dem Aufbau von **Kameras** beschäftigt. Da in der Bundesrepublik auf **dem** Gebiet der Meteoritenforschung bereits eine **große** Aktivität herrscht, hat man geradezu die Verpflichtung, **auch diesen** bisher **vernach-**

* Prof. Dr. J. Zähringer, Max-Planck-Institut für Kernphysik, Heidelberg.

lassigten Bereich der Forschung, die Aufzeichnung von Meteorbahnen, **zu** betreiben.

Die Kenntnis der Bahndaten **ist** aus verschiedenen Gründen für die Meteoriten-Forschung sehr wichtig. Aus der **geozentrischen** Bahn kann man die Lage des **Fallortes** auf wenige **km²** vorausberechnen, so **daß** er in relativ kurzer Zeit gefunden werden kann. Der Meteorit **dient als** Raumsonde und man kann Aussagen über die Intensität der **kosmischen** Strahlung **im** Bereich der Meteoritenbahn **machen**. Man kann also **zeitliche** und örtliche Schwankungen feststellen. Die **Geschwindigkeit** der **Meteorite** beim Eintritt in die Erdatmosphäre gibt zusammen mit **dem** Bestrahlungsalter (Zeit seit **letztem** Auseinanderbrechen aus **großem** Körper) Auskunft, von wo die Körper aus **unserem** Planetensystem kommen können.

Stammen sie vom Mond oder aus dem **Asteroidengürtel** oder von Kometen?

Außer den Meteoriten werden **auch Meteore** (Sternschnuppen) **oberhalb** einer gewissen Helligkeit registriert, und man kann Aussagen über **deren** Häufigkeiten und Massenverteilung und über **deren** Einfallsrichtung **machen**. Aus den Höhen des **Aufglühens** und Verloschens kann man sogar über die **Dichte** der **Atmosphäre** und über Winde in dieser Höhe etwas erfahren.

Die Wahrscheinlichkeit, einen gefallenen Meteoriten in einer bestimmten **Fläche** zu **finden**, steigt **durch** die **Kameras**, um etwa den Faktor 10. Ein **Vorteil**, in Europa ein **solches** Programm zu organisieren, ist die **große** Bevölkerungsdichte. Wir konnten uns einer guten **Zusammenarbeit** des Deutschen Wetterdienstes erfreuen, und dort, wo keine **günstige** Wetterstation **zu finden** war, wurden wir ausnahmslos von **interessierten** Einwohnern unterstützt. Ein **Nachteil** der hohen Bevölkerungsdichte bringt die Beleuchtung (**Straßen**, Autos, **Städte**) mit **sich**. **Außerdem** sind die Wetterbedingungen in Europa natürlich nicht gerade günstig, was die Ausbeute dieses Programms andererseits verringert.

Die 180°-Kamera für Meteoritenphotographie

Die Kamera bildet die Himmelskugel auf einer Leica-Kamera ab, die während der **Nacht** und nur bei schwachem Mondlicht geöffnet wird. Die Fixsterne und **Planeten** **zeichnen sich** als Kreise ab, während ein Meteor **oder** ein Meteorit eine **kurze** Spur **hinterläßt**. Dem **Objektiv** der Kamera ist **außerdem** ein rotierender Sektor vorgeschaltet, der das **Bild** unterbricht. Aus der Reihenfolge der Meteor Spuren **läßt sich** so die Geschwindigkeit des glühenden Körpers ermitteln.

Die Optik besteht aus einem konvexen Spiegel von **36 cm** Durchmesser, der senkrecht auf eine normale **36-mm-Leica-Kamera** (**Objektiv** $\frac{2}{50}$) abgebildet wird (siehe Abb. 1). Die Spiegelhöhe beträgt 7 cm. Der Spiegel ruht fest **auf** einer kreisförmigen **Grundplatte**. Ein **Dreifuß** über **dem** Spiegel **hält** das Gehäuse der **Kamera**. Die Kamera ist **nach** unten auf den Spiegel **gerichtet**. In demselben Gehäuse **ist** vor **dem** **Objektiv** ein rotierendes Segment **zur** **Lichtunterbrechung** angebracht. Die Unterbrechung **dauert** **genausolang** wie die **Belichtung**. Das Segment wird mit **einem Synchronmotor** angetrieben und **macht** **125 Unterbrechungen** pro Sekunde. **Der Spiegel** und **das** Kamera-Gehäuse **werden** **geheizt**, um **Schnee** und **Wasser** zu **beseitigen**. Die **ganze Kamera** **steht** **meist** **ca. 2 m** über **dem Erdboden** auf **einem Gestell** und ist **weit** **genug** von **Häusern**, **Bäumen** etc. **entfernt**, um **möglichst** freien **Horizont** zu **haben**.

Ein Film „Agfa Isopan ISS 21“ wird für die Leica verwendet. Bei Belichtung dieses Films während mehrerer Stunden kann ein Stern der Größenklasse 3^m und 4^m noch nachgewiesen werden. Die Nachweisgrenze einer Meteorspur mit 10²/sec



Die geographische Lage der 25 Meteoriten-Beobachtungs-Stationen. Die Kreise entsprechen einem Radius von 100 km, deuten ungefähr die Sichtweite einer Station an. 1 Stephanshausen, 2 Klippeneck, 3 Uhringen, 4 Wattenheim, 5 Dasing, 6 Glashütten, 7 Seligenstadt, 9 Neukirchen, 10 Eckweisbach, 11 Hetdelberg, 12 Mitteleichenbach, 13 Zell, 14 Leihgestern Neuhof, 15 Marienberg, 16 Hohenpeißenberg, 17 Deuselbach, 18 Schaalheim, 19 Nürnberg, 20 Berus, 21 Gerzen, 22 Schonwald, 23 Wildbad, 24 Neudorf, 25 Bernau, 26 Stotten.

liegt bei = 6^m. Auf dem Film entsprechen 10² einem mm. Die äquivalente Brennweite ist 5.7 mm. In Abb. 2 wird eine solche Aufnahme gezeigt.

Die Kameras sind in Abständen von ca. 100 km aufgestellt, und zur Bestimmung der Bahnelemente sind Aufnahmen von mindestens zwei Stationen erforderlich. Die geographische Aufstellung der Kameras ist auf Abb. 3 ersichtlich.

Bedienung der Kameras

Der Verschluss der Kamera wird mit einer elektrischen Schaltuhr nach vorbereitetem Zeitplan betätigt. Auf der Schaltuhr werden tagsüber die richtigen Schaltzeiten eingestellt und auf Sauberkeit des Spiegels geachtet. Die Genauigkeit der Uhr sollte 10 sec betragen. Die Öffnung der Kamera erfolgt 1 1/2 Std. nach Sonnenuntergang und wird 1 1/2 Std. vor Sonnenaufgang geschlossen. Der Mond wird ca. 1 Woche vor und nach Vollmond mitberücksichtigt.

Die Zeit des Ereignisses ist für die Berechnung der geozentrischen Bahnen nicht erforderlich. Will man die wirkliche Bahn des Körpers im Planetensystem berechnen, dann muß auch die genaue Fallzeit bekannt sein. Hier ist man wiederum auf die Mithilfe der Bevölkerung angewiesen, die durch Vergleich mit anderen Ereignissen (Eisenbahn, Buslinien, etc.) die Zeit meist auf einige Minuten genau anzugeben vermag. Diese Genauigkeit ist zur Bestimmung etwa ausreichend und vergleichbar mit der Genauigkeit der Kameras.

Roullate

Die Erfahrung in der Tschechoslowakei hat gezeigt, daß im Mittel jede Station im Monat eine Meteorbahn größer als = 6ter Größe registriert. Die Auswertung der Filme erfolgt zunächst mit einem Zeiss-Koordinatenmeßgerät, und die Berechnung der Bahnelemente erfolgt mit einem Computer. Dr. Ceplecha in Ondrejov, der Initiator dieses Programms, hat sich bereit-erklärt, die Auswertung für uns zu übernehmen, und das Computer-Programm für unsere Stationen hat er schon vorbereitet. Für den Fall eines Meteoriten, der allerdings bei

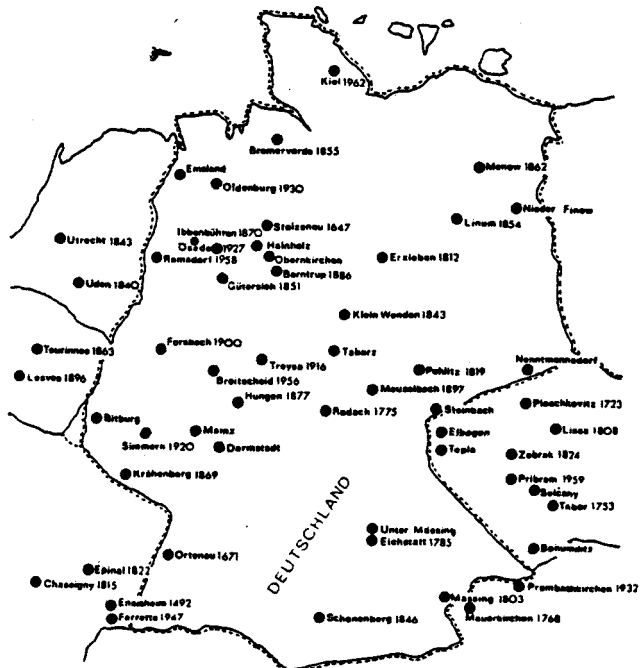
klarem Himmel und bei geöffneter Kamera erfolgen muß, wären wir also vorbereitet.

Der Vollständigkeit halber sei noch erwähnt, daß auch in den USA ein derartiges Beobachtungsnetz, das sogenannte Prairie-Network, in Betrieb ist, das ein zehnmal größeres Gebiet = ca. 10⁶ km² überwacht. Dort sind es 16 Stationen, die auf ganz anderem Prinzip arbeiten als die Ceplecha-Kameras. Die US-Kameras werden durch Helligkeitssensoren gesteuert und filmen die Meteor-Spur mit 4 Filmkameras pro Station, wobei auch die exakte Zeit bestimmt wird. Die Bedienung und Datenentnahme erfolgt drahtlos. Das Netz ist schon seit 3 Jahren in Betrieb und bei der riesigen Fläche hatte man erwartet, daß schon einige Meteorite aufgespürt worden waren. Leider ist bis heute noch kein derartiger Erfolg zu verzeichnen. Eine große Zahl von Meteor-(Sternschnuppen)Bahnen konnte natürlich ermittelt werden. Solche Daten sind in großer Zahl angefallen und wurden bereits ausgewertet. Die Anzahl der sonst gemeldeten Meteoritenfalle ist in den letzten Jahren anormal niedrig und die Natur scheint unserer Statistik einen Streich zu spielen. Abb. 4 gibt zur Übersicht eine Zusammenstellung aller beobachteten Falle und Funde von Meteoriten in Deutschland.

Anerkennungen

Herrn Dr. Ceplecha, Astronomisches Institut in Ondrejov, sind wir in ganz besonderem Maße zu Dank verpflichtet. Er hat uns alle Unterlagen zur Verfügung gestellt und uns jederzeit beraten. Die Übernahme der Auswertung bedeutet für uns eine große Entlastung.

Der Deutschen Forschungsgemeinschaft gilt unser Dank für die Bereitstellung der einmaligen Mittel zum Aufbau der Stationen. Die großzügige Unterstützung des Deutschen Wetter-



Die in Mitteleuropa bekanntgewordenen Meteorite (nach V. F. Buchwald). Der Name richtet sich nach der Gemarkung des Fundortes. Meteorite mit der Jahreszahl sind beobachtete Falle, das andere sind Meteoriten-Funde.

dienstes und insbesondere das persönliche Interesse der Observatoren und der privaten Betreuer hat uns ermutigt, das Programm durchzuführen. Ihnen sind wir sehr zu Dank verpflichtet.

Unser technischer Assistent, Herr Hauth, hat die Aufgabe der Aufstellung der Kameras übernommen und wird zukünftig für die Betreuung verantwortlich sein.

T U N I S I E

Ambassade de Tunisie
Paris.

SCCT/TB/AK

Paris, le 29 Avril 1982

Monsieur,

J'ai bien reçu votre lettre en date du 19/4/82 par laquelle vous me faites part de votre désir d'effectuer une étude sur l'état actuel des recherches dans un domaine scientifique particulier.

En réponse, j'ai l'honneur de vous inviter ,
⊗ à écrire à la Faculté des Sciences - Campus Universitaire à Tunis, qui ne manquera pas de vous fournir les renseignements désirés.

Veillez agréer, Monsieur, l'expression de mes meilleurs sentiments.

Le Conseiller Culturel



M. ZOUARI

Monsieur François LOUANGE
Ingénieur Conseil
9, rue Sainte-Anastase
75003 PARIS

U R U G U A Y

AMBASSADE DE L'URUGUAY

1207/82-737

JE/nd

Paris, le 19 mai 1982

Monsieur François **LOUANGE**
9, rue Sainte-Anastase
75003 **PARIS**

Monsieur,

J'ai pris connaissance avec attention de votre lettre du 19 avril, concernant **l'étude** sur la détection des phénomènes aérospatiaux rares que vous avez entreprise.

Je pense que **l'organisme** compétent uruguayen que vous pourriez contacter pour obtenir des renseignements sur les éventuelles recherches entreprises dans ce domaine est le suivant :

⊗ **Dirección General de Meteorología del Uruguay**
J. Suárez 3747
MONTEVIDEO

Veillez agréer, Monsieur, l'expression de ma considération distinguée.



José E. Etcheverry Stirling
Ambassadeur

III.5.2. Echanges avec les Etats-Unis,

Ce paragraphe comporte 2 comptes-rendus de visites aux Etats-Unis :

- Visite au "Scientific Event Alert Network", organisme mentionné par l'ambassade américaine à Paris,
- Visite à Monsieur Mac Crosky, ancien responsable du réseau Prairie de détection optique des météores.



COMPTÉ-RENDU DE VISITE N° 38/0682

.Visite effectuée par :

NOM : A. ESTERLE

NOM :

NOM :

VISA :

VISA :

VISA :

LIEU : S . E . A . N .

DATE : 3 Juin 1982

OBJET DE LA VISITE : .Visite

LABORATOIRE VISITE : Scientific Event Alert Network

Adresse : National Museum of National History
WASHINGTON D.C.

(202) 357.15.11

Tél. :

PERSONNES RENCONTREES : LINDSAY MAC CLELLAND

DOCUMENT N° CT/GEPAN - 11-0091

du : 29 JUIN 1982

DIFFUSION : François LOUANGE /
Colonel GUYAUX

Depuis 1975, le S.E.A.N. a succédé Center for Short Lived Phenomena qui avait été créée en 1968, Le C.S.L.P. était plutôt tourné vers le public (cf. Condon ?) alors que le S.E.A.N. s'adressait délibérément aux scientifiques. Plutôt que de donner des informations partielles sur tout un tas de phénomènes divers, le S.E.A.N. se concentre sur une information systématique sur quelques domaines particuliers météores, séismes, volcans, etc... Petit à petit, les informations sur les activités volcaniques tendent à supplanter le reste.

Le S.E.A.N. a actuellement 1200 correspondants (dont une dizaine en France), dont un tiers environ sont actifs (envoient des informations). Le bulletin, nécessairement gratuit, est composé sur une machine à traitement de texte, directement par les différents responsables des thèmes. L'avantage est un gain de temps considérable, et la possibilité d'insérer des informations au tout dernier moment (une à deux heures avant éditions). La machine édite ensuite toute seule, à partir du fichier d'adresses.

Le S.E.A.N. n'utilise pas de banque de données, sauf pour les événements volcaniques. S'il y a lieu, les recherches se font sur les numéros antérieurs, surtout si on connaît la date de l'événement concerné. Mais la quantité d'information allant croissant, cela devient de plus en plus difficile.

Pour ce qui est des météores, bolides et autres, Mc CLELLAND se montre intéressé à connaître des résultats des recherches en psychologie de la perception, non pour les publier dans son bulletin mais pour mieux apprécier les informations qu'il reçoit. Il est preneur de toute information récente sur des météores de magnitude - 8 au moins. Il ne connaissait pas le projet GEODSS. Il confirme les difficultés à obtenir des informations ou une aide des militaires américains. Il envisage (vaguement) la possibilité de relancer un projet de caméras d'observation avec des chercheurs jeunes et en utilisant les modèles de vent tels qu'ils sont estimés actuellement. Il recommande de prendre contact avec Ian HALLIDAY au CANADA, qui avait découvert le météore d'INNISFREE en 1977 (SEAN vol 2 n° 2 et 4) à quelques centaines de mètres du lieu de

chute calculé.

Pour ce qui est des séismes, Mc CLELLAND recommande de contacter M. WAVERLY PERSON au National Earthquake Information Service à Denver, Colorado (Ø 303/ 234 -39 -94) qui leur fournit l'essentiel de leurs informations sur le sujet. Pour les événements volcaniques Mc CLELLAND cite un réseau de surveillance automatique, un satellite collectant les mesures des seismographes implantés près de volcans en Amérique Centrale. Il cite un certain Dave Harlow USGS. Menlo Park 94025 CALIFORNIA (Ø /415/328-81-11. ext. 2570, . ou 2479) et son supérieur hiérarchique Peter Ward (ext. 2838). Mais le projet se heurte à des difficultés certaines propres aux implantations dans les pays du tiers-monde : impossibilité de maintenance sur place, vols fréquents pour revendre le matériel au prix de la ferraille.

Les implantations aux U.S.A. se trouvent, soit sur la côte Ouest (Cascade), soit à Hawaï et mesurent les vibrations du sol les gonflements, les changements de champs électriques, la nature et la répartition des gaz d'échappement, etc... Selon lui il n'y a pas de relation claire entre ces gaz et l'historique des événements éruptifs (H. Tazzieff est d'un avis diamétralement opposé). Ceci semble être une des grandes disputes entre volcanologues.

Mc CLELLAND évoque aussi le problème des éruptions à Long Valley, où l'ampleur des éruptions passées est telle que cela soulève maintenant un problème politique aussi bien que technique. Faut-il laisser la population s'implanter à cet endroit ? Pour ce problème, voir Roy Bailey USGS, Reston, Virginia 22092 (Ø 703 860.74.68).

Enfin pour ce qui est de la foudre, Mc CLELLAND reconnaît que le S.E.A.N. n'y travaille pas du tout. Il conseille de voir à la National Oceanic and Atmospheric Administration (NOAA). Il cite Art Krueger, Climate Analysis Center, National Weather Service, Camp Spring, Md. 20233 (Ø 301.763 82 27). Pendant ce temps Nadine Binger téléphone de l'ambassade pour donner les références de 2 personnes de la NOAA, à Silver Spring.

Willan Fritts 301,427 78 41 et pour les questions de protection
des équipements contre les foudroiements ;

Henri Besman 301.427 78 39.



Groupe d'Etude des
Phénomènes Aérospatiaux Non-identifiés

THÈME :

DETECTION

MOTS-CLÉS : METEORE - CAMERA -
OPTIQUE - METEORITE

COMPTE-RENDU DE VISITE N° : 37 / 0682 /

VISITE EFFECTUÉE PAR :

~~APPENDIXE~~ :

NOM : A. ESTERLE

NOM :

NOM :

VISA :

VISA :

VISA :

LIEU : BOSTON (USA)

DATE : 1.06.82

OBJET DE LA VISITE : Réseau PRAIRIE

LABORATOIRE VISITE : Smithsonian Astrophysical
Observatory

ADRESSE : Oak Ridge Observatbry

Pinacle Road - HARVARD

MASSACHUSSETS 01451

TÉL. : (617) 456.3395

N° C.N.R.S. :

PERSONNES RENCONTRÉES - ~~CONTACTÉES~~ : Mac CROSKY

DOCUMENT N° CT/GEPAN - 0084

DU : 15 JUIN 1982

DIFFUSION : F. LOUANGE, Colonel GUYAUX

Monsieur Mc CROSKY fut responsable du réseau Prairie, ensemble de stations de détections optiques qui, de 1964 à 1974, devait permettre d'étudier les trajectoires de météorites (sur allocation de la NASA au Smithsonian Institute). Le projet avait au départ 2 buts :

- * collecter des météores frais (fresh ...) c'est-à-dire des météores n'ayant pas excédé la demi-durée de vie des isotopes décomposés par les rayonnements cosmiques.
- * mieux connaître les trajectoires et la relation masse-brillance.

Quand le projet fut arrêté en 1974, (sur l'avis de Mc CROSKY lui-même) 2700 trajectoires de météorites avaient été étudiées (réf.1) (des milliers de clichés examinés chaque année), mais une seule collecte de météores avait permis de recueillir des fragments (réf. 1 - météore de Lost City - 3 fragments après des mois de recherche, le premier ayant été trouvé très rapidement, sur la route) ; encore s'agissait-il de la meilleure trajectoire optique détectée et calculée.

a) Le réseau :

Il s'agissait de 16 stations couvrant un million de km², distantes de 200 à 250 km. Les caméras et les films provenaient des surplus de l'U.S.A.F.. La surveillance était faite par des fermiers voisins qui changeaient les plaques et postaient les prises de vue. De plus des scientifiques visitaient de temps en temps les stations pour s'assurer que tout allait bien.

Le Middle West avait été choisi comme lieu d'implantation en raison du réseau routier très dense (l'Arizona ou le Nouveau Mexique eussent été meilleurs pour l'observation, mais chercher dans un désert ...)

Les temps de pose étaient de deux heures, Il y avait un système d'observation de l'Etoile Polaire comme révélateur de la

couverture nuageuse : son occultation annulait la séance.

Un système d'occultation (20 fois par seconde) permettait de mesurer la vitesse (et l'accélération) des sources lumineuses. Etant codé, ce système indiquait l'heure. L'horloge était photographiée au début de la séance, puis chaque seconde, une occultation était omise. Le numéro de la seconde concernée était ensuite codé (à base deux ?) sur les 20 occultations qu'elle comportait. De plus, une cellule commandait une photo de l'horloge si la luminosité variait brusquement. Mc CROSKY recommande de toute façon d'assurer une redondance de la mesure du temps.

b) Les météores :

En général, 3 ou 4 stations attrapaient le même météore, ce qui permettait de connaître position, vitesse et accélération, qui pouvaient ensuite être intégrées en arrière (trajectoire d'arrivée) ou en avant (vers le sol).

La brillance s'arrête généralement du fait de la diminution de la vitesse (i-e, d'énergie cinétique), sauf pour les très grosses masses. Pour savoir si une météorite arrive au sol, on peut dire que si elle brille encore à 20 km d'altitude, elle y arrive. De même, si le rapport masse / section est supérieur à 1 (sphère de 10 cm de rayon, de 1kg).

Cependant, le calcul de la chute dépend énormément du modèle de vent utilisé, et c'est de là que proviennent de plus grosses difficultés pour collecter les débris (en INDE un projet prévoit d'utiliser de très nombreuses personnes avec promesse de récompense ...)

c) Divers :

Mc CROSKY n'a rien observé d'anormal sur ses prises de vue (météores, foudre ...) mais il ne garantit pas qu'il n'y a rien (des hectares de photos, qui interdisent toute analyse systématique). D'autre part, le réseau était conçu pour observer en haute altitude, et pas près du sol (ce que me dit spontanément

Mc CROSKY devançant une question que je n'avais pas l'intention de lui poser).

Il existe aussi des réseaux dans d'autres pays en particulier au CANADA (4 ou 5 caméras) et surtout en EUROPE (40 stations en TCHECOSLOVAQUIE, 15 en ALLEMAGNE de l'OUEST etc...) Mc CROSKY recommande de s'adresser à CEPLECHA, leader mondial en la matière. Il n'y a plus rien aux U.S.A., seuls les militaires ont des moyens d'observation de cet ordre, mais il n'y a aucune possibilité d'information.

Par ailleurs, l'observatoire de Oak Ridge comprend un télescope de 16 inches, un de 61 inches, deux instruments de photographie systématique et un radio télescope, inutilisé actuellement, faute de crédit. L'ensemble sert à quelques étudiants et enseignants. Mc CROSKY observe les étoiles binaires réformées par gravitation.

Réf. 1 : Center for astrophysics - Preprint n° 721
60 Garden ST
CAMBRIDGE. Mass. 02138

III.5.3. Echanges avec la Tchécoslovaquie.

.....

Ce paragraphe présente les principales correspondances avec Monsieur Ceplecha, responsable du réseau européen de détection optique des météores, ainsi que le compte-rendu de la visite de son observatoire à Ondrejov.

François LOUANGE
Ingenieur - Conseil

9, rue Sainte-Anastase,
73003 PARIS

Tél. : (1) 277.49.56

No SIRET : 319532503 00012

Dr. Zdenek Cepelchâ
251 65 Ondrejov Observatory
ONDRZJOV (Tchécoslovaquie)

Paris, 21/5/82

Sir,

I have been appointed by a **department** of the french national **space** research centre **CNES** to **undertake** a **survey** of existing **means** and needs in the field of detection of rare aerospace **phenomena**. This topic, **which** is briefly described in the attached **paper**, **includes all sporadic** and non-predictible **luminous** phenonena that **may occur** in **low** atmosphere, such as **lightnings**, fireballs, etc...

The first step in **this work** is obviously to **review**, as far as possible, **ail** existing **equipments** that are **likely to be useful** for **such** a detection (radars, **cameras**, **electromagnetic** detectors, ...). With **this in view**, I **started** getting into touch with **civilian** aviation, **meteorology**, **armies**, etc ..., in France and abroad,

As far as **meteors** and **meteorites** are concerned, I met MM. **Pellas** and **Lorin** (France), **who** confirmed that no systematic detection network **was available** in France, but mentionned **several** countries where **something was done** in **this** field. Besides the american "**Prairie**"^w **project**, your **name** was very often **mentionned** to me, **not only** by french specialists, but **also** through other **channels**, such as the **american SEAN**.

I would be most grateful if you could **provide** me with **technical** data on your **optical detection** system for **fireballs**, and on the **"european network"** you supervise. Maybe the most efficient approach would be for us **to meet**, either if you have an opportunity to **come** in France, or if I may plan a short visit on your **premi-**
ses without disturbing you.

Looking forward to **hear** of you, I **remain**

Yours sincerely,

F. Louange

A handwritten signature in cursive script, reading "F. Louange", with a horizontal line underneath it.

ONDŮEJOV June 1, 1982

Dr. François Louange
9, rue Sainte-Anastase
75003 PARIS
FRANCE

Dear Dr. Louange,

I was very pleased that there is some interest in aerospace phenomena arising again. I am interested in one of them, fireballs and the bodies producing such phenomena. We measure and compute here all photographic records from the so called "European Network", which might become literally European once France would be able to join. Now we have 25 stations in Germany (starting from the French borders to the Czech borders), 2 stations in Austria and 18 stations in Czechoslovakia. There are also few stations in the Netherlands, but only loosely bound to our system: they are amateur stations. The spacings of the stations is 100 km or so. The German and Austrian stations are still using the old optical system, which is a mirror camera about 1 m high, mirror 360 mm diameter and taking the whole 180° field of view on one frame of a 36 mm film. The equivalent optical system is 1:16 with $f=5$ mm. The precision of measuring the directions to any unknown object is $\pm 0.1^\circ$ to $\pm 0.2^\circ$ regularly; stars are used as fiducial points. The cameras are fixed-mounted and beginning of star trails are used for comparison.

In the Czech countries we use now (since 1977) a fish-eye system, which is just marvelous in performance. The objective is Zeiss Distagon 1:3.5, $f=30$ mm, field of view 180° and we use photographic plates 9x12 cm for taking the image (diameter of the image of the entire sky is 80 mm). The precision of measuring directions to unknown objects is ± 1 minute of arc anywhere in the field of view. The objective is relatively small and the camera weighs less than 5 kg. We constructed only simple camera with rotating shutter close to the focal plane (few mm above the photographic emulsion). This shutter with 12.5 breaks of the image

per second gives us the time marks necessary for velocity determinations. I can easily imagine a full-automatic camera operating with film, weighing still around 5 kg: an easy-transportable field system. To my knowledge, the Distagon fish-eye is far the best objective available for accurate high-quality images of the whole half space and it is regularly manufactured.

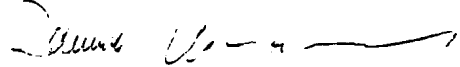
We have problems with absolute timing. Very bright fireballs are usually observed by casual witnesses, which is the easiest way to get time of the fireball passage. We operate one moving fish-eye camera (equatorially mounted) side by side with the fixed fish-eye camera here at the Ondřejov Observatory. Combining these two records we have time passage of even fainter fireballs with precision of several time seconds. Two obvious additional conditions: clear sky and being closer than 500 km to the Observatory. We speculate of several moving systems inside the Network... Another system might be: coding in the shutter breaks*..

Our observational schedule: each clear night (at least clear at the beginning of exposure) and all parts of nights without moonlight; if the Moon is above horizon, we expose when its illuminated part is not bigger than 70%.

In the field of fireball explorations, we still have very insufficient data. Only a dozen bodies or so with masses exceeding 1 ton have been photographed at all. Only three meteorite falls have available accurate data on trajectories and orbits from multistation photographs of their fireballs. In our minds here, the task of obtaining information on more and bigger fireballs is extremely important. We feel that we are attacking "the unknown band" of bodies with dimensions from 10 metres to several 100 metres, the very existence in our solar system we know nothing of.

I am ready to answer any of your questions by mail. If you would have the opportunity to come, you are welcome. Just let me know in time to be sure I will be present. Please, inform me also on your preliminary intentions, what months seems to you the most suitable. I will be not here in July and August.

Sincerely yours


RNDr. Zdeněk Ceplecha, DrSc.

Enclosures: 2 photographs of meteoric fireballs

Czechoslovak Academy of Sciences
ASTRONOMICAL INSTITUTE
Ondřejov Observatory
251 65 Ondřejov
Czechoslovakia
Tel. Praha 72 45 25
Telex 121579

July 3, 1982

A5/261/82

Dr. François Louange

9, rue Sainte-Anastase
75003 PARIS
F R A N C E

Dear Dr. Louange,

choose any period from September 6 to September 10
and let me know place and time of your arrival in time. The questions
you asked in your letter:

The limiting stellar magnitude for an object moving 10° per
second is about 0. The accuracy in computing the impact point of
a meteorite fall depends mostly on aerological data in the last
20 km of the atmosphere: the accuracy of our system of cameras is
usually higher, ± 100 m is a quite typical value, but one sees also
values ± 30 m or ± 300 m. The dark-flight computations on assumption
of symmetrical shape of the body (no lift, only drag) with the
uncertainties of stratospheric winds give quite typically 2 a 1 %
in case of 1 kg mass moving at 45° inclined trajectory. Such com-
putations we start with the measured velocity vector —> deceleration
at the terminal point of the luminous trajectory and we integrate
numerically the equations of motion with drag, gravity, and wind
velocity included, till we reach the ground.

We never used seismic detectors. We have not detected any of
the 3 events you are asking after. In case of the Nov 11, 1980, we
were rather surprised not to have any one photograph. It was seen
also by several people at our Observatory very low on southern
horizon.

Sincerely yours



Zdeněk Ceplecha



Groupe d'Etude des
Phénomènes Aérospatiaux Non-identifiés

THÈME :

DETECTION

MOTS-CLÉS :

CAMERA - OPTIQUE - METEORE - METEOBITE

COMPTE- RENDU DE VISITE N° : 59 / 0982 /

VISITE EFFECTUÉE PAR :

~~APPELÉ DE~~

NOM : F. LOUANGE

NOM :

NOM :

VISA : *F.L.*

VISA :

VISA :

LIEU : ONDREJOV (Tchécoslovaquie)

DATE : 06.09.82 - 07.09.82

OBJET DE LA VISITE : Réseau européen de détection des **météores**

LABORATOIRE VISITÉ : Ondrejov Observatory

ADRESSE :

251 65 ONDREJOV
Tchécoslovaquie

N° C.N.R.S. :

TÉL. :

PERSONNES RENCONTRÉES - ~~CONTACTÉES~~ : Dr. Zdenek CEPLECHA

DOCUMENT N° CT/GEPAN -

DU :

DIFFUSION :

Monsieur CEPLECHA a été le créateur du réseau européen de **détection des météores**, dont il coordonne le **fonctionnement** depuis son observatoire **d'Ondrejov**, pris de Prague, La **visite** a duré deux jours, la première journée étant consacrée à une **présentation** du **réseau** et de ses **composants** ainsi qu'à la visite des installations particulières **d'Ondrejov**, et la **seconde** à la visite **pour maintenance** de routine d'une station **standard** située au sud de la **Tchécoslovaquie** et en **montagne** (**Churanov**, 1105 m).

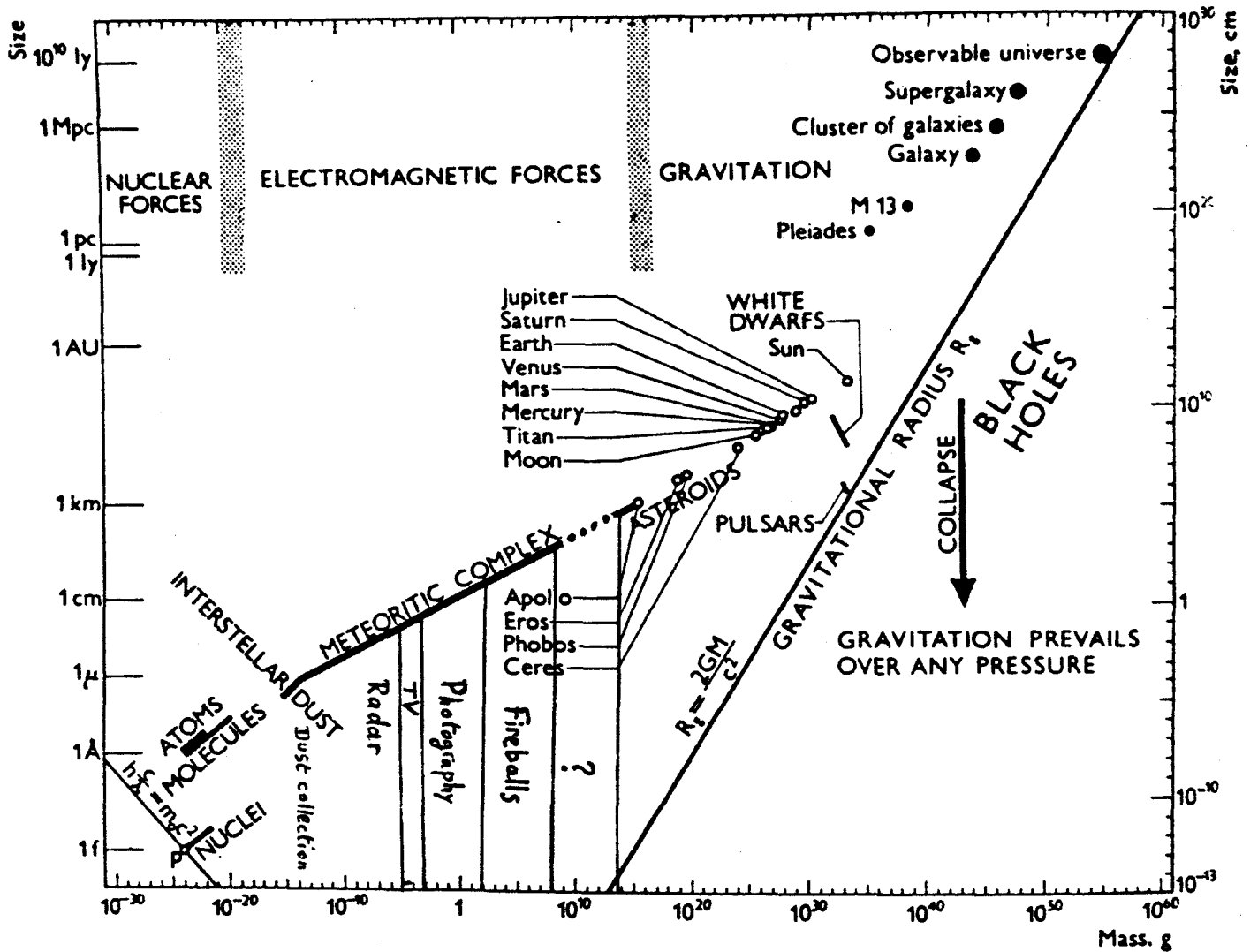
Peu de temps avant cette **visite**, Monsieur CEPLECHA **avait** participé à une **assemblée générale** de l'I.A.U. (**union astronomique internationale**) en Grèce, où une **recommandation** **avait** été formulée pour que se poursuivent les **travaux** sur la **détection** des météores. Celle-ci **apparaîtra** dans les "**Transactions of the International Astronomical Union**".

I. Météores et **moyens** de détection,

Le **diagramme** ci-dessous présente dans un **repère log-log** en **masse** et **taille** l'**ensemble** des structures connues dans l'univers. On y remarque l'**étendue** du "**complexe météorique**".

L'**origine** exacte des étoiles filantes et des **essaims** **n'est pas** vraiment connue, car si l'on peut observer de petits objets, on **n'a pas** suffisamment de **données** pour ceux dont la taille est plus importante (**pointillés** du **diagramme**). L'**origine cométaire** des **essaims** **n'est certainement** qu'une explication partielle, et la possibilité que certaines météorites **aient** une origine **astéroïdale** **n'a pas** encore pu être démontrée : on ne sait pas par quel **mécanisme** ces objets passeraient de la **ceinture astéroïdale** à leur orbite finale. Une nouvelle théorie a **été avancée** pour expliquer les **petits** météores : tous les 10000 ans environ, une comète traverse le **système solaire**, et cela suffirait pour le "**remplir**" à nouveau de ces objets..

Les **annotations** qui figurent **verticalement** sur le diagramme, au-dessous du complexe météorique, indiquent les plages de **fonctionnement optimal** des **différents moyens** de détection **existants**.



Mass and size of structural units in the universe.

Le radar météorique, qui détecte les traînées ionisées permettant une réflexion spéculaire en haute atmosphère, est un outil approprié pour les études à caractère statistique sur les **essaims** (variations d'une année à l'autre, etc...). Il n'a aucun intérêt pour l'étude de la trajectoire d'un objet donné, d'une part en raison de la limitation aux conditions de réflexion spéculaire, et d'autre part parce qu'il ne permet de détecter les objets que 20 Km plus bas que les moyens optiques.

Les systèmes optiques mettant en jeu des techniques de télévision et de traitement d'images video permettent un bon suivi des petits météores (jusqu'à la magnitude 4). Voir à ce sujet un spécialiste qui a fait l'étude de 77 météores :

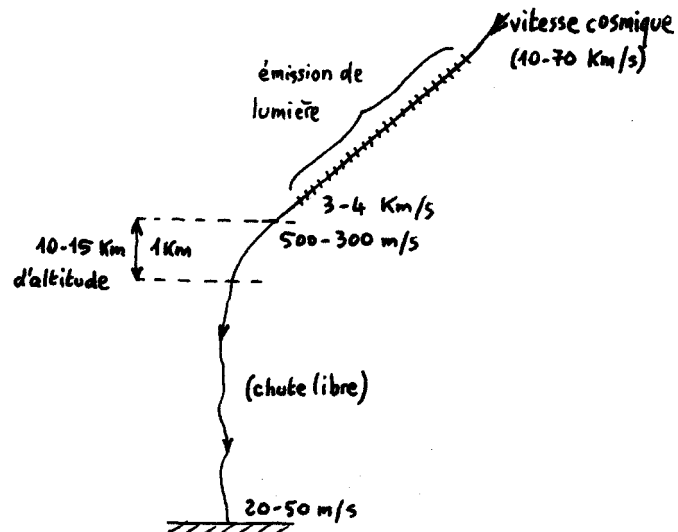
Mr. J. JONES

Physics Dept - University of Western Ontario
London - Ontario - Canada N6A 3K7

Malgré les limitations imposées par la couverture nuageuse, la détection optique est la seule qui permette des **mesures géométriques (trajectographie)** et **photométriques précises**. La trajectoire **angulaire** apparente d'une **étoile filante** couvre **couramment** quelques **dizaines de degrés** (on a **déjà observé** des cas de 110°), tandis que sa vitesse **angulaire** peut aller de 0 (cas du météore radial, **déjà photographié**) à $60^\circ/\text{s}$. En ce qui concerne l'intensité lumineuse, la variation la plus rapide qui ait été **observée** (exceptionnellement) était de **100 magnitudes/s**.

La trajectoire d'arrivée d'une **météorite-type** (1 Kg) est illustrée par le **schéma ci-contre**.

Arrivant de **l'espace** à grande **vitesse**, l'objet commence à émettre de la **lumière** tout en **ralentissant**. Cette émission cesse lorsque la vitesse devient inférieure à environ 3 Km/s . Puis, à une altitude de l'ordre de 12 Km , la trajectoire qui était **jusque là restée pratiquement rectiligne** se coude rapidement (sur 1 Km) et la chute devient très proche d'une **chute libre**, soumise **aux vents**. La vitesse, qui était d'environ 400 m/s au début du "coude" n'est plus que de quelques **dizaines de m/s** à l'arrivée au **sol**. Ceci explique l'**importance** de la **connaissance des vents** lorsqu'on cherche à prévoir le lieu de la chute.



Compte tenu de la **diversité** des cas, on retiendra que pour localiser les points de chute des **météorites**, il faut **pouvoir suivre leurs trajectoires assez bas** (idéalement 10 Km d'altitude). Pour les 3 cas connus de **météorites** retrouvées, les trajectoires ont été suivies **jusqu'aux** altitudes respectives suivantes :

- **PRIBRAM** : 22 Km à cause des limitations du système de l'époque (observations visuelle8 jusqu'à 13 Km).
- **LOST CITY** : 18 Km.
- **INNISFREE** : 18 Km.

Dans le domaine des sons et des infra-sons, Monsieur **CEPLECHA** n'a pas d'expérience particulière, Il signale l'existence jusqu'en 1981 au Canada d'un programme complet d'enregistrement des sons accompagnant toutes aortes de phénomènes (éclipses, ..), à l'aide de stations d'enregistrement continu (jusqu'à 0,1 Hz); à sa connaissance, il n'y a rien sur les météores. Le responsable était :

Dr. **Mc INTOSH**
Planetary Sciences Section
Herzberg Institute of Astrophysics
Ottawa - Canada K1A 0R6

A noter également : "**Anomalous sounds from the entry of meteor fireballs**" par **Colin S.L. Keay**, dans Science du 3/10/80, Vol 210, NO 4465. L'auteur est :

Prof, **C.S.L. Keay**
Physics Dept - Newcastle University
New South Wales, 2308
Australia

En ce qui concerne la détection sismique, il faut tenir compte du fait que la chute tend asymptotiquement vers une chute libre, Monsieur **CEPLECHA** indique qu'il a récemment obtenu une photo d'une météorite tombée aux environs de Berlin, et qu'il a reçu une donnée sismique apparemment corrélée (onde de choc ?).

Selon M. **CEPLECHA**, **Ian HALLIDAY** a publié récemment un papier excellent sur la diatribution des météorites (même adresse que **Mc Intosh** précédemment), Monsieur **WETHERILL**, qui a étudié un dossier militaire déclassifié sur la détection infra-rouge de météores, est l'un des très rares spécialistes qui aient une vision globale de tous les aspects de l'étude des météores et des météorites.

II. Réseau européen de détection optique.

Depuis l'époque de ses études supérieures, M. CEPLECKA est passionné par les travaux scientifiques que l'on peut effectuer à partir de photos d'étoiles filantes. Vers 1951, il installait en Tchécoslovaquie deux stations équipées chacune de 10 appareils photo fixes d'environ 30° de champ et de 180 mm de distance focale. Au bout de 8 ans, il parvint à photographier et à localiser au sol la météorite de PRIBRAM (cas favorable de vent contraire à la météorite, localisation à l'intérieur d'un rectangle de 2 & 3 Km de longueur sur 200 à 300 m de largeur),

Le réseau proprement dit existe depuis 1963 avec son centre de réduction des données à Ondřejov; à cette date, il comportait 3 stations. Il s'est progressivement étendu, et comporte actuellement 18 stations en Tchécoslovaquie, ainsi que 25 stations en RFA et 2 en Autriche (par relations personnelles) et quelques stations d'amateurs en Hollande. Les premiers appareils photo étaient à miroir semi-sphérique (caméra pointée vers le sol), et ces instruments, que M. CEPLECHA qualifie d'archaïques, sont toujours opérationnels en RFA. En Tchécoslovaquie, ils ont été progressivement remplacés par des optiques "fish-eye" de Zeiss. Selon M. CEPLECHA, une petite station équipée d'un fish-eye (focale de 30 mm) donne des résultats aussi précis qu'une des stations canadiennes qui sont équipées de 4 caméras encombrantes de 50 mm de focale : précision de 1 minute d'arc.

M. CEPLECHA se présente lui-même comme étant aussi optimiste pour l'avenir de la détection optique des météores que son ami américain M. Crosky est pessimiste (depuis 10 ans, la NASA n'accorde plus aucun crédit à ce type de recherche). A son avis, l'espacement d'environ 100 Km entre stations qu'il a adopté est beaucoup plus adéquat que celui de 200 Km qu'avait le réseau Prairie (sur lequel il est allé travailler pendant plusieurs mois à ses débuts). Une caméra fish-eye "voit" jusqu'à 500 Km mais ne permet des mesures correctes que jusqu'à 250 Km, et il faut un maillage plus serré pour évaluer la vitesse et la distance des objets. Selon les vents, son réseau permet de localiser une chute dans une aire de 1 à 2 Km².

M, CEPLECHA **confirme** que l'**Anglais** HINDLEY a bien géré un projet important de **détection** pendant 2 ou 3 **ans** (**maximum** vers 1974-75), et qu'ils ont **alors échangé** des données **aux** normes du réseau européen. Il n'en a plus entendu **parler** depuis, D'une façon générale, M, CEPUCHA a toujours eu des **difficultés avec les amateurs** qui, **après** une période active, **se lancent dans** des **disputes** interminables en le prenant à **témoin** (cas de la Hollande).

L'**éventualité** d'une **installation** en France, en particulier dans le prolongement géographique du réseau européen, réjouirait particulièrement M, CEPLECHA, qui se **déclare** prêt à toutes **sortes** de collaborations, et pourrait mettre à **disposition** son **système** de réduction de **données**.

Pour situer **quantitativement** la situation en **matière** de surveillance optique des **météores**, on peut **considérer** que toutes les données **accumulées** dans le monde jusqu'à ce jour **représentent** l'**équivalent** d'une couverture de toute la terre pendant 1,5 **jours...**

III. Les installations d'Ondrejov.

L'observatoire d'**Ondrejov** se situe sur une hauteur à une trentaine de Km de Prague. M, CEPLECHA y a la responsabilité du **département** de matière interplanétaire (22 personnes), **mais conserve** une fraction importante de son temps pour ses propres recherches. L'équipe en charge du réseau comprend 6 **personnes**, **plus** la secrétaire du **département** (à 2/3 de son **temps**) :

- 1 **assistant** fait les mesures sur les **plaques photo**
- 1 **assistante** est **chargée** de l'ordinateur (calculs)
- 2 personnes assurent les observations nocturnes (**caméras**, **spectrogrammes**, catalogues, **développement** des plaques,...)
- 2 **scientifiques** effectuent des travaux théoriques.

Les **installations** d'observation **sont** situées dans une série de petits observatoires astronomiques **avec dômes** (ancienne **propriété** d'un très riche **astronome** de la noblesse locale). On y trouve respectivement :

- 1 station fish-eye fixe (standard) et 1 station **fish-eye** montée sur équatoriale,
- 1 **ensemble** de 4 **caméras groupées** sous un grand obturateur pivotant commun, 2 caméras sont associées à un réseau de diffraction et les 2 autres à un prisme,
- 1 **caméra** à grande focale munie d'un grand réseau de diffraction donnant jusqu'aux ordres 5 et 6 (peu importe une forte dispersion si on observe des lignes d'émission).
- de petits bureaux d'où le **système** est géré,

Pour éviter la formation de buée, ces petits **bâtiments** sont **chauffés** (différence de température optimale avec l'extérieur : 5 degrés).

Les installations **spectrographiques** permettent d'obtenir de **bons** spectres lorsque les conditions sont favorables (**étoile filante** **visibles d'Ondrejov**, **luminosité suffisante**, déplacement **idéalement perpendiculaire** au réseau de diffraction). Le grand réseau, avec 600 lignes, permet d'atteindre une résolution de 0,2 Å entre 3600 Å et 6700 Å. En **moyenne**, un **bon** spectre **est obtenu par an**.

La station fish-eye standard est à la fois **simple** et robuste. Montée dans un coffret **métallique résistant**, elle s'ouvre vers le **haut** par un objectif fish-eye de Zeiss de 35 et 30 mm de focale (**ouverture** équivalente à 8 mm). Le champ angulaire est plus proche de 190° que des 180° nominaux, et l'image des **sources très brillantes** est dédoublée. Une fente est **prévue** pour positionner **les** plaques photo dans le plan focal; ce sont des **plaques** de verre de 400 ASA (meilleures **performances géométriques** que des pellicules), Un obturateur rotatif est **monté très près** du plan focal, **pour assurer** des fronts raides à l'ouverture et à la fermeture. Pour des **raisons** de **simplicité**, un **moteur alimenté** par le secteur **assure** une obturation **périodique** à 12,5 Hz, bien que la fréquence **idéale** soit **aux alentours** de 4 ou 5 obturations par seconde (voir réseau MRP au Canada).

La réduction des données se fait à Ondrejov à l'aide d'un banc optique développé par Zeiss, et permettant d'effectuer sur les **plaques** des mesures géométriques et **photométriques** de façon interactive (microscope binoculaire). Cette **installation** est couplée à un **calculateur (mini)** sur lequel s'exécute un **programme** de 4500 instructions FORTRAN.

IV. La réduction des données.

Par principe-même, seuls sont étudiés les événements qui font l'objet d'au moins deux enregistrements simultanés (à la question "avez-vous observé des phénomènes anormaux à l'aide de votre réseau ?", M. CEPLECHA répond que ses milliers de plaques contiennent une multitude de choses auxquelles il ne s'est jamais intéressé dans la mesure où elles n'affectaient qu'une plaque à la fois).

30 à 60 météores sont photographiés chaque apnée depuis deux stations ou plus, Les papiers fournis en annexe donnent un aperçu de l'activité depuis 30 ans, ainsi que les résultats détaillés d'une année intéressante (1977).

La réduction des données consiste, dans un premier temps, à mesurer sur la plaque photo (négatif) les parties utiles au calcul, c'est-à-dire la trajectoire du météore et entre 15 et 20 étoiles qui permettront de se repérer dans le système de coordonnées équatoriales. Le centre optique des caméras est toujours positionné aussi près que possible du zénit, et les mesures de position sur les plaques se font à la minute d'arc près. Des formules empiriques progressivement mises au point depuis de nombreuses années permettent de retrouver la position d'un point dans le ciel à partir de mesures effectuées sur la plaque (par exemple, la distance zénitale Z est calculée à partir de la distance r du centre optique (supposé au zénit) par une formule de la forme $z = a + br + ce^{dr}$).

L'optique utilisée ne permet pas d'évaluer la taille de l'objet, qui apparaît comme un point (il faudrait une distance focale d'au moins 750 mm pour pouvoir commencer à évaluer les dimensions d'objets brillants).

La reconstruction des données temporelles se fait à l'aide de la caméra mobile d'Ondrejov, par comparaison des positions des étoiles choisies comme repères. Le calcul utilise toujours le temps du début d'exposition, facilement repérable sur les clichés car on démarre les expositions par ciel clair, et parfois le temps de fin d'exposition (les Allemands ont plus de difficulté

car ils **programment** leurs stations à l'aide d'une **minuterie**, et **ne sont donc pas sûrs** de l'état du ciel au début de l'exposition). On obtient couramment une incertitude sur la datation de 10 s à 1σ , cette précision pouvant atteindre 7 s quand la trajectoire est **normale** au mouvement diurne.

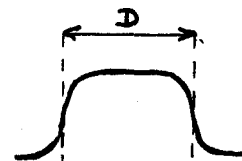
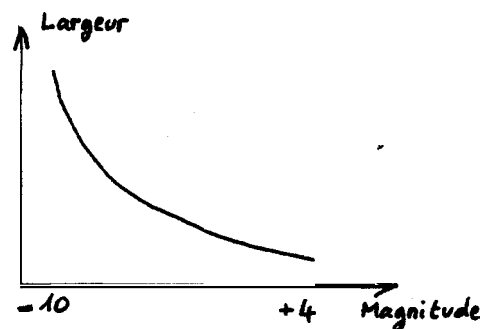
Lorsque des données en **provenance** de plus de 2 stations **sont disponibles**, le **programme fait les calculs de trajectographie** pour toutes les **combinaisons 2 à 2** de ces stations ainsi que pour une combinaison de toutes ces stations. Les **calculs de vitesse font intervenir les pointillés créés par l'obturation cyclique**, et chaque petit segment est **analysé en détail**. Des **corrections fines** mettent en **jeu** la position exacte dans le plan de la plaque du centre de rotation de **l'obturateur (composition du vecteur vitesse apparente du météore avec la vitesse de déplacement du volet de l'obturateur)**.

Les **mesures photométriques** permettent d'évaluer les variations de **magnitude (relative puis absolue)** le long de la trajectoire. Elles **sont effectuées** par comparaison de la **largeur** de la trace sur l'**émulsion** à celle de la trace des étoiles. **Là encore, l'utilisation d'une formule empirique** permet d'atteindre une très bonne précision ($\pm 0,1$ **magn. jusqu'à 70°** du centre optique).

Cette **formule** est de la forme : $M = \ln(aD + b) + k$, où D est la largeur de la trace.

La **précision de la mesure est bonne** en raison du caractère net du profil en intensité de cette trace. On utilise la **meilleure photo** pour faire les mesures et les **calculs photométriques**.

L'**effet de réciprocité** ne **joue pas suffisamment** pour justifier une correction, et la méthode donne de bons **résultats** pour un **domaine de magnitudes** allant jusqu'à -10 ($\pm 0,9$).



L'**extrapolation**, en **localisation comme en brillance**, pose de **sérieux problèmes**.

Le tableau ci-contre indique les correspondances, pour une étoile fixe, entre le diamètre de l'image sur la plaque et la magnitude relative.

\varnothing mm	M
0,02	+ 4
0,05	+ 1,5
0,1	- 1
0,2	- 4
0,3	- 5,5

Les résultats des mesures photométriques sont convertis en magnitudes "absolues" (ramenées & 100 Km de distance), caractéristiques de l'objet lui-même et non de son apparence vu du sol.

A magnitude relative égale, dérivée directement de la mesure photométrique, la contribution à la magnitude absolue de la vitesse angulaire apparente se traduit par la relation :

$$M_1 - M_2 = - 2,5 \log (v_1/v_2)$$

Il en résulte une différence de l'ordre de 7 entre une étoile fixe (15 °/h) et un météore-type (une dizaine de °/s).

La contribution de la distance est donnée de la même manière par :

$$M_1 - M_2 = - 5 \log (d_1/d_2)$$

La pratique a permis de choisir un critère de pondération efficace entre les mesures faites sur différentes plaques pour une même trajectoire : à conditions météorologiques égales, le poids attribué à chaque plaque est proportionnel à la longueur de la trajectoire apparente mesurée sur cette plaque,

Le programme peut extrapoler la trajectoire dans les deux sens : d'une part il "remonte" en amont pour déterminer l'orbite de l'objet, et d'autre part il peut évaluer la fin de la trajectoire (option "dark flight"), en prenant en compte le cas échéant les données disponibles sur l'état des vents (cas où la taille présumée de l'objet permet d'espérer l'arrivée au sol de météorites). Le programme s'exécute en 3 mn sans l'option "dark flight", et en 1 h avec,

V, Gestion du réseau.

La plupart des **caméras** sont **installées** dans des stations **météo-**
rologiques, et **opérées** par le **personnel** de ces stations **moyen-**
nant une petite rétribution (fonction de la **qualité** des **photos**).
Les plaques photos **sont envoyées** par courrier dans des conte-
neurs **spéciaux**, et les **manipulations demandées** aux opérate — s
sont **minimales**.

Les campagnes de prise de vues sont **programmées** depuis **Ondrejov**,
et tiennent compte de l'éclairement **par la lune**. La précision
est de l'ordre de **5 m**, et une condition nécessaire est que le
soleil soit **au moins** à **110** au-dessous de l'horizon. Les **nuits**
sans lune font l'objet d'une seule exposition (**jusqu'à 13 h** en
Décembre), **tandis** que les nuits avec lune sont **décomposées** en
deux périodes d'exposition. Dans un cycle **lunaire** (28 jours),
il y a 22 nuits avec **une** ou deux expositions et **6 nuits sans** ex-
position.

Chaque station (il y en a actuellement **12 équipées** de fish-eye
en **Tchécoslovaquie**) est normalement visitée une fois par **an**
pour l'entretien (c'était le but de la visite à **Churanov**). **Il**
s'agit de nettoyer l'optique et de vérifier le **petit** moteur qui
commande l'obturateur. Il y a en moyenne **une** intervention par
an pour réparer quelque chose sur l'ensemble des 12 stations
(MTBF = **12 ans !..**).

En ce **qui** concerne la collecte des météorites, **il n'y a pas** de
loi **particulière** en Tchécoslovaquie, **mais il n'y a jamais eu** de
problème en **raison** du régime et du sens **très** relatif de la pro-
priété des populations. M. **CEPLECHA** ne **connait pas** de **pays** où
il existe une loi concernant la **propriété** des météorites. En
Tchécoslovaquie, **comme** en RFA, des récompenses **sont** offertes
aux découvreurs, en leur présentant l'effort scientifique re-
présenté et non **une** valeur marchande de l'objet **lui-même**.

VI, Conclusions.

Monsieur CEPLECHA est **certainement** le **meilleur** spécialiste mondial de la détection optique de **météores**. Le **réseau** qu'il gère met en jeu des technologies **très** simples et très éprouvées, et **il** constitue un point de comparaison **unique**.

De **l'aveu-même** de M. CEPLECHA, **l'avenir** appartient certainement à des systèmes plus **sophistiqués** mettant en jeu des technologies de pointe comme les détecteurs CCD et le traitement digital des images, et **il** est **prêt** à mettre son expérience à **la** disposition **des concepteurs** éventuels d'un tel **système**. Compte tenu de la motivation que constituerait pour lui et pour ses **collègues** allemands la prise en compte **d'une** ou de plusieurs stations **françaises** dans le **réseau** européen (avec **son système** de traitement), **il** semble particulièrement **intéressant** de prévoir l'installation d'un premier **prototype** dans le prolongement du réseau européen (ce qui rejoint les **souhaits** de M. PELLAS, cf. CR 570882).

En outre, indépendamment de son lieu d'implantation, **il** serait souhaitable, **lorsqu'une première** maquette sera **expérimentée**, de lui **adjoindre une station** de type "Ceplecha" de façon à disposer d'un point de comparaison bien **connu** pour les performances, M. CEPLECHA partage tout-à-fait ce point de vue.

oooooooooooo

FIREBALLS PHOTOGRAPHED IN CENTRAL EUROPE

Z. Ceplecha, Astronomical Institute of the Czechoslovak Academy of Sciences, **Ondřejov**

Received 11 January 1977

Болиды сфотографированные в средней Европе

Приводятся данные об орбитах и траекториях 42 болидов (большая часть ярче — 8 величины), вычисленных в обсерватории Ондřejов в течении последних трех десятилетий. Болиды были сфотографированы в рамках трех разных программ, которые кратко описаны, равно как планы обсерватории Ондřejов по фотографическому наблюдению метеоров и болидов. Приведены также некоторые результаты этих программ, в частности классификация фотографических метеоров с учетом состава и структуры метеоров и их отношение к другим телам солнечной системы.

The paper contains data on orbits and trajectories of 42 bright fireballs computed at the **Ondřejov Observatory** during the past decades (mostly brighter than magnitude —8). They were photographed during three different projects, which are briefly described. Future prospects of the **Ondřejov** Observatory in photographic recording of meteors and fireballs are outlined. Some results obtained from these and other photographic projects are mentioned; especially the classification of photographic meteors with respect to the meteoroid composition and structure are given and the relation to other bodies of the solar system proposed.

1. Photographic Programs; Their Past and Future

This paper contains orbits and other data on fireballs computed at the **Ondřejov** Observatory during the past 3 decades (1947 to 1976). They form only a small part of all the fireballs photographed: only exceptional cases were reduced. The choice, what to reduce, was directed by taking into account brightness and spectral records before 1963, and the low terminal height, brightness and spectral records from 1963 on. The data before 1963 were collected from the double-station small-camera program described in details elsewhere (Ceplecha, 1957; Ceplecha et al., 1959).

Though some changes were introduced, for most of the 25 years three sets consisting of 30 cameras with Tessar objectives, $1/4.5 f = 180$ mm, and glass photographic plates, 9 x 12 cm, with panchromatic emulsion were used. Of these cameras, 10 are located at the **Ondřejov** Observatory as a fixed aggregate with rotating shutters giving about 48 breaks per second, 10 other cameras are driven and located adjacent to the set of the fixed cameras at the **Ondřejov** Observatory to get known the time of meteor passage. The remaining 10 cameras form a fixed aggregate located 40.388 km away from the **Ondřejov** Observatory at **Prčice** Station.

During 25 years of continuous operation, utilizing each moonless clear night, in about 8000 hours

Table I
Orbital and other data on photographic fireballs.

Fireball No. Name	130 847	131a	641a	15 761	15 811	16051	16 931
Year and Date Time UT	1947 Aug 13 22 h 22 m 44 s ± 1 s	1951 Oct 27 22 h 32 m 47 s ± 1 s	1953 Aug II 21 h 40 m 58 s ± 1 s	1958 Aug 13 22 h 14 m 06 s ± 2 s	1958 Aug 15 21 h 32 m 23 s ± 6 s	1958 Aug 18 23 h 08 m 18 s ± 5 s	1958 Oct 23 2 h 05 m ± 5 m
M_p	9.3	9.6	9.1	7.9	8.8	10.1	10.2
m_∞ kg	0.031	0.15	0.048	1.2	0.30	0.61	0.019
m_E kg	0	0	0	0.02	0	0	0
v_B km/s	60	30	60	22	22	24	71
h_B km	112	99	111	90	96	93	109
v_E km/s	59	24	58	11	19	20	69
h_E km	84	61	79	43	70	68	82
$(\cos z_R)_E$	0.623	0.773	0.561	0.465	0.965	0.879	0.842
h_m km	91	62	86	57	75	75	87
Number of St.	3	2	6	2	2	2	2
α_R° 1950.0	47.36 ± .10	45.68 ± .02	44.733 ± .045	315.508 ± .009	278.79 ± .35	282.40 ± .05	94.9 ± 1.3
δ_R° 1950.0	58.726 ± .017	13.14 ± .03	58.355 ± .008	-12.351 ± .004	47.78 ± .23	55.28 ± .02	17.51 ± .26
v_∞ km/s	60.0 ± .3	30.28 ± .16	59.70 ± .18	22.13 ± .05	22.50 ± .13	23.90 ± .09	70.4 ± .9
λ	40.70 ± .02	78.11 ± .02	40.67 ± .01	98.71 ± .01	102.6 ± .2	96.91 ± .03	26 ± 1
α_G° 1950.0	48.18 ± .10	45.54 ± .02	45.64 ± .05	314.962 ± .010	276.21 ± .37	278.52 ± .06	94.7 ± 1.3
δ_G° 1950.0	58.694 ± .017	11.77 ± .04	58.249 ± .008	-17.39 ± .03	47.19 ± .24	54.49 ± .02	17.32 ± .26
V_G km/s	58.8 ± .3	28.08 ± .17	58.50 ± .18	19.09 ± .06	19.65 ± .15	21.30 ± .10	69.4 ± .9
v_H km/s	41.2 ± .3	36.61 ± .10	40.96 ± .16	37.41 ± .03	38.77 ± .12	38.35 ± .06	44.5 ± 1.0
a A.U.	18 ± 8	1.99 ± .03	12 ± 2	2.521 ± .018	3.56 ± .13	3.14 ± .05	- 4
$1/a$ (A.U.) ⁻¹	0.057 ± .025		0.082 ± .015				- 0.23 ± .10
e	0.946 ± .024	0.825 ± .004	0.922 ± .014	0.725 ± .002	0.722 ± .010	0.682 ± .005	1.13 ± .06
q A.U.	0.9506 ± .0011	0.349 ± .002	0.9527 ± .0005	0.6908 ± .0007	0.9893 ± .0008	0.9963 ± .0001	0.59 ± .03
Q A.U.	34 f 1.6	3.64 ± .07	23 ± 4	4.35 ± .04	6.13 ± .26	5.28 ± .11	-
ω° 1950.0	150.8 ± .5	115.81 ± .06	151.1 ± .3	76.08 ± .03	199.1 ± .3	195.91 ± .04	76 ± 4
Ω° 1950.0	140.348	33.676	138.846	320.33	142.414	145.363	29.04
i° 1950.0	112.16 ± .20	6.12 ± .05	111.97 ± .12	0.180 ± .015	28.83 ± .19	33.04 ± .12	167.4 ± .6
π° 1950.0	291.2 ± .5	149.48 ± .06	289.9 ± .3	36.41 ± .03	341.5 ± .3	341.27 ± .04	105 ± 4
Shower Type	Perseid III Ai	S. Taurid III A (II)	Perseid III Ai	Sporadic II	a Lyrid III B	× Cygnid III A	Orionid III A
Note	-	-	1 PS	1 PS	-	-	-

Table 1 (Cont.)

Fireball No. Name	19 241 Pflibram	19 591	21 911	27 471	32 281	36 221	38 421
Year and Date Time UT	1959 Apr 7 19 h 30 m 21 s ± 1 s	1959 May 9 20 h 50 m 16 s ± 3 s	1959 Sep 8 21 h 43 m 18 s ± 4 s	1960 Oct 27 0 h 13 m 04 s ± 2 s	1961 Nov 13 21 h 49 m 46 s ± 1 s	1962 Sep 26 23 h 18 m 16 s ± 3 s	1963 Apr 21 1 h 13 m 48 s ± 1 s
M_p	-19.2	-14.5	-9.4	-7.4	-9.8	-10.5	-12.4
m_{∞} kg	21 500	2.4	0.036	0.30	0.20	0.36	0.38
m_E kg	50	0	0	0.0002	0	0	0
v_B km/s	21	44	36	26	29	32	32
h_B km	98	115	103	87	96	89	97
v_E km/s	unknown	41	35	12	25	27	32
h_E km	13	72	86	41	66	72	75
$(\cos ZR)_E$	0.678	0.581	0.784	0.755	0.785	0.716	0.965
h_m km	46	83	88	65	72	74	77
Number of St.	2	2	2	2	2	2	2
α_R 1950-0	189.499 ± 0.010	270.55 ± 0.02	252.94 ± 0.12	38.94 ± 0.03	58.044 ± 0.014	22.01 ± 0.03	264.554 ± 0.018
δ_R 1950-0	20.700 ± 0.001	35.59 ± 0.01	75.76 ± 0.03	10.82 ± 0.02	16.451 ± 0.011	7.04 ± 0.03	56.831 ± 0.009
v_{∞} km/s	20.886 ± 0.005	43.58 ± 0.32	35.71 ± 0.16	26.13 ± 0.08	28.86 ± 0.07	31.92 ± 0.20	32.57 ± 0.11
λ°	101.839 ± 0.010	68.57 ± 0.02	81.97 ± 0.03	86.11 ± 0.03	82.665 ± 0.014	71.98 ± 0.03	83.39 ± 0.01
α_G° 1950-0	191.732 ± 0.011	271.34 ± 0.02	248.51 ± 0.12	37.77 ± 0.03	58.154 ± 0.014	21.77 ± 0.03	264.460 ± 0.019
δ_G° 1950-0	17.736 ± 0.002	35.17 ± 0.01	75.21 ± 0.03	8.74 ± 0.03	15.070 ± 0.013	5.58 ± 0.04	57.151 ± 0.009
v_G km/s	17.434 ± 0.006	41.9 ± 0.3	34.01 ± 0.17	23.72 ± 0.09	26.50 ± 0.08	29.85 ± 0.21	30.55 ± 0.12
v_H km/s	37.451 ± 0.005	41.50 ± 0.26	41.84 ± 0.12	36.94 ± 0.05	37.48 ± 0.05	35.00 ± 0.12	40.04 ± 0.08
a A.U.	2.4008 ± 0.0023	25	80	2.108 ± 0.018	2.28 ± 0.02	1.628 ± 0.026	5.46 ± 0.21
$1/a$ (A.U.) ⁻¹		0.039 ± 0.024	0.012 ± 0.011				
e	0.6712 ± 0.0003	0.966 ± 0.021	0.988 ± 0.011	0.764 ± 0.003	0.813 ± 0.002	0.848 ± 0.004	0.817 ± 0.007
q A.U.	0.7894 ± 0.0001	0.8689 ± 0.0013	0.9980 ± 0.0009	0.4982 ± 0.0012	0.4267 ± 0.0008	0.2471 ± 0.0023	0.9969 ± 0.0001
Q A.U.	4.012 ± 0.005	50		3.72 ± 0.04	4.14 ± 0.04	3.01 ± 0.05	9.9 ± 0.4
ω° 1950-0	241.749 ± 0.014	224.3 ± 0.4	168.76 ± 0.07	98.71 ± 0.07	105.54 ± 0.03	129.92 ± 0.10	190.76 ± 0.03
Ω° 1950-0	17.110	48.350	165.352	33.447	51.145	3.212	30.054
f° 1950-0	10.481 ± 0.004	68.1 ± 0.3	53.31 ± 0.16	4.91 ± 0.02	5.041 ± 0.014	4.91 ± 0.05	48.99 ± 0.12
π° 1950-0	258.860 ± 0.014	272.6 ± 0.4	334.12 ± 0.07	132.16 ± 0.07	156.68 ± 0.03	133.13 ± 0.10	220.82 ± 0.03
Shower Type	sporadic I	sporadic III B	sporadic III A ₁	association 85 I	S. Taurid III A	S. Taurid ? core III B crust II	sporadic III A ₁
Note	17 fragments recovered mass 5.8 kg 4 meteorites			I GS 72 and 36 Å/mm	GS 94 + 47 Å/mm	GS 58 Å/mm	GS 57, 28 Å/mm PS

Table 1 (Cont.)

Fireball No. Name	39 141	EN 191 063	EN 160 166 Berounka	EN 031 267 62 061	EN 300 768	EN 151 068 Čechtice	EN 231 068 66 461
Year and Date Time UT	1963 Aug 14 21 h 48 m 34 s ± 5 s	1963 Oct 19 18 h 56 m ± 1 m	1966 Jan 16 1 h 45.1 m ± .6 in	1967 Dec 3 4 h 02 m 15 s ± 7 s	1968 July 30 1 h 15 m ± 15 m	1968 Oct 15 19 h 53.5 m ± .5 m	1968 Oct 23 2 h 12 m 09 s ± 2 s
M_p	(-15.2)	-11.0	-17.0	(-11.3)	(-11.2)	(-15.5)	(-7.6)
m_o kg	(270)	36	550	(14)	(0.3)	(1600)	(0.0013)
m_E kg	0	unknown	0.15	0	0	0.15	0
v_B km/s	25	25	39	27	45	19	67
h_B km	103	79	97	98	94	72	111
v_E km/s	24	unknown	20	24	44	5	67
h_E km	69	49	36	56	73	30	84
$(\cos z_R)_E$	0.948	0.130	0.606	0.562	0.973	0.858	0.828
h_m km	82	64	41	71	76	45	85
Number of St.	2	2	3	5	3	3	4
α_R^o 1950.0	277.275 ± .036	209.3 ± .7	244.0 ± 1.4	77.72 ± .03	326 ± 4	285.2 ± .4	94.510 ± .016
δ_R^o 1950.0	58.939 ± .015	32.77 ± .10	51.4 ± .9	27.758 ± .006	40 ± 2	60.51 ± .18	17.809 ± .013
v_o km/s	24.64 ± .07	25.5 ± .5	38.9 ± .6	27.58 ± .08	45 ± 2	19.02 ± .05	67.26 ± .09
λ_o	94.62 ± .02	78.5 ± .6	70.9 ± .9	83.79 ± .03	66 ± 3	97.9 ± .2	26.84 ± .02
α_G^o 1950.0	274.03 ± .04	206.3 ± .7	245.5 ± 1.4	75.31 ± .03	325 ± 4	277.6 ± .4	94.322 ± .016
δ_G^o 1950.0	58.958 ± 0.016	28.3 ± .2	51.1 ± .9	25.681 ± .014	40 ± 2	59.42 ± .20	17.600 ± .013
v_G km/s	22.07 ± .08	23.2 ± .6	37.1 ± .6	25.52 ± .09	44 ± 2	15.56 ± .06	66.26 ± .09
v_H km/s	38.17 ± .05	34.0 ± .4	39.5 ± .6	37.38 ± .05	41 ± 2	35.53 ± .06	41.79 ± .09
a A.U.	3.008 ± .038	1.42 ± .05	3.6 ± .7	2.206 ± .020	22	1.713 ± .013	24 ± 5
$1/a$ (A.U.) ⁻¹					0.05 ± .20		0.042 ± .008
e	0.666 ± .004	0.580 ± .014	0.73 ± .05	0.7941 ± .0023	0.97 ± .15	0.419 ± .004	0.978 ± .004
q A.U.	1.0063 ± .0001	0.595 ± .009	0.976 ± .003	0.4541 ± .0012	0.72 ± .04	0.9960 ± .0001	0.5205 ± .0017
Q A.U.	5.01 ± .08	2.24 ± .11	6.2 ± 1.4	3.95 ± .04	—	2.43 ± .03	47 ± 9
ω^o 1050.0	190.31 ± .03	84 ± 2	169 ± 2	282.67 ± .07	245 ± 7	184.1 ± .3	87.9 ± .3
Ω 1950.0	141.192	205.48	295.26	250.006	126.7	202.250	29.476
i^o 1950.0	35.06 ± .09	28.2 ± .8	62.5 ± .9	2.71 ± .02	71 ± 4	25.72 ± .09	167.31 ± .03
π^o 1950.0	331.50 ± .03	290 ± 2	104 ± 2	172.67 ± .07	12 ± 7	26.3 ± .3	117.4 ± .3
Slower Type	α Cygnid III B	sporadic I	sporadic II	N. γ Orionid III A	Lacertid! III Ai	sporadic II	Orionid III Ai
Note	PS		Pr. Im. λ 13°31'21" ϕ 49°53'34"	2 GS 67--13 Å/mm I PS	1 GS 23--11 Å/mm I PS	5 fragments 2 GS 56--28 Å/mm 2 PS Pr. Im. λ 15°02'50" ϕ 49°37'24"	1 GS 70--35 Å/mm

Table 1 (Cont.)

Fireball No. Name	EN 100 469 Otterskirchen	EN 080 669 —	EN 270 870 Stuttgart	EN 141 170 Mt. Riffler	EN 170 171 Würzburg	EN 151 071 Hornberg	EN 191 071 Memmingen
Year and Date Time UT	1969 Apr 10 21 h 44.5 m ± 1.5 m	1969 June 8 21 h 18.5 m ± .5 m	1970 Aug 27 1 h 53 m ± 1 m	1970 Nov 24 1 h 47 m ± 1 m	1971 Jan 17 18 h 20 m ± 1 m	1971 Oct 15 19 h 50 m ± 5 m	1971 Oct 19 19 h 35 m ± 3 m
M_p	15.4	9.7	10.7	15.1	17.0	8.7	9.3
m_∞ kg	5000	30	17	3000	3200	4.3	33
m_E kg	5	0.5	0.03	0.9	0	0.006	0.54
v_B km/s	16	17	24	21	16	20	14
h_B km	84	77	86	83	75	71	68
v_E km/s	3	12	6	6	11	11	7
h_E km	24	43	29	26	45	38	34
$(\cos z_R)_E$	0.569	0.294	0.727	0.310	0.248	0.775	0.450
h_m km	45	50	55	41	60	54	48
Number of St.	6	9	10	11	6	5	6
α_R° 1950.0	161.4 ± .5	106.0 ± .3	330.2 ± .4	236.3 ± .3	344.6 ± .3	266.5 ± 1.3	278.6 ± .8
δ_R° 1950.0	- 4.64 ± .14	44.7 ± .2	21.0 ± .3	54.5 ± .4	- 7.77 ± .06	52.0 ± .3	3.38 ± .10
v_∞ km/s	16.08 ± .14	17.44 ± .17	24.4 ± .2	21.17 ± .18	15.7 ± .2	20.4 ± .2	13.8 ± .4
λ°	121.9 ± .5	110.0 ± .2	87.0 ± .4	80.8 ± .2	123.2 ± .5	102.5 ± .5	148.5 ± .9
α_G° 1950.0	157.9 ± .6	99.2 ± .3	327.8 ± .4	242.2 ± .3	335.4 ± .5	260.6 ± 1.4	267.6 ± 1.4
δ_G° 1950.0	-13.86 ± .28	35.2 ± .3	18.8 ± .3	48.9 ± .5	-19.6 ± .4	50.0 ± .3	-10.3 ± 1.3
v_G km/s	11.72 ± .19	13.66 ± .22	21.9 ± .2	17.85 ± .21	11.4 ± .3	17.3 ± .2	8.6 ± .7
v_H km/s	37.26 ± .17	36.34 ± .17	35.80 ± .16	32.52 ± .08	37.8 ± .3	37.6 ± .2	37.5 ± .6
a A.U.	2.32 ± .08	2.08 ± .06	1.87 ± .05	1.199 ± .009	2.35 ± .13	2.43 ± .09	2.35 ± .29
$1/a$ (A.U.) ⁻¹	0.598 ± .013	0.594 ± .012	0.665 ± .008	0.252 ± .005	0.616 ± .021	0.594 ± .016	0.58 ± .05
e	0.934 ± .002	0.844 ± .002	0.627 ± .005	0.896 ± .003	0.9005 ± .0011	0.9888 ± .0014	0.985 ± .001
Q A.U.	3.71 ± .15	3.31 ± .12	3.11 ± .09	1.502 ± .017	3.8 ± .3	3.88 ± .19	3.7 ± .6
ω° 1950.0	35.1 ± .5	123.2 ± .4	267.2 ± .9	122.9 ± 1.2	321.0 ± .5	167.9 ± 1.1	165.8 ± .7
Ω° 1950.0	200.561	77.637	153.106	241.071	116.75	201.49	205.43
i° 1950.0	6.77 ± .08	4.80 ± .18	21.2 ± .3	31.0 ± .4	2.71 ± .05	26.1 ± .3	3.0 ± .5
n° 1950.0	235.7 ± .5	200.8 ± .4	60.3 ± .9	4.0 ± 1.2	77.8 ± .5	9.4 ± 1.1	11.2 ± .7
Shower Type	sporadic II	sporadic II	sporadic I	sporadic I	sporadic core III B crust II	sporadic I	sporadic I
Note	Pr. Im. λ 13°19'58" ϕ 48°38'56"		Pr. Im. λ 9°31'58" ϕ 48°43'28"	Pr. Im. A 10°20'44" ϕ 47°08'26"			Pr. Im. λ 10°26'18" ϕ 48°07'41"

Table 1 (Cont.)

Fireball No. Naine	EN 210 372 B Bramberg	EN 210 372 A Büdingen	EN 220 372 Marburg	EN 120 872 —	EN 020 173 Prague	EN 210473 Nürnberg	EN 200 374 —
Year and Date Time UT	1972 Mar 21 19 h 30 m ± 20 m	1972 Mar 21 21 h 30 m ± 5 m	1972 Mar 22 21 h 30 m ± 20 m	1972 Aug 12 0 h 29 m ± 1 m	1973 Jan 2 3 h 11·1 m ± 1·3 m	1973 Apr 21 20 h 52 m ± 2 m	1974 Mar 20 19 h 42 m ± 2 m
M_p	— 8·9	— 8·7	—11·2	—12·5	— 11·9	— 9·3	— 9·0
m_∞ kg	2·8	26	47	0·42	8·6	14	4·2
m_E kg	0·18	8	0·73	0	0·001	0·08	0·002
v_B km/s	22	12	21	60	34	17	16
h_B km	86	62	73	119	83	72	78
V_E km/s	13	8	10	59	18	10	7
h_E km	36	31	32	76	45	41	39
$(\cos z_R)_E$	0·806	0·791	0·553	0·804	0·698	0·445	0·521
h_m km	47	41	45	83	54	58	64
Number of St.	3	3	3	2	5	7	4
α_R° 1950·0	180 ± 5	134·9 ± 1·4	179 ± 5	44·8 ± 2·3	119·5 ± 4	183·9 ± 6	19·8 ± 2·1
δ_R° 1950·0	48·5 ± 5	14·9 ± 6	— 0·6 ± 5	58·9 ± 1·2	20·6 ± 2	—13·1 ± 4	55·5 ± 5
a km/s	22·1 ± 1·0	12·6 ± 5	21·4 ± 4	60·1 ± 1·1	34·1 ± 3	17·2 ± 2	16·3 ± 3
λ°	105 f 3	136·1 ± 1·6	89 ± 5	41·4 ± 1·2	74·8 ± 4	106·4 ± 6	114·5 ± 1·4
α_G° 1950·0	183 ± 5	129·3 ± 1·9	180 ± 5	45 ± 2	118·2 ± 4	184·1 ± 7	9·8 ± 2·0
δ_G° 1950·0	47·8 ± 6	1·5 ± 2·3	— 5·2 ± 6	59·0 ± 1·2	19·4 ± 2	—22·6 ± 6	47·4 ± 7
v_G km/s	18·9 ± 1·2	6·0 ± 1·0	18·1 ± 5	58·9 ± 1·1	32·4 ± 3	13·0 ± 3	12·1 ± 4
v_H km/s	39·4 ± 1·2	34·5 ± 9	34·8 ± 1·4	41·7 ± 1·1	38·14 ± 26	35·57 ± 22	36·6 ± 4
a A.U.	3·8 ± 1·6	1·50 ± 16	1·55 ± 26	—	2·54 ± 14	1·78 ± 05	2·02 ± 13
$1/a$ (A.U.) ⁻¹	0·26 ± 11			0·01 ± 11			
e	0·77 ± 09	0·35 ± 07	0·59 ± 04	0·99 ± 10	0·892 ± 006	0·519 ± 015	0·546 ± 029
q A.U.	0·888 ± 011	0·979 ± 004	0·63 ± 05	0·959 ± 013	0·274 ± 006	0·854 ± 004	0·919 ± 004
Q A.U.	7 ± 3	2·0 ± 3	2·5 ± 5	—	4·80 ± 28	2·70 ± 11	3·12 ± 26
ω° 1950·0	221 ± 3	21·1 ± 1·6	89 ± 10	153 ± 4	122·0 ± 8	55·9 ± 1·0	141·3 ± 1·6
Ω° 1950·0	1·0	181·06	182·0	139·08	101·34	211·261	359·480
io 1950·0	20 ± 2	2·87 ± 16	2·9 ± 1·1	111 ± 2	2·2 ± 3	7·25 ± 18	12·4 ± 4
π° 1950·0	222 ± 3	202·2 ± 1·6	271 ± 10	292 ± 4	223·3 ± 8	267·2 ± 1·0	140·8 ± 1·6
Showrr Type	sporadic I	sporadic II	sporadic I	Perseid III Ai	sporadic II	sporadic II	sporadic I
Note	Pr. Im. A 10°41'36" gr 50°06'25"	Pr. Im. A 9°07'10" φ 50°19'19"	Pr. Im. A 8°36'26" gr 50°49'58"		GS 53 Å/mm 2 fragments		

Table 1 (Cont.)

Fireball No. Name	EN 210 374	EN 200 474 89 991	EN 300 874 Leutkirch	EN 170 974 —	EN 041 274 Sumava	EN 290 875 Arrach	EN 020 376 Kamyk
Year and Date Time UT	1974 Mar 21/22 20 h 45 m ± 3 h 45 m	1974 Apr 20 0 h 50 m ± 5 m	1974 Aug 30 1 h 25 m ± 5 m	1974 Sep 17 20 h 29 m ± 1 m	1974 Dec 4 17 h 56.6 m ± 3 m	1975 Aug 29 22 h 13 m ± 2 m	1976 Mar 2 19 h 12.0 m ± 3 m
M_p	--12.0	(--10.2)	--10.4	(-12)	(-21)	--13.6	(-13)
m_{∞} kg	130	(26)	311	(0.3)	(100000)	130	(500)
m_E kg	0	0.01	14	0	0	0.009	0.07
v_B km/s	14	17	13	68	27	28	17
h_B km	75	74	71	111	99	64	83
v_E km/s	7	6	4	67	26	11	6
h_E km	38	38	26	95	55	30	32
$(\cos z_R)_E$	0.772	0.574	0.389	0.387	0.460	0.581	0.525
h_m km	53	49	53	96	73	41	43
Number of St.	3	3	6	3	3	3	11
α_R^0 1950.0	66 to 172	194.4 ± 1.3	303.2 ± 1.3	58.9 ± 3	74.51 ± 1.3	333.4 ± 0.9	277.4 ± 1.0
δ_R^0 1950.0	76.3 ± 6	6.11 ± 0.1	8.52 ± 1.2	38.08 ± 1.7	27.51 ± 1.0	-- 4.7 ± 1.0	71.8 ± 3
v_{∞} km/s	14.5 ± 3	17.6 ± 6	12.61 ± 1.1	67.8 ± 1.0	27.0 ± 8	27.8 ± 6	17.40 ± 0.5
z^0	123 to 131	109.1 ± 1.3	138.9 ± 1.7	26.0 ± 2	84.1 ± 2	94.0 ± 9	89.1 ± 4
α_G^0 1950.0	35 to 140	189.9 ± 1.4	286.1 ± 1.7	59.4 ± 3	77.0 ± 2	333.1 ± 9	281.0 ± 8
δ_G^0 1950.0	72.1 ± 7	-- 0.3 ± 0.6	--10.3 ± 7	37.86 ± 1.7	25.6 ± 2	-- 7.3 ± 1.0	63.5 ± 4
v_G km/s	9.4 ± 5	13.9 ± 8	6.48 ± 2.2	66.6 ± 1.0	24.3 ± 9	25.4 ± 7	13.35 ± 0.7
v_H km/s	36.3 ± 4	36.6 ± 5	34.64 ± 1.7	42.1 ± 1.0	36.8 ± 6	40.2 ± 5	32.68 ± 0.8
a A.U.	1.93 ± 1.4	2.08 ± 1.9	1.592 ± 0.33	--	1.98 ± 1.8	6.4 ± 2.0	1.230 ± 0.009
$1/a$ (A.U.) ⁻¹				0.005 ± 0.092		0.155 ± 0.048	
e	0.49 ± 0.04	0.595 ± 0.039	0.385 ± 0.13	1.00 ± 0.07	0.76 ± 0.03	0.91 ± 0.03	0.200 ± 0.006
q A.U.	0.991 ± 0.005	0.844 ± 0.10	0.979 ± 0.03	0.747 ± 0.13	0.471 ± 0.008	0.576 ± 0.13	0.9832 ± 0.0008
Q A.U.	2.9 ± 3	3.3 ± 4	2.21 ± 0.7	--	3.5 ± 4	12 ± 4	1.48 ± 0.2
ω^0 1950.0	165 to 188	235.1 ± 1.8	207.1 ± 1.3	241 ± 3	282.0 ± 4	264 ± 2	161.9 ± 1.0
Ω 1950.0	0.66 ± 1.4	29.30	155.99	174.22	251.78	155.61	341.978
i^0 1950.0	11.6 ± 5	1.4 ± 4	2.30 ± 1.7	147.5 ± 5	2.3 ± 2	2.9 ± 9	24.02 ± 1.1
π^0 1950.0	166 to 189	264.4 ± 1.8	3.1 ± 1.3	55 ± 3	173.8 ± 3	60 ± 2	143.9 ± 1.0
Shower Type	sporadic III A	sporadic II	sporadic I	? Aurigid ? III B	N. χ Orionid III B	sporadic I	sporadic II
Note		2 fragments ?	Pr. Im. λ 9°53'31" ϕ 47°51'05"	PS	4 GS 28--5 Å/mm		4 GS 75--15 Å/mm 9 fragments Pr. Im. λ 14°18'53" ϕ 49°38'41"

of exposure time, 50 000 photographic plates have been exposed and about 1200 double-station **meteors** have been recorded, most of them being sporadic. The **typical** positional precision of these photographs is ± 10 seconds of arc for one position, and **meteors** down to about **visual** magnitude $+1$ could have been photographed. 18 fireballs in this **program** were measured and computed. The data are contained in Tab. 1.

The direct **small-cameras** were accompanied by 7 **cameras** with rotating shutters for **meteor spectroscopy**. Objectives (Tessar 1/6.3, 1/4.5 and 1/3.5, $f = 750$ mm, 360 mm, and 300 mm) with Bausch & Lomb transparent objective gratings with 600 and 400 **grooves** per mm have been used. **Photographic** plates, 30 x 30 cm and 18 x 24 cm, with panchromatic emulsion have been **applied**. **Three cameras** were equipped with objective prisms. Extremely good spectra of many fireballs with dispersions down to 5 Å/mm and with **several** hundred of spectral **lines** in the visible **region** have been photographed. (Rajchl, 1961; Ceplecha, 1971). The best spectra usually initiated the whole reductional procedure of the double-station or multiple-station photographs. The zero **order** images gave the best positional data in some cases and the individual fragments are usually **well** separated and good to measure at **these** large focal distances.

After 8 years and 2500 hours of exposure time of the small-camera double-station **program**, we obtained photographs of the Piibram meteorite **fall** on ten plates of both our stations in April 1959 (Ceplecha, 1961). Among others this inspired us to design a multi-station **program** for photographing the fireballs. We have used one all-sky camera with a rotating shutter having 12.5 breaks per second at each station. A simple system of **photographing** a convex mirror with a standard 36 mm camera has been used. The resulting speed is 1/16 with $f = 5$ mm. The accuracy of positions obtained from **these** photographs is about $\pm 0.1^\circ$, and fireballs brighter **than** magnitude -6 can be photographed. We started **regular** operation of the first stations in **Czechoslovakia** in October 1963, and after Germany joined the **program** in 1968, the whole European Network for fireballs consisted of 45 stations covering **half** million square kilometers for meteorite searches. **Several** hundred of **fireballs** have been photographed. **Trajectories** and **orbits** of very bright, deep penetrating fireballs and of **objects** with spectral records were regularly computed and some of them published. More **details** can be found in papers by Ceplecha and Rajchl (1965), Ceplecha (1967), Zähringer (1969), Ceplecha et al. (1973).

The European Network consists of three operational parts: Czech, Slovak and German. The Czech part is operated by the **Astronomical** Institute of the **Czechoslovak** Academy of Sciences from the Ondřejov Observatory; the Slovak part is operated by the Astronomical Institute of the Slovak Academy of Sciences from Bratislava; the German part is operated by the Max-Planck-Institut für Kernphysik from Heidelberg. The German part covers the **largest** territory of **all** three. The service of the stations and **searches** for meteorites were performed in each of **these** parts independently. The computations and measurements of films were **done** at the **Ondřejov Observatory**.

Altogether data of 27 **fireballs** of this **program** are contained in Tab. 1. The overlap of both the programs (small-camera and **all-sky-camera**) is the **reason** that the total number of different fireball **orbits** computed is 42 at the moment.

Recently a very exciting possibility arose, when a new Fish-Eye Zeiss-Distagon objective (**Opton-Distagon**), $f = 30$ mm, with a field of view of 180" and 1/3.5 focal ratio, giving a very good image quality, **began** to be regularly produced and marketed. The outstanding quality of the objective **enables** to go down to $+12$ stellar magnitude, if the objective is used for a driven camera. **Such** photographs are relatively easy to obtain and, besides **meteors**, they **contain** a lot of other astronomical information (Boček et al., 1976; Ceplecha, 1975b). The **meteors** of zero magnitude are **still** well **above** the sensitivity **limit**. The positional precision is ± 1 minute of arc and **photometric** qualities as far as 70° from the **center** of the field **give** ± 0.1 stellar magnitude accuracy. The dimension of the **entire** celestial hemisphere is 76 mm on the negative.

Thus, we decided to replace gradually the **old** mirror all-sky **cameras** at the Czechoslovak stations by **cameras** equipped with this Fish-Eye objective. The camera has a rotating shutter close to the focal plane with 25 **breaks/second**, and photographic plates 9 x 12 cm with panchromatic emulsion are used. The small size of the camera makes **it** very handy for field operations at a large number of stations. We have already had two of **these cameras**, one driven and one fixed, in operation at the Ondřejov Observatory for more **than 200** nights. The last fireballs in Tab. 1 were photographed with **these** new **cameras** with excellent results (EN 020376 and EN 041274). We are now placing 4 **fixed cameras** more at **various** stations. We hope to finish the replacement of **cameras** at **all 12** stations in the western part of Czechoslovakia by the end of 1978. We want to run this new project for one **decade** at least.

The double-station small-camera program of the Ondřejov Observatory has been terminated at the end of 1976. The mirror all-sky cameras of the multistation fireball program will be replaced by the new Fish-Eye all-sky cameras. The two parallel programs will thus be merged into one multistation program of meteor photography, providing data on fireballs as well. The spectral program will continue together with this multistation program.

2. Orbital and Other Data on Fireballs

Orbital and other data on 42 fireballs, photographed within the period of operation of the programs described in the previous section, are given in Tab. 1. They represent a complete list in the sense that there are no more measured and computed fireballs available at the moment. All the given data are revised values and in some cases they differ from the values published before. Big differences in some cases were caused by gross mistakes contained in the previous computations (namely from the "precomputer" times). The preliminary values published in the Event Reports of the Short-Lived Phenomena Center were in some cases only rough values graphically reduced from the first two photographs we obtained. They contain some gross errors, too.

Slight differences of the revised values in Tab. 1 from the values previously published were caused by a different kilometer equivalent of the astronomical unit used. The old value was 149.5×10^6 km, while the new one used for all orbits in Tab. 1 is 14959787×10^6 km. This change is far from being negligible for well observed fireballs. Also a more precise subtraction of the zenith attraction than done in previous computations is the cause of slight differences. A good example of these small changes is the Příbram fireball, where only the kilometer equivalent of the astronomical unit and a more precise computation of the zenith attraction are responsible for the small change (Ceplecha, 1961).

The radiant and the angular elements of the orbits are related exclusively to 1950.0 in Tab. 1. The computation of zenith attraction and daily aberration was performed using the apparent places; the mean places for the beginning of the current year were used for the computation of the orbital elements and then they were transformed to the standard mean equinox of 1950.0.

Data on many fireballs in Tab. 1 were not published before. The errors given in Tab. 1 are the standard deviations. Tab. 1 contains the following data:

Fireball No. is the recognition number of the fireball. There are three systems of notation corresponding to

three different photographic programs: the double-station programs before and after 1955 and the multistation program (European Network ... EN).

Name contains either the name of the fireball (usually some geographical name close to the terminal point), or the number of the double-station program photographs, if they exist together with the EN data.

Year, Date and Time are given for each fireball in UT. M_p is the maximum absolute (100 km distance) magnitude of the fireball expressed in "panchromatic" magnitudes (magnitudes, which resulted by comparing AO stars with the fireball trail using the panchromatic emulsion). These magnitudes differ in some cases from the values published previously, because of different "color" corrections applied. In any case, no color corrections were applied here for M_p and the "panchromatic" magnitudes given in Tab. 1 are in the same system as used by McCrosky and Posen (1968) and by McCrosky et al. (1977) for the Prairie Network (PN) fireballs. Thus the direct comparison of EN and PN fireballs is possible. m_∞ is the initial photometric mass computed from

$$m_\infty = 2 \int_{t_E}^{\tau} \frac{I dt}{rv^2},$$

where τ was used according to McCrosky's interpretation of the experimental values of Ayers et al. (1970); [the numerical values of τ are contained in the paper by Ceplecha (1975a)]. The same τ and the same system of panchromatic magnitudes as used by McCrosky for the PN fireballs were applied here. The same scale of the mass system resulted and a direct comparison of masses between PN and EN fireballs is possible. In some cases, preliminary photometry of the point of maximum light was the only measured photometric value and the initial mass was then computed according to McCrosky (1968):

$$m_i = \frac{18.5 \times 10^{-14} T \exp(-0.921 M_{\max})}{rv^2 \sqrt{\Delta M}}$$

where m_i resulted in kg, if v was used in km/s and τ in combined units of c.g.s. and of zero stellar magnitude ($0_m : I = 1$). The velocity v and the luminous efficiency τ were taken for the maximum light. The other values are: ΔM the difference in stellar magnitudes between maximum light and the film limit. The total duration of the fireball is given as T seconds. Provisional values of M_p and m_∞ are in parenthesis. m_E is the terminal "dynamic" mass computed from

$$m_E = \left(\frac{1.20 Q_E v_E^2}{(dv/dt)_E \rho_m^{2/3}} \right),$$

where ρ_E is the air density, v_E the velocity and $(dv/dt)_E$ the deceleration at the terminal point, ρ_m is the density of the meteoroid ($\rho_m = 3.7 \text{ g cm}^{-3}$ was used for type I and 2.2 g cm^{-3} for type II fireballs). In case of type II fireballs, the terminal mass is rather a fictitious value and a corresponding terminal mass should be expected rather in a big number of small pieces than in one single body. All masses are given in kg units.

v_B is the velocity at the beginning height h_B of the luminous trajectory of the fireball.

v_E is the velocity at the terminal height h_E of the luminous trajectory of the fireball.

$(\cos z_R)_E$ is the cosine of the zenith distance of the radiant computed for the horizon of the terminal point of the fireball.

h_m is the height of the maximum light.

Number of St. is the number of different stations, at which the fireball was photographed.

α, δ_R are the right ascension and declination of the observed radiant.

v_∞ is the no-atmosphere (initial) velocity.

λ is the angular distance of the Earth's apex from the geocentric (true) radiant.

α, δ_G are the right ascension and declination of the geocentric radiant (observed radiant corrected for the zenith attraction and Earth's rotation).

v_G is the geocentric velocity.

v is the heliocentric velocity.

$a, e, q, Q, \omega, \Omega, i, \pi$ are the orbital elements using the normalized symbols (Q is the aphelion distance).

$1/a$ is given for long period orbits, too.

All angles are given in degrees in Tab. 1.

Table 1 farther contains the shower membership according to Lindblad (1971), Jacchia and Whipple (1961) and McCrosky and Posen (1961), and the "type" of the fireball according to Ceplecha and McCrosky (1976). The "Note" contains geographical coordinates of the predicted impact (Pr. Im.), data on spectral photographs (how many spectral plates and what dispersions. GS . . . grating spectrum, PS . . . prism spectrum) and number of fragments photographed.

The impact point was predicted by computing the dark flight trajectory after the terminal point, starting with the terminal values of velocity, deceleration and air density, and taking into account the wind field, but, of course, with the idealized assumption of spherical shape and no lift forces.

3. Results and Prospects

All fireballs in Tab. 1, except three, are brighter than -8 stellar magnitude. The list of fireballs as bright and brighter than the Full Moon (-12.7_m)

is complete in the sense that all fireballs of such brightness we photographed were computed. The number of these bright objects is quite high. If we take the Ondřejov Observatory as a single station, then 10 fireballs as bright or brighter than the Full Moon were photographed from the Ondřejov Observatory during the whole period. This means that one nighttime fireball comparable in absolute brightness with the Full Moon or brighter is observed once in 2 or 3 years on an average at one station with climatic conditions similar to the Ondřejov Observatory.

On the contrary, meteorites are much rarer. There were only 2 objects photographed at the Ondřejov Observatory within the whole period with a terminal mass in excess of 1 kg (one was recovered: the Piibram case). One meteorite fall photographed during nighttime with a mass of 1 kg or greater may thus be expected to be observed at a single station each 10 or 15 years on an average. The interval for the recovered meteorites must be even bigger. Thus an interval about five times longer is necessary to photograph the fall of a 1 kg or heavier meteorite than to photograph a fireball of Full Moon brightness or more.

The most important result from the photographic fireball networks is the recognition of different compositional and structural groups. Ceplecha and McCrosky (1976) found four groups of different composition and structure among fireballs. Roman numerals, in some cases with a letter suffix, were used to denote these groups. As this notation is used in Tab. 1, here is a brief explanation of the groups: Group I is of the greatest bulk density and the strongest structure and contains the Příbram (Ceplecha, 1961) and Lost City meteorites (McCrosky et al., 1971), the only two meteorite falls scientifically photographed. Thus, the average bulk density of the fireballs in group I was assumed at 3.7 g cm^{-3} using data of these two meteorites as safe calibration values. Group I is evidently connected with ordinary chondrites.*)

The meteoroids of group II have a somewhat lower density of 2.1 g cm^{-3} and they very likely belong to the carbonaceous chondrites. New spectral evidence for this was recently obtained for the Kamýk Fireball (EN 020376).

Fireballs of group III A have average bulk densities of 0.6 g cm^{-3} and direct evidence of cometary origin through showers. Group III A contains orbits of a short period and ecliptical concentration and group III Ai contains long-period randomly-inclined orbits.

*) Note added in proof: Recently a third meteorite fall was photographed. Innisfree meteorite data completely agree with the proposed classification.

Table 2.

Survey of meteoroid populations among photographic **meteors**.
Relationship of **meteor** groups found in **different** photographic data.

Observational material	Super-Schmidt canieras				Small-camera meteors					PN-fireballs					Properties of the meteoroid material		
	typical mass-range				typical mass-range					typical mass-range							
Group	%	Characteristic orbit			Group	%	Characteristic orbit			Group	%	Characteristic orbit			q g/cm ³	log a s ² /cm ²	assumed composition
		obs.	a	e			i	obs.	a			e	i	obs. a)			
"asteroidal" meteors	<1	2.4 c)	.64 c)	15° c)	"asteroidal" meteors	5	2.5 b)	.64 b)	10° b)	I	32	2.4	.68	6°	3.7	-11.5	ordinary chondrites
A	54	2.3	.61	1°	A	37	2.5	.64	4°	II	37	2.3	.61	5°	2.1	-11.3	carbonaceous chondrites
B	6	2.4	.92	5°	B	7	2.5	.90	6°	—	—	—	—	—	1.0	-11.1	dense cometary material
C ₁	9	2.2	.80	6°	C ₁	16	2.5	.80	5°	III A	9	2.4	.82	4°	.6	-10.9	regular cometary material
C ₂	31	≈	.99	random	C ₂	30	≈	.99	random	III A i f)	9	≈	.99	random	.6	-10.9	regular cometary material
D (above C)	<1	3.3 e)	.70 e)	25° e)	D (above C)	5	3.1 b)	.77 b)	10° b)	III B	13	3.0	.70	13°	.2	-10.7	soft cometary material of Draconid type

The data in the Table are based on photographic observations of ≈2600 sporadic **meteors**; the percentage number **does not contain** major **classical showers**; the values of the maxima of statistical distribution of a , e and i are given, if not stated otherwise.

- Q is the **bulk density** of meteoroid, σ is the **ablation coefficient**
- a) rough estimates from the **numbers** of computed **trajectories** (42, 37, 6, 6.9% **respectively**) assuming twice big reduction preference of group I over the group III.
- b) median from 12 cases.
- c) **only two meteors recognized** as asteroidal (No 7946 and 19 816); **their** average elements are given.
- d) **the** biggest bodies photographed within **fireball** networks so far have the mass of the **order** of 10⁹ g.
- e) Draconic shower **orbit**. (2 Super-Schmidt members of the stream).
- f) **all** high-inclined near-parabolic orbits.

The fireballs of group III B have densities of 0.2 g cm^{-3} and they contain fireballs of the Draconid meteor shower. This is a very distinct group and contains a relatively high number of fireballs.

There is evidence from spectral records of fireball 38421 that the group III material may have a relatively high content of carbon, too (Ceplecha, 1971).

The classification of fireballs was recently compared with the classification of fainter meteors (Ceplecha, 1976). The results of this comparison are given in Tab. 2 of this paper. The most important among all masses of the meteoroids outside the Earth's atmosphere are the bodies of group II corresponding to the A group of fainter meteors and perhaps to material similar to carbonaceous chondrites.

The existence of groups of bodies with widely differing structure and composition is the key to the fact that fireballs and meteorite falls are not simply related. If we could somehow organize all the incoming meteoroids to be of the same mass, velocity and angle of incidence, but of different composition and structure as given in Tab. 2, the meteorite fall of an ordinary chondrite would be preceded by the faintest meteor phenomenon of all the 5 different compositional groups. If we observed the brightest possible fireball, we could be sure it belonged to the soft Draconid type of material. This material is ablated high in the atmosphere. On the other hand, the faint fireball, belonging to the meteorite fall of an ordinary chondrite, would have a very long trajectory penetrating very deep into the atmosphere, while the Draconid type would have only a short trajectory, ending very high up. Thus an observation of a very bright fireball does not necessarily mean a meteorite fall. The dependence of the brightness on the mass under real conditions works partly against the paradox and makes the picture quite complicated. Thus decisions, if to search or not to search for meteorites after a bright fireball passage, should rather be made on the basis of criteria, which take into account the terminal height, the mass (or brightness) and the velocity with the angle of incidence (Ceplecha and McCrosky, 1976).

The fireball data from all existing Networks are still limited to less than 400 fireballs. Much more is needed to study different fireball populations. In my view, the fireball networks should run for several decades. I feel they are a typical example of astronomical programs with a time scale exceeding one generation. We should not view the fireball networks as being entirely designed for obtaining photographic data of meteorite falls. We should rather consider them to be a powerful means of obtaining trajectory and

orbital data on fireballs. And, eventually, a meteorite fall may be trapped as well.

Acknowledgment

The orbits and other data on fireballs given in this paper are the result of a long lasting effort in meteor photography. The Ondřejov program was initiated by Prof. V. Guth and Prof. F. Link 30 years ago. The enthusiasm and support of Prof. V. Guth, which continue, were essential for the successful work of a program of such duration.

The German fireball program of the Max-Planck Institut für Kernphysik in Heidelberg was initiated by Prof. J. Zähringer 15 years ago. His interest and intense effort were decisive for the good start of the program. After his sudden death, the program has been successfully directed by Prof. T. Kirsten and Dr. J. Kiko. I am very much indebted to all of them for giving me the possibility to use their observational material. The extensive German part of the Network requires an enthusiastic operator acquainted with the "local language" of the layman. Mr. G. Hauth of Max-Planck Institut in Heidelberg has been successful in this respect and merit is due to him for smooth operation of the all-sky-camera stations in Germany.

Before 1970 the photographic plates and films were measured by the author. From 1970 on, Mr. J. Boček has been doing this important work with excellent results. The materials were prepared for the computers by Miss M. Ježková, who also carried out a lot of numerical computations in the "precomputer times". Her precise work has been very much appreciated.

It is not possible to mention all the observers at all stations in such a short report, but the most important in obtaining the photographic records, including the spectra, was the long-lasting and enthusiastic work of Mr. M. Novák and Mr. M. Brož.

REFERENCES

- Ayers, W. G.; McCrosky, R. E.; Shao, C. - Y.: 1970, *Srnhthson. Astrophys. Obs. Spec. Rep. No. 317*.
 Boček, J.; Ceplecha, Z.; Ježková, M.; Nouak, M.: 1976, *Bull. Astron. Inst. Czech 27*, 190.
 Ceplecha, Z.: 1957, *Bull. Astron. Inst. Czech. 8*, 51.
 —: 1961, *Bull. Astron. Inst. Czech. 12*, 21.
 —: 1967, *Bull. Astron. Inst. Czech. 18*, 233.
 —: 1971, *Bull. Astron. Inst. Czech. 22*, 219.
 —: 1975a, *Bull. Astron. Inst. Czech. 26*, 242.
 —: 1975b, *Sky Telesc. 49*, 353.
 —: 1976, *Meteoroid Populations and Orbits (presented at IAU Colloquium No. 39, Lyon), to be publ. by the Univ. of Toledo in 1977.*

- Ceplecha, Z.: Jeřková, M.; Boček, J.; Kirsten, T.; Kiko, J.:* 1973, Bull. Astron. Inst. Czech. 24, 13.
- Ceplecha, Z.; McCrosky, R. E.:* 1976, J. Geophys. Res. 81, 6257.
- Ceplecha, Z.; Rajchl, J.:* 1965, Bull. Astron. Inst. Czech. 16, 1S.
- Ceplecha, Z.; Rajchl, J.; Sehnal, L.:* 1959, Bull. Astron. Inst. Czech. 10, 204.
- Jocchio, L.; Whipple, F. L.:* 1961, Smithson Contr. Astrophys. 4, No. 4.
- Lindblad, B - A.:* 1971, Smithson. Contr. Astrophys. No. 12 (Space Research XI, 287, Akademie-Verlag, Berlin).
- McCrosky, R. E.:* 1968, Smithson. Astrophys. Spec. Rep. No. 280.
- McCrosky, R. E.; Posen, A.:* 1961, Smithson. Contr. Astrophys. 4, No. 2.
- :* 1968, Smithson, Astrophys. Obs. Spec. Rep. No. 273.
- McCrosky, R. E.; Posen, A.; Schwartz, G.; Shao, C. - Y.:* 1971, J. Geophys. Res. 76, 4090.
- McCrosky, R. E.; Posen, A.; Shao, C. - Y.:* 1978, Meteoritika 37, in press.
- Rajchl, J.:* 1961, Bull. Astron. Inst. Czech. 12, 167.
- Zähringer, J.:* 1969, Sterne u. Weltraum 8, 52.

Z. Ceplecha
Astronomical Observatory
251 65 Ondřejov
Czechoslovakia

European Network Fireballs Photographed
in 1977.

- Z. Ceplecha, J. Boček, M. Nováková-Ježková,
Astronomical Institute of the Czechoslovak
Academy of Sciences,
251 65 Ondřejov, Czechoslovakia
- V. Porubčan, Astronomical Institute of the Slovak
Academy of Sciences, Dúbravská cesta,
899 30 Bratislava, Czechoslovakia
- T. Kirsten and J. Xiko, Max-Planck Institut für
Kernphysik, Postfach 103980, 69 Heidelberg 1,
Bundesrepublik Deutschland

Received May 5, 1982

počet stran: 20

počet tabulek: 4

počet obrázků: 0

Фотографические данные по болидам

Европейской сети в 1977 г.

В работе приведены геометрические, динамические, орбитальные фотометрические данные по 29 болидам сфотографированным Европейской сетью в 1977 г. Для двух случаев предсказано выпадение метеоритов и приведена вычисленная точка и область падения. В работе приведены заметки по нашим методам измерений и вычислений фотографией болидов именно по проблемам стандартных ошибок скоростей.

Geometric, **dynamic**, photometric, and orbital data on all 29 **fireballs** photographed **within** the **European Network** in **the** year 1977 are given. In two **cases**, **meteorite impacts** are **pre-**dicted and their impact points and **areas** given. Few remarks on our **measuring** and reduction **procedures**, especially on the problem of **standard deviations** of **computed velocities**, are **contained**.

1. Observational material and remarks on measurements and computations

This paper contains data on atmospheric trajectories and orbits of all 29 fireballs photographed within the European Network by at least two stations in the year 1977. A brief description of the stations can be found in several preceding papers (Ceplecha et al., 1973, 1976, Ceplecha, 1977a) as well as outlines of some of our measuring technique and computational procedures (Ceplecha et al., 1979). A comparison of European Network with the other photographic fireball networks can be found in a survey paper by Halliday (1973). The most significant change since this Halliday's report lies in implementation of new and more precise fish-eye cameras at five Czech stations.

All photographic plates and films were measured by Zeiss Ascorecord, the rectangular coordinates recorded on magnetic tape and processed by means of a Fortran program, FIRBAL, using the EC1040 computer of the Ondřejov Observatory. The results are given in tables of this paper.

In the year 1977 five Czech stations were equipped with fixed fish-eye cameras ($f/3.5$, $f=30$ mm) giving a positional accuracy of about one minute of arc. The remaining 40 stations were equipped with fixed mirror cameras ($f/16$, $f=5$ mm) giving a positional precision of about 0.1° . One additional moving fish-eye camera at the Ondřejov Observatory were used to obtain time of the fireball passage for the central part of the Network. The whole system covered about one million square kilometers and the equivalent exposure time in the year 1977 resulted in 1280 hours in 166 nights.

Variety of **cameras**, geometrical situations, weather conditions and **absolute** timing went into **wide** variety of precision in **our results**. **Even inside** data holding for one fireball some of them are precise enough and some are just **rough** values. Assigning an indicator of data quality to each **fireball** would not solve the problem of **significance** of **individual values**. Thus each **number** is given with its standard deviation in all tables. The **number** of digits printed in tables corresponds usually to standard deviation in the last digit from 3 to 9 and to standard deviation in the two last digits from 1.0 to 2.9.

The standard deviations of the geometric data were **computed** by two different ways: a) In the case of only a **double-station** record available, the standard deviations of the **parameters** defining the intersection of the two planes (each given by the location of the station and the fireball **trajectory**) were **derived** from standard deviations of one computed position as it **resulted** from positional stars. b) In the case of three and more stations recording the **same** fireball, all statistically weighted intersections of these planes were used for the computation of the **standard** deviation of the average intersection.

We strictly separated the **measurements** of time marks (breaks of the fireball image) from the **measurements** of the apparent fireball trail (great circle). Two types of **rotating** shutters were used, both with ratio of occulted to exposed part as 1:1. The **mirror cameras** have the rotating shutter placed before the objective with 12.5 breaks per second. The rotating shutter is **inside** the fish-eye camera, very close

to the focal plane. The motion of the **shutter** and of the fire-**ball** image superpose **in this case** and a due correction in relative timing of individual breaks was considered. The **number of breaks** per second was **close to 25** in **this case**.

The breaks of **the** image were measured by three different ways depending on the quality and appearance of the **image**. We preferred **measurements** of break heads whenever the quality of the **image** allowed for it. As a second choice, we measured **centers** of dashes in case they were short enough: **sometimes dashes** were **rather** points. As a **third** choice, we measured the breaks, **which** proved to be the **least accurate method** for velocity **determination**.

The great circle of a **fireball** trajectory was measured independently of measuring the time marks (heads, dashes, breaks). The wire settings were pointed to **approximate centers** of 10 or more **suitable** dashes **regularly** spaced **along** the whole fireball trail. **Overexposed** parts were omitted in these **measurements**. Thus the plane containing the station and the fireball trajectory was defined independently of the measurements of the time marks and moreover independently of those parts of the trail, which exhibited bad quality of the image. The geometric precision is significantly increased this way. The average intersection of all planes gave then the fireball trajectory. The measurements of time marks (heads, dashes, breaks) for each station were projected perpendicularly onto **this** average trajectory and the actual length, **l**, along the average trajectory computed. Standard deviation of the distance from the station is readily available and can be combined with standard deviation resulting from applying equation (1) to these average **l**.

The solution for velocity was done by applying an interpolation formula to the distances, l , measured along the trajectory:

$$l = a_1 + a_2 t + a_3 \exp(a_4 t) \quad (1),$$

where a_1, a_2, a_3, a_4 with their standard deviations resulted from the least-squares solution. In some cases of long trajectories, more solutions in separate parts of the trajectory were performed or a linear dependence of velocity on time was assumed close to the terminal point. A new method for computing velocities was published recently (Pecina and Cepelcha, 1983), but not used in this paper (the computations of the fireballs from the year 1977 were terminated before finishing the cited paper).

The standard deviations of parameters in formula (1) were used in computing the standard deviations of velocities and decelerations of individual points. But these standard deviations represent only the spread along the fireball trajectory of the measured distances l . Up to now, all published solutions for l (and velocities and decelerations as well) contained only this component of the standard deviation, assuming implicitly that the distance, r , from the camera to the corresponding point is exact. Since this is not the case, a component, ξ_r , of the standard deviation of r , which is projected along the trajectory, should be added to the standard deviation, ξ_l , of the distance along the trajectory resulting from the least-squares solution of l from (1). And this component, ξ_r , is

not small as it may seem at the first glint: it depends on the geometry of the trajectory against the stations, where the photographs were taken from and amounts usually to values of the same order as ε_1 . With unsuitable geometry, ε_2 may become many times greater than ε_1 .

As an example of applying these considerations to observed velocities, the fireball EN 140977A (the Brno Fireball) can be used. The standard deviations previously published (Cepelcha et al., 1979) and containing only the ε_1 term can be compared with the standard deviations for the same fireball given in this paper with the ε_r term incorporated. The initial velocity $v_\infty = 30.22 \pm 0.04$ km/s converts into 30.22 ± 0.08 km/s with the ε_r term included.

In case of shorter fireballs and less accurate distances, l , available, we used ^asimpler relation than (1), i.e.:

$$v^2 = v_\infty^2 + k \rho \quad (2)$$

where ρ is the air density and k a constant and where the immediate values of v were taken from differences in l of the successive breaks. In these cases, the decelerations were usually quite poor and even those we give in Table 3 (standard deviation less than the value), should be taken with enough precaution. Standard deviations of decelerations resulting from simple formula (2) are rather formalistic values holding only close to the average point of the trajectory.

2. The fireball data,

Preliminary data were given for 4 significant fireballs in 1977 in the SEAN Bulletin (1937). For two of them, the Brno and the Freissing Fireballs, the preliminary data are close to the final values given in tables of this paper. For the other two cases, the Alps and the Wasserburg Fireballs, the final data differ widely from the preliminary values. The graphical reduction we used for obtaining the preliminary data in 1977 is responsible for this in case of the Alps Fireball, which was well outside the network: the distances from stations were from 290 km to 470 km.

In case of the Wasserburg Fireball, the preliminary values deduced from records of the first two stations available at that time depended strongly on the position of the terminal flare due to the fact that both the planes containing one of the stations and the trajectory were almost identical. This unusual method of computing the parallax depends on how sharply the flare is defined and more over the preliminary computations contained a rough mistake.

The fireballs are arranged in tables of this paper according to their succession in dates, denoted ENddmmyy, with dd being the date, mm the month and yy 'the last two digits of the year. Fireballs of the same day are distinguished by an addition of a capital letter after the notation, starting with A, but the alphabetic order does not necessarily follow the time sequence of them: the letters were assigned due to succession, in which they were measured and computed.

Table 1 contains basic data for each fireball starting with the notation (Fireball No.) and name in case we invented any (we usually use geographical names close to the terminal or impact point). The date and time follow.

The time of the fireball passage originates from two different sources;

- a) The moving *fish-eye* camera of the Ondřejov Observatory contained the image of the fireball. The combination of moving camera image either directly with the fixed camera image of the Ondřejov Observatory or with the apparent trail of other fixed cameras recomputed to the Ondřejov-Observatory position through the average trajectory, gave the time with typical standard deviations of several seconds up to several tens of seconds.
- b) The moving fish-eye camera image was missing, but some visual observations by casual witnesses existed. Typical standard deviations are several minutes up to several tens of minutes. In few cases both these possibilities were missing and the middle of the interval, during which all stations with the fireball image took the exposure, was used. Typical standard deviation in these cases usually exceed one hour except some cases, when different stations have different intervals of overcast sky, which is well recorded on the star trails of the fixed-camera records.

The individual entries of Table 1 have the following meaning (most of the values are accompanied with their standard deviations):

M_{\max} is the maximum absolute (100 km distance) magnitude of the fireball expressed in "panchromatic" magnitudes (magnitudes,

which resulted by comparing A0 stars with the fireball trail on our panchromatic emulsions). We corrected stars of other spectral types by

$$V_{\text{panchromatic}} = V + 0.62(B-V) - 0.52(V-R) \quad (3),$$

where V , B , R are the stellar magnitudes in the international system of 5 - color photometry UBVRI and we mostly used data of the Arizona - Tonantzintla Catalogue (1965).

$\int I dt$ is all the energy radiated in the panchromatic pass band (approximately from 3600 to 6600 Å) and is given in J (Joules). Common logarithm of it is given in Table 1. The conversion from the usual units of seconds and $I = 1$ for zero magnitude of A0 star to Joules was done multiplying by 840. Additional multiplying by 10^7 will give the usual c. g. s. units.

m_{∞} is the initial photometric mass including the terminal mass, m_E , dynamically determined. m_{∞} was computed from (4) with $t = t_R$, t_B being the time of the fireball beginning (for more explanatory details see explanation of m_{ph} in Table 3). The photometric masses are in the same system as it was used by McCrosky for the PN fireballs.

m_E is the terminal mass derived from dynamic data and air density at the terminal point from equation (5) and with meteoroid densities ρ_m corresponding to the fireball type. The values of ρ_m used are given in explanations to Table 3 below equation (5). In case of type II fireballs, the terminal mass is rather a fictitious value and a corresponding terminal mass should be expected rather in a big number of small pieces than in one single body,

v_B is the velocity at the beginning height h_B of the luminous trajectory of the fireball.

v_E is the velocity at the terminal height h_E of the luminous trajectory of the fireball

v_{max} is the velocity at the point of maximum light of the fireball

z_R is the zenith distance of the radiant computed for the horizon of the terminal point of the fireball.

Number of St. is the number of different stations, at which the fireball was photographed. Majority of the fireballs were photographed from more than 2 stations, a situation which is widely different from the Prairie Network data.

α_R, δ_R are the right ascension and declination of the observed radiant.

v_0 is the preatmoapheric (initial) velocity

α_G, δ_G are the right ascension and declination of the geocentric radiant (observed radiant corrected for the zenith attraction and Earth's rotation).

v_G is the geocentric velocity

λ_G is the angular distance of the Earth's apex from the geocentric (true) radiant

L_H, B_H are the ecliptic longitude and latitude of the heliocentric radiant.

v_H is the heliocentric velocity.

λ_H is the angular distance of the Earth's apex from the heliocentric radiant.

$a, e, q, Q, \omega, \Omega, i$ are the orbital elements using the normalized symbols (Q is the aphelion distance). The reciprocal semimajor axis $1/a$ is given for all fireballs with its standard

deviation, but the **semimajor axis**, a , itself is not given for very long orbits, where a is not a suitable parameter for describing it. Sometimes both a and $1/a$ have large standard deviations contradicting in fact the definition of the standard deviation to be a relatively small value. There is not much information left in such cases. The **angular orbital elements** as well as **all the right ascensions, declinations, ecliptical longitude and latitude** are given in 1950.0 coordinate system. The most precise element known, the **ascending node**, is usually given without its standard deviation, which has the meaning all given digits are precise. If not, standard deviation is given. Table 1 farther contains the **shower membership based on several photographic catalogues** (Lindblad, 1971; Jacchia and Whipple, 1961; McCrosky and Posen, 1961; Cook, 1973; Southworth and Hawkins, 1963). Except two Perseids, one Southern Piscid, two annual Andromedids and one ν Cetid, all shower identifications are rather spurious, quite typical situation for fireballs in contrast to small-camera and Super-Schmidt meteors.

Type is the fireball type according to classification proposed by Ceplecha and McCrosky (1976) and by Ceplecha (1977b).

Note contains miscellaneous notes on extreme geometry, on light curves and also on spectral records, in case they exist. (Prism spectroscopy ≈ 10 mm for the entire "panchromatic" range.)

Table 2 contains data on the recorded beginning and terminal point of the luminous trajectory and on the point of maximum light of the fireball. For each point, h is the height above the zero level of geoid, λ is the geographic longitude and φ the geographic latitude of the vertical projection of the point

onto the surface of geoid. The standard deviations given for the beginning and terminal point reflect the geometrical precision in computing height, longitude and latitude from the **average intersection** of all planes defined each by the corresponding station and the **fireball trajectory**. Thus the beginning and terminal point **define** the computed average intersection **and its standard deviations**. The actual definition of the beginning or terminal point **along** the trajectory is not important in **this** respect and **thus** the highest or lowest **observed** point from **all** stations was **taken** as an **exact** value. The stellar magnitudes for the beginning and terminal point **can** be **found** in table 3 among the data given for the first and last point of each **fireball**.

Table 3 **contains** geometric, **dynamic** and photometric data at selected points on trajectories of **individual fireballs**. Our **system** of **timing** by rotating-shutter breaks is relative and holding for one station. **We** have usually **chosen** time **equal** zero at the first measurable break (head, **dash**). Thus the beginning points in Table 3 belong **usually** to **negative times**. The **individual entries** of table 3 follow:

t is the relative time in seconds,

h is the height **above** zero level of geoid

v and ϵ_v are the velocity **and** its standard deviation.

dv/dt and $\epsilon_{(dv/dt)}$ are the deceleration and its standard deviation

M and ϵ_M are the **absolute** (100 km distance) panchromatic magnitude and its standard deviation (for more **details** see **explanations** to M_{\max} of table 1)

m_{ph} is the photometric mass computed by integrating M and including the terminal mass, m_E , dynamically determined. m_{ph} was computed from

$$m_{ph} = m_E + 2 \int_{t_E}^t \frac{I dt}{\tau v^2} \quad (4),$$

where $I = 10^{-0.4 M}$ and τ , the luminous efficiency is given according to McCrosky's interpretation of the experimental values of Ayers et al (1970) [the numerical values of τ are contained in a paper by Ceplecha (1975)]. This is the same system of photometric masses as it was used by McCrosky for the PN fireballs.

Among other points, table 3 contains the beginning of the luminous trajectory as the first and the termination of light as the last point. The point of maximum light is always among the selected points.

Fireball EN220177 was too far from both stations and no time marks (breaks) were available. The geometric position of its trajectory is sufficiently precise, but the velocity and orbital data are unknown. The standard deviation given for the maximum light includes the effect of unknown velocity. Absolute magnitude at the beginning of this fireball was -5 ± 2 and at the end -6 ± 2 .

Dynamic masses are not given in Table 3, but they are easy to compute from the given ρ , dv/dt , and h (converted to ρ) according to

$$m_d = (1.20 v^2 \rho)^3 / (\rho_m^2 (dv/dt)^3) \quad (5),$$

where the meteoroid densities ρ_m should be taken according to the fireball type given in table 1: Type I $\rho_m = 3.7 \text{ Mg/m}^3$, Type II $\rho_m = 2.2 \text{ Mg/m}^3$, Type IIIA $\rho_m = 0.6 \text{ Mg/m}^3$ and Type III B $\rho_m = 0.2 \text{ Mg/m}^3$. The standard deviation (not including the unknown standard deviation of shape, of meteoroid density and of drag coefficient for individual fireballs) are given by

$$\epsilon_{m_d} = \left(\frac{36 \epsilon_v^2}{v^2} + \frac{g \epsilon_p^2}{\rho^2} + \frac{g \epsilon_{(dv/dt)}^2}{(dv/dt)^2} \right)^{1/2} m_d \quad (6)$$

Values in Table 2 and 3 enclosed in parentheses originated from extrapolation beyond the interval of the least-squares solution.

Table 4 contains geographical positions of impact points and impact areas of the only two fireballs with terminal masses greater than 100 grams ne photographed in the year 1977. The impact area of the Freising Fireball was too big and the terminal mass too low for any systematic search of meteorites. We only announced the possibility of nateorite fall using public media.

The preliminary graphical data on the Alps Fireball, which was photographed at quite a large distances from our stations (from 290 to 410 km), did not reveal the importance of this fireball. The preliminary distances were underestimated by 40 to 50 km due to small angle of 22° of the intersecting planes. The terminal mass was estimated as less than 100 grams due to overestimated terminal height, Thus no search activities were started. Precise neasurements of the records used in final computations went into much better data than the preliminary

graphical reduction and estimates did. Surprisingly the terminal height proved to be much lower at $h_E = 25.7 \pm 1.0$ km observed with -9.7 stellar magnitude and with mass of 60 kg. Values extrapolated to -2 stellar magnitude on several theoretical assumptions gave the terminal height of 19 km and terminal mass of 30 kg. This possibility of a meteorite fall was recognized as late as in the year 1981 in course of the due reduction of all 1977 fireballs. The announcement was sent to SEAN Bulletin (1981) and to Centre de Recherches sur la Synthèse et Chimie des Minéraux in Orléans, France. The impact area of the Alps Fireball is in a vicinity of Marignier in France about 30 km to ESE from Geneva. Eventual smaller pieces could be found in surrounding of St. Jeoire in France.

Aknowledgement.

We are very much indebted to all observers at the European Network Stations for their devoted service leading to data on fireballs published in this paper. Our special thanks are due to Mr. G. Hauth, who performed all the technical work for the German part of the Network and to Mr. M. Novák, who helped in keeping the Czech stations in regular run.

References

- Arizona - Tonantzintla Catalogue: 1965, Sky and Teles. 30,24
- Ayers, W.G., McCrosky, R.E., Shao, C. - Y: 1970, Smithson.
Astrophys. Obs. Spec. Rep. No. 317
- Cepplecha, Z.: 1975, Bull. Astron. Inst. Czechosl. 26,262
- Cepplecha, Z.: 1977a, Bull.Astron. Inst. Czechosl. 28,328
- Cepplecha, Z.: 1977b, Meteoroid Populations and Orbits, in
"Comets-Asteroids-Meteorites", ed. A.H.Delsemme, The
University of Toledo, p. 143
- Cepplecha, Z., Boček, J., Ježková, M.: 1979, Bull. Astron. Inst.
Czechosl. 30, 220
- Cepplecha, Z., Ježková, M, Boček,J., Kirsten, T.: 1976, Bull.
Astron. Inst. Czechosl. 27, 18
- Cepplecha, Z,, Ježková, M, Boček, J., Kirsten, T., Kiko, J.: 1973,
Bull. Astron, Inst. Czechosl. 24, 13
- Cepplecha, Z., McCrosky, R.E.: 1976, J. Geophys. Res. 81, 6257
- Cook, A.F.: 1973, A Working List of Meteor Streams, in Evolu-
tionary and Physical Properties of Meteoroids (ed.C.L.
Hemenway, P.M.Millman, A.F.Cook), NASA SP-319, Washington,
p. 183
- Halliday, I.: 1973, Photographic Fireball Networks, in Evolu-
tionary and Physical Properties of Meteoroids (ed. C.L.
Hemenway, P.M. Millman, A.F. Cook) NASA SP-319, Washington,
p.1
- Jacchia, L., Whipple, F.L.: 1961, Smithson. Contr. Astrophys.4,No.4
- Lindblad, BA: 1971, Smithson.Contr.Astrophys. No.12 (Space
Research KI,287, Akademie-Verlag, Berlin)
- McCrosky, R.E., Posen,A.: 1961,Smithson.Contr.Astrophys.4, No.2
- Pecina, P., Cepplecha, Z.: 1983, Bull.Astron.Inst.Czechosl. 34,
No. 1 (in print)

References (*continued*)

SEAN Bull., 1977, Meteoritic Events

SEAN Bull. 6: 1981, No. 10, p. 12

Southworth, R.B., Hawkins, G.S. = 1963, *Smithson. Contr.*
Astrophys. 7, 261

Time Ball No	EN08172B	EN051277	EN071277	EN111277	EN111277	EN131277
Acquire	1977 Nov 8	1977 Dec 5	1977 Dec 7	1977 Dec 11	1977 Dec 11	1977 Dec 13
Time and Date	49:45.57 ± 19	19:27.48 ± 15	48:41.50 ± 18	19:41.50 ± 50	4:25.5 ± 18	4:25.5 ± 18
Time UT	-7.41 ± 1.0	-7.61 ± 2	-14.1 ± 2.1	-10.3 ± 0.6	-10.3 ± 0.6	-10.6 ± 1.6
Month	5:04	5:79	8:23	6:81	5:82	5:82
Day of Month	.038	.25	236	21	.038	.038
Year	NONE	NONE	NONE	.03	NONE	NONE
RA	33.4 ± 1.3	31.57 ± 1.04	30.4 ± 1.6	14.33 ± 1.07	65.3 ± 1.5	65.3 ± 1.5
Dec	25 ± 1.8	15 ± 1.3	25 ± 1.1	814 ± 15	57 ± 5	57 ± 5
RA error	32.2 ± 1.7	31.53 ± 1.03	29.7 ± 1.4	13.63 ± 1.03	58 ± 4	58 ± 4
Dec error	39.4 ± 1.7	41.19 ± 1.13	69.55 ± 1.04	19.01 ± 1.05	15.4 ± 1.1	15.4 ± 1.1
Number of St	3	2	3	3	3	3
RA	40.15 ± 1.1	30.39 ± 1.6	38.3 ± 1.09	39 ± 1.3	122 ± 1.5	122 ± 1.5
Dec	42.4 ± 1.1	31.40 ± 1.1	10.17 ± 1.04	31.94 ± 1.05	35.4 ± 1.3	35.4 ± 1.3
RA error	34.1 ± 1.8	31.57 ± 1.04	30.4 ± 1.6	14.28 ± 1.07	65.3 ± 1.5	65.3 ± 1.5
Dec error	41.5 ± 1.8	31.55 ± 1.03	30.4 ± 1.6	38 ± 1.5	172 ± 1.5	172 ± 1.5
RA	42.1 ± 1.1	29.31 ± 1.04	8.52 ± 1.0	27.72 ± 1.2	35.3 ± 1.3	35.3 ± 1.3
Dec	32.1 ± 1.9	31.00 ± 1.1	28.10 ± 1.6	9.10 ± 1.5	64.4 ± 1.1	64.4 ± 1.1
RA error	84.9 ± 1.7	31.82 ± 1.08	85.8 ± 1.1	12.5 ± 1.1	31.8 ± 1.3	31.8 ± 1.3
Dec error	3.4 ± 1.8	5.54 ± 1.0	29.1 ± 1.7	2.0 ± 2.3	142 ± 1.8	142 ± 1.8
RA	48.7 ± 1.0	38.68 ± 1.06	-10.22 ± 1.06	3.0 ± 1.9	48 ± 1.4	48 ± 1.4
Dec	42.0 ± 1.4	13.53 ± 1.7	39.1 ± 1.4	36.3 ± 1.3	41.8 ± 1.5	41.8 ± 1.5
RA error	40.5 ± 1.8	2.91 ± 1.05	13.53 ± 1.7	168.2 ± 2.0	54.2 ± 2.1	54.2 ± 2.1
Dec error	9.8 ± 1.7	38.70 ± 1.00	3.9 ± 1.6	1.8 ± 1.4	194 ± 1.3	194 ± 1.3
RA	50.3 ± 1.12	38.74 ± 1.00	14.87 ± 1.00	4.9 ± 1.08	188 ± 1.07	188 ± 1.07
Dec	269.6 ± 1.6	5.44 ± 1.09	7.3 ± 1.12	92 ± 1.03	218 ± 1.4	218 ± 1.4
RA error	225.865	28.9 ± 1.3	94.8 ± 1.2	2.7 ± 1.7	260.67 ± 1.013	260.67 ± 1.013
Dec error	26.6 ± 1.9	253.449	7.166	216 ± 1.2	128 ± 1.3	128 ± 1.3
RA	.03 ± 1.13	8.35 ± 1.15	14.1 ± 1.2	260.23 ± 1.04	.06 ± 1.15	.06 ± 1.15
Dec		34.3 ± 1.006	26 ± 1.04	3.1 ± 1.9		
RA error		N None ?	57.00 ± 2	55 ± 1.1		
Type	III B	II	II	II	II	II A
Notes		900 mg mechanism 60 film ipitrim mechanism				Terminated plate

	1	2	3	4	5	6	7	8	9	10
-0.197	68.82	12.7	.5	-0.20	.05	-0.2	2.6	55		
.044	65.39	18.5	.5	-.5	.1	-8.7	0.9	55		
.205	63.43	18.6	.5	-.6	.2	-10.3	1.6	13		
.359	60.73	18.4	.5	-.8	.2	-10.2	1.6	51		
.533	78.19	18.3	.5	-.7	.3	-9.2	1.1	49		
.680	55.39	18.1	.4	-1.4	.3	-12.6	2.2	43		
.861	53.21	17.8	.4	-2.1	.5	-11.6	1.9	30		
1.025	50.73	12.4	.4	-2.8	.6	-9.6	1.2	22		
1.189	48.55	16.8	.4	-3.7	.8	-7.5	1.5	22		
1.352	46.18	16.1	.5	-5.1	1.1	-11.3	1.8	18		
1.517	43.94	14.9	.7	-.7	.2	-9.9	1.4	5		
1.762	41.91	13.4	1.0	-.9	.2	-9.5	1.2	3		
1.824	41.17	12.6	1.3	-1.0	.3	-9.3	1.1	0.9		
1.926	40.33	11.6	1.6	-1.2	.3	-7.3	0.5	0.12		
2.245	32.99	7	4	-2.0	.5	0.2	2.6	0		

	1	2	3	4	5	6	7	8	9	10
-0.012	83.12	33.2	.5						-2.3	1.3
0.000	82.09	33.2	.6						-5.2	.3
0.148	87.39	33.1	.5						-5.6	.3
0.260	86.19	33.0	.5						-5.7	.3
0.320	84.78	32.9	.4						-5.9	.3
0.502	83.59	32.8	.4						-5.9	.3
0.541	83.18	32.8	.4					-1.0	.8	-6.2
0.633	82.19	32.7	.4						-6.1	.3
0.746	80.99	32.5	.4						-6.1	.3
0.860	79.79	32.3	.4						-5.9	.3
0.993	78.39	32.1	.5						-5.3	.3
1.108	77.19	31.8	.7						-5.9	.3
1.254	75.6	31.4	1.0						-2.3	1.3

EN 010672

EN 200477A										
0.172	83.42	42.39	.24						-2.3	.6
0.000	84.71	42.38	.23						-4.54	.21
0.150	81.97	42.36	.22	-.17	.16	-4.64	.20	.022		
0.200	79.24	42.34	.20	-.30	.24	-4.64	.20	.021		
0.300	76.51	42.30	.18	-.5	.4	-4.48	.22	.020		
0.400	73.78	42.23	.14	-.9	.5	-4.45	.22	.019		
0.500	71.07	42.10	.11	-1.6	.7	-5.09	.18	.018		
0.600	68.36	41.88	.11	-2.9	.9	-5.57	.21	.016		
0.700	65.68	41.50	.17	-5.0	1.0	-5.29	.19	.014		
0.800	64.08	41.14	.22	-7.0	1.0	-5.93	.26	.013		
0.900	63.02	40.83	.25	-8.8	1.0	-5.31	.19	.012		
1.000	60.44	39.6	.3	-15.4	1.4	-5.35	.20	.009		
1.100	57.95	37.6	.3	-27	5	-5.49	.22	.006		
1.200	55.64	34.0	1.0	-47	14	-5.63	.24	.002		
1.300	53.54	27	3	-86	36	-7.9	.6	0		

-0.241	77.87	26.38	.11						-0.40	.013	-2.8	1.0	5240
0.000	75.63	26.92	.11						-.05	0.2	-3.6	.9	5240
0.400	71.17	26.94	.10						-.09	.02	-8.7	.5	5240
0.800	68.21	26.90	.09						-.13	.03	-12.3	.6	5240
1.200	63.78	26.82	.07						-.22	.04	-13.3	.6	5210
1.600	60.85	26.74	.06						-.31	.05	-14.4	.7	5170
2.000	57.70	26.58	.04						-.48		-14.7	.7	5070
2.400	53.59	26.34	-.04						-.76	.08	-16.0	.8	4800
2.800	50.05	25.96	0						-1.18	.08	-14.7	.7	4600
3.200	46.58	25.36	.07						-1.85	.07	-15.3	.8	4400
3.600	43.24	24.43	.08						-2.89	.09	-15.8	.8	3900
3.920	40.68	23.32	.07						-.47	.2	-16.9	.9	3400
4.400	37.29	20.73	.17						-6.4	.2	-15.9	.8	2200
4.800	35.23	18.16	.20						-6.4	.2	-15.3	.8	1300
5.200	33.38	15.58	.23						-6.4	.2	-14.7	.8	690
5.600	31.61	13.0	.3						-6.4	.2	-13.4	.7	350
6.000	29.92	10.4	.4						-6.4	.2	-9.6	.5	29
6.816	26.09	5.2	1.0						-6.4	.2	-2.6	.9	0.7

EN 200477B

0.11	76.53	12.67	.05						-3.3	.2	390		
0.20	73.46	17.67	.05						-7.4	.2	390		
0.30	70.55	17.67	.05						-8.0	.2	390		
0.40	67.64	17.67	.05						-9.5	.2	388		
0.50	64.73	17.67	.05	-.013	.009	-11.0	.3	386					
0.600	61.81	17.67	.04	-.025	.016	-10.9	.3	380					
0.700	58.90	12.66	.04	-.05	.03	-11.3	.3	375					
0.800	56.00	17.65	.04	-.09	.04	-12.6	.4	362					
0.900	53.09	17.62	.03	-.18	.07	-12.2	.4	344					
1.000	50.19	17.57	.03	-.34	.10	-12.6	.4	321					
1.100	47.31	17.47	.04	-.66	.14	-12.6	.4	296					
1.200	44.44	17.29	.07	-1.22	.18	-13.2	.4	261					
1.300	43.34	17.17	.08	-1.65	.18	-14.0	.5	233					
1.400	41.62	16.93	.10	-2.44	.17	-13.1	.4	184					
1.500	38.89	16.24	.11	-4.7	.3	-12.7	.4	93					
1.600	36.32	14.92	.14	-9.0	1.3	-11.8	.3	49					
1.700	34.05	12.4	.5	-17	4	-9.8	.2	5					
1.800	32.38	7.6	1.8	-33	10	-2.4	.3	0					

EN 090677

-0.025	86.83	27.45	.23								-2.2	1.6	.17
0.000	86.25	27.45	.23								-6.4	.3	.17
0.100	83.89	27.45	.22								-6.7	.3	.14
0.200	81.53	27.44	.19								-7.2	.4	.12
0.300	79.18	27.43	.13								-6.6	.3	.097
0.420	76.35	27.3	.3								-7.4	.4	.071
0.500	74.47	27.2	.7								-7.2	.4	.038
0.570	72.81	26.7	1.1						-9	3	-6.2	.4	.021
0.600	72.17	26.4	1.0						-13	6	-5.8	.4	.017
0.650	71.05	25.5	.5								-5.6	.4	.012
0.700	69.99	24	.3								-6.2	.4	.006
0.749	69.06	21	.13								-2.7	1.6	0

EN 120677

0.00	78	14.1	.8								-5.6	.8	850
0.11	77	14.1	.8								-8.2	.5	850
0.44	74	14.1	.7								-9.3	.6	840
0.98	69	14.1	.7								-9.9	.8	830
1.64	63	14.1	.7								-10.2	.8	810
2.18	58	14.1	.6								-10.3	.8	780
2.73	53	14.0	.6								-10.7	.9	750
3.36	47.3	13.9	.6								-11.5	1.1	690
3.96	41.9	13.7	.5						-2	.1	-12.1	1.3	600
4.54	36.8	13.4	.5						-1.0	.2	-12.4	1.3	460
5.18	31.5	12.0	.7						-1.8	.3	-12.6	1.4	280
5.53	28.9	10.7	.9						-2.7	.5	-12.8	1.5	180
6.03	25.7	8.9	1.1						-3.9	.9	-9.7	.8	60
(19)	3.6	2	2								-2	2	30

EN 160777

-0.21	83.3	26.8	.7								-1.5	1.3	.42
0.00	79.0	26.7	.6								-8.2	.3	.40
0.08	77.3	26.6	.5								-8.4	.4	.33
0.16	75.7	26.5	.5								-8.3	.4	.21
0.22	74.4	26.3	.7								-8.0	.5	.12
0.32	72.3	26	.2									.3	.01
0.55	71.7	26	.2								-2.7	.3	.001
0.39	70.8	25	.3								-2.3		0

EN 210477

0.22	91.16	22.13	.13								-2.5	.4	.36
0.30	88.57	22.07	.10								-5.03	.13	.36
0.40	84.17	22.00	.07								-5.49	.19	.34
0.50	81.79	21.86	.04								-.9	.3	.31
0.60	79.43	21.61	.06								-1.7	.3	.29
0.70	77.11	21.14	.10								-3.14	.20	.27
0.80	75.97	20.78	.10								-4.27	.17	.26
0.90	74.83	20.28	.09								-5.8	.4	.26
1.00	73.78	19.59	.06								-7.9	1.0	.25
1.10	72.74	18.67	.15								-10.8	1.9	.25
1.20	71.96	12.7	.3								-14	3	.14
1.30	70.94	15.8	.8								-20	6	.02
1.40	69.28	9.0	2.3								-41	18	0

						M	=E _m	Group
-0.000	81.25	15.10	.7			-1.5	.7	.100
0.100	82.25	15.10	.3			-4.18	.2	.093
0.200	83.25	15.34	.24			-4.18	.3	.084
0.300	84.61	15.31	.17			-4.2	.3	.077
0.400	83.44	15.17	.12			-4.6	.2	.068
0.500	82.28	15.12	.13			-4.7	.3	.058
0.600	81.12	15.35	.18			-4.4	.2	.057
0.700	79.74	15.63	.22			-5.2	.2	.040
0.800	78.22	15.53	.22			-3.8	.3	.032
0.900	77.69	15.37	.22			-4.0	.3	.024
1.000	76.57	15.2	.5			-4.4	.2	.012
1.100	75.47	14.9	1.1			-4.4	.2	.002
1.250	73.87	14	3			-1.3	.2	0

EN 12 08 77

0.000	100.0	61.1	1.7			-6.0	1.2	.120
0.033	98.4	61.1	1.7			-7.9	.3	.120
0.116	94.2	61.1	1.7			-8.2	.3	.115
0.199	90.1	61.1	1.6			-9.2	.5	.105
0.280	86.1	61.1	1.4			-9.8	.8	.084
0.360	82.1	60.1	1.4			-10.1	.9	.050
0.439	78.2	56	3			-9.9	.9	.009
0.563	77.2	52	3			-6.0	1.2	.001
-	74.6	-	-			-4.2	1.4	0

EN 17 08 77

-0.009	101.40	62.1	2.7			-4.1	.3	.0049
0.000	100.88	62.1	2.6			-5.85	.15	.0049
0.102	95.28	62.0	2.5			-6.05	.14	.0038
0.200	89.88	61.9	2.2			-6.10	.13	.0030
0.303	84.88	61.7	2.3			-5.82	.14	.0021
0.361	81.08	61.4	4.0			-7.20	.12	.0010
0.412	78.88	61	6			-5.20	.17	.0001
-	77.14	60	8			-3.0	.3	0

EN 14 09 77B

-0.033	104.90	72	6			-4.1	.8	.0019
0.000	102.39	71	5			-5.7	.5	.0019
0.040	99.59	71	5			-6.5	.4	.0016
0.080	96.79	71	4			-6.2	.4	.0012
0.120	94.06	70	4			-6.5	.4	.0008
0.160	91.99	69	5			-6.2	.4	.0005
0.202	89.59	66	11			-6.5	.4	.0001
0.248	87.51	65	15			-3.7	.8	0

EN 14 09 77C

-0.232	109.90	67.9	.7			-4.6	.4	.0040
0.000	96.93	67.8	.6			-6.4	.2	.0040
0.050	94.13	67.7	.5			-6.8	.2	.0032
0.100	91.33	67.5	.4			-6.5	.2	.0025
0.151	88.53	67.1	.5			-6.7	.2	.0018
0.200	85.83	66.6	1.0			-8.8	.2	.0005
0.242	83.52	65.9	2.9			-4.4	.4	0

EN 14 09 77A

0.000	97.41	30.22	.08			-4.2	.2	1500
0.033	89.26	30.22	.08			-6.7	.2	1500
0.066	88.40	30.22	.08			-5.7	.2	1500
0.100	83.48	30.21	.08			-8.5	.2	1500
0.133	77.85	30.20	.07			-11.2	.4	1500
0.166	70.60	30.16	.06			-10	.5	1350
0.200	64.21	30.06	.04			-15.0	.6	1140
0.233	63.03	29.98	.03			-15.0	.6	1070
0.266	61.16	29.88	.03			-15.2	.6	990
0.300	60.44	29.83	.04			-16.2	.6	910
0.333	58.30	29.73	.05			-15.6	.6	820
0.366	57.44	29.52	.06			-15.4	.6	700
0.400	55.62	29.08	.05			-15.3	.6	580
0.433	53.84	28.17	.05			-15.5	.6	440
0.466	52.11	27.24	.05			-15.3	.6	350
0.500	50.43	27.03	.06			-14.9	.6	240
0.533	48.87	27.85	.06			-14.5	.6	150
0.566	47.33	24.66	.06			-14.2	.5	97
0.600	45.76	23.54	.06			-15.0	.6	42
0.633	44.37	21.91	.10			-12.1	.4	11
0.666	43.10	19.95	.2			-10.2	.3	1.6
0.700	41.95	18.2	0			-11.5	.2	.5
0.733	40.82	16.2	1.2			-7.0	.1	.007

-0.034	80.41	25.66	.20									-2.6	.8	.002
0.000	79.26	25.66	.29									-5.4	.4	.002
0.153	77.02	25.63	.27									-4.8	.4	.002
0.3186	74.20	25.57	.22									-5.4	.4	.002
0.480	72.08	25.52	.19									-5.2	.6	.002
0.6472	69.27	25.40	.13									-5.9	.3	.002
0.8162	66.48	25.18	.13									-6.1	.3	.002
0.9853	63.73	24.80	.20									-5.8	.3	.002
1.1540	61.37	24.35	.25									-6.0	.3	.002
1.3232	60.37	23.93	.27									-6.7	.4	.002
1.4924	58.44	23.63	.26									-5.4	.4	.002
1.6616	56.59	21.7	.4									-5.6	.3	.002
1.8308	54.88	19.7	1.1									-4.8	.4	.002
2.0000	53.20	16.1	2.9									-2.5	.8	0

EN 08 10 77

-0.000	93.94	24.30	.14									-3.26	.26	.460
0.032	91.39	24.30	.13									-5.33	.19	.457
0.063	87.89	24.28	.13									-5.71	.18	.443
0.098	85.91	24.27	.12									-4.97	.20	.434
0.130	82.85	24.24	.10									-5.72	.18	.420
0.166	80.71	24.20	.09									-5.88	.18	.409
0.200	76.67	24.10	.06									-6.77	.17	.389
0.232	74.18	23.99	.05									-5.77	.18	.370
0.266	69.82	23.66	.05									-6.55	.17	.292
0.299	68.34	23.48	.06									-7.34	.17	.270
0.333	67.23	23.31	.07									-6.72	.17	.245
0.366	66.14	23.11	.08									-8.93	.19	.191
0.399	64.88	22.83	.09									-6.49	.17	.135
0.433	62.62	22.13	.08									-6.15	.18	.102
0.466	61.94	21.85	.08									-7.2	.17	.094
0.500	60.29	21.00	.14									-9.7	.14	.078
0.533	58.35	20.36	.22									-11.6	.20	.042
0.566	58.46	19.6	.4									-14	.3	.006
0.600	58.82	17.2	.8									-19	.4	0

Handwritten note:
 ...
 ...

0.100	22.22	32.22	.22	-2.4	.4	-3.9	.4	.27
0.100	22.22	32.22	.16	-1.9	.4	-2.2	.2	.26
0.100	22.22	32.22	.12	-2.6	.5	-2.6	.2	.25
0.100	69.23	32.22	.08	-3.6	.5	-2.6	.2	.23
0.100	69.23	32.22	.05	-4.8	.5	-2.6	.2	.20
0.100	63.21	32.22	.06	-6.5	.4	-2.2	.2	.17
0.100	62.03	32.22	.06	-7.4	.4	-2.9	.2	.16
0.100	60.82	32.22	.07	-8.4	.3	-2.5	.2	.14
0.100	58.83	32.22	.08	-10.3	.3	-2.4	.2	.11
0.100	57.40	32.22	.08	-12.0	.4	-2.4	.2	.086
0.100	56.00	32.22	.07	-13.9	.7	-2.0	.2	.066
0.100	54.00	32.22	.08	-16.2	.7	-2.9	.2	.049
0.100	53.29	32.22	.11	-18.9	1.6	-2.2	.2	.033
0.100	51.99	32.22	.20	-21.9	2.3	-2.2	.2	.026
0.100	50.73	32.22	.3	-26	3	-2.4	.2	.014
0.100	48.99	29.6	.6	-32	5	-3.8	.4	.004

EN161077

-0.233	26.0	33.8	1.8	-1.5	.6	-5.3	.4	.88
-0.093	22.2	33.8	1.8	-3.0	1.1	-7.2	.2	.87
0.175	25.1	32.1	1.4	-7	.3	-2.1	.2	.77
0.261	22.8	31.3	1.3	-10	.4	-11.4	.4	.57
0.341	21.9	30.4	1.1	-13	.5	-8.8	.2	.28
0.441	20.5	28.9	1.2	-18	.7	-12.4	.5	.16
0.467	19.3	28.5	1.2	-20	.8	-12	.4	.006
0.747	18.6	22	.4	-38	1.4	-4.5	.5	.0

EN 181077

-0.134	24.9	17.13	.3	-1.6	.3	-3.4	.7	1.9
-0.116	24.6	17.3	.3	-1.6	.3	-6.1	.3	1.8
0.002	23.3	17.22	.20	-1.7	.4	-7.4	.3	1.6
0.119	22.4	17.14	.16	-1.8	.5	-8.1	.3	1.4
0.149	21.7	17.01	.12	-1.9	.5	-7.9	.3	1.1
0.179	20.5	16.81	.15	-1.1	.7	-8.4	.3	.55
0.200	19.9	16.22	.18	-1.2	.7	-8.0	.3	.32
0.219	18.0	16.57	.26	-1.3	.8	-8.8	.4	.08
0.277	17.7	16.5	.3	-1.4	.9	-3.4	.2	.0

EN 311077

0.095	94.87	35.7	.5	-0.12	.005	-3.2	.6	2.80
0.100	94.87	35.7	.5	-0.15	.008	-5.6	.3	2.80
0.120	88.94	35.7	.5	-0.29	.015	-7.4	.3	2.80
0.140	87.07	35.7	.5	-0.55	.028	-7.9	.3	2.80
0.160	84.62	35.6	.5	-1.0	.05	-6.9	.3	2.80
0.180	82.87	35.6	.5	-1.18	.09	-8.1	.4	2.80
0.200	81.42	35.6	.5	-1.30	.13	-9.6	.7	2.79
0.220	79.42	35.5	.5	-1.5	.2	-10.6	.8	2.79
0.240	78.87	35.5	.5	-1.8	.4	-11.7	1.0	2.78
0.260	78.67	35.4	.4	-1.2	.6	-12.3	1.1	2.75
0.280	78.42	35.2	.4	-1.18	.9	-13.1	1.3	2.73
0.300	78.27	35.0	.4	-2.2	1.4	-14.1	1.4	2.64
0.320	77.47	34.7	.5	-4	2	-14.5	1.5	2.49
0.340	77.27	34.2	.6	-6	3	-14.9	1.6	2.22
0.360	77.07	33.6	1.0	-8	5	-14.7	1.5	2.00
0.380	76.87	32.8	1.6	-13	9	-14.8	1.5	1.74
0.400	76.67	31	3	-17	14	-15.2	1.6	1.40
0.420	76.50	(27	5			-13.7	1.3	1.00
0.440	76.32	(25	8			-15.9	1.7	.61
0.460	76.15	(20	16			-9.7	.6	0.44
0.480	75.98	(17	≈			-2.2	.3	0.29
0.500	75.87	(7	≈			-3.8	.6	0

EN 071177

0.100	66.24	14.14	.03	-1.30	.03	-2.23	.19	.70
0.100	65.41	14.11	.03	-1.33	.03	-3.54	.12	.70
0.100	63.70	14.03	.03	-1.42	.03	-4.57	.10	.68
0.100	62.00	13.938	.04	-1.52	.04	-4.62	.10	.66
0.100	60.34	13.821	.04	-1.66	.04	-4.98	.11	.64
0.100	58.63	13.674	.04	-1.82	.04	-4.53	.10	.61
0.100	57.07	13.489	.04	-1.93	.03	-4.61	.10	.58
0.100	55.57	13.287	.04	-2.10	.03	-4.45	.10	.53
0.100	54.14	12.992	.04	-2.25	.02	-6.16	.10	.43
0.100	52.76	12.709	.04	-2.05	.03	-5.70	.09	.33
0.100	51.43	12.439	.04	-2.57	.06	-4.58	.10	.22
0.100	50.15	12.170	.04	-3.23	.12	-4.30	.10	.14
0.100	48.92	11.903	.05	-4.1	.2	-4.19	.10	.07
0.100	47.74	11.638	.05	-5.1	.3	-1.31	.19	.01

-0.17	112.92	53.13	.5					
0.000	107.28	53.13	.5					
0.100	104.62	53.12	.4					
0.200	101.86	53.12	.4					
0.300	98.26	53.05	.25					
0.400	95.67	52.6	.5	-9	5			
0.439	93.84	52.1	.7	-14	5			
0.500	91.94	52.0	.7	-28	14			
0.570	89.87	51.8	2.3					
0.635	88.62	47	11					

EN 0811277

-0.045	92.73	33.4	1.3					
0.070	89.72	32.9	.9					
0.160	87.54	32.2	.7					
0.280	84.58	30.7	1.6					
0.523	79.31	25	8					

EN 051277

-0.182	98.99	31.57	.04					
0.100	95.42	31.57	.04					
0.200	91.16	31.57	.04					
0.400	86.90	31.57	.04	-0.18	.010			
0.600	82.63	31.56	.04	-0.06	.03			
0.800	78.38	31.53	.03	-0.23	.08			
1.000	74.13	31.44	.03	-0.25	.19			
1.200	69.89	31.06	.05	-3.8	.3			
1.400	67.79	29.62	.08	-11.5	.4			
1.600	62.04	25.4	.3	-35	4			
1.838	58.99	5	3	-150	30			

EN 071277

-0.085	79.5	30.4	.6					
0.203	76.4	30.3	.6					
0.406	74.2	30.3	.6					
0.609	72.2	30.3	.6					
0.812	70.0	30.3	.5					
1.015	68.8	30.3	.5					
1.218	65.6	30.2	.5					
1.421	61.8	30.1	.5					
1.624	58.0	29.9	.4					
1.827	54.5	29.7	.4					
2.030	50.6	29.3	.6					
2.233	46.4	28.4	1.2					
2.436	39.0	25	4					

EN 111277

-0.145	64.92	14.33	.07	-1.11	.03	-3.5	.5	21
0.100	62.26	14.31	.06	-1.16	.04	-5.1	.3	21
0.200	57.91	14.24	.04	-1.30	.06	-7.4	.3	21
0.300	55.20	14.16	.03	-1.46	.08	-8.6	.4	20
0.400	53.05	14.07	.02	-1.63	.08	-7.8	.3	19
0.500	50.91	13.96	.02	-1.87	.09	-9.0	.4	18
0.600	48.80	13.79	.02	-2.20	.09	-9.7	.5	16
0.700	47.24	13.63	.03	-2.63	.08	-10.3	.6	14
0.800	44.66	13.25	.04	-3.16	.07	-10.0	.5	9.5
0.900	43.17	12.94	.04	-3.79	.11	-9.16	.5	6.1
1.000	40.77	12.22	.04	-4.4	.3	-8.16	.4	3.2
1.100	40.30	12.03	.05	-4.8	.4	-9.5	.5	2.5
1.200	39.85	11.83	.06	-5.2	.4	-7.9	.3	2.0
1.300	39.40	11.62	.07	-5.6	.5	-8.8	.4	1.8
1.400	38.53	11.13	.12	-6.6	.7	-6.2	.2	1.0
1.500	37.71	10.56	.18	-7.7	.9	-7.3	.3	.7
1.600	36.93	9.9	.3	-9.1	1.3	-7.5	.3	.2
1.700	35.68	8.4	.5	-12.1	2.0	-3.7	.5	.0

EN 131222

-0.053	102.79	65.13	1.5					
0.100	99.48	65.12	1.5					
0.200	94.28	65.1	1.4					
0.300	88.48	64.1	1.2	-14	8			
0.400	82.28	62.1	1.5					
0.500	78.88	60.1	2.3					
0.600	76.48	58	4					
0.700	75.10	57	5					

	h_{min}	α°	γ°	h_{min}	α°	γ°			
EN20177	68.98 ±.16	9.022 ±.003	47.723 ±.002	56.3	8.901	42.902	37.99 ±.11	8.726 ±.002	±.002
EN205177	87.0 ±.4	18.747 ±.017	48.167 ±.016	79.5	18.862	48.192	73.2 ±1.5	18.958 ±.017	48.213 ±.016
EN200477A	89.42 ±.03	14.8165 ±.0004	48.6631 ±.0003	64.1	15.038	48.886	53.54 ±.03	15.1326 ±.0025	48.8797 ±.0003
EN200477B	76.5 ±.3	7.372 ±.006	48.419 ±.005	43.3	7.092	48.503	32.4 ±.2	6.999 ±.004	48.530 ±.003
EN210477	91.16 ±.02	14.8822 ±.0002	49.6245 ±.0002	72.0	15.220	49.771	69.28 ±.04	15.2680 ±.0005	49.7713 ±.0004
EN160577	89.19 ±.10	16.2818 ±.0010	49.2365 ±.0007	83.2	16.707	49.339	75.60 ±.10	15.8828 ±.0010	49.4700 ±.0007
EN010677	77.9 ±.6	12.627 ±.002	47.282 ±.004	40.7	11.983	48.083	26.99 ±.02	11.7311 ±.0002	48.3896 ±.0002
EN090677	86.83 ±.08	14.356 ±.002	50.385 ±.001	76.3	14.320	50.436	69.06 ±.05	14.295 ±.002	50.471 ±.001
EN120677	78 ±.3	5.98 ±.05	46.72 ±.03	28.9	6.352	46.262	25.7 ±1.0	6.377 ±.016	46.239 ±.009
							(≈ 19)	6.427	46.178
EN160777	83.25 ±.11	17.4240 ±.0023	49.3328 ±.0012	74.4	17.414	49.270	70.77 ±.05	17.4100 ±.0010	49.2438 ±.0005
EN220777	88.64 ±.09	17.3032 ±.0014	49.5208 ±.0012	79.7	17.411	49.500	73.87 ±.09	17.4818 ±.0014	49.4863 ±.0012
EN120877	100.0 ±.3	11.730 ±.007	46.861 ±.005	82.0	11.606	46.787	74.6 ±.3	11.556 ±.006	46.757 ±.005
EN170877	101.40 ±.02	12.657 ±.0004	50.2788 ±.0003	81.0	16.933	50.206	77.14 ±.02	16.9099 ±.0004	50.1958 ±.0003
EN140977B	104.90 ±.03	13.754 ±.002	49.850 ±.002	94.1	13.724	49.857	87.51 ±.03	13.707 ±.002	49.861 ±.002
EN140977C	109.90 ±.04	16.9155 ±.0008	49.5222 ±.0006	85.7	16.697	49.486	83.52 ±.03	16.6770 ±.0006	49.4220 ±.0005
EN140977A	97.8 ±.5	18.707 ±.003	48.639 ±.004	60.4	12.305	48.980	40.1 ±.4	16.494 ±.002	49.157 ±.003
EN061072	80.41 ±.21	16.986 ±.004	49.730 ±.002	60.4	17.044	49.911	53.2 ±.3	17.066 ±.005	49.926 ±.002
EN061022	93.9 ±.6	15.420 ±.012	49.756 ±.007	66.1	15.277	49.945	56.8 ±.4	15.229 ±.008	50.009 ±.004
EN081077	78.66 ±.03	15.9879 ±.0005	49.0227 ±.0004	60.8	16.129	49.702	48.98 ±.02	16.2601 ±.0005	49.1543 ±.0003
EN081077	86.0 ±.5	10.985 ±.010	48.726 ±.006	68.5	11.061	48.619	62.6 ±.5	11.050 ±.010	48.582 ±.006
EN081077	74.9 ±.14	15.957 ±.011	48.703 ±.014	68.0	16.123	48.733	67.7 ±.17	16.130 ±.013	48.735 ±.016
EN311077	94.6 ±.3	12.985 ±.018	48.629 ±.012	37.1	12.192	48.339	32.8 ±1.0	12.562 ±.027	48.317 ±.016
EN31177	65.24 ±.03	15.4092 ±.0003	48.9520 ±.0003	53.4	15.617	49.027	46.60 ±.02	15.7285 ±.0003	48.9520 ±.0003
EN31277	82.92 ±.06	14.1036 ±.0009	48.3464 ±.0003	93.8	13.992	48.538	88.07 ±.04	13.9784 ±.0006	48.8739 ±.0002
EN31277	72.7 ±.17	14.1581 ±.0005	50.4931 ±.0007	87.5	14.450	50.486	79.21 ±.17	14.358 ±.003	50.4728 ±.0002

EN 101 : 10-10-10

Fireball No	Beginning			Maximum Light			Terminal		
	h km	$\lambda^\circ E$	$\varphi^\circ N$	h km	$\lambda^\circ E$	$\varphi^\circ N$	h km	$\lambda^\circ E$	$\varphi^\circ N$
EN 051277	98.99 ± 0.5	14.9416 ± 0.006	49.8617 ± 0.0006	78.4	14.633	49.860	58.99 ± 0.05	14.3399 ± 0.0006	49.8571 ± 0.0006
EN 071277	79 ± 3	19.873 ± 0.018	49.07 ± 0.03	54.5	19.004	49.16	39 ± 3	18.447 ± 0.017	49.21 ± 0.03
EN 111277	64.92 ± 1.0	18.303 ± 0.005	50.714 ± 0.003	47.2	18.286	50.762	35.62 ± 0.09	18.275 ± 0.004	50.802 ± 0.002
EN 131277	102.79 ± 0.7	18.743 ± 0.004	50.016 ± 0.002	76.5	18.713	50.077	75.5 ± 0.4	18.712 ± 0.020	50.079 ± 0.013

Astronomischen Instituts der Tschechoslowakischen Akademie der Wissenschaften auf eine optimale Lösung, die die Effektivität dieses ausgezeichneten Gerätes wesentlich erhöht, zielte. Die Konstrukteure des VEB Carl Zeiss JENA und von VILATI Budapest stellten sich den Forderungen an eine moderne Ausrüstung des 2-m-Teleskops, denn auf diesem Gerät baut der langfristige Plan der wissenschaftlichen Arbeit des Astronomischen Instituts der Tschechoslowakischen Akademie der Wissenschaften in beträchtlichem Maße auf. Dieser Plan umfaßt auch die Untersuchung von Sternen, Sternsystemen und interstellarer Materie.

Im Jahre 1978 wurde ein Vertrag über die Modernisierung des 2-m-Teleskops abgeschlossen, die in der Zeit vom November 1982 bis März 1984 erfolgen wird. Folgende Änderungen werden verwirklicht:

Die Drehmelder im Ablesesystem werden durch zwei inkrementelle Geber mit hoher Auflösung, angetrieben durch Reibungsgetriebe, ersetzt. Aus dem Übersetzungsverhältnis ergibt sich die Größe eines Inkrements von 0,1", so daß eine Genauigkeit der differentiellen Einstellung in einem Feld von 4 × 4' etwa ± 1" und eine angemessene Genauigkeit bei der Vorwahl des Teleskops in der Größenordnung von ± 10" zu erwarten sind.

Der Einbau des Meßsystems neben der unerläßlichen Kontrolle des Hauptlagers und der komplette Kabelaustausch erfordern die volle Demontage des Teleskops und die Rekonstruktion einiger seiner Teile im Herstellerbetrieb.

Ein Teil der Modernisierung umfaßt den Austausch des Spaltkopfes des Coudé-Spektrographen gegen einen neuen Typ, der am 2-m-Teleskop in Bulgarien erfolgreich erprobt wurde, sowie den Einbau eines Kreuzschlittens am Cassegrain-Fokus, der außeraxiale Nachführung bei der direkten Fotografie und beim Scanning der flachenhaften Objekte unter eventueller Anwendung eines Fotometers ermöglicht.

Der bedeutendste Beitrag zur Modernisierung ist die Anwendung der Mikroprozessortechnik zur Steuerung des Teleskops. Es ist nicht notwendig, alle Vorteile eines progressiven elektronischen Systems aufzuzählen. Unter anderem wird eine neue Art der Spektrenverbreiterung und der Derotation im Coudé-Spektrographen realisiert, und zwar ohne Lichtverluste, da die jetzt verwendeten optischen Glieder entfallen. Dank der großen Reserve in der Speicherkapazität und der Möglichkeit ihrer Erweiterung werden die Vorverarbeitung und einfache Reduktion der Beobachtungsdaten möglich sein, insbesondere wenn als Lichtempfänger elektrooptische Elemente benutzt werden.

Im Rahmen der Modernisierung soll auch die Fernsehtechnik schrittweise zur Anwendung kommen. Im Fortgang dieser Entwicklung werden wir uns auf die Verarbeitung der Bildinformation bei gleichzeitiger Nutzung der durch den Mikroprozessor gegebenen Möglichkeiten konzentrieren.

Diese so umfassende Modernisierung des größten optischen Gerätes in der ČSSR ist keine geringe Aufgabe. Die oben angeführten Änderungen erfordern bauliche Maßnahmen im Beobachtungsgeschoß der Kuppel sowie eine wesentlich höhere Qualifikation der Mitarbeiter, die in Zukunft mit diesem modernen Teleskop arbeiten werden.

An der Modernisierung des 2-m-Teleskops arbeiten bei allen beteiligten Partnern neue Spezialistenkollektive, deren Anzahl aus Gründen der Vertiefung der Spezialisierung wesentlich vergrößert wurde. Um so wichtiger ist andererseits die Koordinierung dieser Kollektive zur Erreichung des abgesteckten Ziels. Das enge Zusammenwirken aller beteiligten Partner wird garantieren, daß das modernisierte 2-m-Teleskop im Observatorium Ondřejov ein weiteres positives Beispiel der sozialistischen Integration sein wird.

Der Vertrag über die wissenschaftlich-technische Zusammenarbeit, abgeschlossen zwischen dem Astronomischen Institut der Tschechoslowakischen Akademie der Wissenschaften und dem VEB Carl Zeiss JENA, bietet die Voraussetzungen dafür, daß sich die schöpferischen Leistungen des großen Kollektivs der Fachleute dieses Werkes mit ihren wissenschaftlichen Kenntnissen, Erfahrungen und dem fachlichen Niveau der Mitarbeiter des Astronomischen Instituts zum gemeinsamen Nutzen vereinigen.

Literaturstatistik

Aus der Arbeit des Observatoriums Ondřejov sind erschienen:

- 65 Arbeiten in 4 tschechoslowakischen und 22 ausländischen Publikationen.
- 18 Arbeiten im Bull. Astron. Inst. Čsl.
- 4 Arbeiten im Astron. Astrophys.
- 1 Arbeit in Astrophys. Letters.
- 9 Arbeiten im Inf. Bull. Var. Stars.
- 6 Arbeiten im IAU Circ.
- 8 Arbeiten in Symposia und Colloquia IAU.

An den Arbeiten beteiligten sich 38 Wissenschaftler, darunter 22 aus der ČSSR und 16 aus dem Ausland: Kanada: 3, BRD: 3, Holland: 2, Bulgarien: 1, Jugoslawien: 2, UdSSR: 1, Italien: 2, Polen: 2.

Das Zweikoordinatenmeßgerät ASCORECORD 3 DP im Dienste des Europäischen FEUERKUGEL-Programms

Zdeněk Cepelcha

Institut für Astronomie der Tschechoslowakischen Akademie der Wissenschaften, Observatorium Ondřejov

Ein systematisches Programm für die Fotografie von Feuerkugeln über der zentral-europäischen Region wurde 1963 durch das Astronomische Institut der Tschechoslowakischen Akademie der Wissenschaften begonnen. Jede der heute bestehenden 46 Stationen ist mit einer all-sky-Kamera ausgerüstet. Es werden zwei Typen dieser Kamera verwendet. Die eine Kamera besteht aus einem 360-mm-Konvexspiegel und einer Kleinbildkamera, mit derselben nach unten belichtet wird. Das Gesamtsystem hat eine sehr kurze

Brennweite, sie ergibt annähernd einen Maßstab von 1 mm pro 10'. Der andere Kameratyp verwendet ein Fischaugenobjektiv, das einen Abbildungsmaßstab von etwa 1 mm pro 2' im Zentrum gewährleistet. Für diese Kameras werden ORWO-NP-27-Fotoplatten verwendet. Beide Kameras sind mit rotierenden Verschlussblenden ausgerüstet, die 12,5 Zeitmarken/s (Unterbrechungen der Leuchtspur des Meteors) ergeben.

Die mit den Kameras gewonnenen Aufnahmen von Feuerkugeln wurden am Obser-

vatorium Ondřejov mit einem ASCORECORD aus dem VEB Carl Zeiss JENA [1] gemessen und die geometrischen, dynamischen und photometrischen Daten mit einem Rechner EC 1040 ausgewertet. Das Rechnerprogramm FIRBAL enthält 4500 Fortran-Befehle, ein Beweis, wie kompliziert das Problem der Berechnung von Bahn, Geschwindigkeit und Umlaufbahn von Feuerkugeln aus Aufnahmen mehrerer Stationen ist. Als Berechnungsbasis dienen die gemessenen rechtwinkligen Koordinaten einer Reihe von

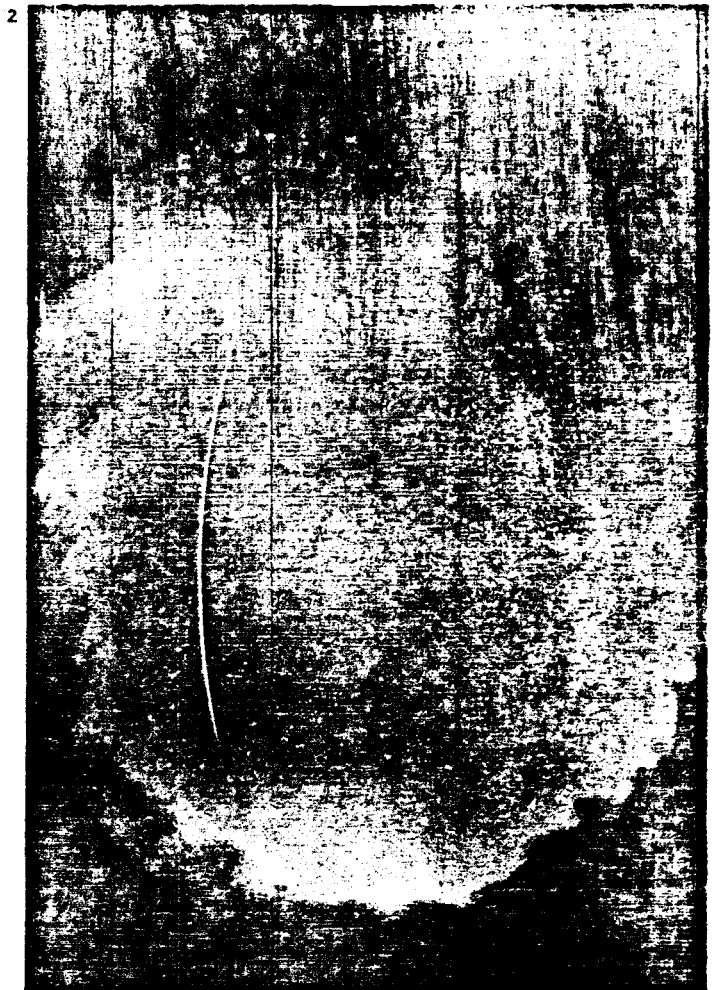


Bild 1: Feuerkugel von Mälnik, aufgenommen am 22. Juni 1979, 22^h00^m47^s im Observatorium Ondřejov mit einem Fischaugenobjektiv. Der Durchmesser des Gesamthimmels beträgt auf dem Originalnegativ 80 mm. Die Zeitmarken folgen im Intervall von 0,08 s, die Flugrichtung verläuft von Süd nach Nord. Die Gesamtlänge beträgt 105° entsprechend einer Entfernung von 140 km. im Raum zurückgelegt in 6,4 s. Die maximale Hellig-

keit entspricht der des Vollmondes. Mit 15 Sternen, die mit dem ASCORECORD entlang der Feuerkugelspur (beginnend bei den Sternspuren bei 21^h02^m04^s UT) gemessen wurden, betrug die Standardabweichung für einen Stern $\pm 0,020''$. Die Standardabweichung des Radianten von $\pm 0,06''$ und die Anfangsgeschwindigkeit von $24,10 \pm 0,03$ km/s wurden aus einer Reihe von in 5 Stationen gemachten Aufnahmen berechnet.

Bild 2: Feuerball von Mälnik, aufgenommen am 22. Juni 1979 im Observatorium Ondřejov mit einem bewegten Fischaugenobjektiv ohne Zeitmarken. Die Kombination dieser Abbildung mit Bild 1 zeigt die Durchgangszeit der Feuerkugel mit einer Genauigkeit von ± 8 s. Mit 15 mit dem ASCORECORD entlang der Bahn gemessenen Sternen betrug die Standardabweichung pro Stern 0,016''.

Meßpunkten auf jeder Aufnahme: Für die Berechnungen einer hellen Feuerkugel, die von mehreren Stationen aufgenommen wurde, sind in der Regel 2000 Messungen mit dem ASCORECORD notwendig. Hier soll detailliert beschrieben werden, welche Punkte und Objekte gemessen und wie diese Datenmenge auf einfache Weise mit Hilfe eines Coniputerprogramms ausgewertet wurden.

Das Koordinatensystem der mit beiden Kameratypen gewonnenen Negative wird mit Hilfe von Umgebungssternen definiert. Die feststehende Kamera gewährleistet eine strichformige Aufnahme der Sternspur. Die Zeiten des Beginns und des Endes der Belichtung sind bekannt. Damit ist die annähernde Zenit- und Südorientierung einfach zu realisieren, indem das auf einem Kreuztisch befindliche Negativ gedreht wird. Der Kreuztisch gehört zur Standardausrüstung des ASCORECORD.

Beginn oder Ende der Sternspuren werden dann mindestens viermal gemessen. Dabei wird bei der Hälfte der Einstellungen das

direkte, bei der anderen Hälfte das um 180° gedrehte Bild verwendet. Die Zahl der verwendeten Sterne liegt meist zwischen 10 und 20, da die Höchstzahl aller freien Parameter in den zweidimensionalen Reduktionsformeln pro Stern 7 ist. Alle Daten werden automatisch auf Lochstreifen gestanzt, wenn eine Einstellung des Fadenkreuzes erfolgt ist. Der gesamte Meßprozeß wird mit einem Kleinrechner KSR 4100, dessen Software die Wahl unterschiedlicher Arbeitsabläufe gestanzt, realisiert. Anmerkungen zu jeder Messung können mit einer Fernschreiber-tastatur auf Lochstreifen übertragen werden. Es wurde eine sehr einfache Bezeichnung der Meßobjekte gewählt, die Numerierung von 1, 2, bis x, wobei mit jedem neuen Objekttyp wieder bei 1 begonnen wird. Die Orientierung, welche Daten im Moment gelesen werden, ist in das Computerprogramm FIRBAL einbezogen. Dieses Arbeitsregime bietet dem Operateur des ASCORECORD mehr Zeit, sich auf die Hauptaufgabe – die Fadenkreuzeinstellung – zu konzentrieren.

Die Meßgenauigkeit des ASCORECORD

von 0,0001 mm in den x- und y-Koordinaten über einen Bereich von 300 mm x 300 mm ist größer, als für den tatsächlich gemessenen Bildtyp erforderlich ist. Die interne Genauigkeit für einen Meßpunkt liegt bei den verwendeten Kameras und Emulsionen um 0,0005 mm. Die Genauigkeit der Übereinstimmung der gemessenen Sternpositionen mit den Katalogwerten beträgt etwa 1 Bogenminute für den gesamten, mit dem 3,5/30-Fischaugenobjektiv sowie 0,1' für den mit der 16/6-Spiegelreflexkamera fotografierten Himmel. Sie hängt von der richtigen Wahl der Sterne ab, wobei scharfe, schwachere Sternbilder in dieser Hinsicht zu bevorzugen sind.

In unserem Fall ist das Objekt mit unbekannter Rektaszension und Deklination ein Feuerkugelschweif, der einen Teil eines Großkreises bildet. Die Leuchtspur (Bild 1) ist durch die periodischen Unterbrechungen der rotierenden Verschlussblende aufgegliedert. Angewendet wurden zwei Typen von ASCORECORD-Messungen der x- und y-Koordinaten für die Feuerkugelabbildung im

gleichen System wie die Sterne. in dem die Beziehungen $\lambda = \lambda(x, y)$, $\delta = \delta(x, y)$ gelten.

Zuerst werden 10 bis 20 Punkte der beleuchteten Spuren des Feuerkugelschweifes ausgewählt, wobei alle zu breiten Spuren vermieden werden, um eine gute Fadenkreuz-Okulareinstellung zu garantieren. Bei einer sehr hellen Feuerkugel muß man sich oft auf den Anfang oder das Schweifende beschränken. Die Bedingung, daß alle Meßpunkte auf dem gleichen Großkreis (in der gleichen Ebene) liegen, sowie die Verwendung der qualitativ besseren Bilder von den äußeren Zonen des Schweifes führen zu genaueren Ergebnissen als das Messen aller Punkte einschließlich der breiten Bilder in der Nähe des Leuchtmaximums der Feuerkugel, wo unterschiedliche Abbildungseffekte die Genauigkeit der einzelnen Einstellungen verschlechtern. Diese Messungen von geeigneten Abschnitten des Feuerkugelschweifes legen dann die Ebene der Feuerkugelbahn fest, die sich aus einem Kamerastandort ergibt. Die aus mehreren Standorten berechneten Ebenen sollten sich im Idealfall auf einer Linie schneiden, der Feuerkugelbahn im Raum. In der Praxis werden aus den Schnittpunkten aller verfügbaren Ebenen eine gemittelte Feuerkugelbahn berechnet und die Standardabweichung aus den Abweichungen der Ebenen von diesem Mittelwert bestimmt.

Der zweite Schritt der Messungen mit dem ASCORECORD befaßt sich mit den von der rotierenden Verschlussblende erzeugten Unterbrechungen. Es gibt mehrere Möglichkeiten, wie man in Abhängigkeit von der Bahngeschwindigkeit einstellt. Ist der Abstand der Unterbrechungen groß genug, um die einzelnen Abschnitte zu erkennen, wird die Einstellung für deren Anfänge vorgenommen. Auf Grund des Nachleuchtphänomens wird niemals der hintere Teil des Schweifabschnittes verwendet. Sind die Abschnitte so schmal, daß sie eher Punkten gleichen, müssen diese direkt gemessen werden. Oft sind sie zu lang, um eine geeignete mittlere Einstellung zu erhalten, aber zu schmal für eine gute Einstellung des Abschnittanfangs, so daß man sich auf die Unterbrechungen der Leuchtspur beziehen muß. In jedem Fall werden alle sichtbaren Zeitmarken des Feuerkugelschweifes gemessen. Bei der Berechnung projizieren wir alle Messungen senkrecht auf den Großkreis des Feuerkugelschweifes, der vom ersten Satz der Meßwerte bestimmt wird. Durch senkrechte Projektion der gemessenen Zeitmarken auf die mittlere Feuerkugelbahn verbleiben nur die Abweichungen von der Flugrichtung der Feuerkugel in den Messungen der einzelnen Zeitmarken (Unterbrechungen, Abschnitte, Spitzen). Die momentane Geschwindigkeit und ihre Veränderung sind die Ergebnisse dieser Messungen. Die Anfangsgeschwindigkeit (außerhalb der Atmosphäre) ergibt zusammen mit dem Vektor der Feuerkugelbahn (Radiant) die Umlaufbahn um die Sonne.

Die Aufnahmen enthalten eine Vielzahl von Sternspuren, und es ist schwierig, die

Helligkeit der Feuerkugel mit einem klassischen Mikrodensitometer zu bestimmen. Die mit dem Fischaugenobjektiv gewonnenen Aufnahmen können zur photometrischen Messung der Breiten der Sternspur und des Feuerkugelschweifes mit dem ASCORECORD verwendet werden. Dabei handelt es sich um relative Messungen, deren Genauigkeit weitgehend von guten Einstellungen abhängt. Diese lassen sich bei den mit dem Fischaugenobjektiv erhaltenen Bildern außerordentlich gut realisieren [2]. Die Breiten der Sternabbildungen ergeben zusammen mit denen aller Spuren der Feuerkugel nach den entsprechenden Korrekturen die charakteristische Dichtekurve, und die absoluten Helligkeitswerte, bezogen auf 100 km Entfernung entlang der Feuerkugelbahn, können berechnet werden. Die kleinsten meßbaren Breiten betragen 0,01 mm, die größten 0,5 mm. Dieser Bereich umfaßt etwa fünfzehn Sterngrößenklassen mit typischen Standardabweichungen von $\pm 0,2$ Größenordnungen am dunkleren und $\pm 0,6$ Größenklassen am helleren Ende, vorausgesetzt, daß genügend Vergleichssterne über den gesamten Helligkeitsbereich zur Verfügung stehen.

Die Ergebnisse aller mit dem ASCORECORD durchgeführten Messungen werden vorwiegend auf Lochstreifen gespeichert, der dann auf Magnetband übertragen wird, um mit dem Rechner auswerfen zu können. Dazu wird ein einfacher Konverter mit Lochstreifenleser und Magnetbandschreiber verwendet. Das FIRBAL-Programm verwendet ein Magnetband, ist aber auch in der Lage, den Lochstreifen direkt zu lesen. Ein Spezialprogramm CORTAP dient zu notwendigen Korrekturen des Magnetbandes, insbesondere dann, wenn einige der verwendeten Sterne während des Rechenprozesses aus dem Datenkomplex ausgeschlossen werden sollen. Wenn der Operateur des ASCORECORD eine beliebige Datenreihe unmittelbar während der Messung streichen will, so kann das Objekt mit einer „Unbekannten“ (hohen Ziffer) numeriert werden, was vom Programm FIRBAL berücksichtigt wird. Das ASCORECORD gibt automatisch zwei ganze Zahlen für jede Messung. Die feste Zahl dient als Standortziffer, die zweite, die automatisch jede abgeschlossene Einstellung zählt, dient als Bezugszahl zur betreffenden Datenreihe.

Der für alle Messungen erforderliche Zeitaufwand hängt allein davon ab, inwieweit der Operateur in der Lage ist, eine gute Einstellung des Strichkreuzes vorzunehmen, da die Zeit für eine Aufzeichnung einer ASCORECORD-Messung demgegenüber wesentlich geringer ist. Die typische Genauigkeit der geometrischen Meßergebnisse mehrerer Stationen im Abstand von 100 km, die dieselbe Feuerkugel beobachten, entspricht den Standardabweichungen von 10 bis 100 m bei der Berechnung von Höhe, Entfernungen und Positionen der vertikalen Projektion auf die Oberfläche. Bei einer Feuerkugel mit einer Leuchtdauer von mehreren Sekunden liegen die Standardabweichungen der Geschwindigkeiten in der Größenordnung von

0,01 km/s, und die Standardabweichungen des Radianten haben einen typischen Wert von $0,2^\circ$. Die Vorhersage eines Meteoritenfalls hängt bei einem tief eindringenden Objekt (in der Regel 35 km über der Erdoberfläche) weitgehend von der Genauigkeit der aerologischen Daten (Hohenwinde) ab. Die mit dem ASCORECORD erzielten Meßergebnisse sind meistens um mindestens eine Größenordnung besser, als es für diese Berechnungen erforderlich ist.

Der Einsatz des ASCORECORD mit dem Kleinrechner KSR 4100 ermöglicht die Durchführung des gesamten Projektes zur Überwachung des europäischen Feuerkugelnetzes mit nur einem Operateur. Die vorläufigen Ergebnisse werden regelmäßig im SEAN-Bulletin [3, 4] veröffentlicht, die Endergebnisse erscheinen im Bulletin des Astronomischen Instituts der Tschechoslowakei [5, 6].

Literatur

[1] BECK, H. G. und R. TIETSCH: Koordinatenmeßgerät ASCORECORD 3 DP. Jenaer Rundschau 17 (1972) 7, S. 349–353.

[2] BOČEK, J., u. a.: Fish-Eye Camera Photographs of Nova Cygni 1975, Bull. Astr. Inst. Czechosl. 27 (1976). 190–191.

[3] CEPLECHA, Z.: Bull. SEAN 4 (1979) 6, 11–14.

[4] CEPLECHA, Z.: Bull. SEAN 6 (1981) 2, 14–17.

[5] CEPLECHA, Z., u. a.: Photographic Data on the Brno Fireball. Bull. Astr. Inst. Czechosl. 30 (1979). 220–225.

[6] CEPLECHA, Z., u. a.: Photographic Data on the Zvolen Fireball and Suspected Meteorite Fall. Bull. Astr. Inst. Czechosl. 31 (1980), 176–182.

Hinweis an die **Bezieher** der JENAER RUNDSCHAU

Im Interesse sicherer und schneller Zustellung der JENAER RUNDSCHAU wird gebeten, bei der Mitteilung von Anschriftenänderungen **außer** der neuen **auch** die **alte** Anschrift mit anzugeben, **unter** der die **Hefte** bisher empfangen wurden. Bitte unbedingt ausgeschnittene Anschrift mit **allen** Angaben (**Kurzzeichen**) vom **letzten** Versandumschlag **übersenden**.
Die Redaktion